



MONASH University

**Development and Characterization of Cocoa Butter Alternatives
from Palm-based Oils for Chocolate Application**

Nirupam Biswas
BSc Hons, MSc

A thesis submitted for the degree of Doctor of Philosophy (PhD) at

Monash University in 2017

School of Science

Copyright notice

© Nirupam Biswas 2017

I certify that I have made all reasonable efforts to secure copyright permission for third-party content included in this thesis and have not knowingly added copyright content to my work without the owner's permission.

Abstract

The principle ingredient of chocolates is cocoa butter (CB). CB is expensive due to high market demand and limited production. As such the search for alternatives to CB is attracting a lot of attention. This study aimed to develop and characterize cocoa butter alternatives (CBAs) by blending and enzymatic interesterification of palm-based oils, such as palm mid-fraction (PMF), refined bleached deodorized palm kernel oil (RBDPKO) and palm stearin (RBDPS) for use in chocolate production. A multi-methodological approach was used for characterization of the samples which included gas chromatography (GC) for fatty acid, high performance liquid chromatography (HPLC) for triacylglycerol (TAG), differential scanning calorimetry (DSC) for melting, pulsed nuclear magnetic resonance (pNMR) for solid fat content (SFC), X-ray diffraction (XRD) for polymorphism, polarized light microscopy (PLM) for crystal morphology, master-sizer for particle size distribution (PSD), rheometer for flow behavior, texture analyser for hardness and stereomicroscopy for bloom formation.

The physical and chemical properties of binary mixtures of PMF, RBDPKO and RBDPS for cocoa butter substitutes (CBSs) were investigated. Using 20-40% of PMF in RBDPKO, 30-50% of RBDPS in RBDPKO and 50-80% of PMF in RBDPS, the blends showed broad melting endotherms at 20-38°C, comparable to that of CB. Although the polymorphism, fatty acid and TAG composition were different, these blends exhibited a desirable monotectic effect (compatibility) at 10-25°C, indicating their potential for use as CBSs.

The physicochemical properties of ternary mixture of PMF, RBDPKO and RBDPS were also examined. Eight blends of various ratios of ternary mixtures were studied based on the results of binary mixtures. The composition of palmitic (P) and oleic (O) fatty acids, POP TAG and crystal morphology of the ternary blend (14.9% PMF/59.6% RBDPKO/25.5% RBDPS) resembled closely to CB. Although its melting profile (18.5 and 37°C) and polymorphism were different, it showed a desirable monotectic effect at 20-25°C, pointing to potentials for use as CBS.

As ternary blends lacked stearic-oleic fatty acids, commercial stearic-oleic acids were added to these blends to get fatty acids composition to resemble that of CB. The blend (80% ternary mixture/15% stearic/5% oleic) with fatty acids composition resembling closely to CB was then selected for enzymatic interesterification. Using the optimized conditions (4% lipase incubated for 6 h at 60°C) for enzymatic interesterification, the blend showed a single

melting endotherm at 33.5°C, similar to CB. The composition of POST (28.4%) and StOSt (19.5%) of the interesterified fat was significantly ($P<0.05$) increased along with a gradual decrease in POP (17.7%) compared to non-interesterified fat. In addition, the interesterified fat revealed a desirable X-ray diffraction peak (albeit smaller) at near 4.5 Å, indicating β polymorph. Although the interesterified fat had considerably lower SFC, it could be used as CBS as it had comparable melting profile, fatty acids and TAGs composition to CB.

Subsequently, the compatibility of enzymatically produced CBS with CB was examined. Six blends at various ratios of CBS/CB mixtures were studied. The mixtures using 5-20% of CBS in CB showed similar melting endotherm to CB, with comparable TAG composition and polymorphism (dominating β -crystal). Iso-solid phase diagrams of these mixtures exhibited a desirable monotectic effect at 15-25°C. Thus, 5-20% of CBS could be potentially mixed with CB for chocolate formulation.

Finally, the physical and sensory characteristics of dark chocolate made using the CBS were evaluated. Dark chocolates with CB (without CBS), 5% and 20% CBS were produced. The chocolates with 5% and 20% CBS showed melting profile similar to CB-chocolate. Significant ($P<0.05$) differences in PSD, flow behavior, hardness and sensory characteristics were observed for 20% CBS-chocolate whilst no significant difference ($P\geq 0.05$) was observed for 5% CBS-chocolate compared to CB-chocolate. Stereomicroscope images of all the chocolates did not show bloom at 24°C for up to 8 weeks. Conversely, at $29\pm 1^\circ\text{C}$, bloom formation was only observed for CB-chocolate and 5% CBS-chocolate after two weeks. Noticeable changes in X-ray diffraction peaks were observed for bloomed chocolate. Overall, 5% CBS-chocolate was similar to CB-chocolate in terms of physical and sensory properties while 20% CBS-chocolate exhibited significantly different sensory profiles particularly taste acceptance and hardness compared to CB-chocolate.

In summary, CBS with comparable melting profile and TAG composition to CB was developed in this study, which could be potentially used to partially replace CB in chocolate production and other confectioneries as a lower cost ingredient.

Declaration

I hereby declare that this thesis contains no material which has been accepted for the award of any other degree or diploma at any university or equivalent institution and that, to the best of my knowledge and belief, this thesis contains no material previously published or written by another person, except where due reference is made in the text of the thesis.

Student: Nirupam Biswas

Signature:



Date: 5/4/2017

Main Supervisor: Dr Lee Fong Siow

Signature:



Date: 4/4/2017

Publications during enrolment

International peer-reviewed journals

- i) **Biswas N.**, Cheow Y. L., Tan C. P. & Siow L. F. (2016) Blending of palm mid-fraction, refined bleached deodorized palm kernel oil or palm stearin for cocoa butter alternative. *Journal of American Oil Chemists' Society*, 93(10): 1415-1427.
- ii) **Biswas N.**, Cheow Y. L., Tan C. P., Kanagaratnam S. & Siow L. F. (2017) Cocoa butter substitute (CBS) produced from palm mid-fraction/palm kernel oil/palm stearin for confectionery fillings. *Journal of American Oil Chemists' Society*, 94(2): 235-245.
- iii) **Biswas N.**, Cheow Y. L., Tan C. P. & Siow L. F. (2017) Physical properties of enzymatically produced palm oils-based cocoa butter substitute (CBS) with cocoa butter mixture. Submitted to *European Journal of Lipid Science and Technology*. Under review
- iv) **Biswas N.**, Cheow Y. L., Tan C. P. & Siow L. F. (2017) Physical, rheological and sensorial properties, and bloom formation of dark chocolate made with cocoa butter substitute (CBS). *LWT-Food Science and Technology*, 82: 420-428.

Conference contributions

Oral

- i) **Biswas N.**, Cheow Y. L., Tan C. P. & Siow L. F. Enzymatically produced palm oils based cocoa butter substitute (CBS) in chocolate formulation, Monash Science Symposium, 21st – 23rd November 2016, Monash University Malaysia, Malaysia.

Poster

- i) **Biswas N.**, Cheow Y. L., Tan C. P. & Siow L. F. Phase behavior of ternary fat mixture for cocoa butter alternative formulation, 49th Annual AIFST (Australian Institute of Food Science and Technology) convention, 27th – 28th June 2016, Brisbane, Queensland, Australia.

ii) Biswas N., Cheow Y. L., Tan C. P. & Siow L. F. Cocoa butter substitute prepared from enzymatic interesterification of fractionated palm oils. 107th AOCS Annual Meeting & Expo, 1st-4th May 2016, Salt Lake Convention Centre, Salt Lake City, Utah, USA.

iii) Biswas N., Cheow Y. L., Tan C. P. & Siow L. F. Phase behaviour of binary fat mixtures for confectionery applications, 9th MIFT (Malaysian Institute of Food Technology) Food Science & Technology Seminar, 21st – 22nd March 2015, UCSI University, Kuala Lumpur, Malaysia.

iv) Biswas N., Cheow Y. L., Tan C. P. & Siow L. F. Melting and crystallization behaviour of palm mid fraction and refined bleached deodorized palm kernel oil mixture for confectionery applications, 21st MSMBB Annual Scientific Meeting, 1st - 3rd October 2014, Monash University Malaysia, Malaysia.

Thesis including published works General Declaration

I hereby declare that this thesis includes two original papers published in peer reviewed journals and two papers currently under reviewed for publication. The core theme of the thesis is “Development and characterization of cocoa butter alternatives from palm-based oils for chocolate application”. The ideas, development and writing up of all the papers in the thesis were the principal responsibility of myself, the candidate, working within the School of Science under the supervision of Dr Lee Fong Siow.

The inclusion of co-authors reflects the fact that the work came from active collaboration between researchers and acknowledgements input into team-based research.

In all the papers, my contribution to the work involved the following:

Paper	Publication Title	Publication Status	Nature and extent (%) of candidate's contribution
I	Blending of palm mid-fraction, refined bleached deodorized palm kernel oil or palm stearin for cocoa butter alternative	Published	100%. Experimental design, samples preparation, conduct, data collection, result interpretation, statistical analysis, manuscript preparation.
II	Cocoa butter substitute (CBS) produced from palm mid-fraction/palm kernel oil/palm stearin for confectionery fillings	Published	100%. Experimental design, samples preparation, conduct, data collection, result interpretation, statistical analysis, manuscript preparation.
III	Physical properties of enzymatically produced palm oils-based cocoa butter substitute (CBS) with cocoa butter mixture	Submitted	100%. Experimental design, samples preparation, conduct, data collection, result interpretation, statistical analysis, manuscript preparation.
IV	Physical, rheological and sensorial properties, and bloom formation of dark chocolate made with cocoa butter substitute (CBS)	Published	100%. Experimental design, samples preparation, conduct, data collection, result interpretation, statistical analysis, manuscript preparation.

I have not renumbered sections of submitted or published papers in order to generate a consistent presentation within the thesis.

Student Signature



Date: 5/4/2017

The undersigned hereby certify that the above declaration correctly reflects the nature and extent of the student and co-authors contributions to this work.

Main Supervisor Signature:



Date: 4/4/2017

Acknowledgements

First of all, I would like to express my deepest gratitude to God, the almighty, for his mercy extended to me to work and manage each and everything soundly for this research.

I feel immense pleasure to express my gratitude to my main PhD supervisor, Dr Lee Fong Siow, for her advice and guidance from the very early stage of this research, as well as sharing her extraordinary experiences in Food Science throughout my work. I am also grateful to her for giving me the opportunity to attend two international conferences; the AOCS, Utah in USA and AIFST, Brisbane in Australia. Above all, she provided me unflinching encouragement and support in various ways.

I wish to thank my co-supervisors, Dr Cheow Yuen Lin and Prof Chin Ping Tan (University Putra Malaysia), for their knowledge, experience and time. Prof Tan deserves special thanks for arranging the much needed help, for me to work in Malaysian Cocoa Board.

I am also thankful to the School of Science at Monash University Malaysia, Fundamental Research Grant Scheme (FRGS/1/2013/SG01/MUSM/03/2) and Monash University Higher Degree Research Scholarship for financial support of the current study. I am also grateful to the Monash University Postgraduate Research travel grant for funding my international conference travel.

I would like to thank my PhD review panel members, Prof Sadeq, Dr Pushpa and Dr Choo for their constructive remarks and suggestions during my PhD milestone review which gave me the right directions for my work.

I thank all lab staffs, particularly Ms Amirah and Mr Jegan for their technical assistance. Special thanks to Mr Nasrun at the School of Engineering for XRD technical assistance. Many thanks to Malaysian Cocoa Board for chocolate making facility and Malaysian Palm Oil Board (MPOB) for NMR experiments. A massive thank you to Dr Sivaruby, MPOB for her kind assistance of the NMR experiments. I also need to thank Dr Satoshi and Ms Rachel at the School of Medicine for their technical assistance on stereomicroscope experiment. Thanks to Mr Purush for his effort to correct my English. My sincere thanks to Mr Ragavan for proofreading the entire manuscript and for his helpful comments.

I am grateful to my lab mates and office mates for their cooperation and for maintaining a healthy working environment. A big thank you to Monash University Postgraduate Association (MUPA) for arranging nice tea-break, coffee talk session, Annual Dinner, Christmas event which gave me the opportunity to meet new friends. I would like to acknowledge my HDR colleagues in School of Science for their prompt help and participating in my sensory study. I have to thank all the academic and administrative staff members in the School of Science for being so cooperative and nice to me, making me feel very comfortable throughout my PhD journey.

Finally, I must thank my wife, Tama Sarkar. She is always there cheering me up and stands by my side through the good times and bad. I am also thankful to my family members for giving their greatest encouragement and most sincere support in whatever decision that I made.

To my parents, brother, sisters and brother-in-law

Table of contents

Abstract	ii
Publications during enrolment	v
Acknowledgements	ix
Table of contents	xii
List of figures	xvii
List of tables	xx
List of equations	xxii
List of abbreviations and acronyms	xxiii

Chapter 1

1 Literature review	1
1.1 Cocoa butter	1
1.1.1 Overview of world cocoa production	1
1.1.2 Chemical composition	2
1.1.3 Thermal characterization	4
1.1.3.1 Basic principles of DSC.....	4
1.1.3.2 Basic principles of <i>p</i> NMR.....	4
1.1.4 Polymorphism	6
1.2 Cocoa butter alternatives (CBAs)	10
1.2.1 Cocoa butter equivalents (CBEs).....	10
1.2.2 Cocoa butter replacers (CBRs)	10
1.2.3 Cocoa butter substitutes (CBSs)	11
1.3 Legislation	11
1.4 Sources for CBAs	11
1.4.1 Palm mid-fraction (PMF).....	12
1.4.2 Refined bleached deodorized palm kernel oil (RBDPKO).....	12
1.4.3 Refined bleached deodorized palm stearin (RBDPS).....	13
1.5 Production of CBAs	13
1.5.1 Blending.....	14
1.5.2 Interesterification	15
1.5.2.1 Chemical interesterification	15
1.5.2.2 Enzymatic interesterification	16
1.6 Production of chocolate	18
1.6.1 Mixing.....	18
1.6.2 Refining.....	18
1.6.3 Conching.....	20
1.6.4 Tempering.....	20

1.6.5	Moulding, cooling and de-moulding.....	21
1.7	Research gap and motivation.....	21
1.8	Research questions	22
1.9	Thesis objectives	23

Chapter 2

2	Characterization and physicochemical properties of binary mixtures of PMF, RBDPKO or RBDPS for CBSs formulation.....	25
2.1	Introduction	25
2.2	Materials and methods.....	26
2.2.1	Materials	26
2.2.2	Preparation of oil blends	26
2.2.3	Fatty acid analysis.....	27
2.2.4	Triacylglycerol (TAG) analysis	27
2.2.5	Solid fat content (SFC) analysis	27
2.2.6	Melting behavior.....	28
2.2.7	Crystal analysis	28
2.2.8	Statistical analysis.....	28
2.3	Results and discussion.....	29
2.3.1	Fatty acid composition.....	29
2.3.2	Triacylglycerol (TAG) composition	30
2.3.3	Solid fat content (SFC) and iso-solid diagrams of the blends	35
2.3.4	Melting behavior.....	37
2.3.5	Polymorphism	42
2.4	Conclusion.....	45

Chapter 3

3	Evaluation of physical and chemical properties of ternary mixtures of PMF/RBDPKO/RBDPS for CBS.....	48
3.1	Introduction	48
3.2	Materials and methods.....	49
3.2.1	Materials	49
3.2.2	Preparation of fat blend.....	49
3.2.3	Fatty acid analysis.....	50
3.2.4	Triacylglycerol (TAG) analysis	50
3.2.5	Solid fat content (SFC)	50
3.2.6	Melting behavior.....	51
3.2.7	Polymorphism.....	51
3.2.8	Crystal morphology	51
3.2.9	Statistical analysis.....	51
3.3	Results and discussion.....	52

3.3.1	Fatty acid composition	52
3.3.2	Triacylglycerol (TAG) composition	52
3.3.3	Melting behavior	53
3.3.4	Solid fat content (SFC)	56
3.3.5	Iso-solid diagrams of ternary blends	57
3.3.6	Polymorphism	58
3.3.7	Crystal morphology	60
3.4	Conclusion	62

Chapter 4

4	Investigation on the enzymatic interesterification of PMF/RBDPKO/RBDPS blend with commercial stearic/oleic fatty acids for CBS	67
4.1	Introduction	67
4.2	Materials and methods	68
4.2.1	Materials	68
4.2.2	Preparation of oil blends	69
4.2.3	Enzymatic interesterification	70
4.2.4	Blending of enzymatically produced CBS and CB	71
4.2.5	Fatty acid analysis	71
4.2.6	Melting behavior	71
4.2.7	Triacylglycerol analysis	71
4.2.8	Solid fat content (SFC)	71
4.2.9	Polymorphism	71
4.2.10	Crystal morphology	72
4.2.11	Statistical analysis	72
4.3	Results and discussion	72
4.3.1	CBS production and its characterization	72
4.3.1.1	<i>Fatty acid composition</i>	<i>72</i>
4.3.1.2	<i>DSC melting thermograms</i>	<i>75</i>
4.3.1.3	<i>Optimization of the reaction parameters</i>	<i>76</i>
4.3.1.4	<i>Triacylglycerol (TAG) composition</i>	<i>78</i>
4.3.1.5	<i>Free fatty acid (FFA) analysis</i>	<i>79</i>
4.3.2	Physical properties of enzymatically produced CBS (interesterified B2) and CB blends	81
4.3.2.1	<i>TAG composition of the CBS/CB blends</i>	<i>81</i>
4.3.2.2	<i>Thermal properties and iso-solid diagrams of the developed CBS/CB blends</i>	<i>81</i>
4.3.2.3	<i>Polymorphism</i>	<i>85</i>
4.3.2.4	<i>Crystal morphology</i>	<i>86</i>
4.4	Conclusion	89

Chapter 5

5 Physical properties of enzymatically produced CBS and CB mixture, and physical and sensory characteristics of dark chocolate made from the enzymatically produced

CBS	92
5.1 Introduction	92
5.2 Materials and methods	93
5.2.1 Materials	93
5.2.2 Chocolate production	94
5.2.3 Triacylglycerol (TAG) analysis	95
5.2.4 Melting profile	95
5.2.5 Polarised light microscopy (PLM).....	95
5.2.6 Particle size distribution (PSD).....	96
5.2.7 Flow behavior	96
5.2.8 Texture analysis	96
5.2.9 Bloom formation on chocolate surface	96
5.2.10 Polymorphism	97
5.2.11 Sensory evaluation	97
5.2.12 Statistical analysis	97
5.3 Results and discussion	98
5.3.1 TAG composition.....	98
5.3.2 Melting behavior.....	100
5.3.3 Particle size distribution (PSD) of the dark chocolates	101
5.3.4 Flow behavior	103
5.3.5 Textural behavior	104
5.3.6 Bloom formation and X-ray diffraction during storage.....	105
5.3.7 Sensory evaluation	109
5.4 Conclusion	110

Chapter 6

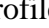
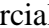
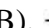




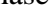
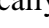






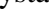

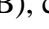
6 General conclusions and Future work	112
6.1 General conclusions	112
6.1.1 Overall conclusions.....	114
6.2 Suggestions for future work	116
References	117

Appendix A List of chemicals used in this study	127
Appendix B (Chapter 2) GC chromatogram	128
Appendix C (Chapter 2) HPLC chromatogram	129
Appendix D (Chapter 2) Statistical analysis using OriginPro software	130

Appendix E (Chapter 5) Statistical analysis using SPSS software	131
Appendix F (Chapter 5) Sensory questionnaire form	132
Appendix G (Chapter 5) Control chocolate and bloomed chocolate	133
Appendix H (Chapter 2) Publications during enrolment.....	134
Appendix I (Chapter 3) Publications during enrolment	147
Appendix J (Chapter 5) Publications during enrolment.....	158

List of figures

Figure 1.1	Magnetization decay of a fat used in the determination of the solid fat content by pNMR.....	6
Figure 1.2	Principle of XRD in fat samples.....	7
Figure 1.3	Three different polymorphic structures of a TAG. (a) Sub-cell structures and (b) chain length structures.....	8
Figure 1.4	Overview of polymorphism in cocoa butter with melting temperature.....	10
Figure 1.5	Blending process scheme for production of CBAs.....	15
Figure 1.6	Chemical and enzymatic interesterification mechanism of two TAGs (XXX, YYY) and TAG (XXX) with commercial stearic (St) fatty acid.....	17
Figure 1.7	Overview of chocolate manufacturing process.....	21
Figure 2.1	SFC versus temperature profiles for CB (—▲—), PMF (—●—), RBDPKO (—■—) and RBDPS (—×—).....	35
Figure 2.2	Binary iso-solid phase diagrams for mixtures of (a) PMF/RBDPKO, (b) RBDPS/RBDPKO, and (c) PMF/RBDPS.....	37
Figure 2.3	Differential scanning calorimetry melting curves of (a) PMF/RBDPKO mixtures, (b) RBDPS/RBDPKO mixtures, and (c) PMF/RBDPS mixtures.....	39
Figure 3.1	DSC melting curves for ternary mixtures (A-H) of PMF/RBDPKO/RBDPS.....	56
Figure 3.2	Solid fat content of ternary mixtures (A-H) of PMF/RBDPKO/RBDPS.....	57
Figure 3.3	Ternary iso-solid phase diagrams for PMF/RBDPKO/RBDPS mixtures at a 10°C, b 20°C, and c 25°C. The straight lines represent monotectic effect and curves represent eutectic effect.....	58
Figure 3.4	X-ray diffractograms of PMF, RBDPKO, RBDPS, their blends and commercial CB at 24°C.....	60
Figure 3.5	Polarised light microphotographs (40× lens) of (a) individual CB, (b) PMF, (c) RBDPKO, (d) RBDPS, and (e) ternary blend of PMF/RBDPKO/RBDPS (14.9/59.6/25.5, %w/w) obtained at 24°C.....	61
Figure 4.1	DSC melting thermograms of commercial stearic acid, commercial oleic acid, ternary-blend 1 (14.9% PMF/59.6% RBDPKO/25.5% RBDPS) or ternary-blend 2 (33.3% PMF/33.3% RBDPKO/33.3% RBDPS), their mixture (referring to A1 to D2 as per Table 4.1) and commercial CB.....	76

Figure 4.2	DSC melting thermograms of (A) 2% Enzyme, (B) 4% Enzyme and (C) 6% Enzyme concentrations for sample B2 (referring in Table 4.1).....	78
Figure 4.3	DSC melting thermograms of enzymatically produced CBS (interesterified B2) and commercial CB mixtures: a (5%CBS/95%CB), b (10%CBS/90%CB), c (20%CBS/80%CB), d (30%CBS/70%CB), e (40%CBS/60%CB) and f (50%CBS/50%CB).....	82
Figure 4.4	Solid fat content profiles of  enzymatically produced CBS (interesterified B2),  commercial CB, and their blends:  a (5%CBS/95%CB),  b (10%CBS/90%CB),  c (20%CBS/80%CB),  d (30%CBS/70%CB),  e (40%CBS/60%CB),  f (50%CBS/50%CB), and  non-interesterified B2. Data represent averages of three measurements with standard deviations lower than 1.5% in all cases.....	84
Figure 4.5	Binary iso-solid phase diagrams constructed with OriginPro 9.1 software for blends of enzymatically produced CBS and commercial CB. Numbers in curves represent the percentage of solids.....	85
Figure 4.6	X-ray diffractograms of  enzymatically produced CBS (interesterified B2),  commercial CB and their blends:  a (5%CBS/95%CB),  b (10%CBS/90%CB),  c (20%CBS/80%CB),  d (30%CBS/70%CB),  e (40%CBS/60%CB) and  f (50%CBS/50%CB), and  non-interesterified B2.....	87
Figure 4.7	Overview of crystal morphology for enzymatically produced CBS (interesterified B2), commercial CB and their blends: a (5%CBS/95%CB), b (10%CBS/90%CB), c (20%CBS/80%CB), d (30%CBS/70%CB), e (40%CBS/60%CB) and f (50%CBS/50%CB).....	88
Figure 5.1	DSC Melting thermograms of CB-chocolate, 5% CBS-chocolate and 20% CBS-chocolate. *Significantly different from CB-chocolate, $P < 0.05$. All measurements were performed in triplicate and the standard error for each sample was below 1.2%. Abbreviations: Onset temperature (T_{onset}), endset temperature (T_{end}), maximum peak temperature (T_{max}), melting enthalpy (ΔH_{melt}).....	101
Figure 5.2	PLM micrographs (20 \times lens) of A) CB-chocolate, B) 5% CBS-chocolate and C) 20% CBS-chocolate at 24 $^{\circ}$ C.....	102
Figure 5.3	Particle size distribution of CB-chocolate, 5% CBS-chocolate and 20% CBS-	

	chocolate at D_{90} (>90% finer).....	103
Figure 5.4	A) Casson yield stress (Pa) and B) Casson viscosity (Pa s) of CB-chocolate, 5% CBS-chocolate and 20% CBS-chocolate.....	104
Figure 5.5	Hardness of — CB-chocolate, 5% CBS-chocolate and — 20% CBS-chocolate at 24°C.....	105
Figure 5.6	Bloom formation of CB-chocolate, 5% CBS-chocolate and 20% CBS-chocolate stored at 24±1°C and 29±1°C.....	107
Figure 5.7	X-ray diffraction spectrum of A) — CB-chocolate and bloomed-chocolate, B) — 5% CBS-chocolate and bloomed-chocolate and C) — 20% CBS-chocolate and bloomed chocolate.....	108
Figure 5.8	Sensory evaluation of CB-chocolate, 5% CBS-chocolate and 20% CBS-chocolate.....	109
Figure 6.1	Schematic diagram of the production of produced CBS in chocolate application.....	115

List of tables

Table 1.1	Overview of fatty acids and TAGs composition (wt %) of CB from different geographical origins.....	3
Table 1.2	Tempering protocol of the fat samples described in the AOCS official method Cd 16b-93.....	6
Table 1.3	Short spacings characteristic of various crystal polymorphs of CB as determined by powder XRD wide angle reflections.....	9
Table 1.4	TAG composition of vegetable fats and oils for CBAs.....	12
Table 1.5	Literature enumeration of production of CB-like fats by blending.....	15
Table 1.6	Literature enumeration of production of CB-like fats by enzymatic interesterification.....	19
Table 2.1	Fatty acid composition (peak area %) for PMF/RBDPKO mixtures.....	31
Table 2.2	Fatty acid composition (peak area %) for RBDPS/RBDPKO mixtures.....	32
Table 2.3	Fatty acid composition (peak area %) for PMF/RBDPS mixtures.....	33
Table 2.4	Overview of TAGs (peak area %) in PMF/RBDPKO, RBDPS/RBDPKO and PMF/RBDPS mixtures.....	34
Table 2.5	Overview of T_{Onset} , T_{Endset} and melting enthalpy (ΔH) in PMF/RBDPKO, RBDPS/RBDPKO and PMF/RBDPS mixtures.....	43
Table 2.6	Overview of Polymorphic forms (%) in PMF/RBDPKO, RBDPS/RBDPKO and PMF/RBDPS mixtures.....	44
Table 3.1	Experimental design of PMF/RBDPKO/RBDPS mixtures.....	50
Table 3.2	Fatty acid composition (% peak area) of PMF/RBDPKO/RBDPS mixtures.....	54
Table 3.3	Overview of TAGs (peak area %) in PMF/RBDPKO/RBDPS mixtures.....	55
Table 4.1	Blending ratios (w/w) of ternary-blend (14.9% PMF/59.6% RBDPKO/25.5% RBDPS or 33.3% PMF/33.3% RBDPKO/33.3% RBDPS), commercial stearic (18:0) and oleic (18:1) fatty acids.....	70
Table 4.2	Fatty acid composition of commercial stearic acid, commercial oleic acid, ternary-blend 1 (14.9% PMF/59.6% RBDPKO/25.5% RBDPS) or ternary-blend 2 (33.3% PMF/33.3% RBDPKO/33.3% RBDPS), their mixture (blend component according to the blending ratios in Table 1) and commercial CB....	74

Table 4.3	Overview of TAGs composition of individual CB, enzymatically produced CBS (interesterified B2) and different blends (a-f) of enzymatically produced CBS/CB, and non-interesterified B2 (80% ternary blend/15% stearic/5% oleic).....	80
Table 5.1	Overview of TAGs composition of individual CB and enzymatically produced CBS.....	99
Table 6.1	Overall production cost of CBS.....	116

List of equations

Eq. 1.1	$\text{SFC} = \frac{(\text{E11}-\text{E70}) \times \text{F} \times 100}{\text{E70} + [(\text{E11}-\text{E70}) \times \text{F}] + \text{D}}$5
Eq. 1.2	$n\lambda = 2d \sin \theta$6
Eq. 2.1	$\% \beta'_1 = \frac{I \beta'_1 \times 100}{I \beta'_1 + I \beta'_2 + I \beta_2}; \% \beta'_2 = \frac{I \beta'_2 \times 100}{I \beta'_1 + I \beta'_2 + I \beta_2}; \% \beta_2 = \frac{I \beta_2 \times 100}{I \beta'_1 + I \beta'_2 + I \beta_2}$28

List of abbreviations and acronyms

α	Alfa
β	Beta
γ	Gamma
μl	Microliter
$^{\circ}\text{C}$	Degree Celsius
\AA	Angstrom
ΔH	Melting enthalpy
i.e.	That is
a.u.	Arbitrary units
e.g.	Example
$\text{C}_{8:0}$	Caprylic acid
$\text{C}_{10:0}$	Capric acid
$\text{C}_{12:0}$	Lauric acid
$\text{C}_{14:0}$	Myristic acid
$\text{C}_{16:0}$	Palmitic acid
$\text{C}_{18:0}$	Stearic acid
$\text{C}_{18:1}$	Oleic acid
$\text{C}_{18:2}$	Linoleic acid
$\text{C}_{20:0}$	Arachidic acid
CB	Cocoa butter
CBA	Cocoa butter alternative
CBE	Cocoa butter equivalent
CBS	Cocoa butter substitute
CBR	Cocoa butter replacer
DSC	Differential scanning calorimetry
EI	Enzymatic interesterification
FAME	Fatty acid methyl esters
FID	Flame ionisation detector
GC	Gas chromatography
HPLC	High performance liquid chromatography
mg	Milligram
min	Minute

ml	Milliliter
pNMR	Pulsed nuclear magnetic resonance
PMF	Palm mid-fraction
PLM	Polarised light microscopy
PSD	Particle size distribution
RBDPKO	Refined bleached deodorized palm kernel oil
RBDPS	Refined bleached deodorized palm stearin
SFC	Solid fat content
SFA	Saturated fatty acid
SD	Standard deviation
SSS	Total content of tri-saturated triacylglycerol
SUS	Total content of monounsaturated triacylglycerol
SUU	Total content of di-unsaturated triacylglycerol
TAG	Triacylglycerol
t_1	Transition temperature
T_m	Melting temperature
T_{onset}	Onset temperature
T_{endset}	Endset temperature
T_{peak}	Peak temperature
T_{max}	Maximum temperature
USFA	Unsaturated fatty acid
UUU	Total content of polyunsaturated triacylglycerol
v/v	Concentration expressed as volume by volume
w/w	Concentration expressed as weight by weight
w	Weight
XRD	X-ray diffraction

Chapter 1

1 Literature review

1.1 Cocoa butter

1.1.1 Overview of world cocoa production

Cocoa butter (CB) is derived from the seeds (beans) of cocoa tree (*Theobroma cacao*), which was introduced to Latin America (Mexico) over 500 years ago, thereafter to Europe and other parts of the world [66]. The major cocoa beans producing countries are Ghana, Ivory Coast, Malaysia, Cameroon, Indonesia, Nigeria, Ecuador, and Brazil, contributing approximately 90% of the total world cocoa production [47]. Approximately 68% of the total global cocoa was produced in Africa followed by Asia, Oceania and America in 2009/2010. The production of world cocoa beans was 3.7 million tons in 2007/2008, whilst it dropped to 3.6 million tons in 2009/2010 [69]. According to Malaysian Cocoa Board [98], production of cocoa beans was 15,654 tons in 2010 while it declined to 1,757 tons in 2016. Based on the report of International Cocoa Organization (2009/2010), the production of cocoa beans varies depending on the climate. A 2011 study by Magalhaes *et al.* [41] stated that almost three-fourths of the total world's cocoa consumption comes from Nigeria, Ghana and Ivory Coast. Since the last decade, the production of cocoa is decreasing day by day while its consumption has increased [2,73]. This high demand leads to the increasing market price of cocoa beans. According to ICCO, the price of cocoa beans has increased from US\$1549 per ton in 2005 to US\$2288 per ton in 2016 [67]. Therefore, due to this high market demand and limited production, the price of the main ingredient of chocolate, cocoa butter (CB), is also increasing.

Cocoa powder is extracted from the cocoa beans and also used in confectionery products such as chocolates. Cocoa bean is made up of approximately 85% cotyledon (nib) and 15% shell. The nibs have around 55% CB. The nibs are ground to make cocoa mass/liquor, which is directly used in chocolate [14,69].

Cocoa, usually used in chocolate, contains alkaloid such as theobromine, which is responsible for the stimulating effect of diuretic and cardiac muscle contraction [105]. Cocoa prevents cardiovascular disease and has other health benefits because cocoa beans and its products such as chocolate are rich sources of antioxidants and polyphenols [77,134]. Several researchers have identified (-)epicatechin, (+)catechin and procyanidins as major polyphenols and quercetin, isoquercitrin, apigenin, luteolin and naringenin as minor polyphenols present

in cocoa [10,17,58,101]. Due to its high content in polyphenols, cocoa and cocoa-derived products are highly consumed in many countries particularly Europe and United States [12,104].

CB is used not only in food but also in different pharmaceutical products such as medicinal suppositories due to its unique melting characteristics, highly solid at 25°C (room temperature) and melts at 37°C (body temperature). It is also used in personal skin care products such as soaps, cosmetics and lotion because of its pleasant fragrance, emollient properties and smooth texture [110].

1.1.2 Chemical composition

Chemical composition of fats/oils is responsible for its melting, solid fat content (SFC) and polymorphism [62,111]. The chemical composition describes the fatty acids and triacylglycerols (TAGs) of fats/oils. Table 1.1 illustrates the main fatty acids and TAGs composition of CB from different geographical origins.

Fatty acid is a key component of TAGs and its chemical structure is made up of a carbon chain of variable length (odd or even) with a carboxylic acid group attached at the end. Fatty acids can be classified into two major groups namely “saturated” (no double bond; palmitic acid) and “unsaturated” (one or more double bonds; oleic acid and arachidonic acid). The three major fatty acids in CB are 18.9-22.6% palmitic acid (16:0), 33.7-40.2% stearic acid (18:0) and 26.3-35.0% oleic acid (18:1), which account for approximately 98% of all the total fatty acids [13,53]. Other minor fatty acids of CB are linoleic (18:2), arachidic (20:0) and myristic (14:0) acids.

TAGs are made out of three fatty acids in a glycerol backbone. Molecules where the glycerol backbone contains less than three fatty acids are termed as partial glycerols namely monoacylglycerols (MAGs) and diacylglycerols (DAGs). TAG with palmitic, oleic and stearic acid in sn-1, 2, 3 positions of a glycerol backbone is represented as POST. The fatty acids in sn-1 and 3-positions are “equivalent” fatty acids, for example “POST” is the same as StOP.

Table 1.1. Overview of fatty acids and TAGs composition (wt %) of CB from different geographical origins [53].

Chemical Properties (%)	Country of origin					
	Ivory Coast	Nigeria	Indonesia	Brazil	Ecuador	Malaysia
Palmitic (P)	25.6	26.5	26.1	25.1	27.1	25.7
Stearic (St)	36.5	37.1	37.3	34.3	35.4	37.1
Oleic (O)	34.1	33.1	33.3	36.4	33.7	33.7
Linoleic (L)	2.8	2.3	2.4	3.4	2.6	2.4
Arachidic (A)	1.1	1.1	1.2	1.3	1.0	1.2
POP	18.3	18.3	17.5	17.0	18.9	17.8
POSt	41.7	43.0	41.8	38.7	41.0	40.7
StOSt	25.2	25.1	25.8	23.8	25.2	25.9
POO	2.4	1.8	2.4	5.0	2.4	2.4
StOO	2.9	2.1	2.8	6.0	2.9	2.8
PPP	0.3	0.5	0.3	0.2	0.3	0.2
MOP	0.2	0.2	0.2	0.2	0.3	0.2
PPSt	0.6	0.8	0.5	0.5	0.9	0.8
PLP	1.7	1.3	1.9	2.1	1.5	1.84
PStSt	0.3	0.4	0.2	0.3	0.6	1.0
PLO	0.3	0.3	0.4	0.3	0.3	0.4
StStSt	0.2	0.2	0.1	0.2	0.6	0.5
StOA	1.2	1.3	1.2	1.0	1.3	1.3

TAGs are divided into four groups according to their degree of saturation namely tri-saturated (SSS): tripalmitin (PPP); mono-unsaturated (SUS): POP, POSt, StOSt; di-unsaturated (SUU): POO; and poly-unsaturated (UUU): OOO. CB has mainly three symmetrical TAGs namely POSt, StOSt and POP, contributing about 92-96% of the total TAGs composition [52]. Due to this TAGs composition, CB melts quickly over a narrow temperature ranging between 30 and 35°C [127]. The StOSt is responsible for the high melting fraction, whereas the POP and POSt are responsible for the low melting fraction. In addition, CB contains other minor TAGs such as POO, StOO, PLP and StOA (Table 1.1).

CB has also other minor chemical components namely free fatty acids, monoacylglycerols and diacylglycerols. The composition of free fatty acids and DAGs of CB ranges between 1.2 and 2.8%, 0.6 and 2.2% respectively. These components are responsible for the crystallization process [32,52,97].

1.1.3 Thermal characterization

There are several techniques that are used to study the thermal characteristics of fats/oils. These techniques involve differential scanning calorimetry (DSC), thermal mechanical analysis (TMA), differential thermal analysis (DTA) and pulsed nuclear magnetic resonance (pNMR). The DSC and pNMR were used in this study. The principle of these techniques will be discussed in the following section.

1.1.3.1 Basic principles of DSC

DSC is typically used to measure the melting/crystallization profile and changes in enthalpy of fats/oils [11,31].

DSC involves the measurement of heat differences between a sample and a reference. The variation in the amount of energy (heat) needed to raise the melting temperature of a sample compared to an empty reference is monitored as a function of temperature [60]. It is sensitive to the changes associated with phase transitions such as melting/crystallization that the sample undergoes. Phase transitions in the fat crystals correspond to absorption or evolution of heat in the differential heat flow recorded as a peak. The area under the peak of a thermal event is proportional to the enthalpy change and the peak also shows either endothermic (energy flow to the sample) or exothermic (energy flow from the sample) [54,86].

Based on the mechanism of operation, there are two different types of DSC systems such as heat-flux DSC and power compensation DSC. In the current study, a heat flux DSC was performed to determine the melting behavior of the different fat samples. The heat-flux DSC heats the sample and reference sample using the same heating source and measures the heat flow rate or the difference in power. The temperature difference observed in a heat flux DSC is strictly proportional to the heat flow.

1.1.3.2 Basic principles of pNMR

Pulsed (low resolution) nuclear magnetic resonance (pNMR) is performed to determine the percentage of solid/crystalline fat present in fats/oils at a specific temperature. This method uses a short intense pulse of radio frequency energy in a magnetic field to capture the response of hydrogen nuclei (protons) in the sample. A magnetized signal is induced in a sample when a radio frequency pulse is applied. This initial signal is proportional to the

number of protons in the sample. When more than one protons containing solid and liquid fat is present in the sample, the signal decay for each component will be different. This difference in decay rate (at two different convenient time intervals: t_A and t_B as shown in Figure 1.1) is used to calculate the percentage of solid or liquid component [28,29,93,112].

The solid fat content (SFC) of the fat samples was measured using pNMR (Bruker Minispec PC 120, Karlsruhe, Germany). According to the American Oil Chemists' Society (AOCS), two methods are used to determine SFC of the fats: the direct method (AOCS official method Cd 16b-93) and the indirect method (AOCS official method Cd 16-81). In the current study, the direct method was used to determine the SFC of the different fat samples (this method is suitable for fats that have stable β -crystal form or high amounts of 2-oleo-disaturated triacylglycerols). The SFC is calculated using the formula [51] as shown in equation 1.1; where E11 and E70 represent the NMR signals measured at 11 μ s and 70 μ s after the pulse respectively, F represents an empirical correction factor (calibration standards) for the detector dead time and D is the digital offset factor (to correct for the detector offset during calibration).

$$\text{SFC} = \frac{(E11 - E70) \times F \times 100}{E70 + [(E11 - E70) \times F] + D} \dots\dots\dots (1.1)$$

The fat samples were melted at 100°C, then placed in NMR tubes and submitted to the tempering treatments as described in the AOCS official method Cd 16b-93 (Table 1.2). The SFC was measured at 5, 10, 15, 20, 25, 30, 35, 37, 40, 45 and 50°C following 60 min incubation at each temperature.

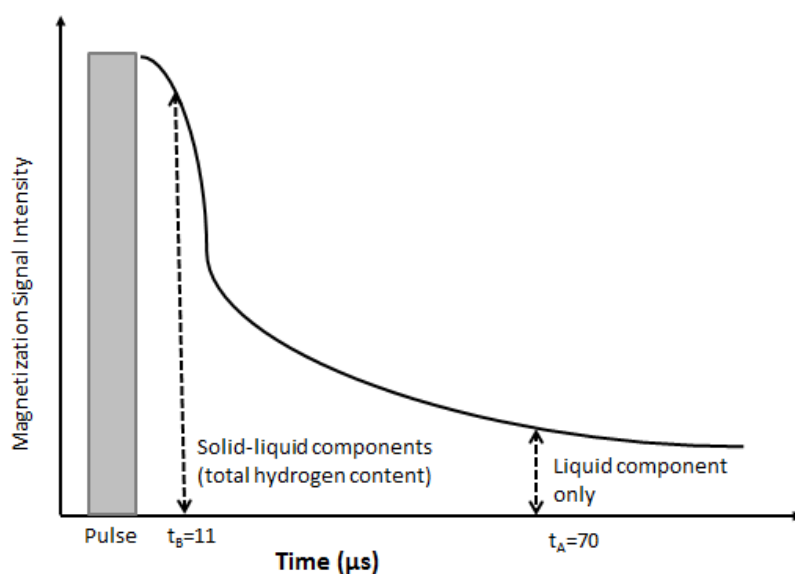


Figure 1.1. Magnetization decay of a fat used in the determination of the solid fat content by pNMR. Source: Ref [93]

Table 1.2. Tempering protocol of the fat samples described in the AOCS official method Cd 16b 93.

Tempering protocols for SFC measurement

- 1) Melt at 100°C
 - 2) Hold at 60°C for 15 min
 - 3) Cool to 0°C, hold for 90 min
 - 4) Heat to 26°C, hold for 40 h
 - 5) Cool to 0°C for 90 min
 - 6) Hold for 60 min at the desired measuring temperatures before SFC is determined
-

1.1.4 Polymorphism

Polymorphism of fats/oils is generally determined using X-ray diffraction (XRD). The crystallography is the relations of the incident rays with a crystal, produces a diffracted ray whenever conditions satisfy the Bragg's law as shown in equation 1.2, where n is an integer (the order of diffraction, usually $n = 1$), λ (Å) is the wavelength, d (Å) is the distance between the reflecting planes (methyl end groups of the TAGs) and θ (°) is the incident angle.

$$n\lambda = 2d \sin \theta \dots\dots\dots (1.2)$$

This is related to the wavelength (λ) of electromagnetic radiation to the diffraction angle (θ) and the lattice spacing (d) in a fat sample. A diffraction pattern is observed by determining the intensity of the scattered radiation as a function of the scattering angle θ (Figure 1.2). The strong intensities (Bragg peaks) are observed in the diffraction pattern where the scattering waves satisfy the Bragg's condition [23,148].

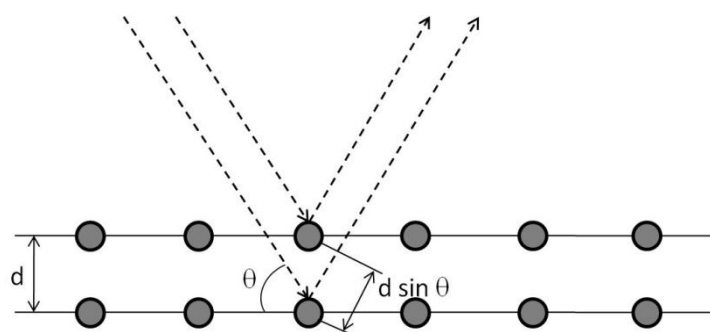


Figure 1.2. Principle of XRD in fat samples.

Polymorphism refers to the ability of a TAG molecule to crystallize in different crystal forms with different melting temperatures [121]. TAGs of a fat can crystallize into three main polymorphs: α (alpha), β' (beta-prime) and β (beta) in order of increasing stability ($\alpha \rightarrow \beta' \rightarrow \beta$) and melting temperature. The α form have a hexagonal sub-cell (H); β' forms have an orthorhombic-perpendicular sub-cell (O_{\perp}); and β forms have a triclinic-parallel sub-cell (T_{\parallel}) (Figure 1.3a) [111,124].

The chain-length structure of TAG illustrates a repetitive sequence of the hydrocarbon chain involved in a unit cell lamella along with the long-chain axis (Figure 1.3b). A double chain-length structure (DCL) is formed when the TAGs contain similar three fatty acid components. In contrast, a triple chain-length structure (TCL) is formed when the TAGs contain largely different one/two of the fatty acid components. When the DCL fats are mixed with the TCL fats, polymorphism of the fats mixture occurs readily.

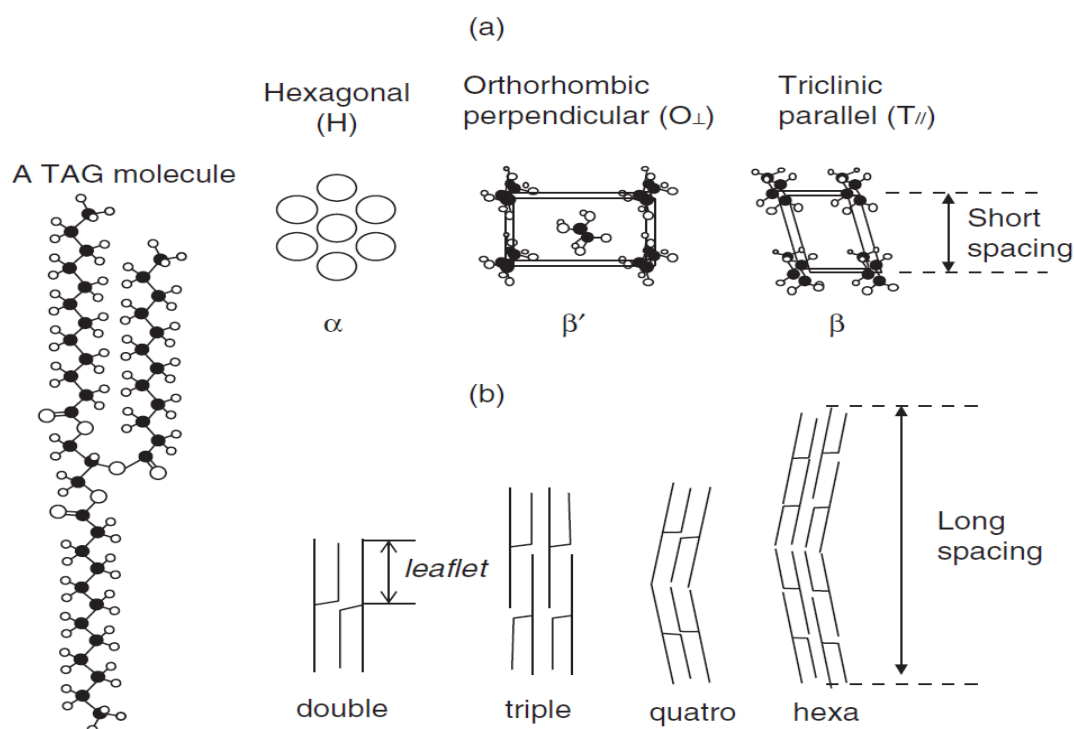


Figure 1.3. Three different polymorphic structures of a TAG. (a) Sub-cell structures and (b) chain length structures. Source: Ref [124]

Polymorphism (crystal forms) of a fat is characterized by determining the long-spacing and short-spacing (d -spacing). The crystal forms are identified through interpretation of the X-ray diffraction pattern [29,43,94,96,112]. Long-spacing (small angles) corresponds to the distance between methyl end-groups of TAGs and is generally comprised of two [72], three [57], or four [123] chain-lengths of the fatty acid components of the TAG (Figure 1.3). Long spacing for TAGs increases with increasing fatty acyl chain-length and decreases with increasing the angle of tilt. Polymorphs α and β' (I-IV) have a DCL structure displaying long-spacings from 22.1 to 55.1°C, while polymorphs β (V-VI) have a TCL structure showing long-spacings between 63.0 and 66.0 Å [33,149]. Short-spacing (wide angles), in contrast, denotes to the cross sectional packing of the acyl chains, and is independent of the chain length [43]. Short spacing is usually used for characterizing the different crystalline polymorphs, which differ in their chain length packing sub-cell. The β crystal has a triclinic sub-cell with a d -spacing at 4.5/4.6 Å, while the β' crystal has an orthorhombic sub-cell structure with multiple d -spacings between 3.8 and 4.3 Å. The α crystal has a hexagonal sub-cell with a d -spacing at 4.15 Å [124]. Table 1.3 illustrates the short spacings characteristic of various crystal polymorphs of CB as determined using XRD with wide angle reflections.

Table 1.3. Short spacings characteristic of various crystal polymorphs of CB as determined by powder XRD wide angle reflections [85,99].

Polymorphic form	Short (<i>d</i>) spacing (Å)
I or γ (sub- α)	3.87(m), 4.17(s)
II or α	4.20(vs)
III or β'_2	3.87(vw), 4.20(vs)
IV or β'_1	3.75(m), 3.88(w), 4.13(s), 4.32(s)
V or β_2	3.65(s), 3.73(s), 3.87(w), 3.98(s), 4.22(w), 4.58(vs), 5.13(w), 5.38(m)
VI or β_1	3.67(s), 3.87(m), 4.01(w), 4.21(vw), 4.53(vs), 5.09(vw), 5.37(m)

Relative peak intensity noted as very weak (vw), weak (w), medium (m), strong (s) or very strong (vs).

Polymorphism of fats/oils is much complicated, particularly those with a relative homogenous TAG composition. Figure 1.4 shows an overview of polymorphism in CB with corresponding melting temperatures. CB exhibits six polymorphic forms namely I (sub- α or γ), II (α), III (β'_2), IV (β'_1), V (β_2) and VI (β_1) in ascending stability and melting temperature [37,149]. Polymorph I (sub- α or γ) is the most unstable form with melting temperature of 16-18°C. Polymorph II (α) is found to have melting temperature of 19-24°C and can crystallize directly from polymorph I during storage. Polymorph III (β'_2) can form by transformation of polymorph II (α) with melting temperature of 24-26°C. Polymorph IV (β'_1) can be crystallized from the unstable polymorph III (β'_2). It has a melting temperature of 26-30°C. Polymorph V (β_2) is a more stable form with melting temperature of 30-34°C, which can be obtained directly from the IV (β'_1) and/or III (β'_2) polymorphs. Finally, the most stable polymorph VI (β_2) with melting temperature of 34-36°C can be obtained from the V (β_2) polymorph during storage [16].

Polymorphic transitions of CB take place through either a solid-state transition or by melt-mediation. Generally, the stable V(β_2)-crystal is preferred in chocolate as it has a desirable melting temperature and sensorial characteristic [118,136]. On the other hand, metastable β' -crystals are desirable for confectionery fillings and compound chocolates because it melts at low temperature with fine crystal structures [136,145].

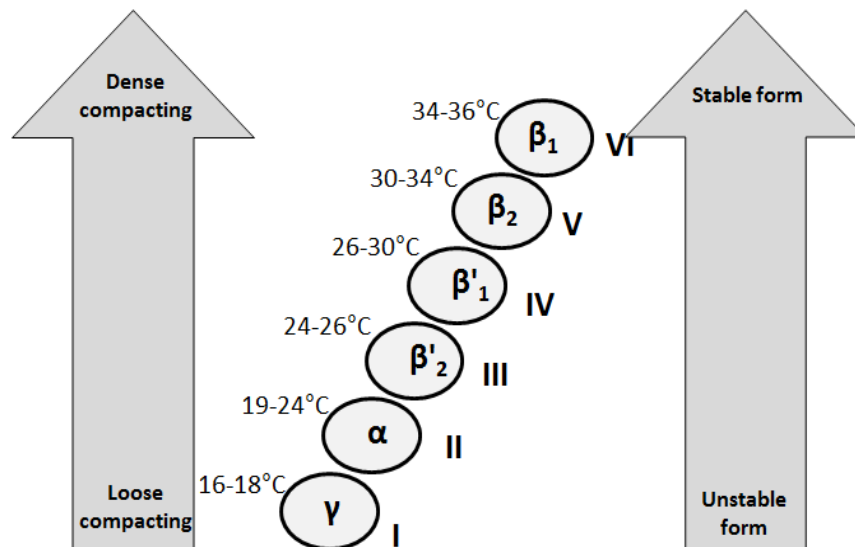


Figure 1.4. Overview of polymorphism in cocoa butter with melting temperature. Source: Ref [16]

1.2 Cocoa butter alternatives (CBAs)

CBAs are derived from vegetable fats and oils, used in replacement of CB. CBAs can be divided into three groups according to their functionality and similarity to CB: i) cocoa butter equivalents (CBEs), ii) cocoa butter replacers (CBRs), and iii) cocoa butter substitutes (CBSs).

1.2.1 Cocoa butter equivalents (CBEs)

CBEs are combinations of polymorphic non-lauric fats such as sal, mango seed, shea, palm oil, kokum and illipe. CBEs provide similar fatty acid/TAG composition, melting/crystallization properties and polymorphism to those of CB [26]. Ideally, CBEs can be added in any amount with commercial CB without presenting any eutectic behavior (indicating fats mixtures are not compatible) [44]. CBEs can be obtained by blending POP rich fat and POST/StOSt rich fats [22].

1.2.2 Cocoa butter replacers (CBRs)

CBRs are non-polymorphic and non-lauric fat (12:0) based on hydrogenated oils such as hydrogenated mango kernel. CBRs can be partially compatible with commercial CB due to the presence of β' polymorphs [53].

1.2.3 Cocoa butter substitutes (CBSs)

CBSs are lauric-based fats (12:0) such as palm kernel oil (PKO) and coconut oil. CBSs show similar melting/crystallization properties to that of CB, with different fatty acid and TAG composition [27,109,135]. CBSs can only be mixed in small quantities with commercial CB as they are usually not compatible [27]. Generally, production of the fat is obtained by blending low melting rich fats (such as PMF) and high melting rich fats (such as palm stearin).

1.3 Legislation

According to DIRECTIVE 2000/36/EC and Malaysian Food Regulation 1985, the maximum amount of CBAs can be used in chocolate, is limited to 5% only [45,114]. The non-European Union countries have their own regulations. For example, the United States does not allow the use of CBAs in chocolates, but permits its use as coatings on chocolate products. Generally, most countries allow higher levels of CBAs in chocolate, but this is labelled as “compound chocolate” [14,39,75,141].

1.4 Sources for CBAs

In 2000 an amendment on the EU DIRECTIVE 2000/36/EC stated that only the six vegetable fats/oils are permitted to be used as CBAs. These oils are shea (*Burtyrospermum parkii*), illipe (*Shorea spp.*), sal (*Shorea robusta*), palm oil (*Elaeis guineensis*, *Elaeis olifera*), mango kernel oil (*Mangifera indica*) and kokum gurgi (*Garcinia indica*). These oils are the rich sources of SUS TAGs: POP, POST and StOSt, have a large difference in the SUS TAGs composition as shown in Table 1.4. Among all the six fats/oils, illipe fat has comparable POST to CB whereas the other five fats have different TAGs composition. However, illipe is rarely used due to its availability and quality. None of the six vegetable fats/oils shows POP:POST:StOSt ratio that is similar to that of CB. Therefore, blending of the components is needed to produce a suitable CBA.

Table 1.4. TAG composition of vegetable fats and oils for CBAs [53,137].

TAGs	CB	Palm fraction	Shea fraction	Illipe fat	Sal fraction	Kokum fat	Mango kernel fraction
POP	16	66	1	7	Trace	Trace	1
POSt	37	12	7	34	10	6	16
StOSt	26	3	74	45	60	72	59
Total	79	81	82	86	70	78	76

Oil palm is the major export commodities in Malaysia, which is one of the largest contributors to its overall economy. Palm oil is extracted from the mesocarp layer of the palm fruits (*Elaeis guineensis*) and palm kernel oil is derived from the kernel of the same fruits. The oils are further fractionated and refined. Palm kernel has approximately 45-50% oil. Although palm oil and palm kernel oil are extracted from same palm fruits, they have different chemical and physical properties [69]. Apart from different palm oil fractions, palm mid-fraction, refined bleached deodorized palm kernel oil or palm stearin used in this study will be discussed in the following section.

1.4.1 Palm mid-fraction (PMF)

PMF is a fraction of palm oil that shows melting temperatures between 9.8 and 32.8°C [21]. PMF contains 51.8% of POP among three main TAGs, which leads to a steep SFC versus temperature curve. Almost all CBAs contain some proportion of PMF that contributes most of the POP to the blend. PMF tends to crystallize in the β' form and is therefore an attractive option for producing confectionery fillings and fat spreads [131].

1.4.2 Refined bleached deodorized palm kernel oil (RBDPKO)

RBDPKO refers to extract palm kernel oil that has been refined, bleached and deodorized. It is a semi-solid fat at room temperature, with a melting temperature of approximately 26-28°C. The oil has a high percentage of short-chain fatty acids such as lauric (12:0, 47.7%) and myristic acids (14:0, 22.6%) [150,152]. Although this oil contains high levels of undesirable short-chain fatty acids, it is broadly used as a suitable raw material for the production of confectioneries [130]. In this application, RBDPKO shows melting characteristic and crystallization behavior similar to CB, but chemical composition of these

two fats differ considerably. In CB, the composition of long-chain fatty acids such as palmitic (16:0, 24.4%), stearic (18:0, 33.6%), and oleic acids (18:1, 37.0%) are high, whereas short-chain fatty acids such as lauric acid and myristic acid compositions are in very low amounts [21]. In RBDPKO, the composition of short-chain fatty acids is high, whereas the composition of long-chain fatty acids is relatively low compared to that of CB. Hence, the high short-chain fatty acid content and low long-chain fatty acids (palmitic/oleic) content of RBDPKO makes it unsuitable as a direct use as CBS. Blending RBDPKO with palmitic and oleic acids rich fats such as PMF and/or palm stearin, however, could decrease the short-chain fatty acid composition whilst increasing the long-chain fatty acid composition [152]. This process may produce high-quality CBSs with a fatty acid composition more similar to that of CB.

1.4.3 Refined bleached deodorized palm stearin (RBDPS)

RBDPS is obtained from palm stearin by separating olein which has been refined, bleached and deodorized. The physical behavior of RBDPS differs from other palm oil products because it is a solid fat with high melting temperature (44-56°C). This needs to be mixed with lower melting temperature oils such as PMF and RBDPKO to yield a melting profile similar to that of CB. In addition, this oil contains low amount of linoleic acid (18:2), making it less prone to oxidation [46,130]. The applications of RBDPS have been well reviewed, and the stearin has also been reported to be a suitable coating material [78,91].

1.5 Production of CBAs

Many researches have been performed for the production of CBAs from different vegetable fats/oils. Due to the economic advantages, the vegetable fats/oils have been used to replace CB in chocolate and other confectionery applications. Different methods such as blending, supercritical carbon-dioxide (SC-CO₂), fractionation, hydrogenation, chemical interesterification and enzymatic interesterification are used to obtain CBAs with fatty acid/TAG composition, melting profile and other physical characteristics similar to that of CB. Among the methods, blending is a simple modification method which leads to a change in physical properties such as melting profile but it does not change the TAG molecule. The fatty acids in the TAG still remain the same in their original positions after blending two or more fats/oils. Interesterification process changes both physical and chemical properties of a fat/oil or blend. Interesterified fats/oils have a different TAG profile than the blend, and

interesterification rearranges fatty acids in the glycerol backbone to modify the physicochemical properties of a fat/oil or blend such as TAGs and melting profile. In the current study, blending and enzymatic interesterification were used to produce CBAs. These will be discussed in the following section.

1.5.1 Blending

Blending is a physical technique to produce CBAs using different vegetable fats/oils. Two or three fats are mixed together to resemble their fatty acid/TAG composition and melting temperature as per CB (Figure 1.5). For example, palm oil mid-fraction has a melting endotherm of 10-30°C while mango seed almond fat shows a high melting endotherm of 35-37°C. Blending of these components produced CBEs with similar melting/crystallization, fatty acid and TAG composition to CB [76].

A group of researchers has produced CB-like fat by blending different vegetable fats and oils (Table 1.5). CBRs were prepared by blending mango seed fat and palm stearin [70]; mango seed fat and PMF [68]; and PKO and palm oil [152]. Whereas CBEs were produced from blending mango kernel fat and PMF [131]; and high oleic-high stearin sunflower hard stearin and PMF [21]. In another study, Wang *et al.* [145] prepared CBSs by blending hydrogenated PKO and palm kernel stearin.

In these works, the melting profile, SFC as a function of temperature and fatty acid/TAG composition were analysed that were comparable to CB. However, the crystal polymorphism was not investigated in these studies. Crystal polymorphism is responsible for the textural and sensory characteristics of chocolates. Moreover, mango seed fat and mango kernel fat are unavailable in the market. Hence, production of CBAs specifically CBSs by blending followed by interesterification of PMF, RBDPKO and RBDPS remains an unexplored area of research.

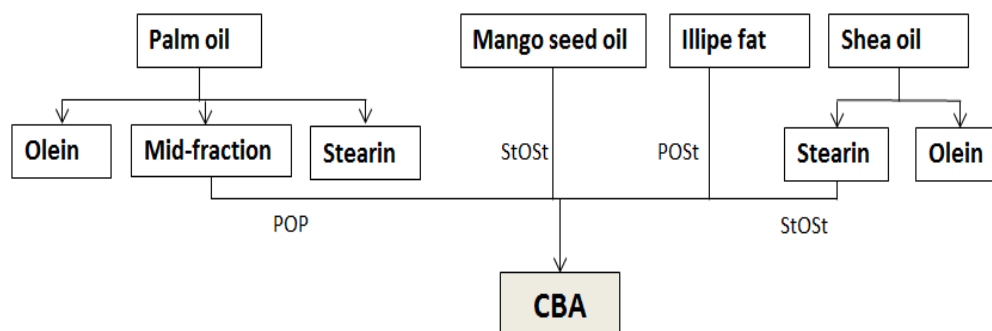


Figure 1.5. Blending process scheme for production of CBAs. Source: Ref [137]

1.5.2 Interesterification

Interesterification, an acyl rearrangement reaction is used to modify TAG and melting profile of fats/oils (Table 1.6). Interesterification rearranges the fatty acids within and between TAGs (Figure 1.6). There are two ways to carry out interesterification: chemical and enzymatic.

Table 1.5. Literature enumeration of production of CB-like fats by blending.

Blending	CB-like characteristic	Reference
Palm stearin/mango seed fat	Melting, crystallization, crystal morphology with major three TAGs	[70]
Mango seed fat/PMF	Melting, crystallization, crystal morphology with major three TAGs	[68]
Mango kernel fat/PMF	Melting, polymorphism with major three TAGs	[131]
High oleic-high stearin sunflower hard stearin/PMF	Melting, compatibility with major three TAGs	[21]
Hydrogenated PKO and palm kernel stearin	Melting and crystallization	[145]
PKO/palm oil	Slip melting, SFC, saponification/iodine value	[152]

1.5.2.1 Chemical interesterification

In chemical interesterification, fatty acids are randomly distributed over the glycerol backbone of a fat (Figure 1.6). Chemical interesterification employs a metal catalyst (sodium methoxide) which randomly distributes fatty acids among all possible TAG positions while enzymatic interesterification involves the application of lipase enzyme which can be random

or regio-specific (1, 3-specific or 2-specific) [95]. In confectionery products, this process is usually not applicable because of deficiency in positional specificity [151]. Hence, enzymatic interesterification offers a great potential for the production of a specialty fat with developed physicochemical characteristics.

1.5.2.2 Enzymatic interesterification

Enzymatic interesterification is performed to exchange the fatty acids attached to the glycerol backbone of a fat. Usually, lipases *sn* 1,3-positions are used to modify TAG composition that produce CB-like fats, which are preferred in confectionery products [80]. The important sources of lipase enzymes are *Mucor miehei*, *Rhizopus arrhizus*, *Thermomyces lanuginose*, *Porcine pancreas* and *Rhizomucor miehei*.

Enzymatic interesterification is a fat modification technology to improve physicochemical characteristics of fats/oils for confectionery and other applications [79,116]. The interesterification reactions of oils permit the production of new fats without any trans-fatty acid residues [100,154]. The advantages of this process are: low investment cost, simple, no undesirable trans-fatty acids production and no undesirable solvents/chemicals. In the current study, enzymatic interesterification was performed.

Production of CBAs from different vegetable fats/oils is one of the most promising applications of the enzymatic interesterification process. This is because of the structural composition of CB where the major TAGs namely POP, POST and StOSt contain only oleic fatty acid (O) in the *sn*-2 position of the glycerol backbone. Various vegetable fats/oils have been investigated and used to produce special fats resembling the TAG composition and other physical properties to CB. Table 1.6 summarizes the literature of different fats and oils modified by enzymatic interesterification for the production of CBAs over the last decades.

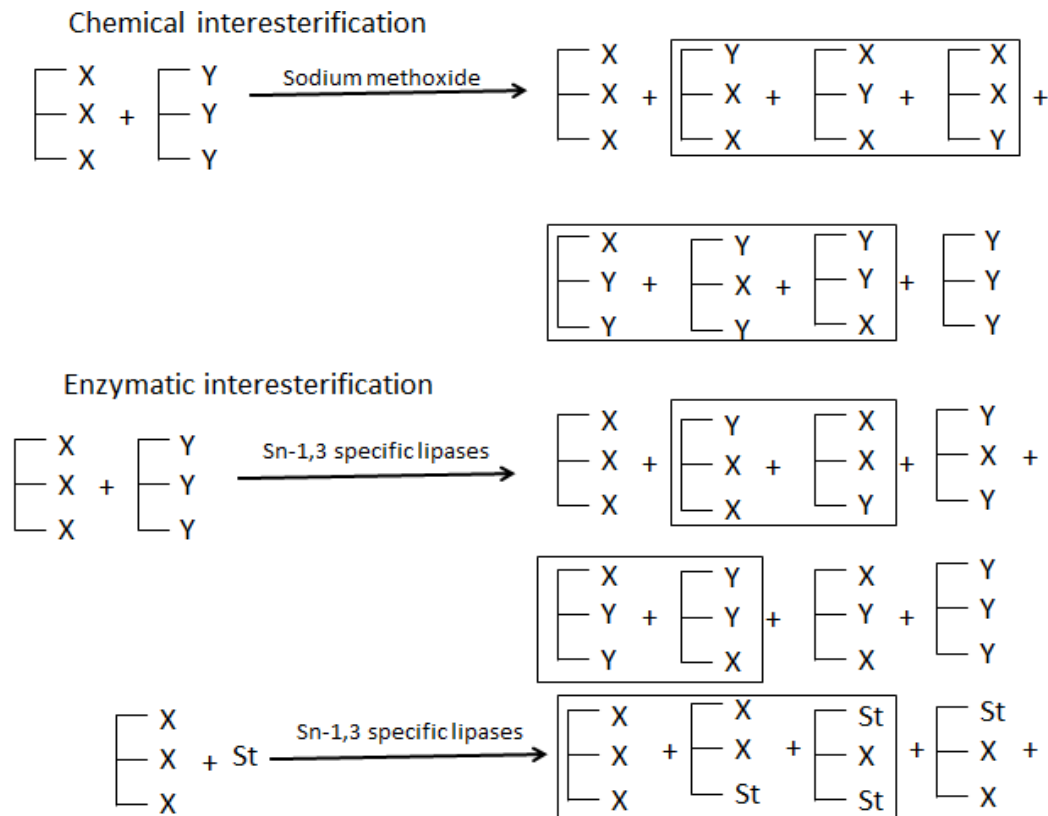


Figure 1.6. Chemical and enzymatic interesterification mechanism of two TAGs (XXX, YYY) and TAG (XXX) with commercial stearic (St) fatty acid.
Source: Ref [151]

In a recent study, Mohamed [102] produced CBEs from olive oil and stearic fatty acid mixture through enzymatic interesterification using 10% *Mucor miehei* enzyme at 24 h reaction time with *n*-hexane system. Kadivar *et al.* [75] used solvent free fractionation to produce CBEs through enzymatic interesterification of high-oleic sunflower oil with 10% *Rhizomucor miehei* enzyme at 6 h reaction time. Many other researchers have also prepared CBEs through enzymatic modification of PMF and palmitic-stearic fatty acid [103]; high-oleic sunflower oil and stearic-palmitic acid [113]; tea seed oil with fatty acid methyl esters [147]; and palm oil with hydrogenated soybean oil [1]. In another study, Zarrianghalami *et al.* [153] prepared CBRs from hydrogenated and solid fraction of tea seed oil through enzymatic interesterification using acetone solvent system at 4 h reaction time.

In most of the researches, the effect of several parameters such as enzyme-substrate ratio, initial ratio of commercial fatty acids, incubation time/temperature and solvents were studied. The TAGs produced from these works exhibited similar melting thermograms to CB.

Although the potential to achieve a composition virtually similar to CB through enzymatic interesterification is high, no work has been reported using PMF, RBDPS and RBDPKO mixtures to produce CBS with TAGs composition, melting profile, SFC and polymorphism that resemble CB.

1.6 Production of chocolate

Chocolate is made up of sugar, cocoa powder/cocoa liquor, CB, soy lecithin and/or milk powder [6,49]. There are mainly three varieties of chocolate: dark chocolate, milk chocolate and white chocolate. Dark chocolate is composed of sugar, CB, cocoa powder/cocoa liquor, while milk chocolate contains additional milk fat in the mixture. White chocolate, however, contains milk fat but does not include cocoa powder/cocoa liquor [45]. To produce chocolate, the following stages are involved: mixing, refining, conching and tempering [14]. Figure 1.7 displays the flow diagram of the main steps of the chocolate manufacturing process.

1.6.1 Mixing

In the first step, the basic ingredients of dark chocolate (sugar, cocoa powder and CB) are mixed together. A thermostat controlled mixer is generally used to ensure the mixture with a plastic consistency and rough texture. Approximately 2-10 min of mixing is necessary in large-scale manufacturing [6].

1.6.2 Refining

The mixture is then refined using a vertical three roll refiners. The chocolate paste is fed through the gap between the first two rollers and a knife blade fitted with the third roller is used to collect the chocolate flakes. This stage is used to reduce the particle size to smaller than 35 μ m in diameter, which is the optimum size of particles required in chocolate production [8]. Small crystals provide smooth mouth-feel and cool sensation during chocolate consumption, whereas large crystals provide a sandy or waxy mouth-feel [39,42].

Table 1.6. Literature enumeration of production of CB-like fats by enzymatic interesterification.

Parameter	Lipase	Substrate	CB-like characteristic	Reference
Solvent: hexane Enzyme concentration: 10% Tm: 60°C T: 24 h	Lipozyme (<i>Mucor miehei</i>)	Olive oil/palmitic-stearic acid	38.5% POST, 27.2% POP and 15.4% StOSt	[102]
Solvent free Enzyme concentration: 10% Tm: 65°C T: 6 h	Lipozyme (<i>Rhizomucor miehei</i>)	High-oleic sunflower oil	59.1% StOSt	[75]
Solvent: hexane Enzyme concentration: 10% Tm: 60°C T: 24 h	Lipozyme (<i>Mucor miehei</i>)	Palm mid-fraction/palmitic-steric acid	40.1% POST, 30.7% POP, 14.5% StOSt, 9.0% POO and 5.7% StOO	[103]
Solvent free Enzyme concentration: 2% Tm: 70°C T: 5 h	Lipozyme (<i>Rhizopus oryzae</i>)	High-oleic sunflower oil/stearic-palmitic acid	CB-like containing StOSt	[113]
Solvent free Enzym concentration: 10% Tm: 60°C T: 8 h	Lipozyme (<i>Thermomyces lanuginose</i>)	Hydrogenated tea seed oil/solid fraction of tea seed oil	17.4% POST, 10.7% POP and 11.1% StOSt	[153]
Solvent free Enzyme concentration: 10.4% Tm: 35°C T: 60 h	<i>Porcine pancreas</i>	Tea seed oil/fatty acid methyl esters	35.3% POST, 32.4% POP, and 29.2% StOSt	[147]
Solvent: acetone Enzyme concentration: 10% Tm: 70°C T: 4 h	Lipozyme (<i>Rhizomucor miehei</i>)	Palm oil/hydrogenated soybean oil	39% POST, 23% StOSt and 11.0% POP	[1]

1.6.3 Conching

After the refining, conching is performed to achieve the desirable texture, viscosity and sensory characteristics of the chocolate product. Viscosity refers to the energy needed to maintain the flow of a fluid. High viscous chocolates are not desirable due to sticky mouth-feel [39]. Proper hardness (textural behavior) of the chocolate provides pleasant mouth-feel sensation and good snap. Conching is usually achieved by mixing chocolate at approximately 45°C for 6 h [16]. During this phase, the mixture turns into a paste as the viscosity is reduced. In the last stage of the conching, the residual ingredient (soy lecithin as emulsifier) is added to obtain the desired flow characteristics.

1.6.4 Tempering

The next most important step is tempering, which is a time-temperature process to ensure the formation of chocolate in the right crystal form (β). The tempering process involves reducing the temperature of the chocolate to induce crystallization (27°C) of both stable and unstable crystals. This is then followed by melting the unstable crystals by increasing the temperature to 30-32°C, which leaves behind only the stable crystals [4].

The stable β -crystal form is desired in chocolates as it melts at 32-34°C. It also provides the desired good snap, glossy appearance, sensory mouth-feel and resistance to fat bloom [16,97,136]. Poorly crystallized chocolate causes the formation of fat bloom (sticky greyish-white surface) upon storage as the crystal form β'_{IV} rapidly transforms into polymorph β_V . Bloom formation may also arise due to slight (i.e., $\pm 2-3^\circ\text{C}$) or larger temperature variations which causes the melting and re-crystallization of TAG in CB, where the liquid fat from the chocolate matrix migrates through pores and microfractures to the surface forming bloom [42,118,129]. Un-tempered chocolate is usually soft due to the presence of unstable crystals and does not lend itself to effective de-moulding [6].

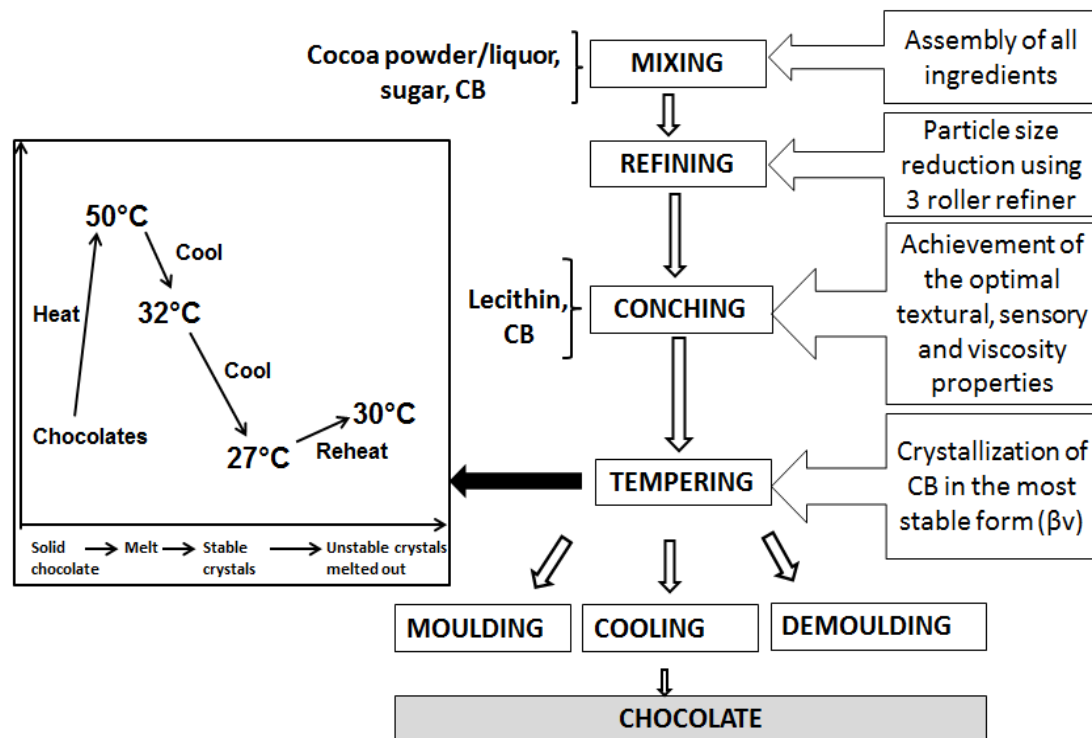


Figure 1.7. Overview of chocolate manufacturing process. Source: Ref [4,55]

1.6.5 Moulding, cooling and de-moulding

Finally, the chocolate is moulded and chilled at approximately 15°C for 60 min to solidify the chocolate [40]. Prior to packaging, the chocolate bars are de-moulded.

1.7 Research gap and motivation

CB is largely used as a raw material in chocolates and confectioneries due to its unique melting properties. However, its high price and limited production warrants researchers to produce alternatives to CB with similar melting and other physical properties. One of the alternative fats is known as CBS. Generally, CBS is derived from lauric based fats such as palm kernel oil using hydrogenation. This process is concerned on human health due to the presence of trans-fatty acids (undesirable saturation level) that may increase the risk of coronary heart disease. Alternatively, blending or enzymatic interesterification is a simple, easy and cost-effective process by which special fats like CBS can be produced by rearranging the structure of readily available vegetable fats/oils. The existing literature review on the production of CB-like fats through blending and enzymatic interesterification is summarized in Tables 1.5 and 1.6, and described in this chapter.

The development of CBSs by blending and enzymatic interesterification of palm mid-fraction, refined bleached deodorized palm kernel oil and palm stearin has not been done. Hence in order to overcome the research gaps, this study was carried out to investigate the development of CBS by blending and enzymatic interesterification of palm mid-fraction, refined bleached deodorized palm kernel oil and palm stearin. Melting, compatibility, polymorphism, fatty acids and triacylglycerols of CBS/CB mixture were determined for chocolate formulation. This study provides fundamental knowledge on the phase behavior and physicochemical characteristics of fats mixture for chocolate application.

1.8 Research questions

The specific research questions that the thesis has investigated were:

1. Are the binary mixtures of PMF/RBDPKO, PMF/RBDPS and RBDPS/RBDPKO compatible? If so, at what composition? What is the phase behavior of PMF, RBDPKO and RBDPS as binary mixture?
2. Is the ternary mixture of PMF/RBDPKO/RBDPS compatible? If so, at what composition? What is the phase behavior of PMF/RBDPKO/RBDPS mixture? Which composition will mimic cocoa butter in terms of fatty acid and triacylglycerol constituents, solid fat content, melting and polymorphism?
3. What is the effect of enzymatic interesterification of ternary mixture of PMF/RBDPKO/RBDPS using commercial stearic and oleic acids on triacylglycerol composition and melting profile for CBS development?
4. Is the enzymatically produced CBS compatible with commercial CB? If so, at what composition? What are the physical properties of enzymatically produced CBS and CB mixture for chocolate formulation?
5. What are the physical, rheological and sensorial properties, and bloom formation of dark chocolate made with enzymatically produced CBS?

1.9 Thesis objectives

The specific objectives of this study were:

1. To evaluate the physicochemical properties of binary mixtures of PMF, RBDPKO or RBDPS for CBSs formulation.
2. To examine the physical and chemical properties of ternary mixtures of PMF/RBDPKO/RBDPS for CBSs development.
3. To investigate the enzymatic interesterification of PMF/RBDPKO/RBDPS mixture with commercial stearic/oleic fatty acids for CBS development.
4. To examine the physical properties of enzymatically produced CBS and CB mixtures for chocolate formulation, and
5. To investigate the physical and sensory characteristics of dark chocolates made with enzymatically produced CBS.

Chapter 2

Work that is presented in this chapter is published in *Journal of the American Oil Chemists' Society* (2016), 93(10): 1415-1427 with minor adjustments in Figure/Table number to fit into the current thesis format. A copy of the research paper is included as appendix H in page 134.

2 Characterization and physicochemical properties of binary mixtures of PMF, RBDPKO or RBDPS for CBSs formulation

2.1 Introduction

Cocoa butter (CB) is a natural fat obtained from cocoa seeds (*Theobroma cacao*), commonly used as an important ingredient for the production of chocolate. CB consists of three main triacylglycerols (TAGs) such as glycerol-1,3-dipalmitate-2-oleate (POP; P palmitic, O oleic), glycerol-1-palmitate-2-oleate-3-stearate (POST; St stearic) and glycerol-1,3-distearate-2-oleate (StOSt) [21,59]. These TAGs are responsible for the melting profiles, crystallization and polymorphism of CB. CB becomes highly solid at 20°C and melts between 30 and 35°C [69]. This melting profile is desired in confectionery applications such as chocolates. CB has a complex polymorphic behavior, with an α polymorph (melting temperature, T_m 17-24°C, short spacing at 4.15 Å); a β'_1 polymorph (T_m 26-30°C, 3.8 and 4.2 Å); a β'_2 polymorph (T_m 24-26°C, 4.1 and 4.3 Å); a β_1 polymorph (T_m 34-36°C, 3.7 and 4.6 Å) and a β_2 polymorph (T_m 32-34°C, 4.5 Å) [37]. Generally, the stable polymorph (β_2) is preferred in chocolates as it melts at high melting temperature with small to moderate crystal sizes allowing for smooth products [136].

CB is expensive among all commercial fats and oils due to its low availability and strong market demand. Therefore, many studies have been performed to produce alternatives to CB by blending different proportions of palm kernel oil and palm oil [56,150,152]; palm mid-fraction and mango kernel fat [131]; palm kernel oil and milk fat [150]; and palm stearin and mango seed fat [70]. The melting profile of CBSs is similar to that of CB, but chemical composition and crystallization behavior in terms of stable polymorphic forms are completely different to CB. CBEs show similar melting profile, polymorphism and chemical composition as per CB [135].

Binary systems of fats/oils are gaining interest recently in producing CBAs for chocolates and other confectionery applications because fats/oils such as PMF, RBDPKO and RBDPS as described in section 1.4 are comparatively cheap and are easily available in the market. Recent studies produced CBRs by blending palm kernel oil and palm oil [152], mango seed fat and palm stearin [70], and also reported fatty acid composition, solid fat content and slip

melting point closer to commercial CB. Some studies also investigated the compatibility and melting behavior via chemical interesterification of palm olein and palm kernel oil [56], palm stearin and palm kernel olein [107] for producing confectionery products such as spreads. From the literature, it has also been noted that there are a few reports on the melting behavior, compatibility and microstructure of palm kernel oil, palm stearin or palm olein for producing margarines, shortenings and fat spreads [48,155]. Hence, production of CBAs especially CBSs with PMF, RBDPKO or RBDPS remains an unexplored area of research. Oil blending in the current study is helpful in understanding their potential application in confectionery. CBSs produced from blending of fat mixtures could be used as a suitable partial replacement of CB.

In the present study, PMF, RBDPKO and RBDPS were mixed two at a time at different proportions to determine their suitability as a CBA. PMF has a high percentage of POP, RBDPKO has a short melting range, and RBDPS has a wider range of melting points. These oils/fats were mixed to see how close their physicochemical characteristics resemble those of CB. Hence, the objective of this study was to evaluate the fatty acid composition, triacylglycerol, solid fat content, melting behavior and polymorphism of PMF/RBDPKO, RBDPS/RBDPKO and PMF/RBDPS mixtures for CBSs formulation.

2.2 Materials and methods

2.2.1 Materials

Palm mid fractions (PMF), refined bleached deodorized palm kernel oil (RBDPKO) and refined bleached deodorized palm stearin (RBDPS) were obtained from Sime Darby Research Sdn. Bhd. (Selangor, Malaysia). Cocoa butter (CB) was purchased from Le Bourne Sdn. Bhd. (Selangor, Malaysia). All chemicals and solvents used were of Analytical Reagent or HPLC grades (Fisher Scientific, Loughborough, UK). Fatty acid methyl ester (FAME) standards and TAG standards were obtained from Lab Science Solution Sdn. Bhd. (Selangor, Malaysia) and Sigma Aldrich (St. Louis, MO, USA).

2.2.2 Preparation of oil blends

Mixtures (w/w) of two fats (PMF/RBDPKO, RBDPS/RBDPKO and PMF/RBDPS) were prepared from 0 to 100% in 10% increments. The samples were melted at 80°C and mixed thoroughly and then stored at room temperature for further analysis.

2.2.3 Fatty acid analysis

Fatty acid composition was determined in terms of fatty acid methyl esters (FAME). The samples (50 mg) were weighed and dissolved in 1 ml of heptane inside a 1.5 ml centrifuge tube. The mixtures were then added to 50 μ l of 1 M sodium methoxide in anhydrous methanol and then mixed vigorously for 1 min by using a vortex mixer. After the sedimentation of sodium glycerolate, 1 μ l of the clear supernatant was injected into a gas chromatograph (Perkin Elmer Clarus 500 GC, Norwalk, USA) fitted with an elite FFAP column (30 m length \times 0.32 mm i.d. \times 0.25 μ m film thickness). A flame ionization detector (FID) was used to detect the FAME [120]. The injection and detection temperatures were both 250°C. The oven temperature was programmed as follows: heat from 110°C to 140°C (30°C/min), hold at 140°C for 1 min, heat from 140°C to 240°C (15°C/min) and hold for 7 min at 240°C. The carrier gas (helium) flow rate was 0.9 ml/min. The peaks were identified by comparing the retention times with the FAME standards and quantified by using a peak area normalization method.

2.2.4 Triacylglycerol (TAG) analysis

The TAG profiles of the fat mixtures were analysed using high performance liquid chromatography (Agilent HPLC series 1260, Santa Clara, USA) according to AOCS Official Method, Ce 5b-89 [51]. The column used was ZORBAX C-18 (4.6 \times 250 mm, 5 μ m, Agilent Technologies Inc., Santa Clara, USA) and maintained at 35°C by a column oven. Isocratic elution was carried out at a flow rate of 1.5 ml/min with a mixture of acetone/acetonitrile (70:30, v/v) as the mobile phase. A refractive index detector (RID, Agilent 1260 Infinity, Santa Clara, USA) was used. The injection volume with an auto-injector was 10 μ l of 5% (w/v) oil in acetone. TAG peaks were identified based on the retention time of TAG standards. The percentage of TAGs was determined by using a peak area of the chromatogram.

2.2.5 Solid fat content (SFC) analysis

The SFC of the fat mixtures was determined using pulsed nuclear magnetic resonance with a Bruker Minispec PC 120 NMR analyzer (Karlsruhe, Germany), following the method developed by Fiebig and Lüttke [50]. The fat samples (2-3 g) were placed into the NMR tubes and melted at 80°C for 30 min followed by tempering at 60°C for 5 min, 0°C for 90 min, 26°C for 40 h, 0°C for 90 min, and finally kept it for 30 min at the desired measuring

temperatures of 5, 10, 15, 20, 25, 30, 35, 40 and 45°C before SFC is measured. Iso-solid phase diagrams of the fat mixtures were constructed with OriginPro 9.1 software (OriginLab Corp., Northampton, MA, USA) based on SFC value obtained from NMR for each temperature ranging from 5 to 40°C.

2.2.6 Melting behavior

Melting behavior of the fat mixtures was determined using differential scanning calorimetry (DSC, Perkin-Elmer Pyris 4000 DSC, Norwalk, USA), following the method developed by Williams et al. [150]. Nitrogen gas was used at a flow rate of 20 ml/min. The instrument was calibrated with indium and n-dodecane. The samples (5-10 mg) were hermetically sealed in an aluminum pan. An empty, covered aluminum pan was used as the reference. The samples were cooled to -50°C at 10°C/min, held at -50°C for 5 min and then heated to 80°C at 5°C/min.

2.2.7 Crystal analysis

The polymorphic forms of the fat crystals were determined at 24°C (room temperature) with a D8 Discover X-ray diffraction (XRD, Bruker, Karlsruhe, Germany) fitted with Cu-K α radiation ($k = 1.5418 \text{ \AA}$, voltage 40 kV and current 40 mA). The samples were analysed at 2θ angles of 10°-30° with a scan rate of 1.5 °/min. X-ray data was processed using the diffraction software to calculate the absorption intensity background, intensity and peak width in degrees for each crystalline form and the relative contents of β'_1 , β'_2 and β_2 crystals. The β'_1 , β'_2 and β_2 polymorphs were calculated from the intensity of the short spacings at 3.8 & 4.2 Å, 4.1 & 4.3 Å, and 4.5 Å, respectively [37]. Each polymorph present was calculated using the formula [115], where $I\beta'_1$, $I\beta'_2$ and $I\beta_2$ were the peak intensities of β'_1 , β'_2 and β_2 polymorphs, respectively.

$$\% \beta'_1 = \frac{I \beta'_1 \times 100}{I \beta'_1 + I \beta'_2 + I \beta_2}; \% \beta'_2 = \frac{I \beta'_2 \times 100}{I \beta'_1 + I \beta'_2 + I \beta_2}; \% \beta_2 = \frac{I \beta_2 \times 100}{I \beta'_1 + I \beta'_2 + I \beta_2} \dots\dots\dots 2.1$$

2.2.8 Statistical analysis

The data were statistically analyzed by one-way analysis of variance (ANOVA) using the OriginPro 9.1 software (OriginLab Corp., Northampton, MA, USA). Tukey's test was applied to determine the significant differences at a $P < 0.05$ level. NMR data represented single determination. DSC diagrams and XRD analyses were conducted in triplicate.

2.3 Results and discussion

2.3.1 Fatty acid composition

The fatty acid profiles of the different mixtures of PMF/RBDPKO, RBDPS/RBDPKO and PMF/RBDPS are shown in Table 2.1, Table 2.2 and Table 2.3. PMF and RBDPS were rich in palmitic (51.9% and 68%) and oleic (36.1% and 21%) acids respectively. RBDPKO contained a high percentage of lauric acid (48.3%), followed by myristic (15.6%), oleic (15.1%), palmitic (8%), and linoleic (3%) acids. The compositions of all the individual fats were consistent with the earlier findings [21,131,138,150], who reported that the fatty acid profiles of CB are described in the introduction.

Since none of these fats mimicked the fatty acid profile of CB, so it was decided that they must be blended in different proportions and combinations. In Tables 2.1, 2.2 and 2.3, the fatty acid constituents among the blends were significantly ($P<0.05$) affected by the ratios of the mixtures. In PMF/RBDPKO mixtures (Table 2.1), the constituents of short-chain fatty acids (lauric and myristic) increased gradually ($P<0.05$) with increasing RBDPKO. Although the compositions of long-chain fatty acids such as palmitic, oleic and linoleic acids were comparable to commercial CB (Table 2.1), the compositions of short-chain fatty acids were significantly higher ($P<0.05$) in blends G to I (20-40% of PMF in RBDPKO). A similar trend was also observed in mixtures F to H (30-50% of RBDPS in RBDPKO) of RBDPS/RBDPKO blends as described in Table 2.2. In PMF/RBDPS mixtures (Table 2.3), the palmitic and oleic acids with the exception of stearic were significantly ($P<0.05$) higher in mixtures B to F (50-90% of PMF in RBDPS) compared to commercial CB. Calliauw and co-workers [27] also produced CBSs via two-stage static fraction of palm kernel oil, and reported the fatty acid profiles: lauric (56.3%), myristic (19.6%), palmitic (8.9%) and stearic (2.0%). Jahurul and co-workers [71] also studied the fatty acids in different blends of mango seed fat extracted by supercritical carbon-dioxide and palm stearin at various ratios to obtain CB replacers, and reported that the fatty acid profiles of certain blends were comparable to commercial CB. Therefore, the fatty acid compositions of mixtures G to I of PMF/RBDPKO, mixtures F to H of RBDPS/RBDPKO and mixtures B to F of PMF/RBDPS were the closest to commercial CB compared to other fat mixtures. Though these fatty acids were chemically different from those present in CB, they may have similarity on their solid fat content and melting behaviors as per CB, thus making them suitable substitutes for CB.

2.3.2 Triacylglycerol (TAG) composition

The TAG profiles of the different mixtures are shown in Table 2.4. CB contained predominantly monounsaturated TAGs (88.2% SUS: POP, POSt and StOSt; P palmitic, O oleic, St stearic), which was consistent with previous studies [21] as described in the introduction. PMF and RBDPS were high in SUS (60.1 and 40.7%), followed by diunsaturated (SUU: PLL, POO, StOO; L linoleic) TAGs (26.9 and 21.6%). RBDPKO was rich in trisaturated TAGs (70.4% SSS: LaLaLa, LaLaM, MMM; La lauric, M myristic). In Table 2.4, variations of TAG constituents were observed among the blends. All the blends of PMF/RBDPKO, RBDPS/RBDPKO and PMF/RBDPS had a mixture of SSS, SUS, SUU and UUU (polyunsaturated; OOL and OOO) TAGs. In respect of PMF/RBDPKO mixtures, SUS and SUU contents decreased significantly ($P < 0.05$), while SSS content increased with the addition of RBDPKO. A similar trend was also observed for RBDPS/RBDPKO and PMF/RBDPS mixtures. There were significant differences among all the binary mixtures except some blends of UUU TAGs (Table 2.4). The StOSt TAG is responsible for β crystal formation, whereas POP/POSt TAGs for β' crystals [142]. Therefore, these TAGs though being chemically different from those of CB, they may have a significant influence on the solid fat content, melting properties and polymorphism of the mixtures, making them suitable substitutes for CB.

Table 2.1. Fatty acid composition (peak area %) for PMF/RBDPKO mixtures.

Blend	Fatty acid composition							
	<C _{12:0}	C _{12:0}	C _{14:0}	C _{16:0}	C _{18:0}	C _{18:1}	C _{18:2}	C _{20:0}
A (100:0)	-	0.16±0.11j	1.0±0.09k	49.40±0.10a	4.59±0.09b	37.68±0.10a	7.17±0.10a	-
B (90:10)	0.77±0.13	4.86±0.25i	2.56±0.10j	45.71±0.18b	4.18±0.11b	35.28±0.10b	6.64±0.13b	-
C (80:20)	1.32±0.21	8.40±0.08h	3.77±0.10i	41.85±0.21c	4.26±0.04b	34.16±0.12c	6.24±0.10b	-
D (70:30)	2.03±0.10	14.82±0.14g	5.96±0.08h	35.79±0.12d	4.04±0.05bc	31.69±0.10e	5.67±0.04c	-
E (60:40)	2.36±0.16	17.47±0.11f	6.93±0.05g	33.93±0.04e	3.87±0.20cd	30.11±0.11f	5.33±0.12cd	-
F (50:50)	2.78±0.14	20.34±0.21e	8.07±0.13f	31.16±0.10f	3.72±0.15cd	28.84±0.11g	5.09±0.10d	-
G (40:60)	3.29±0.10	25.72±0.07d	10.04±0.10e	26.36±0.12g	3.48±0.08cd	26.45±0.12h	4.66±0.10e	-
H (30:70)	4.17±0.17	30.72±0.14c	11.89±0.12d	21.58±0.25i	3.27±0.07cd	24.24±0.10i	4.20±0.06e	-
I (20:80)	6.13±0.08	37.34±0.12b	13.06±0.18c	17.31±0.45j	2.57±0.13e	20.15±0.14j	3.44±0.10f	-
J (10:90)	3.92±0.17	37.73±0.11b	14.77±0.28b	15.90±0.10k	2.95±0.07cde	21.20±0.14k	3.53±0.12f	-
K (0:100)	7.74±0.07	46.79±0.10a	16.21±0.21a	8.77±0.17l	2.20±0.14e	15.78±0.16l	2.51±0.11g	-
CB	-	Trace	0.73±0.02k	25.69±0.28h	36.15±0.26a	33.24±0.19d	3.13±0.22f	1.04±0.07

Values within the same column with different letters are significantly different ($P<0.05$). Each value in the table represents the mean \pm S.D. of three measurements. Abbreviations: Palm mid-fraction (PMF), refined bleached deodorized palm kernel oil (RBDPKO) and cocoa butter (CB).

Table 2.2. Fatty acid composition (peak area %) for RBDPS/RBDPKO mixtures.

Blend	Fatty acid composition							
	<C _{12:0}	C _{12:0}	C _{14:0}	C _{16:0}	C _{18:0}	C _{18:1}	C _{18:2}	C _{20:0}
A (100:0)	-	0.23±0.08k	1.17±0.05j	54.28±0.28a	4.47±0.14b	33.39±0.20a	6.46±0.10a	-
B (90:10)	0.96±0.03	10.15±0.12j	4.49±0.21i	42.15±0.34b	4.54±0.12b	31.88±0.08b	5.83±0.14b	-
C (80:20)	1.08±0.10	11.21±0.40i	4.75±0.10i	42.96±0.54c	4.39±0.21bc	30.03±0.13c	5.58±0.24bc	-
D (70:30)	1.7±0.10	13.73±0.21h	6.04±0.14h	39.56±0.31d	4.22±0.21bc	29.46±0.17d	5.29±0.30cd	-
E (60:40)	1.97±0.08	16.73±0.40g	7.32±0.21g	37.02±0.12e	4.0±0.10cd	27.96±0.24e	5.0±0.12d	-
F (50:50)	2.73±0.11	22.27±0.12f	9.05±0.14f	31.43±0.32f	3.74±0.12d	26.21±0.21f	4.57±0.14e	-
G (40:60)	3.4±0.20	27.68±0.10e	11.12±0.21e	25.49±0.14g	3.52±0.10de	24.59±0.24g	4.20±0.14e	-
H (30:70)	3.42±0.21	29.59±0.10d	12.01±0.40d	23.99±0.20h	3.40±0.14de	23.45±0.13h	4.14±0.21e	-
I (20:80)	4.38±0.07	32.07±0.21c	13.70±0.12c	20.40±0.13i	3.25±0.21e	22.41±0.10i	3.79±0.18f	-
J (10:90)	4.8±0.13	34.30±0.57b	16.97±0.70b	15.81±0.21j	3.12±0.15e	21.46±0.40j	3.54±0.10fg	-
K (0:100)	7.74±0.07	46.79±0.10a	16.21±0.21a	8.77±0.17k	2.20±0.14f	15.78±0.16k	2.51±0.11f	-
CB	-	Trace	0.73±0.02k	25.69±0.28g	36.15±0.26a	33.24±0.19a	3.13±0.22g	1.04±0.07

Values within the same column with different letters are significantly different ($P<0.05$). Each value in the table represents the mean \pm S.D. of three measurements. Abbreviations: Refined bleached deodorized palm stearin (RBDPS), refined bleached deodorized palm kernel oil (RBDPKO) and cocoa butter (CB).

Table 2.3. Fatty acid composition (peak area %) for PMF/RBDPS mixtures.

Blend	Fatty acid composition							
	<C _{12:0}	C _{12:0}	C _{14:0}	C _{16:0}	C _{18:0}	C _{18:1}	C _{18:2}	C _{20:0}
A (100:0)	-	0.16±0.11a	1.0±0.09a	49.40±0.10a	4.59±0.09c	37.68±0.10a	7.17±0.10a	-
B (90:10)	0.02±0.03	0.15±0.06a	0.96±0.03a	49.66 ± 0.46b	4.76±0.17bc	37.55±0.11a	6.90±0.10ab	-
C (80:20)	0.03±0.01	0.16±0.06a	0.98±0.05a	49.86 ± 0.31b	4.79±0.12bc	37.28±0.17a	6.90±0.14ab	-
D (70:30)	0.03±0.01	0.16±0.07a	0.96±0.03a	50.04 ± 1.36c	4.81±0.52bc	37.18±0.75a	6.82±0.32ab	-
E (60:40)	0.03±0.01	0.16±0.12a	0.97±0.09a	50.87 ± 1.08d	4.78±0.41bc	36.43±0.47b	6.76± 0.21ab	-
F (50:50)	0.04±0.03	0.16±0.08a	1.0±0.14a	51.34 ± 0.57e	4.80±0.41bc	36.06±0.64b	6.65±0.10b	-
G (40:60)	0.07±0.02	0.17±0.05a	1.01±0.10a	51.89 ± 0.40e	4.76±0.18bc	35.48±0.54c	6.62±0.21b	-
H (30:70)	0.10±0.01	0.19±0.05a	1.07±0.12a	52.44 ± 0.21f	4.75±0.12bc	34.72±0.32d	6.73±0.17b	-
I (20:80)	0.09±0.02	0.19±0.12a	1.07±0.14a	52.58 ± 0.80f	4.90±0.08b	34.44±0.23d	6.73±0.12b	-
J (10:90)	0.11±0.03	0.19±0.02a	1.04±0.08a	52.96 ± 0.65g	5.0±0.21b	34.19±0.13de	6.51±0.24b	-
K (0:100)	-	0.23±0.08a	1.17±0.05a	54.28±0.28h	4.47±0.14bc	33.39±0.20e	6.46±0.10b	-
CB	-	Trace	0.73±0.02a	25.69 ± 0.28i	36.15±0.26a	33.24±0.19e	3.13±0.22c	1.04±0.07

Values within the same column with different letters are significantly different ($P<0.05$). Each value in the table represents the mean \pm S.D. of three measurements. Abbreviations: Palm mid-fraction (PMF), refined bleached deodorized palm stearin (RBDPS) and cocoa butter (CB).

Table 2.4. Overview of TAGs (peak area %) in PMF/RBDPKO, RBDPS/RBDPKO and PMF/RBDPS mixtures.

Blend	PMF/RBDPKO					RBDPS/RBDPKO					PMF/RBDPS				
	SSS	SUS	SUU	UUU	Others	SSS	SUS	SUU	UUU	Others	SSS	SUS	SUU	UUU	Others
A (100:0)	4.8±0.1k	60.1±1.7b	26.9±0.7a	7.4±0.2a	0.8	29.1±1.8k	40.7±1.7b	21.6±1.2a	6.1±0.7a	2.5	4.8±0.4k	60.1±0.4b	26.9±1.1a	7.4±0.4a	0.8
B (90:10)	10.6±0.5j	58.2±0.8c	25.2±0.4b	5.2±0.2bc	0.8	33.7±1.1j	39.2±1.1c	17.8±1.4b	5.7±0.5ab	3.6	7.3±0.1j	58.3±0.5c	26.5±1.0ab	7.1±0.1ab	0.8
C (80:20)	18.5±0.4i	52.3±1.1d	23.1±0.6c	4.9±0.2c	1.2	36.5±1.2i	38.7±0.7d	15.7±1.2c	5.5±0.1bc	3.6	8.1±0.1i	57.6±0.4d	26.2±0.8b	6.8±0.1bc	1.3
D (70:30)	20.7±0.1h	50.7±0.8e	22.4±0.5d	4.7±0.1cd	1.5	37.3±1.1h	38.3±0.3e	15.2±0.4c	5.4±0.2bc	3.8	10.1±0.2h	56.1±1.8e	25.7±0.8cd	6.8±0.1bc	1.3
E (60:40)	27.9±0.5g	44.7±0.5f	21.0±0.7e	4.7±0.1cd	1.7	42.0±0.7g	36.8±0.8f	12.3±0.5d	5.1±0.5cd	3.8	11.7±0.1g	55.4±1.4f	25.2±1.0d	6.4±0.1cd	1.3
F (50:50)	31.5±0.7f	42.3±0.7g	19.7±0.2f	4.6±0.1cd	1.9	43.0±0.5f	36.4±0.4fg	11.7±0.4e	5.1±0.2cd	3.8	12.4±0.2f	54.7±1.2g	24.8±0.7e	6.4±0.1cd	1.7
G (40:60)	38.7±1.0e	41.0±0.9h	13.4±0.1g	4.5±0.1cde	2.4	45.5±1.2e	36.1±0.8g	9.5±0.1f	4.7±0.2d	4.2	14.8±0.2e	52.7±0.8h	24.4±0.4ef	6.4±0.1cd	1.7
H (30:70)	42.3±0.8d	39.4±0.5i	11.2±0.1h	4.5±0.2cde	2.6	50.5±1.3d	32.4±0.4h	8.2±0.1g	4.7±0.4d	4.2	15.0±0.1d	52.1±0.3h	24.1±0.2f	6.4±0.1cd	2.4
I (20:80)	45.7±0.7c	37.8±0.4j	9.5±0.5i	4.3±0.1cde	2.7	61.5±1.4c	21.7±0.8i	7.9±0.4gh	4.5±0.1de	4.4	19.8±0.2c	48.3±0.4i	23.3±0.6g	6.2±0.1cd	2.4
J (10:90)	60.8±1.1b	24.2±0.4k	7.3±0.2j	4.3±0.2cde	3.4	69.0±1.2b	14.7±0.4j	7.4±0.1h	4.5±0.2de	4.4	21.0±0.4b	47.1±0.5j	22.7±0.5h	6.2±0.1cd	3.0
K (0:100)	70.4±1.4a	14.2±0.4l	6.8±0.2k	4.1±0.2e	4.5	70.4±1.7a	14.2±0.5j	6.8±0.2i	4.1±0.4e	4.5	29.1±1.2a	40.7±0.5k	21.6±0.4i	6.1±0.1d	3.5
CB	0.7±0.1 _l	88.2±0.7a	5.3±0.2l	0.4±0.0f	5.4	0.7±1.8l	88.2±1.5a	5.3±0.2j	0.4±0.0f	5.4	0.7±0.0l	88.2±1.3a	5.3±0.5j	0.4±0.0e	5.4

Values within the same column with different letters are significantly different ($P<0.05$). Each value in the table represents the mean \pm S.D. of two measurements. Abbreviations: Triacylglycerols (TAG), trisaturated (SSS: LaLaLa, LaLaM, MMM, PPP; La lauric, M myristic, P palmitic), monounsaturated (SUS: POP, POST, StOST, LaOLa; O oleic, St stearic), diunsaturated (SUU: PLL, POO, StOO; L linoleic), polyunsaturated (UUU: OOL, OOO), palm mid-fraction (PMF), refined bleached deodorized palm kernel oil (RBDPKO), refined bleached deodorized palm stearin (RBDPS) and cocoa butter (CB).

2.3.3 Solid fat content (SFC) and iso-solid diagrams of the blends

The SFC profiles of individual CB, PMF, RBDPKO and RBDPS are shown in Figure 2.1. CB showed a high SFC ($\geq 70\%$) up to 20°C , followed by a rapid SFC drop between 20 and 35°C and 0% SFC was observed at or above 40°C . This is presumably due to its high content of SUS TAGs (Table 2.4). This finding was consistent with the earlier studies by Kadivar *et al.* [74], who reported a high SFC ($\geq 75\%$) at 20°C , a rapid decrease from 25 to 35°C and 0% at or above body temperature. PMF and RBDPKO exhibited a high SFC ($\geq 50\%$) up to 20°C , followed by a rapid decrease from 20 to 30°C . PMF was completely liquefied at 35°C , while RBDPKO showed 0% SFC at and above 40°C . These variations in the SFC are mainly caused by the differences in the fatty acids (Table 2.1) and TAGs of PMF and RBDPKO (Table 2.4). RBDPS exhibited the highest SFC ($\geq 60\%$) at less than 25°C and melted completely at and above 50°C (Figure 2.1), possibly due to its high content of SSS TAGs (Table 2.4).

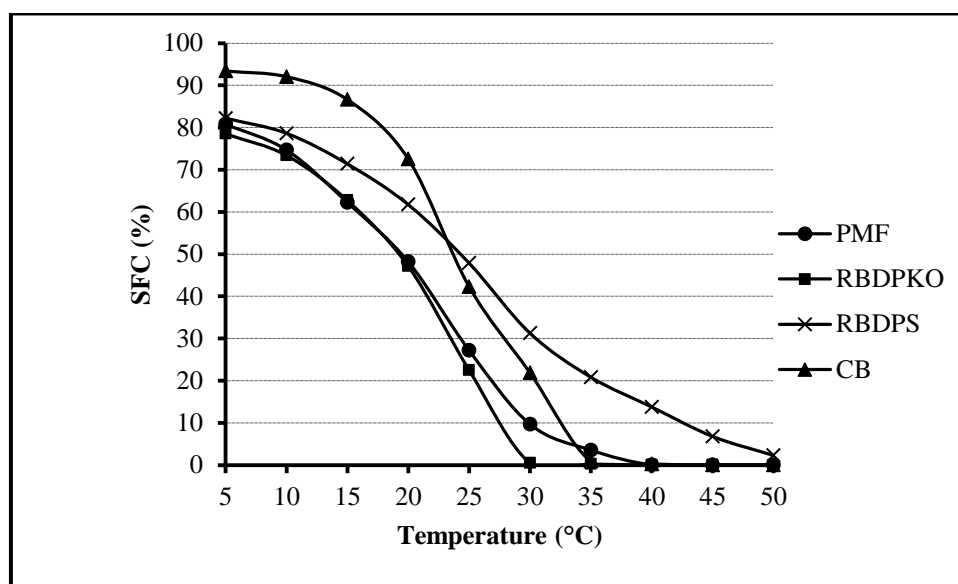


Figure 2.1. SFC versus temperature profiles for CB (—▲—), PMF (—●—), RBDPKO (—■—) and RBDPS (—×—).

The phase behavior of fat mixtures can be explained by iso-solid phase diagrams which have been used to illustrate the eutectic and monotectic effects as it is useful to understand the compatibility of mixed fats systems at a given temperature [64,145]. For example, eutectic effect occurs when theoretically the contour lines of constant SFC are not straight, with some blend compositions having lower melting temperatures than expected. This indicates that the

fat mixtures are not compatible (eutectic). The monotectic effect (compatibility) is seen by a straight line connecting the SFC of each pure component, indicating fats in a blend are mixed well [74,139]. In Figure 2.2a, the PMF/RBDPKO mixtures especially 10-70% PMF in RBDPKO displayed a eutectic effect at temperatures above 15°C ($\text{SFC} \leq 40\%$). A eutectic effect was observed at 5°C for 30-90% PMF in RBDPKO. However, the contour lines were almost straight for 20-50% PMF in RBDPKO between 10 and 15°C (Figure 2.2a). This may be due to the considerable contents of SUS and UUU TAGs (which have similar melting profiles and polymorphs) in PMF and RBDPKO (Table 2.4). A similar iso-solid diagram (monotectic effect) was observed between 10 and 20°C for 40-80% RBDPS in RBDPKO (Figure 2.2b). This behavior was also observed by Bootello and co-workers [21] for sunflower hard stearins (SHSs) and PMF mixtures. They also reported a eutectic effect for 20-60% SHS-65 in PMF between 10 and 20°C, and monotectic effect for 70-85% SHS-95 in PMF above 20°C. Therefore, according to the iso-solid diagrams, 20-50% PMF at 10-15°C and 40-80% RBDPS at 10-20°C could be blended with RBDPKO to avoid the undesirable eutectic effect which is responsible for unpleasant mouth feel and softer texture [21].

In Figure 2.2c, the iso-solid lines of PMF/RBDPS mixtures were almost linear and exhibited a monotectic effect at less than 30°C. The absence of eutectic effect in Figure 2.2c indicated that PMF and RBDPS do not show incompatibilities as these oils contained similar pattern of long-chain fatty acids (Table 2.3) with corresponding TAGs (Table 2.4). Approximately 40% of SFC was observed at 25°C for 50 to 80% PMF in RBDPS and it is also within the monotectic area of the iso-solid diagram (Figure 2.2c). This observation was in accordance with Timms [139], who suggests a fat adequate for confectionery usage should display at least 40% SFC value at 25°C. Therefore, 50 to 80% PMF in RBDPS could be used as CBSs because of the monotectic effect and SFC profiles.

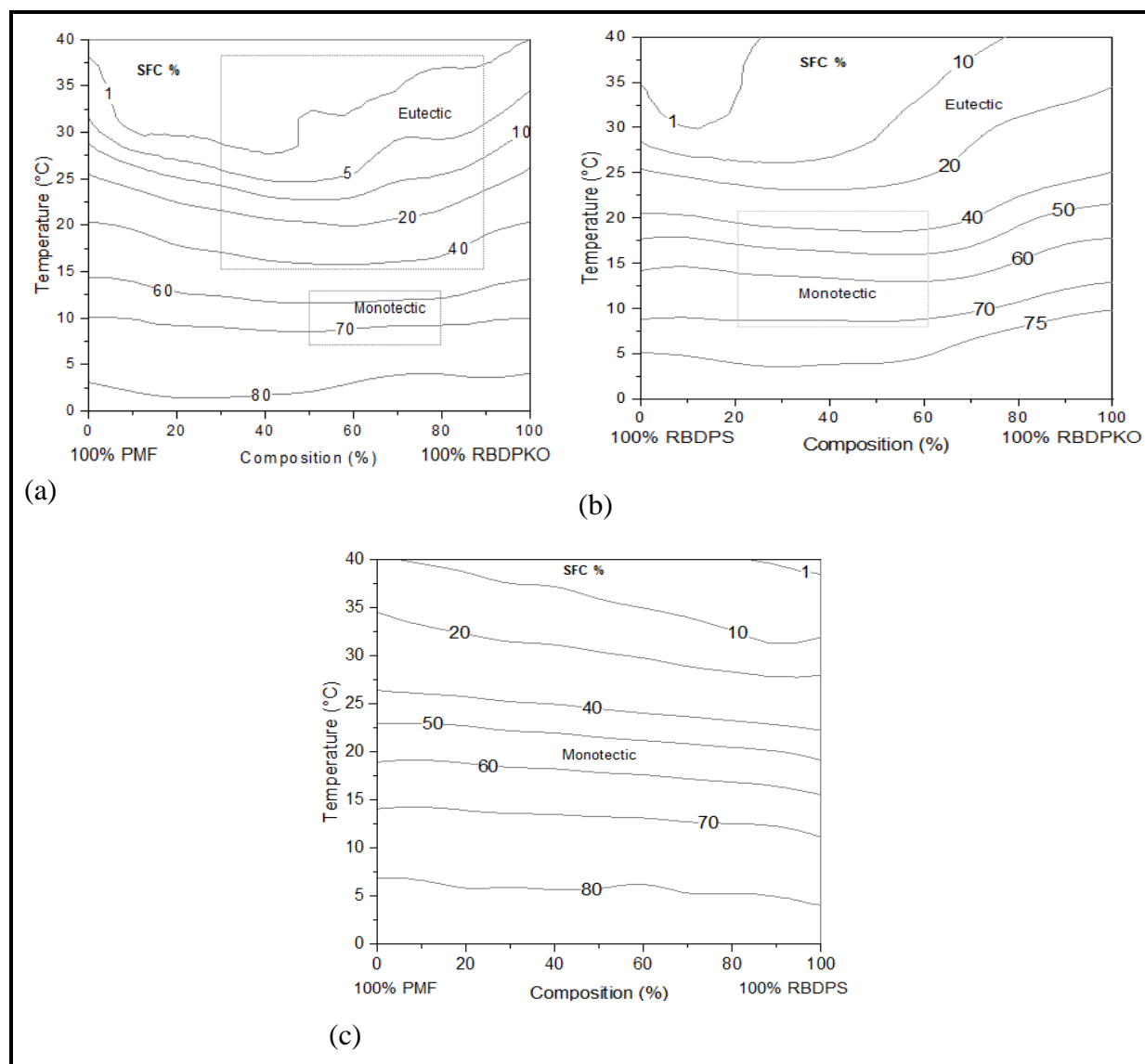


Figure 2.2. Binary iso-solid phase diagrams for mixtures of (a) PMF/RBDPKO, (b) RBDPS/RBDPKO, and (c) PMF/RBDPS.

2.3.4 Melting behavior

The DSC melting curves of the selected individual fats: CB, PMF, RBDPKO and RBDPS were shown in Figure 2.3. CB exhibited one sharp endotherm (T_1) at approximately 33°C with one/two small endotherms (Figure 2.3a). The small endotherms may be due to the considerable contents of SSS and SUU TAGs (Table 2.4). The onset temperature (T_{Onset}) at 22.1°C, endset temperature (T_{Endset}) at 37.2°C and melting enthalpy (ΔH) at 114.2 J/g were also observed for CB (Table 2.5). PMF exhibited two broad endotherms (T_1 10°C and T_2 22°C) with an exotherm (endothermic trough) between them. Melting is one of the endothermic behaviors and crystallization is one of the exothermic behaviors. This exotherm

is likely caused by the polymorphic transformation during the DSC melting [138]. PMF also showed T_{Onset} (4.5°C), T_{Endset} (27.3°C) and ΔH (34.8 J/g) as described in Table 2.5. RBDPKO had a broad endotherm (T_1) at approximately 27°C, with multiple small peaks. The T_{Onset} , T_{Endset} and ΔH of RBDPKO were observed at 17.2°C, 29.8°C and 84.9 J/g respectively (Table 2.5). RBDPS exhibited two distinct broad endotherms at 10 and 40°C (T_1 and T_2) with an exotherm between them (Figure 2.3b). The lower temperature endotherm (T_1) is probably related to the small content of oleic fraction, while the higher temperature endotherm (T_2) corresponded to the stearin fraction (Figure 2.3b). The melting of RBDPS started at -4.1°C and ended at 55.2°C, with melting enthalpy at 73.9 J/g (Table 2.5). Similar DSC melting profiles have been reported by other researchers [21,138]; endothermic peaks at 32.5°C for commercial CB, 9.8 to 32.8°C for PMF, - 9.12 to 26.03°C for RBDPKO, and -18.4 to 55.0°C for RBDPS.

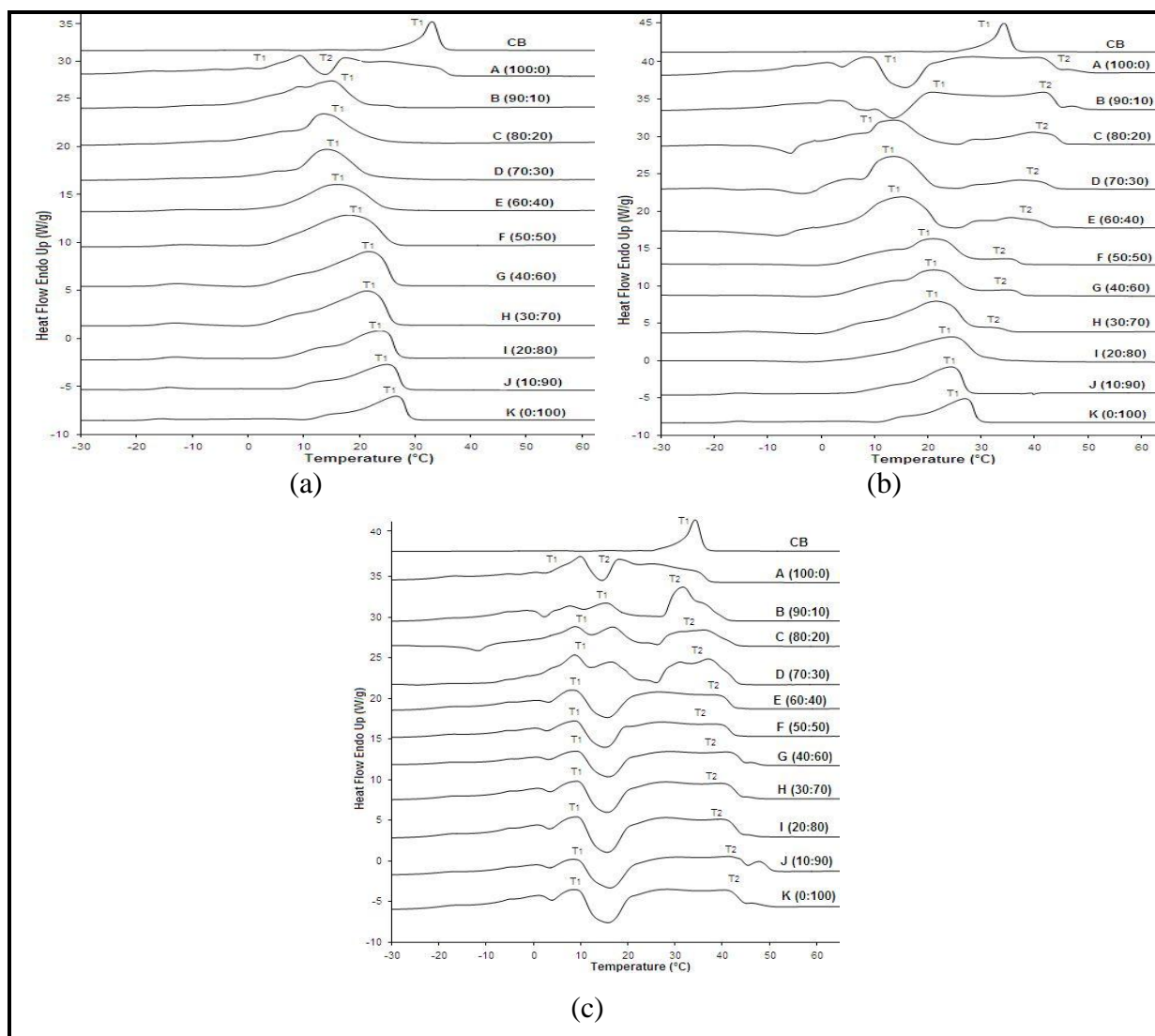


Figure 2.3. Differential scanning calorimetry melting curves of (a) PMF/RBDPKO mixtures, (b) RBDPS/RBDPKO mixtures, and (c) PMF/RBDPS mixtures.

The DSC melting profiles of the different binary mixtures of PMF/RBDPKO, RBDPS/RBDPKO and PMF/RBDPS are shown in Figure 2.3a-c. All mixtures of PMF/RBDPKO showed one primary broad endothermic peak between 15.7 and 25.8°C with one/two small shoulder peaks (Figure 2.3a). The shoulder peaks are probably caused by the presence of UUU TAGs both from PMF and RBDPKO (Table 2.4). Mixtures B to F of PMF/RBDPKO showed one broad endotherm between 16 and 20°C with a small exothermic peak, different onset temperature (T_{Onset}), endset temperature (T_{Endset}) and melting enthalpy (ΔH). The exothermic peak could be probably explained by the polymorphic transformation in PMF. The T_{Onset} , T_{Endset} and melting enthalpy of these blends ranged from 4.8 to 9.2°C, 27.5 to 28.4°C and 42.2 to 61.2 J/g, respectively (Table 2.5). However, the T_{Onset} from 10.4 to

16.4°C, T_{Endset} from 28.3 to 29.3 °C and melting enthalpy from 64.7 to 80.9 J/g were observed for blends G to J of PMF/RBDPKO. There were also significant differences ($P < 0.05$) among all the blends except blends C and D of the T_{Endset} temperature (Table 2.5). The blends G to J also exhibited one broad endotherm at 25 and 26°C with two small shoulder peaks. The small difference of the melting peak could be due to the variation of fatty acids, SSS and SUS TAGs in PMF and RBDPKO (Table 2.1 and Table 2.4). Moreover, this behavior agreed with the monotectic formation in the iso-solid diagram (Figure 2.2a). These findings were in agreement with those reported by Jahurul and co-workers [68], who obtained CB replacers by blending supercritical carbon-dioxide extracted mango seed fat and PMF. They also reported two maxima at 16.4 and 19.1°C, with T_{Onset} (-14.1 to -15.2°C), T_{Endset} (36.3 to 36.8°C) and ΔH (68 to 69.3 J/g) closer to commercial CB. In the present study, mixtures G to J with 10-40% of PMF in RBDPKO showed one maxima at 25 to 26°C with T_{Onset} , T_{Endset} and ΔH , which are comparable to commercial CB (Figure 2.3a). Therefore, mixtures G to J of PMF in RBDPKO may be used as CBS-based filling fats require to have less than 50% SFC at 20°C with melting temperature ranging between 21 and 23°C [136].

In Figure 2.3b, the RBDPS/RBDPKO mixtures showed one or two broad endotherms with multiple small peaks. The shoulder peaks may be due to the presence of unsaturated fatty acids, SUU and UUU TAGs in RBDPS and RBDPKO (Table 2.2 and Table 2.4). Mixtures B to H with 30 to 90% of RBDPS in RBDPKO demonstrated two broad endotherms (T_1 and T_2) at temperatures ranging from 5 to 36°C. The lower temperature endotherm (T_1) is possibly related to the presence of low melting SUU and UUU TAGs both from RBDPS and RBDPKO (Table 2.4). However, the high temperature endotherm (T_2) indicates the presence of high melting SSS (PPP) and SUS TAGs from RBDPS (Table 2.4). In addition, these results suggest eutectic formation, although the iso-solid phase diagram for the 40-80% RBDPS in RBDPKO showed monotectic behavior at 10 to 20°C (Figure 2.2b). With respect to the mixtures I and J, the DSC melting curves exhibited one broad endotherm at approximately 26°C (T_1). This may be due to the presence of medium melting SSS TAGs from RBDPKO (Table 2.4). With decreasing RBDPS in the mixtures, the T_{Onset} increased while the T_{Endset} decreased both significantly ($P < 0.05$), and they ranged from -3.7 to 16.4°C and 53.7 to 34.7°C respectively. The increase in T_{Onset} can be explained by the presence of increased proportion of short-chain saturated fatty acids and SSS TAGs (Table 2.2 and Table 2.4). The decrease in T_{Endset} can be due to the presence of decreased long-chain palmitic and oleic fatty acids, SUS (especially POP) and SUU (especially POO) TAGs (Table 2.2 and 2.4).

Melting enthalpies (75.8-82.7 J/g) also decreased gradually ($P<0.05$) with the addition of RBDPKO in the mixtures (Table 2.5). This observation was consistent with a previous report by Jahurul and co-workers (10), who successfully produced hard CB replacers by blending supercritical carbon-dioxide extracted mango seed fat and palm stearin. And they also reported melting profiles (17.6 to 36.9°C) with T_{Onset} (-13.4°C) and T_{Endset} (40.0°C) closer to CB. A recent study, Bootello and co-workers [21] also reported two maxima at 22.8 and 36.51°C for commercial CB. In the present study, mixtures F to H with 30-50% RBDPS in RBDPKO showed melting profiles of 20-38°C with T_{Onset} , T_{Endset} and ΔH , which are the closest to commercial CB. Therefore, mixtures F to H of RBDPS/RBDPKO can be used as CBSs in compound chocolates because of their compatibility (Figure 2.2b) and melting profiles (Figure 2.3b and Table 2.5).

In Figure 2.3c, the PMF/RBDPS mixtures showed two broad endotherms (T_1 and T_2) with an exotherm between them. As the RBDPS increased in the mixtures, the higher temperature endotherm (T_2) increased from 30 to 40°C. This may be due to the increased proportion of SSS TAGs (PPP) from RBDPS (Table 2.4). All the mixtures showed different T_{Onset} , T_{Endset} , and ΔH . For example, the T_{Onset} at 4.2°C and T_{Endset} at 32.1°C were observed for mixture B, whereas T_{Onset} at -0.8°C and T_{Endset} at 50.7°C for mixture J (Table 2.5). There were gradual increases in the ΔH of all mixtures (41.7 to 70.6 J/g) with the addition of RBDPS (Table 2.5). This behavior can be probably caused by the presence of increased proportion of saturated fatty acids and SSS (especially PPP) TAGs (Table 2.3 and Table 2.4). These findings also agreed with the monotectic effect in the iso-solid diagram (Figure 2.2c). Most of the PMF/RBDPS mixtures were significantly ($P<0.05$) different for the T_{Onset} , T_{Endset} and melting enthalpy (Table 2.5). These findings are consistent with a previous report by Sonwai and co-workers [131], who reported the melting profiles of mango kernel fat/PMF blend that resemble CB with two maxima at 17 and 36.2°C. In another study, Chaiseri and Dimik [32] also noted two maxima at 11.6 and 22.8°C for commercial CB. Similarly, in the present study, mixtures C to F with 50-80% PMF in RBDPS showed melting characteristics of 20-38°C with T_{Onset} , T_{Endset} and ΔH , which are comparable to commercial CB. Therefore, mixtures C to F of PMF in RBDPS can be used as CBSs in compound chocolates due to their monotectic effect with approximately 40% SFC value at 25°C (Figure 2.2c) and melting profiles (Figure 2.3c and Table 2.5).

2.3.5 Polymorphism

The purpose of the polymorphism study using XRD was to observe if the crystal polymorph of binary mixtures resembles that of CB. The polymorphic structures of the different fat mixtures are presented in Table 2.6. CB showed a mixture of β'_1 , β'_2 and β_2 crystals due to the presence of 88.2% SUS (Table 2.4), and this agreed with the earlier studies [37]. PMF and RBDPKO showed only β'_1 and β'_2 polymorphs, while RBDPS exhibited a mixture of β'_1 , β'_2 and β_2 polymorphs. For PMF/RBDPKO mixtures, the proportion of β'_1 crystal decreased gradually while the proportion of β'_2 crystal increased accordingly ($P<0.05$) with the addition of RBDPKO. This behavior could be due to the decreased proportion of SUS (especially POP) and increased proportion of SSS TAGs (Table 2.4). In DSC melting thermograms, blends G to J with 10 to 40% PMF in RBDPKO showed melting temperatures of 25-26°C that is close to CB with a mixture of β'_1 and β'_2 polymorphs ($\beta'_1 \gg \beta'_2$) (Figure 2.3a and Table 2.6).

A similar trend was observed for PMF/RBDPS mixtures. In the PMF/RBDPS mixtures, percentage of β_2 crystal increased ($P<0.05$) with increasing RBDPS (Table 2.6). This may be related to the presence of increased proportion of SSS TAGs especially PPP (Table 2.4). Blends C to F with 50-80% PMF in RBDPS showed a mixture of β'_1 , β'_2 and β_2 polymorphs ($\beta'_1 \gg \beta'_2 > \beta_2$) with melting temperatures of 20-38°C that is comparable to CB (Table 2.6 and Figure 2.3c).

Table 2.5. Overview of T_{Onset} , T_{Endset} and melting enthalpy (ΔH) in PMF/RBDPKO, RBDPS/RBDPKO and PMF/RBDPS mixtures.

Blend	PMF/RBDPKO			RBDPS/RBDPKO			PMF/RBDPS		
	T_{Onset} (°C)	T_{Endset} (°C)	ΔH (J/g)	T_{Onset} (°C)	T_{Endset} (°C)	ΔH (J/g)	T_{Onset} (°C)	T_{Endset} (°C)	ΔH (J/g)
A (100:0)	4.5±0.1j	27.3±1.2f	34.8±0.3l	-4.1±0.1k	55.2±0.3a	73.9±1.0l	4.5±0.3b	27.3±1.1k	34.8±1.0k
B (90:10)	4.8±0.1j	27.5±0.9f	42.2±0.3k	-3.7±0.3j	53.7±0.8b	75.8±1.2k	4.2±0.3ac	32.1±1.0j	41.7±0.7j
C (80:20)	5.7±0.1i	27.6±0.8f	44.6±0.5j	-3.4±0.3j	52.4±0.6c	77.4±0.8j	4.0±0.3bc	33.6±1.2i	50.3±1.0i
D (70:30)	6.8±0.3h	27.8±0.6f	50.3±0.3i	-2.2±0.3i	49.3±0.1d	78.1±0.7i	3.7±0.1cd	35.4±0.3h	57.6±0.8h
E (60:40)	8.3±0.3g	28.1±0.7e	55.4±0.3h	-0.5±0.0h	46.4±1.1e	79.6±0.6h	3.6±0.5cd	37.2±1.2g	66.4±0.5g
F (50:50)	9.2±0.3f	28.3±0.9de	61.2±0.3g	5.4±0.3g	42.3±1.2f	80.4±0.8g	3.2±0.3d	42.1±0.3f	68.5±0.7f
G (40:60)	10.4±0.3e	28.5±1.1de	64.7±0.5f	9.7±0.7f	39.4±1.0g	81.2±0.5f	2.6±0.2e	44.3±1.0e	69.4±1.0e
H (30:70)	12.5±0.2d	28.7±1.0d	71.2±1.1e	13.2±0.8e	37.6±0.8h	81.8±0.5e	2.3±0.2e	45.6±1.1d	70.4±0.7d
I (20:80)	14.7±0.1c	29.1±1.1c	74.6±1.2d	14.8±0.7d	36.4±0.8i	82.3±0.7d	1.7±0.3f	49.4±1.0c	70.6±0.8d
J (10:90)	16.4±0.4b	29.3±0.3bc	80.9±0.3c	16.4±1.0c	34.7±0.6j	82.7±0.8c	-0.8±0.0g	50.7±0.8b	72.1±0.5c
K (0:100)	17.2±0.6b	29.8±0.3b	84.9±0.8b	17.2±0.8b	29.8±0.7k	84.9±1.1b	-4.1±0.0h	55.2±0.7a	73.9±1.2b
CB	22.1±0.3a	37.2±0.6a	114.2±0.7a	22.1±0.4a	37.2±0.4l	114.2±1.0a	22.1±0.5a	37.2±0.3g	114.2±0.8a

Values within the same column with different letters are significantly different ($P < 0.05$). Each value in the table represents the mean \pm S.D. of three measurements. Abbreviations: Palm mid-fractions (PMF), refined bleached deodorized palm kernel oil (RBDPKO), refined bleached deodorized palm stearin (RBDPS) and cocoa butter (CB).

Table 2.6. Overview of Polymorphic forms (%) in PMF/RBDPKO, RBDPS/RBDPKO and PMF/RBDPS mixtures.

Blend	PMF/RBDPKO			RBDPS/RBDPKO			PMF/RBDPS		
	β'_1	β'_2	β_2	β'_1	β'_2	β_2	β'_1	β'_2	β_2
A (100:0)	82.4±0.9a	17.6±1.2a	-	34.7±0.7i	37.1±1.2a	28.2±1.2b	82.4±0.2a	17.6±0.7a	-
B (90:10)	80.7±0.7b	19.3±1.1b	-	35.4±1.1h	37.0±0.7a	27.6±0.4c	72.7±1.5b	18.3±0.8b	9.0±0.4k
C (80:20)	80.2±1.2b	19.8±1.0b	-	36.9±0.7g	36.8±0.7a	26.3±0.4d	67.3±0.4c	18.7±0.7b	14.0±0.8j
D (70:30)	74.5±0.7c	25.5±1.1c	-	37.5±0.7f	36.8±0.7a	25.7±0.7e	64.0±0.3d	19.0±0.1c	17.0±0.7i
E (60:40)	72.3±0.8d	27.7±0.7d	-	40.0±0.7ef	36.8±1.2a	23.2±0.7f	59.1±0.7e	19.5±0.2c	21.4±0.7h
F (50:50)	71.4±1.1e	28.6±0.7e	-	40.4±0.2e	36.8±1.1a	22.8±0.7g	57.5±0.7f	19.7±0.7c	22.8±0.8g
G (40:60)	70.4±1.4f	29.6±0.3f	-	42.0±0.2e	36.8±1.4a	21.2±0.8h	55.4±0.8g	21.4±0.7d	23.2±0.4f
H (30:70)	66.2±0.4g	33.8±0.3g	-	43.6±1.1d	36.7±0.2a	19.7±0.7i	51.4±0.7h	24.3±0.7e	24.3±0.4e
I (20:80)	64.7±0.4h	35.3±0.2h	-	47.7±0.3c	36.7±0.7a	15.6±0.7j	47.1±0.7i	27.2±1.2f	25.7±1.2d
J (10:90)	64.2±0.4h	35.8±0.3h	-	51.0±1.4b	36.7±0.7a	12.3±0.3k	41.7±0.8j	31.2±0.2g	27.1±0.4c
K (0:100)	63.3±0.4i	36.7±0.2i	-	63.3±1.4a	36.7±0.3a	-	34.7±0.9k	37.1±0.7h	28.2±0.4b
CB	25.4±0.7j	4.1±0.2j	70.5±0.4	25.4±0.7j	4.1±0.2b	70.5±0.4a	25.4±0.7i	4.1±0.2i	70.5±0.4a

Determined by X-ray diffraction; Values within the same column with different letters are significantly different ($P<0.05$). Each value in the table represents the mean \pm S.D. of three measurements. Abbreviations: Palm mid-fraction (PMF), refined bleached deodorized palm kernel oil (RBDPKO), refined bleached deodorized palm stearin (RBDPS) and cocoa butter (CB).

For RBDPS/RBDPKO mixtures, the proportion of β'_1 crystal increased, while the proportion of β'_2 and β_2 crystals decreased gradually with increasing RBDPKO. There were significant differences ($P < 0.05$) in the amount of β'_1 and β_2 polymorphs among all the blends, however blends C to J showed similar percentage of β'_2 polymorph (Table 2.6). These variations in the crystals are likely due to the differences in the TAGs content (Table 2.4). Blends F to H (30-50% RBDPS in RBDPKO) showed melting temperatures of 20-38°C that is comparable to CB with a mixture of β'_1 , β'_2 and β_2 polymorphs ($\beta'_1 > \beta'_2 \gg \beta_2$) (Figure 2.3b and Table 2.6). A similar observation was reported in the blends of mango kernel fat and PMF, which revealed a mixture of β' and β polymorphs comparable to CB [131]. In the present study, the amounts of β'_1 and β'_2 -crystals were found to be higher than CB for all the mixtures, while the amount of β_2 -crystal was reasonably lower compared to commercial CB. In a previous study, more than 70% β' crystals compared to β -crystal have been reported to be desirable for compound chocolates and coatings [145]. Therefore, 20 to 40% of PMF in RBDPKO, 30 to 50% of RBDPS in RBDPKO and 50 to 80% of PMF in RBDPS mixtures may be used as CBSs in chocolates.

2.4 Conclusion

The melting profile of 20-40% PMF in RBDPKO, 30-50% RBDPS in RBDPKO and 50-80% of PMF in RBDPS mixtures approximated that of CB, and even though the polymorphism, fatty acid profile and TAG composition were different. Furthermore, 20-40% of PMF in RBDPKO and 30-50% of RBDPS in RBDPKO mixtures showed a monotectic behavior at 10-20°C, suitable to be used as CBSs in chocolates and fillings. Up to 50-80% of PMF in RBDPS mixtures also displayed a monotectic behavior at less than 30°C, making the mixtures potentially for use as CBSs in chocolates and other confectionery applications.

Chapter 3

Work that is presented in this chapter is published in *Journal of the American Oil Chemists' Society* (2017), 94(2): 235-245 with minor adjustments in Figure/Table number to fit into the current thesis format. A copy of the research paper is included as appendix I in page 147.

3 Evaluation of physical and chemical properties of ternary mixtures of PMF/RBDPKO/RBDPS for CBS

3.1 Introduction

Cocoa butter (CB) is traditionally used for the formulation of chocolates, coatings, confectionery fillings and other confectionery products. CB is solid at room temperature and melts quickly above 30-32°C [59] as discussed in section 2.1 (Chapter 2). CB exhibits complex polymorphic forms namely γ , α , β' and β in ascending stability [37]. The stable polymorph (β) is typically preferred in chocolates and coatings because it melts at high melting temperature with small to moderate crystal sizes, allowing for smooth mouth-feel products [136]. The metastable β' polymorphs are desirable for confectionery fillings and compound chocolates because it melts at low temperature with a fine arrangement and a large surface area of solid crystals [136,145].

Cocoa butter is expensive compared to other commercial vegetable fats and oils because of its limited supply and high market demand. Therefore, manufacturers are looking for alternatives to CB. CBSs are generally used in confectionery fillings such as truffles, compound chocolates and other confectionery products [136]. CBSs contain high amount of lauric acid (12:0, 54.6%), followed by myristic acid (14:0, 20.7%), palmitic acid (16:0, 9.2%) and stearic acid (18:0, 8.7%), resulting in short-chain TAGs [119]. CBSs show solid fat content as a function of temperature and crystal morphology (size and shape) similar to those of CB, while the polymorphism, melting profile, TAG composition and fatty acid profile are different from CB [27,87,135]. In addition, CBSs with low melting temperature of 21-23°C are used in confectionery fillings [136].

In compound chocolates, coatings and fillings, different vegetable fats such as palm kernel oil, palm kernel stearin, palm oil or cocoa butter are commonly modified or blended. The modification of palm kernel oil to CBS is traditionally performed through hydrogenation. This process, however, has always been regarded to produce trans-fatty acids that increase undesirable low-density lipoprotein cholesterol [84]. Therefore, many studies have been performed to produce for CBS-based compound chocolates and coatings by blending different proportions of palm kernel oil, palm kernel stearin, palm oil or cocoa butter [131,145,146]. Vereecken *et al.* [144] studied the crystallization behavior, microstructure and

macroscopic properties of the lauric-based and palm-based fats for confectionery fillings. However, no information has been obtained with respect to the melting behavior, polymorphisms and crystal morphology of ternary mixtures of PMF/RBDPKO/RBDPS, which are important in producing CBSs in confectionery fillings.

PMF, RBDPKO and RBDPS oils are less expensive than other vegetable oil products, making them a cost-effective ingredient in confectionery fillings and compound chocolates. The present study aimed to evaluate the physical and chemical characteristics of ternary fat mixtures of PMF/RBDPKO/RBDPS in terms of their fatty acid profiles, triacylglycerol constituents, melting behavior, solid fat content, polymorphism and crystal morphology to produce CBSs in confectionery fillings. The ternary fat mixtures were combined based on our preliminary study of binary fat mixtures [18].

3.2 Materials and methods

3.2.1 Materials

The materials of this chapter are similar to the previous chapter as described in section 2.2.1.

3.2.2 Preparation of fat blend

Blends (%w/w) of PMF, RBDPKO and RBDPS were mixed in various ratios (Table 3.1) according to binary fat mixtures in our preliminary study [18]. The blends were melted at 80°C for 30 min to erase the crystal memory. The samples were kept at room temperature for further analysis.

Example of ternary relation from binary mixtures: $\text{PMF}:\text{RBDPKO}:\text{RBDPS} = (\text{PMF}:\text{RBDPKO}) \times (\text{PMF}:\text{RBDPS})$. Where, $\text{PMF}:\text{RBDPKO} = 2:3$ (40/60); $\text{RBDPKO}:\text{RBDPS} = 1:1$ (50/50), therefore, $\text{PMF}:\text{RBDPKO}:\text{RBDPS} = 2:3:3$ (25/37.5/37.5).

Table 3.1. Experimental design of PMF/RBDPKO/RBDPS mixtures.

Code	Proportion by weight (%)		
	PMF	RBDPKO	RBDPS
A(e)	11.1	44.4	44.4
B(g)	25.0	37.5	37.5
C(h)	33.3	33.3	33.3
D(f)	28.6	42.8	28.6
E(c)	14.9	59.6	25.5
F(d)	31.0	48.3	20.7
G(a)	16.6	66.6	16.6
H(b)	26.6	62.0	11.4

Small letters, (a)-(h) are used to label samples with decreasing order of RBDPKO; and capital letters, A-H, are used to label samples with decreasing order of RBDPS. Abbreviations: Palm mid-fraction (PMF), refined bleached deodorized palm kernel oil (RBDPKO) and refined bleached deodorized palm stearin (RBDPS).

3.2.3 Fatty acid analysis

Fatty acid composition of the investigated fat mixtures was determined using gas chromatography fitted with FID as described in section 2.2.3.

3.2.4 Triacylglycerol (TAG) analysis

The TAG profiles of the selected samples were analyzed using high performance liquid chromatography equipped with RID as described in section 2.2.4.

3.2.5 Solid fat content (SFC)

SFC of the selected fats was determined using pulsed nuclear magnetic resonance with a Bruker Minispec PC 120 NMR analyzer (Bruker, Karlsruhe, Germany), according to the AOCS Official Method Cd 16b-93 for stabilizing confectionery fats. Samples were melted at 100°C for 15 min and filled into NMR tubes (10 mm o.d. × 75 mm length, up to 3 cm in height). Samples were tempered at 60°C for 5 min, followed by 0°C for 90 min, 26°C for 40 h, 0°C for 90 min, and finally kept for 60 min at the desired measuring temperatures of 5, 10, 15, 20, 25, 30, 35, 37, 40, and 45°C before SFC was measured. Iso-solid phase diagrams of

the fat mixtures were constructed with OriginPro 9.1 software (OriginLab Crop., Northampton, MA, USA) based on SFC value obtained from NMR at 10, 20 and 25°C.

3.2.6 Melting behavior

Melting behavior of the fat mixtures was determined using differential scanning calorimetry (DSC) fitted with nitrogen gas flow rate of 20 ml/min as described in section 2.2.6.

3.2.7 Polymorphism

The polymorphic forms of the fat crystals were determined at room temperature (24°C) with a D8 Discover X-ray diffraction fitted with Cu-K α radiation as described in section 2.2.7. Assignments of polymorphs were based on the following short spacing characteristics of CB: α form ($d = 4.15$ Å); β' forms ($d = 3.8$ – 4.3 Å) and β forms ($d = 4.5$ – 4.6 Å or 5.2 Å) [37].

3.2.8 Crystal morphology

Polarized light microscopy (PLM, Olympus BX51, Tokyo, Japan) equipped with digital camera (Nikon, DS-Filc, Tokyo, Japan) at 24°C was used to observe the crystal network microstructure of individual CB, PMF, RBDPKO, RBDPS, and ternary mixtures of PMF/RBDPKO/RBDPS. The method described by Narine and Marangoni [106] was used for the crystallization of fat blends. The sample was melted at 80°C for 20 min to destroy the crystal memory. About 15 μ l of melted sample was placed on a glass slide, heated to 80°C, and covered carefully by a coverslip. The slides were then stored in a temperature controlled cabinet at $24 \pm 1^\circ\text{C}$ for 48 h to ensure proper crystallization. The liquid phase appears black, while the solid phase appears grey. NIS-Element Imaging Software (Version 4.20, Nikon Instruments Inc. Melville, USA) was used to obtain images.

3.2.9 Statistical analysis

Data were statistically analysed by one-way analysis of variance (ANOVA) using the OriginPro 9.1 software (OriginLab Crop., Northampton, MA, USA). Tukey's test was applied to determine the significant differences at $P < 0.05$ level. NMR analysis was performed in duplicate. DSC diagrams, XRD and PLM analyses were conducted in triplicate.

3.3 Results and discussion

3.3.1 Fatty acid composition

Table 3.2 shows the fatty acid profiles of ternary mixtures of PMF/RBDPKO/RBDPS. When the RBDPKO decreased in the mixtures, the concentration of short-chain fatty acids (lauric and myristic) significantly ($P<0.05$) decreased along with a gradual increase in the concentration of long-chain fatty acids such as palmitic and oleic (Table 3.2). The fatty acid concentrations in all ternary blends were significantly ($P<0.05$) affected by the ratios of the mixtures. Calliau and co-workers [27] also produced CBSs via two-stage static fraction of palm kernel oil, and reported the fatty acid profiles: lauric (56.3%), myristic (19.6%), palmitic (8.9%) and stearic (2.0%). Zaidul *et al.* [152] also studied the fatty acids in different blends of supercritical carbon-dioxide extracted palm kernel oil fractions and palm oil in various ratios to obtain CB replacers, and they reported that the fatty acid profiles of certain blends were comparable to those of commercial CB. In the present study, the concentrations of long-chain fatty acids such as palmitic, oleic and linoleic with the exception of stearic and short-chain fatty acids in blend (c) were observed to be comparable to those of commercial CB (Table 3.2).

3.3.2 Triacylglycerol (TAG) composition

The TAG profiles of the different PMF/RBDPKO/RBDPS mixtures are shown in Table 3.3. CB contained predominantly monounsaturated TAGs: POP (18.1%), POSt (39.2%) and StOSt (29.7%). PMF contained high concentration of unsaturated TAGs: POP (50.7%), POO (12.9%), PLP (10.2%; L linoleic) and POSt (9.1%). RBDPS had high concentration of both saturated and unsaturated TAGs: PPP (28.4%) and POP (32.1%). RBDPKO was rich in saturated TAGs: LaLaLa (La lauric), LaLaM (M myristic), LaMM at 27.2, 17.0 and 15.1%, respectively. These findings were consistent with the results reported in previous studies [21,138]. Blending of PMF/RBDPKO/RBDPS shows variations in TAG constituents (Table 3.3). All eight mixtures of the PMF/RBDPKO/RBDPS blend contained a mixture of SSS (trisaturated), SUS (monounsaturated), SUU (diunsaturated) and UUU (polyunsaturated) TAGs. In the mixtures, the trisaturated SSS TAGs: CLaLa (C capric), LaLaLa, LaLaM, LaMM and MMM decreased, whereas the unsaturated SUS TAGs especially POP and PLP increased gradually ($P<0.05$) with the reduction of RBDPKO. This can be explained by the presence of decreasing amount of short-chain saturated fatty acids and increasing amount of

long-chain both saturated and unsaturated fatty acids (Table 3.2). The most remarkable difference between the ternary mixtures and CB was the content of SUS TAGs specially POSt and StOSt. Sabariah *et al.* [119] reported that CBS contains a mixture of short-chain fatty acids: lauric, myristic, and long-chain fatty acids: palmitic, stearic with corresponding TAGs. In the present study, the constituent of POP with the exception of POSt and StOSt TAGs in blend (c) was found to be comparable to that of CB.

3.3.3 Melting behavior

DSC melting curves of ternary mixtures of PMF/RBDPKO/RBDPS are shown in Figure 3.1. All ternary mixtures demonstrated two broad endothermic peaks, with T_1 ranging from 17.1 to 19.7°C and T_2 ranging from 36.7 to 37.5°C. Only small differences in melting temperatures were observed among all the eight blends. These differences are most likely caused by the variation in fatty acid constituents (Table 3.2) and TAG contents in PMF, RBDPKO and RBDPS (Table 3.3). When the RBDPS was reduced in mixtures A-H, the first broad endothermic peak (T_1) slowly increased towards a temperature of 19.7°C and the second peak (T_2) decreased to 36.7°C. For instance, blend A with 44.4% RBDPS showed its first broad endotherm (T_1) at 17.1°C and second endotherm (T_2) at 37.5°C, whereas the first endotherm (T_1) was observed at 19.7°C and the second endotherm (T_2) was observed at 36.7°C for mixture H with 11.4% RBDPS. This observation was consistent with a previous report by Jahurul *et al.* [70], who successfully produced high melting profiles of CB replacers by blending supercritical carbon-dioxide extracted mango seed fat with palm stearin. The authors reported the melting profiles of mango seed fat/palm stearin blends that resemble CB with two endotherms at 17.6 and 36.9°C. Sonwai *et al.* [131] also produced CBE by blending mango kernel fat and PMF, and reported two maxima at 22.8 and 36.5°C. In the current study, blend E of 14.9/59.6/25.5 PMF/RBDPKO/RBDPS contains 25.74% palmitic, 24.51% oleic and 3.95% linoleic acids (Table 3.2). The melting profile of blend E spanning from 18.5 to 37°C (Figure 3.1) is reasonably different from commercial CB, leading to its potential use as a CBS in confectionery fillings [117,136].

Table 3.2. Fatty acid composition (% peak area) of PMF/RBDPKO/RBDPS mixtures.

FA (%)	Blend								CB
	(a)	(b)	(c)	(d)	(e)	(f)	(g)	(h)	
C _{8:0}	2.75±0.1a	2.58±0.1a	2.47±0.4a	2.07±0.1b	2.04±0.0b	1.78±0.1c	1.70±0.2c	1.69±0.4c	-
C _{10:0}	2.24±0.1a	2.05±0.4a	2.01±0.1a	1.76±0.1b	1.71±0.0b	1.47±0.1bc	1.43±0.4bc	1.38±0.4bc	-
C _{12:0}	30.32±0.7a	29.69±0.5b	29.06±0.6c	26.47±0.3d	26.36±0.5d	23.31±0.4e	23.27±0.7e	23.24±0.3e	Trace
C _{14:0}	10.26±0.8a	9.63±0.1b	9.14±0.1c	8.86±0.4d	8.74±0.4d	8.17±0.3e	8.11±0.9e	8.09±0.4e	0.73±0.0f
C _{16:0}	24.85±0.2f	24.88±0.2f	25.74±0.4e	26.89±0.9d	29.46±1.1c	30.76±0.1b	30.82±0.8b	33.00±0.7a	25.69±0.2e
C _{18:0}	3.00±0.1d	3.09±0.4d	3.12±0.0d	3.96±0.4b	3.37±0.4c	3.36±0.4c	3.34±0.5c	3.29±0.4c	36.15±0.5a
C _{18:1}	22.56±0.4g	23.34±0.8f	24.51±0.8e	25.14±0.8d	25.26±0.9d	26.62±0.1c	26.78±0.8b	26.84±0.7b	33.24±0.3a
C _{18:2}	4.02±0.1c	4.74±0.1b	3.95±0.4c	4.85±0.4a	3.06±0.4d	4.53±0.1b	4.55±0.4b	2.47±0.3e	3.13±0.4d
C _{20:0}	-	-	-	-	-	-	-	-	1.04±0.1
SFA	73.42±1.1a	71.92±1.0b	71.54±1.1c	70.01±1.1d	71.68±1.1c	68.85±0.6e	68.67±1.4e	70.69±1.1f	63.63±1.0g
USFA	26.58±0.7f	28.08±0.8e	28.46±0.9d	29.99±0.4b	28.32±0.3de	31.15±0.8b	31.33±0.4b	29.31±0.5c	36.37±0.7a

Values within the same row with different letters are significantly different ($p < 0.05$). Each value in the table represents the mean \pm S.D. of three measurements. Abbreviations: Fatty acid (FA), saturated fatty acid (SFA), unsaturated fatty acid (USFA), palm mid-fraction (PMF), refined bleached deodorized palm kernel oil (RBDPKO), refined bleached deodorized palm stearin (RBDPS) and cocoa butter (CB).

Table 3.3. Overview of TAGs (peak area %) in PMF/RBDPKO/RBDPS mixtures.

TAG %	Blend								PMF	RBDPKO	RBDPS	CB
	(a)	(b)	(c)	(d)	(e)	(f)	(g)	(h)				
CCLa	1.7±0.01b	1.5±0.01b	1.0±0.0b	0.8±0.0b	-	-	-	-	-	8.7±0.01a	-	-
CLaLa	6.4±0.01b	5.7±0.04bc	5.3±0.01c	5.3±0.01c	2.4±0.07d	2.4±0.01d	2.1±0.07d	2.1±0.01d	-	11.4±0.50a	-	-
LaLaLa	18.1±0.01b	17.0±0.01b	15.4±0.40c	15.1±0.40c	14.3±1.10d	13.7±0.07d	13.2±0.05d	10.3±0.70e	-	27.2±1.10a	-	-
LaLaM	10.2±0.03b	9.7±0.01c	9.2±0.01c	8.8±0.01c	7.5±0.01d	6.8±0.02de	6.4±0.02e	6.4±0.01e	0.9±0.01f	17.0±0.01a	-	-
LaMM	7.2±0.01b	6.7±0.07b	6.7±0.01b	6.4±0.01b	4.8±0.01c	4.3±0.02c	3.8±0.01d	3.4±0.01d	-	15.1±0.50a	-	-
MMM	4.7±0.01b	4.4±0.31b	3.8±0.01bc	3.4±0.01c	2.6±0.00d	2.2±0.01d	1.7±0.01de	1.2±0.01e	0.7±0.01f	8.4±0.01a	0.7±0.00g	-
PLO	4.1±0.01b	3.8±0.01b	3.7±0.01b	3.4±0.01b	3.4±0.01b	3.1±0.01bc	2.6±0.03c	2.3±0.01c	6.2±0.01a	-	6.1±0.01a	0.6±0.01d
PLP	1.4±0.01e	1.7±0.01e	3.7±0.01c	2.3±0.01de	1.2±0.01e	2.8±0.01d	2.4±0.02de	6.7±0.40b	10.2±1.20a	-	5.5±0.01b	2.1±0.01de
POO	6.2±0.05b	5.4±0.01bc	5.0±0.01c	3.8±0.01d	4.6±0.01cd	3.5±0.03d	5.4±0.01bc	2.1±0.01	12.9±1.10a	2.4±0.01e	13.5±0.50a	-
POP	34.7±0.10f	34.3±1.20f	25.4±1.50h	34.6±1.10f	37.5±1.10e	38.6±1.10d	39.4±1.20c	44.2±1.70b	50.7±1.4a	0.9±0.01	32.1±1.10g	18.1±0.70i
PPP	4.4±0.01e	3.8±0.01e	5.4±0.01d	4.8±0.01d	10.3±0.01b	8.9±0.02c	9.7±0.01b	10.1±0.01b	3.2±0.01f	1.1±0.01g	28.4±1.10a	0.7±0.01h
POSt	0.4±0.01g	5.4±0.01e	7.1±0.01d	5.9±0.01e	4.2±0.01f	5.7±0.01e	5.0±0.01e	7.6±0.01c	9.1±0.01b	-	3.8±0.01f	39.2±1.10a
StOSt	-	-	0.7±0.01	0.5±0.01	-	0.2±0.01c	-	1.2±0.01b	1.9±0.01b	-	-	29.7±1.10a
SSS	51.0±1.20b	47.3±0.70c	45.8±1.70d	43.8±0.70e	41.9±1.10f	38.3±1.10g	36.9±0.40h	33.5±1.20i	4.8±0.01k	80.2±1.50a	29.1±0.01j	0.7±0.00l
SUS	35.1±0.11f	39.7±0.40e	33.2±0.50g	41±0.01d	41.7±1.00d	44.5±1.10d	44.4±1.10d	53.0±1.10c	61.7±1.10b	0.9±0.00h	35.9±0.60f	87.0±1.20a
SUU	7.6±0.02e	7.1±0.01e	8.7±0.01cd	6.1±0.01f	5.8±0.01f	6.3±0.01f	7.8±0.01de	8.8±0.01c	23.1±0.70a	2.4±0.01g	19.0±0.01b	2.1±0.01g
UUU	4.1±0.01b	3.8±0.01b	3.7±0.01b	3.4±0.01bc	3.4±0.01bc	3.1±0.02bc	2.6±0.00c	2.3±0.01d	6.2±0.01a	-	6.1±0.01a	0.6±0.01e
Others	0.5	0.6	7.6	4.9	7.2	7.8	8.3	2.4	4.2	7.8	9.9	9.6

Each value in the table represents the mean ± S.D. of two measurements. Abbreviations: Triacylglycerol (TAG), C capric, La lauric, M myristic, P palmitic, O oleic, St stearic L linoleic, trisaturated (SSS), monounsaturated (SUS), diunsaturated (SUU), polyunsaturated (UUU), palm mid-fraction (PMF), refined bleached deodorized palm kernel oil (RBDPKO), refined bleached deodorized palm stearin (RBDPS) and cocoa butter (CB).

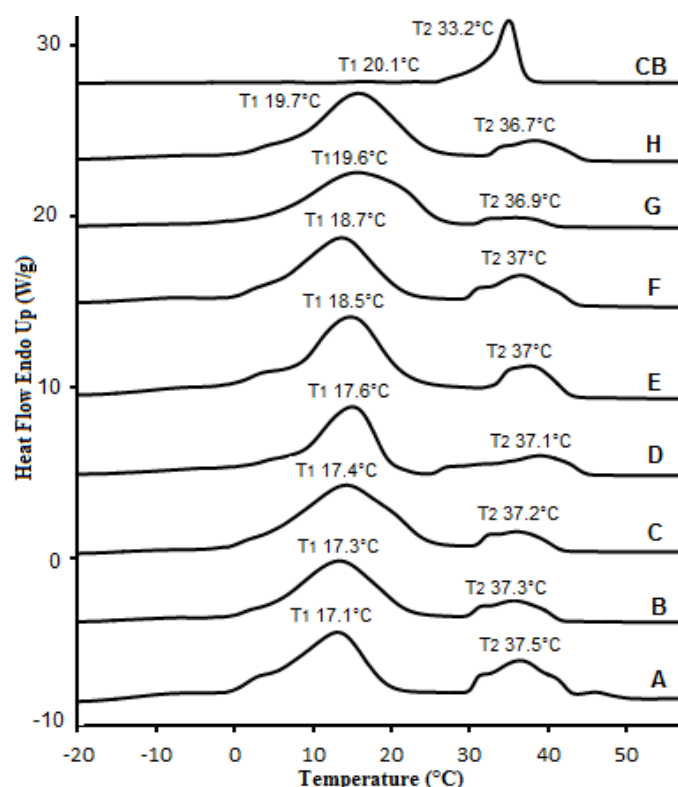


Figure 3.1. DSC melting curves for ternary mixtures (A-H) of PMF/RBDPKO/RBDPS.

3.3.4 Solid fat content (SFC)

The SFC profile of the investigated fat samples was shown in Figure 3.2. CB showed a high SFC ($\geq 70\%$) up to 20°C , followed by a steep decline between 25 and 35°C and 0% SFC was detected at or above 37°C (Figure 3.2). This finding was in agreement with previous studies by Kadivar *et al.* [74], who reported there were more than 75% SFC up to 20°C , followed by a steep decrease between 25 and 35°C and no solids above the body temperature. It was observed from Figure 3.2 that the SFC of all the eight ternary mixtures decreased gradually with increasing temperature. The SFC of the ternary mixtures showed a maximum decline at temperatures ranging from 15 to 25°C . This behavior was likely caused by the decreased proportion of unsaturated fatty acids (Table 3.2) and SUS TAGs (Table 3.3), which melted over this temperature range. The SFCs for mixtures A to E were found to be different from those of mixtures F to H (Figure 3.2). In the present study, blend E showed approximately 40% SFC at 20°C , 30% SFC at 25°C which are comparatively lower than that of CB (Figure 3.2). This was close to a report by Timms [140] who suggested that confectionery fat (e.g., chocolate) should exhibit approximately 63% SFC at 20°C , 40% SFC at 25°C and 0% SFC at 37°C . In another study of Talbot [135], fat with less than 50% SFC at 20°C is suitable as

confectionery fillings. In this regard, blend E could potentially be used as a CBS in confectionery fillings.

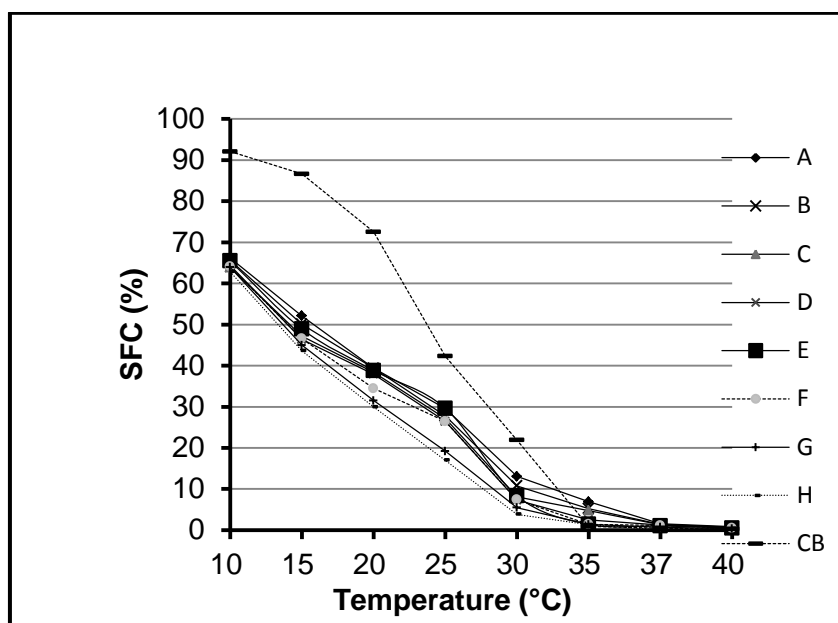


Figure 3.2. Solid fat content of ternary mixtures (A-H) of PMF/RBDPKO/RBDPS.

3.3.5 Iso-solid diagrams of ternary blends

Ternary iso-solid phase diagrams of PMF/RBDPKO/RBDPS mixtures at 10, 20 and 25°C are shown in Figure 3.3a-c. The ternary blends showed slightly curvatures at 10°C, which indicated the eutectic effect (Figure 3.3a). This behavior could be caused by the differences in SSS TAGs and SFC at low temperature among PMF, RBDPKO and RBDPS (Figure 3.2). As the temperature increased from 10 to 25°C, the eutectic effect gradually shifted to a monotectic effect. The contour lines of all the eight mixtures were nearly straight at 25°C (Figure 3.3c), indicating fats are compatible. In the case of blend E (14.9/59.6/25.5 PMF/RBDPKO/RBDPS), approximately 30% of SFC was observed at 25°C (Figure 3.2), which is within the monotectic area of the iso-solid diagram (Figure 3.3c).

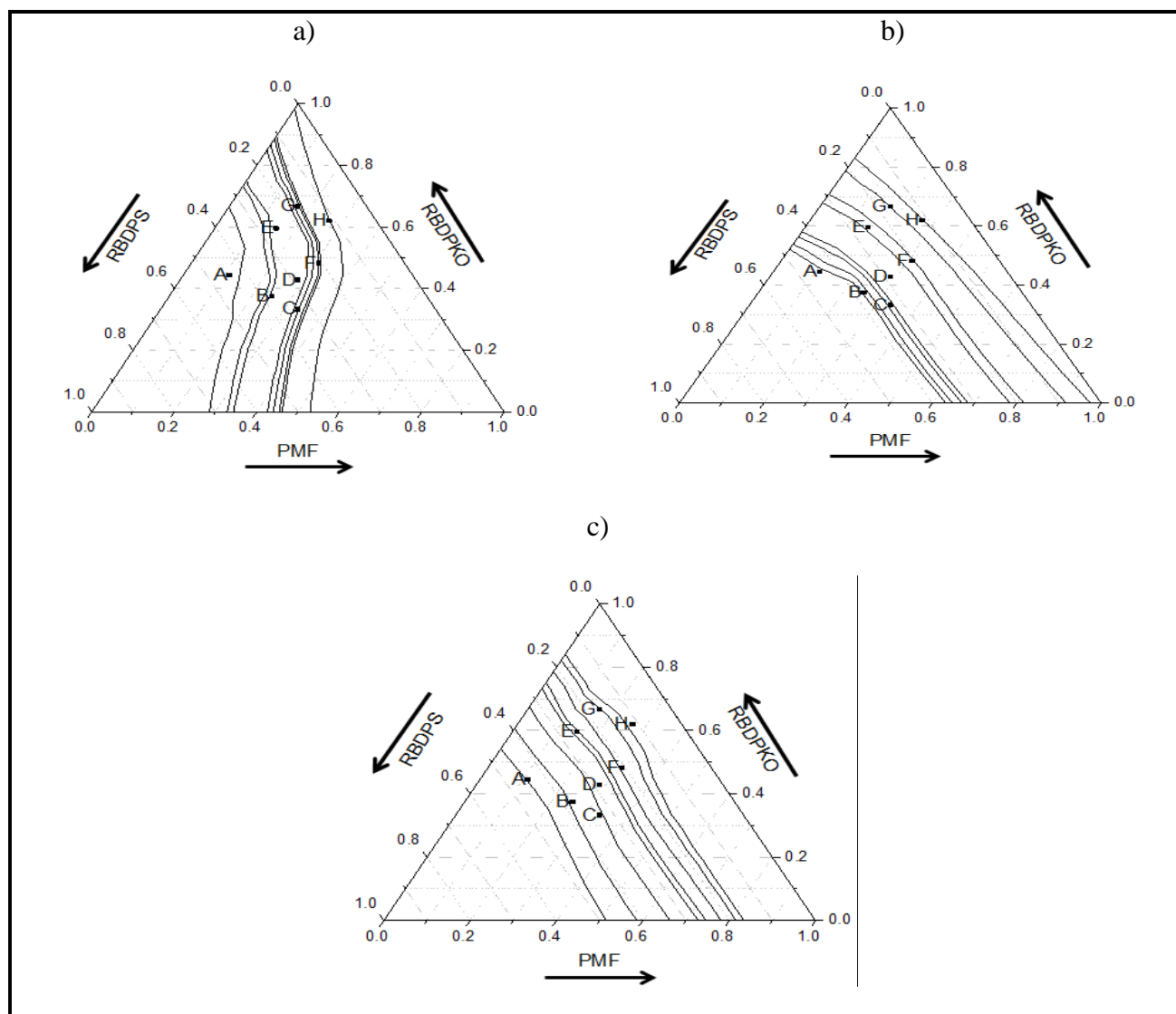


Figure 3.3. Ternary iso-solid phase diagrams for PMF/RBDPKO/RBDPS mixtures at a) 10°C, b) 20°C, and c) 25°C. The straight lines represent monotectic effect and curves represent eutectic effect.

3.3.6 Polymorphism

The polymorphic structures of individual PMF, RBDPKO, RBDPS, their ternary mixtures (A-H) and commercial CB were identified by XRD at 24°C (Figure 3.4). CB showed multiple diffraction peaks at $d = 3.8\text{--}4.3\text{ \AA}$ and 4.5 \AA , indicating a mixture of β' and β polymorphs. Two diffraction peaks at $d = 3.8$ and 4.3 \AA indicating the β' forms were observed for individual PMF. Similar XRD patterns were found for RBDPS with a major diffraction peak near 4.5 \AA , representing the β form. RBDPKO exhibited mainly three

diffraction peaks at $d = 3.8, 4.1$ and 4.3 \AA which are characterized by the β' forms. These findings were in agreement with previous studies [37,131,155].

Sato [122] reported that fat with high levels of PPP and SSS TAGs was responsible for β forms and POP/POSt were responsible for β' forms. RBDPS had a high percentage of PPP while PMF was rich in POP (Table 3.3), so RBDPS tends to have β crystals whereas PMF tends to have β' crystals. Timms [140] stated that palm kernel oil tends to crystalize in the stable β' form due to the presence of high percentage of LaLaLa TAG. In the present study, it was observed that with decreasing the concentration of RBDPS into the blends (A-H) resulted in disappearance of the major diffraction peak at $d = 4.5 \text{ \AA}$ (β formation) (Figure 3.4). This could be explained by the decreased proportion of PPP in RBDPS (Table 3.3). Blends A to E exhibited diffraction peaks at $d = 3.8, 4.2, 4.3 \text{ \AA}$ with a major peak at $d = 4.5 \text{ \AA}$, representing combinations of β' and β polymorphs. For blends F to H, peaks at $d = 3.8-4.3 \text{ \AA}$ (only β' formation) was observed. Vereecken *et al.* [144] reported that β' form is desired for confectionery fillings because it melts at low temperature with a fine arrangement, whilst β form gives hardness as well as rough and sandy textures. Blend E with 14.9/59.6/25.5 PMF/RBDPKO/RBDPS showed comparable fatty acid composition to CB, but its melting profile (18.5 to 37°C), 30% SFC at 25°C with polymorphism are different from CB, making it potentially useful as a CBS in confectionery fillings.

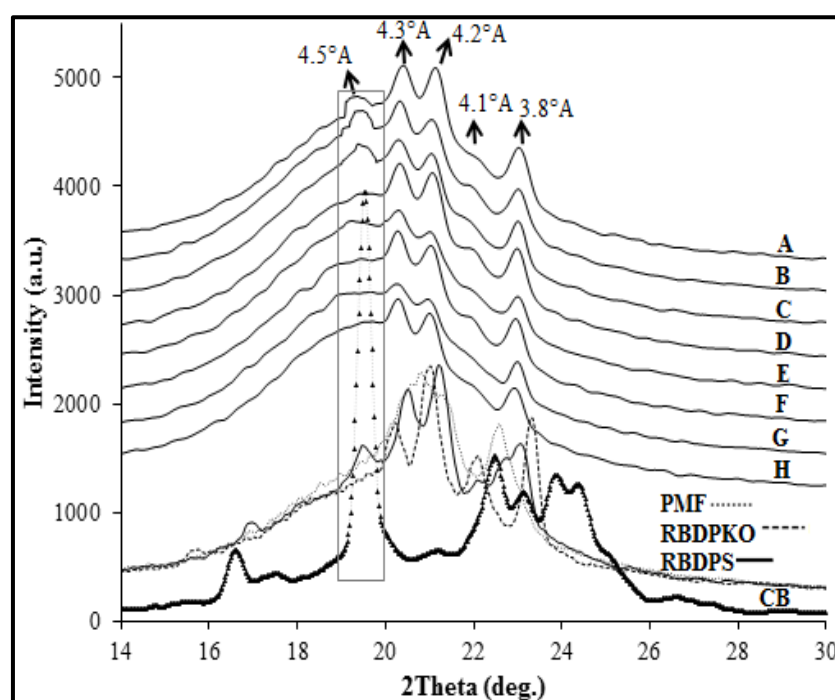


Figure 3.4. X-ray diffractograms of PMF, RBDPKO, RBDPS, their blends and commercial CB at 24°C.

3.3.7 Crystal morphology

The crystal morphology of individual PMF, RBDPKO, RBDPS, their ternary blend and CB were observed using PLM at 24°C (Figure 3.5). Commercial CB displayed spherulitic crystals (10-100 μm in diameter) consisting of needle-like crystals branching outward from the central nuclei (Figure 3.5a). The microstructure of individual PMF showed continuous granular crystals in the shape of very small spherulites (10-50 μm in diameter) with an orderly packed structure (Figure 3.5b). Similar granular crystals (densely packed) were observed for RBDPS with a size of less than 20 μm in diameter (Figure 3.5d). Large spherulitic crystals (100-300 μm in diameter) with a tight nucleus were observed in RBDPKO (Figure 3.5c). The morphology of RBDPKO was found to be consistent with that observed by Schmelzer *et al.* [125], who reported large spherulitic crystals.

The crystal network morphologies of all ternary blends were found to be a mixture of tightly packed spherulites and granular structures. With the addition of RBDPKO in the formulations, the spherulitic granular crystals shifted to large needle-like crystals. This variation could be related to the differences in the fatty acid composition (Table 3.2) and

TAG species (Table 3.3). Another possible reason for the differences in crystalline structure (size and shape) could be the differences in textural properties among PMF, RBDPKO and RBDPS [35]. A blend of 14.9/59.6/25.5 PMF/RBDPKO/RBDPS showed small spherulites ($\geq 50 \mu\text{m}$ in diameter) consisting of needle-like crystals radiating and branching outward from the central nuclei (Figure 3.5e). This behavior was explained by Jahurul et al. who reported spherulites exhibiting needle-like structures when blending mango seed fat and PMF [68]. No drastic change in microstructure in terms of size and shape was observed between CB and 14.9/59.6/25.5 PMF/RBDPKO/RBDPS blend. However, CB still had densely and orderly packed crystals compared to the ternary blend (Figure 3.5).

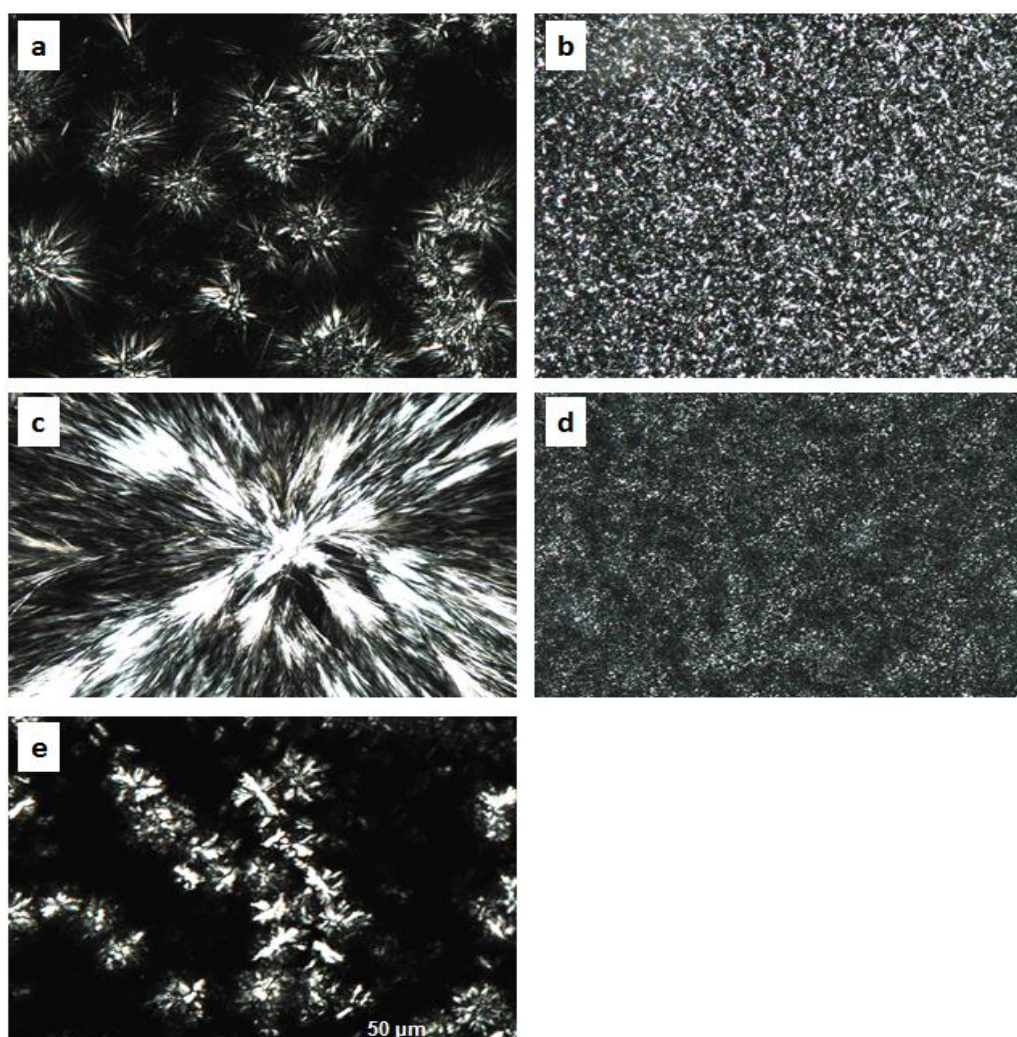


Figure 3.5. Polarised light microphotographs (40 \times lens) of (a) individual CB, (b) PMF, (c) RBDPKO, (d) RBDPS, and (e) ternary blend of PMF/RBDPKO/RBDPS (14.9/59.6/25.5, %w/w) obtained at 24°C.

3.4 Conclusion

The composition of palmitic (P) and oleic (O), POP, and crystal morphology (spherulitic crystals and $\geq 50\text{ }\mu\text{m}$ in diameter) of PMF/RBDPKO/RBDPS [14.9/59.6/25.5 (%w/w)] mixture were comparable to CB, while its melting profile (18.5 and 37°C), SFC at 20°C and polymorphism were different from CB. The iso-solid diagrams of the mixture displayed a monotectic effect at 20-25°C. Therefore, the 14.9/59.6/25.5 PMF/RBDPKO/RBDPS mixture could be used as a CBS in confectionery fillings because of the palmitic/oleic and POP composition, and crystal morphology comparable to those of CB.

Chapter 4

Work that is presented in this chapter is submitted to *European Journal of Lipid Science and Technology*, entitled “Physical properties of enzymatically produced palm oils-based cocoa butter substitute (CBS) with cocoa butter mixture” in May 2017

4 Investigation on the enzymatic interesterification of PMF/RBDPKO/RBDPS blend with commercial stearic/oleic fatty acids for CBS

4.1 Introduction

Cocoa butter (CB) is a core ingredient in chocolates and characterised predominantly with three main fatty acids: palmitic, stearic, and oleic acids corresponding to three major triacylglycerols (TAGs): POP, POSt and StOSt [21,88] as described in section 2.1 (Chapter 2). These TAGs dominate the melting characteristic, solid fat content as a function temperature and polymorphism of CB. CB becomes highly solid at 20°C and melts between 30 and 35°C [128]. CB has complex polymorphic forms namely γ , α , β' and β in ascending stability [37]. Usually, the stable polymorph β is preferred in chocolate because of its desirable melting characteristics [136].

CB is expensive among all the vegetable fats and oils due to its limited production and high market demand. Therefore, many studies have been performed to produce alternatives to CB.

In the earlier phase of this research (Chapter 3), RBDPKO was mixed with PMF and RBDPS to produce CBS [19] and the results showed low amount of stearic/oleic fatty acids compared to CB and several melting temperatures instead of a single melting peak between 30 and 35°C as shown by CB. To increase the fatty acids, addition of commercial stearic/oleic acids was considered in this study. Generally, TAGs which are responsible for the melting profile of the fat mixture, do not react with commercial fatty acids without the help of enzymatic interesterification [35,82,154]. Melting is the main characteristic that is used for the evaluation of an enzymatically produced CBA [151]. Enzymatic interesterification rearranges the fatty acids of TAGs and this process changes the melting temperatures. In this study, enzymatic interesterification is used to modify the melting profile of the fat mixture to resemble that of CB.

Enzymatic interesterification with sn-1, 3 specific lipases is now receiving more attention in the production of CBAs as enzyme lipases are usually cheap and reusable, and have high specificity and efficiency in acyl exchange reaction. Vegetable fats/oils such as PMF, palm olein, palm oil, fatty acid methyl ester, palmitic acid, stearic acid, mango seed, kokum, sal and tea seed oil have been used to prepare CBAs by enzymatic interesterification

[20,34,89,103,143]. Sridhar *et al.* [133] produced CBS from the lipase-catalysed interesterification of sal fat, kokum fat, mahua fat, dhupa fat and mango fat with methyl palmitate and/or stearate in an organic solvent *n*-hexane system, which showed the solid fat content and melting profile of interesterified kokum fat resembling those of CB. Abigor *et al.* [1] also produced CB-like fats from lipase-catalysed interesterification of palm oil and hydrogenated soybean oil, and reported major TAGs with melting profile similar to CB. However, no work has been reported using fat mixtures of PMF, RBDPS and RBDPKO to produce CBS with fatty acid and triacylglycerol constituents, melting properties and solid fat content of CBS that resemble of CB.

PMF, RBDPKO and RBDPS are readily available in the market at a reasonable price, making them cost-effective ingredients in chocolates and other confectionery products. The present study aimed to determine the effect of enzymatic interesterification of palm oil fractions mixture using commercial stearic/oleic fatty acids, with an ultimate goal to produce suitable CBS that have similar fatty acid and triacylglycerol constituents, melting properties and solid fat content to CB. CBS can only be mixed in small quantities with CB as they are usually not compatible (eutectic) [53,140]. When a CBS is mixed with commercial CB for chocolate formulation, it is important to consider the fatty acid, triacylglycerol constituents, melting profile, solid fat content as a function of temperature, polymorphism and crystal morphology of CBS that resemble those of CB. Therefore, the other objective of this study was to determine the compatibility of enzymatically modified palm oils-based CBS and CB mixtures for use in chocolate application.

4.2 Materials and methods

4.2.1 Materials

The materials of this chapter are similar to the previous chapter as described in section 2.2.1. Commercial stearic acid (18:0) and commercial oleic acid (18:1) known as palmera A9218 and palmera A1813 were purchased from Palm-Oleo Sdn. Bhd. (Klang, Malaysia). Lipozyme TL IM (*Thermomyces lanuginosa* lipase), a 1, 3 specific lipase (Activity, 250 IUN/g and immobilized on a non-compressible silica gel carrier) was kindly donated by Novozymes (Bagsvaerd, Denmark). The enzyme is optimally used at temperatures of 60-70°C.

4.2.2 Preparation of oil blends

Two ternary-blends with comparable major palmitic/oleic fatty acids and POP TAG to CB were selected for the current study from our preliminary study [19]. These blends are 14.9% PMF/59.6% RBDPKO/25.5% RBDPS (ternary-blend 1) and 33.3% PMF/33.3% RBDPKO/33.3% RBDPS (ternary-blend 2) (Chapter 3, Table 3.2). Firstly, commercial stearic acid and oleic acid at various ratios (%w/w) were added to the ternary-blend 1 (14.9% PMF/59.6% RBDPKO/25.5% RBDPS) to resemble the major fatty acids (palmitic, stearic and oleic) composition to CB as shown in Table 4.1. All the samples were melted at 100°C. Results showed that the constituent of stearic and oleic fatty acids increased, while the palmitic acid composition decreased considerably for samples A1 to D1 compared to CB. Taking this into account, ternary-blend 2 was chosen and examined. This blend (33.3% PMF/33.3% RBDPKO/33.3% RBDPS) had higher amount of palmitic acid with comparable amount of other fatty acids compared to that of ternary-blend 1, in addition to multiple melting peaks as per the blend 1. After the addition of different ratios (%w/w) of commercial stearic/oleic fatty acids to blend 2, similar trend of the fatty acids composition was observed in samples A2 to D2. Among all the eight samples, blend B2 (80% ternary-blend/15% stearic/5% oleic) with major fatty acids composition resembling closely that of CB was then selected for enzymatic interesterification.

Table 4.1. Blending ratios (w/w) of ternary-blend (14.9% PMF/59.6% RBDPKO/25.5% RBDPS or 33.3% PMF/33.3% RBDPKO/33.3% RBDPS), commercial stearic (18:0) and oleic (18:1) fatty acids.

Sample code	Blending ratio (w/w)		
	Ternary-blend	Stearic	Oleic
A1 or A2	75	15	10
B1 or B2	80	15	5
C1 or C2	80	10	10
D1 or D2	85	15	0

Abbreviations: Palm mid-fraction (PMF), refined bleached deodorized palm kernel oil (RBDPKO) and refined bleached deodorized palm stearin (RBDPS). 14.9% PMF/59.6% RBDPKO/25.5% RBDPS blend referring to “1” and 33.3% PMF/33.3% RBDPKO/33.3% RBDPS blend referring to “2”.

4.2.3 Enzymatic interesterification

Experiments were conducted to find out the optimum reaction time, reaction temperature, enzyme concentration and substrate ratio. Three different concentrations of Lipozyme TL IM (2, 4 and 6% w/v) were added to substrate oil (10 ml) in 50 ml conical flask. The flask was covered with aluminum foil and agitated in an incubator shaker (temperature controlled) at 250 *rpm*. The incubation temperature was maintained at 60°C to prevent solidification of the substrate. Enzymatic interesterification was monitored from 0 to 10 h at 2 h intervals. The interesterification reaction was stopped by filtering out the enzyme through a double layer of cheese cloth. The free fatty acids (FFA) were removed by alkaline neutralization as described by Kuleasan [83] with minor modifications. Twenty ml of the oil was placed in a 100 ml glass beaker with magnetic stirring at 800 *rpm*. Thereafter, 1 ml of caustic solution (20% w/v NaOH) was added to the sample. The mixture was heated at 70°C for 25 min (to break any emulsion) and then centrifuged immediately at 4000 *rpm* for 20 min to remove the soap. The centrifuge was maintained at 40°C to prevent solidification of the oil. The FFA was determined according to the AOCS Official Method Ca 5a-40, as percentage of stearic acid [51].

4.2.4 Blending of enzymatically produced CBS and CB

Enzymatically produced CBS (interesterified B2, as described in the section 4.2.2) and commercial CB were mixed at proportions (CBS/CB, %w/w) of 5:95 (blend a), 10:90 (blend b), 20:80 (blend c), 30:70 (blend d), 40:60 (blend e) and 50:50 (blend f), and the TAG composition, melting and compatibility behaviors, polymorphism and crystal morphology of these blends were analyzed.

4.2.5 Fatty acid analysis

Fatty acid composition was determined using gas chromatography fitted with FID as described in section 2.2.5 with minor modification [21]. The samples (15 mg) were weighed and dissolved in 1.5 ml of methanol/toluene/sulphuric acid (88/10/2) inside a 5 ml glass vial. The mixtures were added to 1 ml of heptane and then mixed vigorously for 1 min by using a vortex mixer.

4.2.6 Melting behavior

Melting profile of the samples was determined using differential scanning calorimetry (DSC) fitted with nitrogen gas flow rate of 20 ml/min as described in section 2.2.6 [18].

4.2.7 Triacylglycerol analysis

The TAG profile of the selected samples was analysed using high performance liquid chromatography equipped with RID as described in section 2.2.4 [18].

4.2.8 Solid fat content (SFC)

SFC profile of the selected fats was determined using pulsed nuclear magnetic resonance (pNMR), according to the AOCS Official Method Cd 16b-93 for stabilizing confectionery fats as described in section 3.2.5 [19].

4.2.9 Polymorphism

The polymorphic forms of the fat samples were determined at 24°C (room temperature) using a D8 Discover X-ray diffraction (XRD, Bruker, Karlsruhe, Germany) fitted with a Cu-K α radiation ($k = 1.5418 \text{ \AA}$, voltage 40 kV and current 40 mA) as described in section 3.2.7.

4.2.10 Crystal morphology

Polarized light microscope (PLM) equipped with digital camera (Nikon, DS-Filc, Tokoyo, Japan), was used to observe the crystal network microstructure of enzymatically produced CBS (interesterified B2) and CB mixture as described in section 3.2.8 [106].

4.2.11 Statistical analysis

Data were statistically analysed by one-way analysis of variance (ANOVA) using the OriginPro 9.1 software (OriginLab Corp., Northampton, USA). Tukey's test was applied to determine the significant difference at $P < 0.05$ level. DSC, XRD and PLM analyses were conducted in triplicate. NMR and FFA analyses were performed in duplicate.

4.3 Results and discussion

4.3.1 CBS production and its characterization

4.3.1.1 Fatty acid composition

Table 4.2 illustrates the fatty acid profiles of individual commercial stearic acid (18:0), oleic fatty acid (18:1), ternary-blend 1 (14.9% PMF/59.6% RBDPKO/25.5% RBDPS), ternary-blend 2 (33.3% PMF/33.3% RBDPKO/33.3% RBDPS) and commercial CB. Commercial stearic fatty acid had 93.43% stearic and 5.43% palmitic acids. Commercial oleic fatty acid showed 80.5% oleic, followed by 11.25% linoleic, 4.14% palmitic and 2.83% stearic acids. The results of the commercial stearic and oleic fatty acids were consistent with the literature [152]. Commercial CB exhibited 36.15% stearic, followed by 33.24% oleic, 25.69% palmitic and 3.13% linoleic acids. This was in agreement with the existing literature [21].

The fatty acid profiles of the different mixtures of ternary-blend 1 or 2/stearic/oleic (A1 to D2) are shown in Table 4.2. With the addition of commercial stearic/oleic acids to the ternary-blend 1 (14.9% PMF/59.6% RBDPKO/25.5% RBDPS), the amount of stearic and oleic acids increased, whereas the amount of palmitic, lauric (12:0) and myristic (14:0) acids decreased considerably ($P < 0.05$) for samples A1 to D1 (Table 4.2). In samples A1 to D1, the amount of undesirable lauric and myristic acids was found to be higher, while the amount of palmitic, stearic and oleic acids was significantly ($P < 0.05$) lower than commercial CB. Likewise by adding commercial stearic and oleic acids to ternary-blend 2 (33.3% PMF/33.3% RBDPKO/33.3% RBDPS), similar trend of the fatty acids composition was found for

samples A2 to D2 (Table 4.2). However, samples A2 to D2 had almost two-times lower amount of undesirable lauric and myristic acids than samples A1 to D1 (Table 4.2). Besides, the composition of major palmitic, stearic and oleic acids in samples A2 to D2 was found to be comparable to commercial CB. The findings of the current study were compared to the existing literatures: Calliauw *et al.* [27] produced CBSs through two-stage static fraction of palm kernel oil, and reported the fatty acid profile as lauric (56.3%), myristic (19.6%), palmitic (8.9%) and stearic (2.0%). Zaidul *et al.* [152] also studied the fatty acids of different blends of supercritical carbon-dioxide extracted palm kernel oil fractions and palm oil in various ratios to obtain CB replacers, and reported that the fatty acid profile of certain blends was comparable to commercial CB.

Table 4.2. Fatty acid composition of commercial stearic acid, commercial oleic acid, ternary-blend 1 (14.9% PMF/59.6% RBDPKO/25.5% RBDPS) or ternary-blend 2 (33.3% PMF/33.3% RBDPKO/33.3% RBDPS), their mixture (blend component according to the blending ratios in Table 4.1) and commercial CB.

Sample	Fatty acid (area %)								
	C _{8:0}	C _{10:0}	C _{12:0}	C _{14:0}	C _{16:0}	C _{18:0}	C _{18:1}	C _{18:2}	C _{20:0}
Commercial stearic acid	-	-	-	-	5.43±0.1h	93.43±0.5a	-	-	1.14±0.0a
Commercial oleic acid	-	0.25±0.0b	0.45±0.0i	0.16±0.1i	4.14±0.1h	2.83±0.0i	80.5±0.6a	11.25±0.2a	0.42±0.0a
Ternary-blend 1	2.47±0.1a	2.01±0.1a	29.06±0.2a	9.14±0.1a	25.74±0.3bc	3.12±0.1i	24.51±0.2g	3.95±0.1bc	-
Ternary-blend 2	1.69±0.1a	1.38±0.1a	23.24±0.3b	8.09±0.0b	33.00±0.5a	3.29±0.1i	26.84±0.4de	2.47±0.1d	-
A1	0.4±0.0b	0.2±0.0b	19.64±0.5d	4.65±0.1e	17.68±0.1f	27.59±0.8g	26.36±0.4e	3.48±0.1c	-
B1	0.3±0.1b	0.3±0.0b	20.12±1.1d	5.22±0.7d	14.51±0.4g	31.30±0.5e	25.25±0.4f	3.0±0.2cd	-
C1	0.5±0.1b	0.3±0.1b	18.42±0.7e	3.73±0.1f	17.24±0.4f	28.12±1.1f	27.24±0.7d	4.45±0.1b	-
D1	0.7±0.1b	0.6±0.1b	21.45±0.5c	6.24±0.4c	18.56±0.6f	32.25±0.2d	17.84±0.7h	2.36±0.2d	-
A2	-	0.4±0.0b	8.04±0.4h	1.43±0.2h	20.35±1.0e	37.95±0.5b	27.91±0.5d	4.32±0.2b	-
B2	-	0.2±0.1b	8.52±0.1h	1.13±0.2h	24.81±0.6cd	32.33±0.7d	29.10±0.5c	3.91±0.3bc	-
C2	Trace	0.4±0.1b	12.41±0.4g	4.11±0.2ef	23.03±0.5d	26.41±0.7h	29.16±0.6c	4.38±0.2b	-
D2	0.3±0.1b	Trace	15.53±0.3f	2.83±0.3g	26.03±0.5b	32.73±0.3d	19.76±0.7	2.74±0.1d	-
CB	-	-	Trace	0.73±0.1h	25.69±0.2bc	36.15±0.5c	33.24±0.3b	3.13±0.4c	1.04±0.1a

Values within the same column with different letters are significantly different ($P<0.05$). Each value in the table represents the mean \pm SD of three measurements. Abbreviations: Palm mid-fraction (PMF), refined bleached deodorized palm kernel oil (RBDPKO), refined bleached deodorized palm stearin (RBDPS) and cocoa butter (CB). 14.9% PMF/59.6% RBDPKO/25.5% RBDPS blend referring to “1” and 33.3% PMF/33.3% RBDPKO/33.3% RBDPS blend referring to “2”.

4.3.1.2 DSC melting thermograms

The DSC melting thermograms of individual commercial stearic acid, oleic fatty acid, ternary-blend 1 (14.9% PMF/59.6% RBDPKO/25.5% RBDPS), ternary-blend 2 (33.3% PMF/33.3% RBDPKO/33.3% RBDPS) and commercial CB are shown in Figure 4.1. Commercial stearic acid and oleic acid showed a sharp endotherm at 70°C and 9.6°C respectively. Both ternary-blends 1 and 2 had two broad endotherms between 17 and 37°C as described in our earlier study [19]. Commercial CB exhibited a single endotherm at approximately 33°C. The DSC melting thermogram of CB was found to be consistent with previous studies [150], who reported a single endotherm at 32.8°C.

The DSC melting profiles of the different mixtures of ternary-blend 1 or 2/stearic/oleic are shown in Figure 4.1. When commercial stearic and oleic acids were added to ternary-blend 1 and ternary-blend 2, the DSC melting thermograms showed mainly two broad endotherms, first maxima (T_1) between 13.6 and 20°C and second one (T_2) between 50.1 and 53.6°C. The first endothermic peak (T_1) corresponded to the low melting unsaturated fatty acids (Table 4.2). The second endothermic (T_2) event was likely due to the high melting stearic acid (Table 4.2). Thus, all the samples (A1 to D2) were not suitable as alternatives to CB because of their undesirable multiple melting profiles. Hence, enzymatic interesterification was used to modify the TAG composition and melting profile resembling that of CB. In the current study, sample B2 (80% ternary-blend/15% stearic/5% oleic) was chosen for enzymatic interesterification as it showed undesirable multiple melting peaks as per other samples A1 to D2 (Figure 4.1) and major fatty acids composition resembling closely that of commercial CB (Table 4.2).

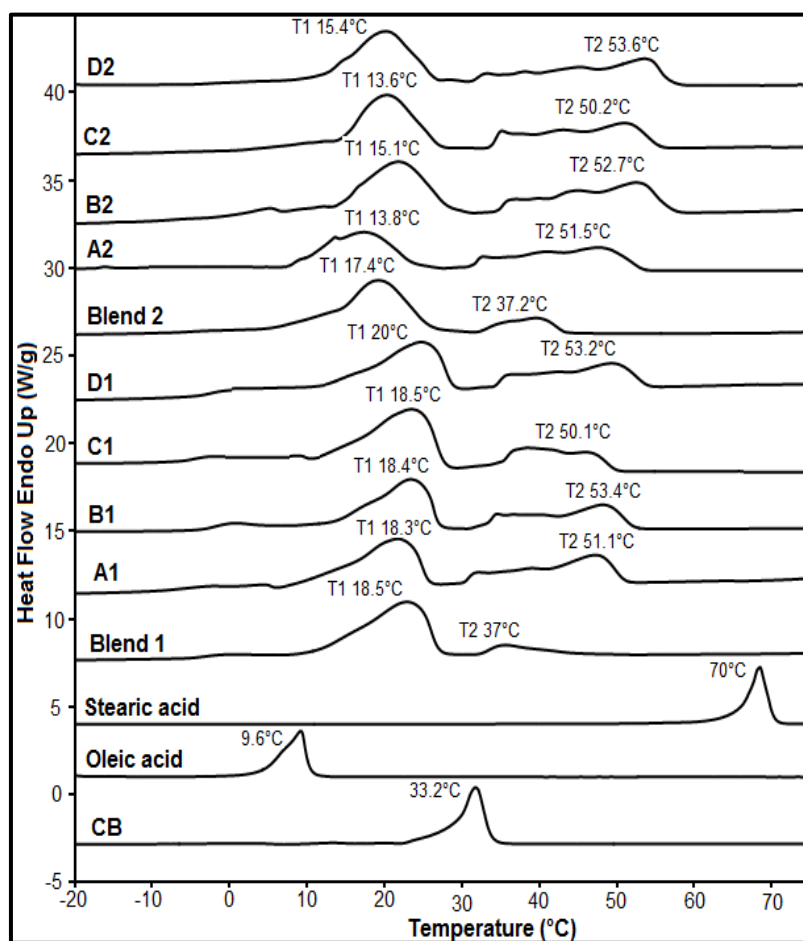


Figure 4.1. DSC melting thermograms of commercial stearic acid, commercial oleic acid, ternary-blend 1 (14.9% PMF/59.6% RBDPKO/25.5% RBDPS) or ternary-blend 2 (33.3% PMF/33.3% RBDPKO/33.3% RBDPS), their mixture (referring to A1 to D2 as per Table 4.1) and commercial CB.

4.3.1.3 Optimization of the reaction parameters

Enzymatic interesterification was performed to determine the optimum enzyme concentration with substrate ratio (2-6% w/w), reaction temperature (60°C) and reaction time (0-10 h).

Two endotherms were observed between 17.3°C and 50.5°C at 2% enzyme at 0 h (control) (Figure 4.2). With increasing the reaction time to 6 h, the melting peaks gradually shifted to 13.7°C and 31.1°C respectively. After 8 h treatment, a broad endotherm was observed at 28.9°C. When the reaction time increased to 10 h, the broad endotherm was reduced to 27.2°C. Likewise, by increasing the enzyme concentration to 4% (w/w), two endotherms were observed similar to 2% enzyme concentration for 0 h (control), indicating reaction time has a considerable impact on esterification process (Figure 4.2). When the reaction time was

increased to 6 h, the endotherms shifted and formed a new endotherm near 33.5°C, indicating the formation of high melting TAGs. Similar trend was found at 6% enzyme concentration at 6 h, in which a new endotherm was observed at 28.1°C. After 8 h incubation at 4 and 6% enzyme concentrations, two endotherms were observed between 16.5°C and 35.5°C, probably due to the rearrangement of fatty acids (Table 4.2). Among all the interesterification conditions, interesterified B2 under optimized interesterification conditions (using 4% enzyme incubated for 6 h reaction time at 60°C) showed a single broad melting endotherm at 33.5°C, which is similar to commercial CB (Figure 4.2). Wang *et al.* [147] produced CBE through enzymatic interesterification of tea seed oil with fatty acid methyl esters and reported a new high melting peak at 37.7°C, which was observed after 60 h treatment at 35°C using 10% enzyme. Abigor *et al.* [1] prepared a CB-like fat with a single melting peak at 33.8°C from palm oil and hydrogenated soybean oil using 10% lipase enzyme after incubating 4 h at 70°C. Similarly in the present study, interesterified B2 using 4% lipase enzyme after incubating 6 h at 60°C showed a desirable single melting peak at 33.5°C, therefore, interesterified B2 could be potentially used as CBS.

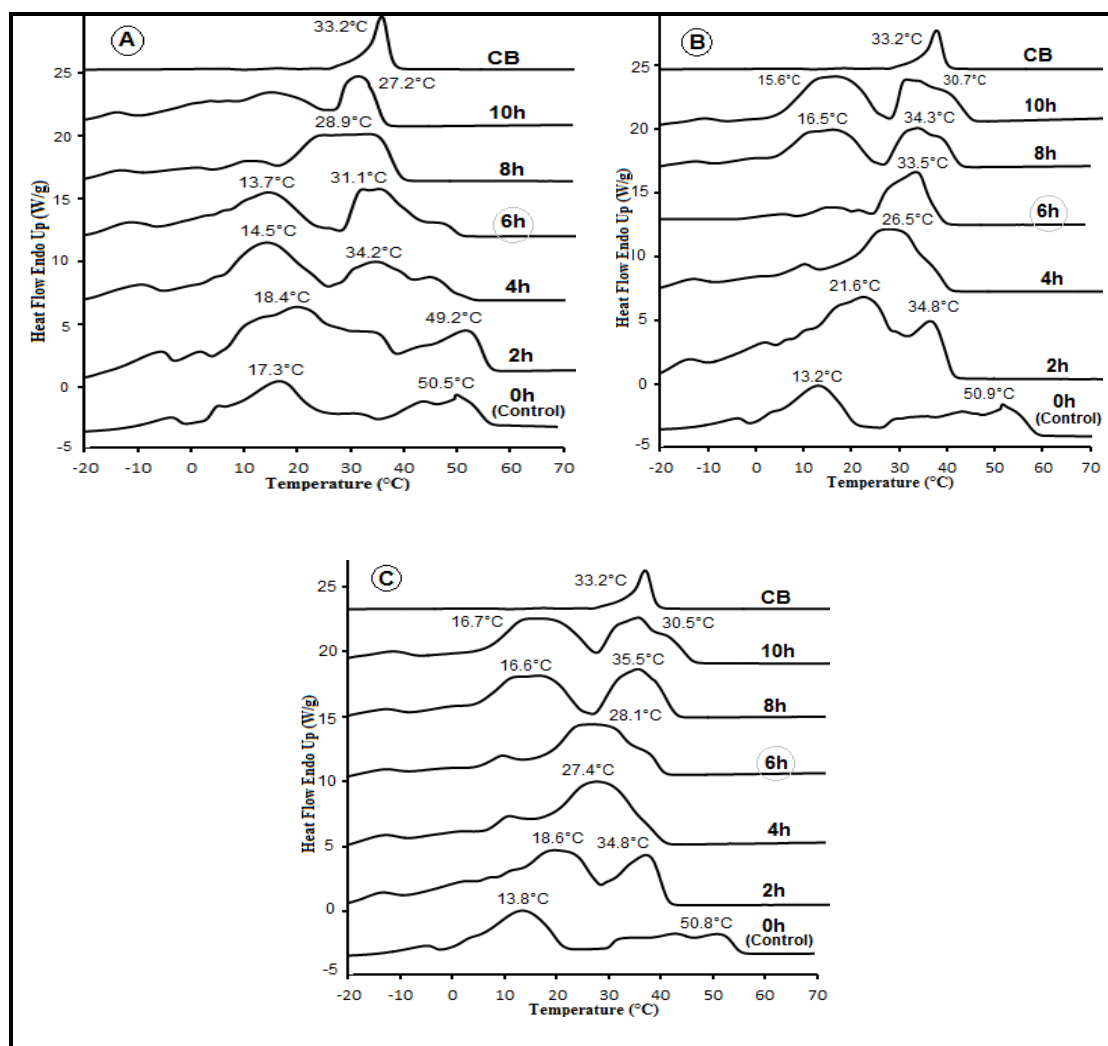


Figure 4.2. DSC melting thermograms of (A) 2% Enzyme, (B) 4% Enzyme and (C) 6% Enzyme concentrations for sample B2 (referring in Table 4.1).

4.3.1.4 Triacylglycerol (TAG) composition

After interesterification, substantial changes ($P < 0.05$) of the TAG species in the interesterified B2 were observed compared to its non-interesterified B2 (Table 4.3). The composition of POP (17.7%) and PLP (1.4%) of the interesterified B2 rapidly decreased, whereas the composition of POST (28.4%), StOSt (19.5%), PLO (6.1%) and StOO (1.3%) increased correspondingly after interesterification (Table 4.3). The changes in the TAGs composition were due to the rearrangement of the fatty acids during interesterification (Figure 4.2). Other forms of SSS TAG species such as PPP, PPSt, LaLaLa (La lauric) and LaLaM (M myristic) were also observed in the interesterified B2 (Table 4.3). These TAGs may be responsible for shoulder peaks at the main melting region with small endotherms below 25°C of the interesterified B2 (Figure 4.2). These findings coincided with the results

obtained by Undurraga & co-workers [143], who produced CBE from enzymatic interesterification of palm mid-fraction and stearic acid, and also reported POP (23.4%), POSt (38.5%) and StOSt (20.2%). In another study [88], the composition of three TAGs: POP (23%), POSt (39.9%) and StOSt (13.5%) was observed upon Lipozyme IM-20 interesterification of lard and tri-stearin using a supercritical-CO₂ system.

4.3.1.5 Free fatty acid (FFA) analysis

The percentage of FFA was found to be slightly higher in the interesterified B2 compared to commercial CB (Table 4.3). During enzymatic interesterification, fatty acids are cleaved off the glycerol backbone, and not all of these fatty acids reattach to the TAG, resulting in FFA. Alkaline neutralization reduced FFA to 1.7%.

Table 4.3. Overview of TAGs composition of individual CB, enzymatically produced CBS (interesterified B2) and different blends (a-f) of enzymatically produced CBS/CB, and non-interesterified B2 (80% ternary blend/15% stearic/5% oleic).

TAG (area %)		CB	Blend						CBS (IE B2)	Non-IE
			a	b	c	d	e	f		
SSS	PPP	0.1±0.0f	0.9±0.2e	1.5±0.4e	2.1±0.3d	2.5±0.2d	4.2±0.1c	4.4±0.4c	8.4±0.2b	10.1±0.3a
	PPSt	0.5±0.0cd	0.2±0.1d	1.0±0.2c	1.3±0.3b	1.3±0.1b	2.0±0.2a	2.1±0.2a	2.4±0.4a	-
	StPSt	-	0.2±0.0c	0.5±0.1bc	0.6±0.0bc	0.7±0.1ab	0.7±0.0ab	0.8±0.2ab	1.2±0.2a	-
	CLaLa	-	-	-	-	-	-	-	-	2.1±0.1
	LaLaLa	-	0.3±0.0f	1.2±0.2e	1.7±0.2de	2.1±0.2cd	2.4±0.0c	2.7±0.0c	4.7±0.3b	10.3±0.7a
	LaLaM	-	0.1±0.0e	0.4±0.0de	0.5±0.2de	0.8±0.0cd	1.3±0.2c	1.4±0.2c	2.3±0.1b	6.4±0.1a
	LaMM	-	-	-	-	-	-	-	-	3.4±0.1
	MMM	-	0.1±0.0b	0.2±0.0b	0.2±0.0b	0.3±0.0b	0.4±0.3b	0.5±0.2b	1.1±0.2a	1.2±0.1a
	Total	0.6	1.8	4.8	6.4	7.7	11.0	11.9	20.1	33.5
SUS	POP	18.1±0.8b	18±0.3b	17.8±1.0b	17.7±1.2b	17.7±0.7b	17.7±0.5b	17.7±0.7b	17.7±1.6b	44.2±1.7a
	POSt	39.2±1.2a	38.9±1.2a	38.4±1.5b	37.9±1.3c	37.2±0.9d	34.5±0.8e	33.8±1.0f	28.4±1.2g	7.6±0.1h
	StOSt	29.7±0.7a	29.2±1.1a	28.3±0.7b	27.8±1.2c	26.4±1.2d	24.7±0.7e	24.2±0.7f	19.5±0.8g	1.2±0.1h
	LaOLa	-	0.1±0.0b	0.2±0.0ab	0.3±0.0ab	0.2±0.0ab	0.4±0.0ab	0.5±0.2ab	0.7±0.2a	0.4±0.3ab
	AOSt	1.9±0.5a	1.8±0.1a	1.2±0.7c	1.0±0.2cd	0.7±0.0cde	0.5±0.0de	0.5±0.0de	0.6±0.1de	0.2±0.3e
	PLP	1.1±0.0b	1.2±0.2b	1.2±0.0b	1.3±0.2b	1.3±0.2b	1.3±0.1b	1.3±0.0b	1.4±0.3b	6.7±0.4a
	MLP	0.6±0.0cd	0.6±0.2cd	0.8±0.0bc	0.9±0.0abc	1.0±0.2abc	1.1±0.1abc	1.2±0.0ab	1.4±0.2a	0.2±0.3d
	Total	90.6	89.7	87.9	86.9	84.5	80.2	79.2	69.7	60.5
SUU	PLL	0.5±0.0a	0.5±0.0a	0.5±0.0a	0.5±0.0a	0.6±0.2a	0.6±0.0a	0.7±0.0a	0.8±0.0a	0.2±0.3a
	PLO	0.6±0.2f	0.7±0.0f	1.3±0.2e	1.9±0.0d	3.7±0.1c	4.9±0.7b	5.0±0.2b	6.1±0.7a	2.3±0.1d
	POO	2.8±0.4a	2.7±0.2a	1.8±0.1bc	1.7±0.2c	1.3±0.1c	1.3±0.0c	1.3±0.2c	1.3±0.2c	2.1±0.1b
	StOO	2.4±0.1a	2.3±0.4a	1.7±0.0b	1.2±0.2b	1.2±0.2b	1.2±0.0b	1.3±0.2b	1.3±0.0b	-
	Total	6.3	6.2	5.3	5.3	6.8	8.0	8.3	9.5	4.6
UUU	LLO	0.4±0.0a	0.4±0.2a	0.4±0.0a	0.3±0.2a	0.3±0.0a	0.2±0.0a	0.1±0.2a	0.1±0.0a	0.3±0.1a
	OOL	0.7±0.1a	0.6±0.0a	0.6±0.0a	0.6±0.2a	0.4±0.0a	0.3±0.0a	0.2±0.0a	0.2±0.0a	0.4±0.1a
	OOO	1.4±0.2a	1.3±0.0a	1.0±0.2ab	0.5±0.0bc	0.3±0.0c	0.3±0.0c	0.3±0.0c	0.4±0.0c	0.7±0.1a
	Total	2.5	2.3	2.0	1.4	1.0	0.8	0.6	0.7	1.4
FFA		1.2±0.3a	-	-	-	-	-	-	1.7±0.3a	0.6±0.3b

Values within the same row with different letters are significantly different ($P<0.05$). Blends a (5%CBS/95%CB), b (10%CBS/90%CB), c (20%CBS/80%CB), d (30%CBS/70%CB), e (40%CBS/60%CB) and f (50%CBS/50%CB). Each value in the table represents the mean \pm SD of two measurements. Abbreviations: Triacylglycerol (TAG), cocoa butter (CB), cocoa butter substitute (CBS), free fatty acid (FFA), interesterified fat (IE), total content of tri-saturated (SSS), total content of mono-unsaturated (SUS), total content of di-unsaturated (SUU), total content of poly-unsaturated (UUU), P palmitic, St stearic, C capric, O oleic, La lauric, L linoleic, M myristic, A arachidic.

4.3.2 Physical properties of enzymatically produced CBS (interesterified B2) and CB blends

4.3.2.1 TAG composition of the CBS/CB blends

The TAG profiles of the CBS and CB blends are presented in Table 4.3. The composition of mono-unsaturated (SUS: POST and StOSt), di-unsaturated (SUU: POO and StOO) and poly-unsaturated (UUU: OOO, OOL and LLO) TAGs decreased gradually with increasing CBS in blends a-f, whereas the composition of tri-saturated (SSS: PPP, LaLaLa, LaLaM and PPSt) TAG increased significantly ($P < 0.05$). It was also observed that the major TAGs composition (POP, POST and StOSt) of blends a and b (5-10% of CBS in CB) did not change significantly. However, by adding more than 10% CBS in blends c-f, SSS TAG content was significantly ($P < 0.05$) increased along with a gradual decrease in SUS particularly POST and StOSt. In this regard, blends a and b (5-10% of CBS in CB) were found to be the most compatible blend formulation to that of CB in terms of TAG content.

4.3.2.2 Thermal properties and iso-solid diagrams of the developed CBS/CB blends

The melting profiles of the different mixtures (a-f) of enzymatically produced CBS and commercial CB are shown in Figure 4.3. CB showed a sharp melting peak at 33.2°C with onset temperature (T_{onset}) at 30.2°C and endset temperature (T_{endset}) at 36.1°C. When the proportion of CBS increased in blends a-f, the DSC melting thermogram became broad. This may be due to the differences in long-chain fatty acids (Table 4.2) and TAG contents of CBS and CB (Table 4.3). However, the melting peak temperature remained unchanged. Blends a-c (5-20% of CBS in CB) showed comparable onset and endset of the melting temperature to CB, whereas blends d-f (>20% of CBS in CB) displayed a lower T_{onset} with a broader peak. This can be explained by the higher content of SSS TAG in CBS (Table 4.3). Enzymatically produced CBS exhibited a broad melting peak at 33.5°C with T_{onset} at 25.2°C and T_{endset} at 37.6°C (Figure 4.3). The broader melting peak can lead to a waxy mouth-feel, less cooling sensation and less intense flavour release [74]. In the present study, the melting profile of blends a-c (5-20% of CBS in CB) was comparable to that of CB.

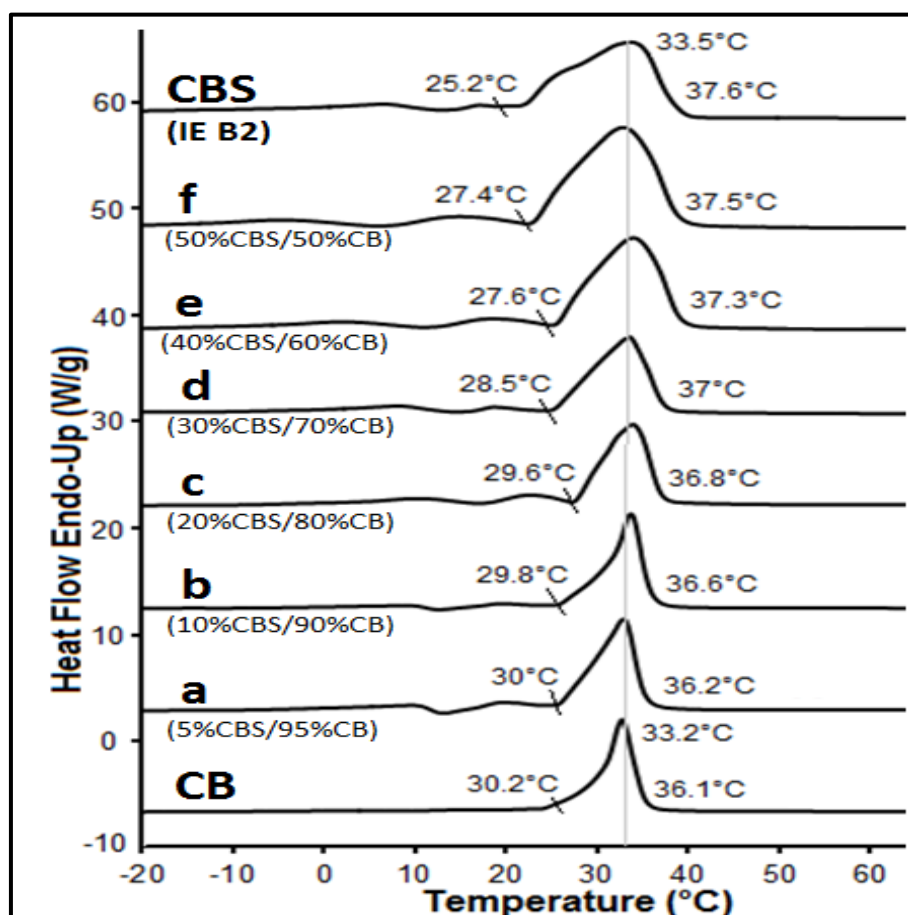


Figure 4.3. DSC melting thermograms of enzymatically produced CBS (interesterified B2) and commercial CB mixtures: a (5%CBS/95%CB), b (10%CBS/90%CB), c (20%CBS/80%CB), d (30%CBS/70%CB), e (40%CBS/60%CB) and f (50%CBS/50%CB).

In Figure 4.4, commercial CB displayed a high SFC ($\geq 70\%$) up to 20°C , followed by a steep decline between 20 and 35°C , and 0% SFC was detected at or above 37°C . This finding was in agreement with previous studies [74], who reported a high SFC value ($\geq 75\%$) at 20°C , a steep decrease between 25 and 35°C , and no solids above body temperature. There was a significant change ($P < 0.05$) of SFC at all temperatures before interesterification and after interesterification of the sample B2. Before interesterification, the sample B2 showed just below 40% SFC at 20°C and approximately 1% SFC at 37°C . However, after interesterification, the SFC value of the interesterified B2 was observed at approximately 48% at 20°C and 0% at or above 37°C . The difference of the SFC trend between non-interesterified and interesterified B2 could be probably explained by the variation of fatty acid (Table 4.2) and TAG composition (Table 4.3). However, interesterified B2 showed

considerably lower SFC values between 10 and 30°C than commercial CB. This behavior was most likely due to the differences of POSt and StOSt TAGs (Table 4.3). Kadivar and co-workers [74] produced enzymatic interesterification of sunflower oil-based CBEs and also reported approximately 45% SFC at 20°C and 1% SFC at 37°C. An earlier study [139] suggested that confectionary fats (e.g., chocolate) should exhibit approximately 63% SFC at 20°C, 40% SFC at 25°C and 0% SFC at 37°C. In the present study, the interesterified B2 had considerably lower SFC values at 10-25°C compared to the above literatures and commercial CB (Figure 4.4), making it potential for use as CBS in terms of melting profile (Figure 4.3) and fatty acid/TAG composition (Table 4.2 and Table 4.3).

The SFC profile of all the blends a-f showed a significant ($P < 0.05$) decrease between 10 and 30°C with increasing percentage of CBS (Figure 4.4). Blends c to f (20-50% CBS) had a lower SFC value at those mentioned temperatures, due to the presence of SSS TAG content in CBS (Table 4.3). Regarding blends a and b (5-10% of CBS in CB), SFC values at all the temperatures were found to be similar as per CB. This was most likely due to the comparable content of SUS TAG (Table 4.3).

Iso-solid phase diagrams are used to illustrate the eutectic and monotectic behavior of binary fat mixtures because they are useful in understanding the compatibility of mixed fat systems [145]. For instance, the eutectic effect occurs, when the contour lines of constant SFC are not straight, with some blend compositions having lower melting temperatures than expected. This indicates that the fat blends are not compatible (eutectic). Monotectic effect (dilution effect or miscible) is manifested by a straight line connecting the SFC of each pure component, indicating that fats in a blend are mixed well [139]. Binary iso-solid phase diagrams of the CBS/CB blends are shown in Figure 4.5. The binary blends showed slightly curvature above 25°C, which indicated an undesirable eutectic effect (Figure 4.5). This behavior could be mainly caused by the differences in TAG content between CBS and CB (Table 4.3). The iso-solid plot of all the six blends was nearly straight at 15 to 25°C, showing that fats are mixed well (compatible). Blends a and b (5-10% of CBS in CB) displayed approximately 70% SFC at 20°C (Figure 4.4), which are within the desirable monotectic area of the iso-solid diagram (Figure 4.5).

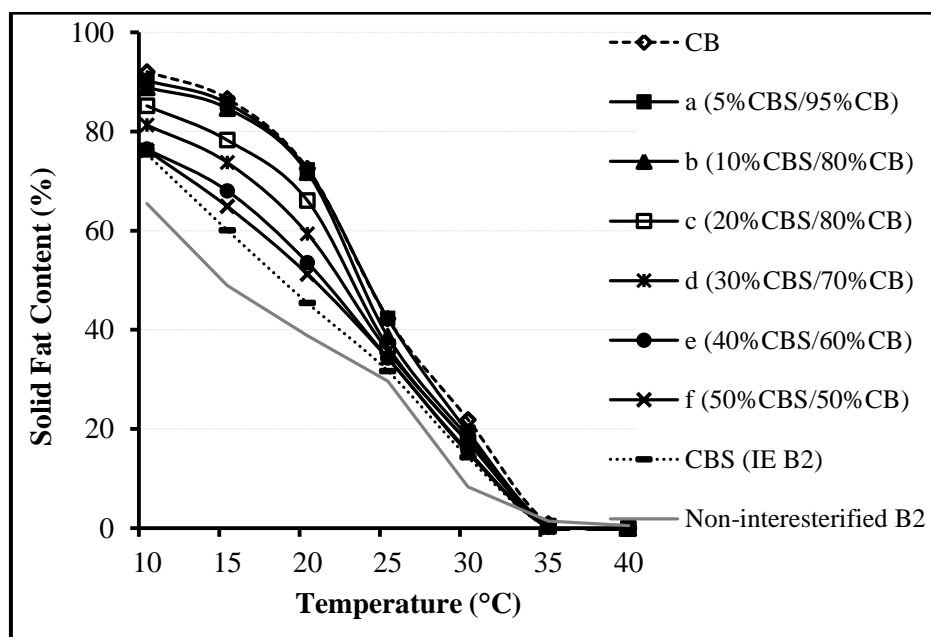


Figure 4.4. Solid fat content profiles of enzymatically produced CBS (interesterified B2), commercial CB, and their blends: a (5%CBS/95%CB), b (10%CBS/90%CB), c (20%CBS/80%CB), d (30%CBS/70%CB), e (40%CBS/60%CB), f (50%CBS/50%CB), and non-interesterified B2. Data represent averages of three measurements with standard deviations lower than 1.5% in all cases.

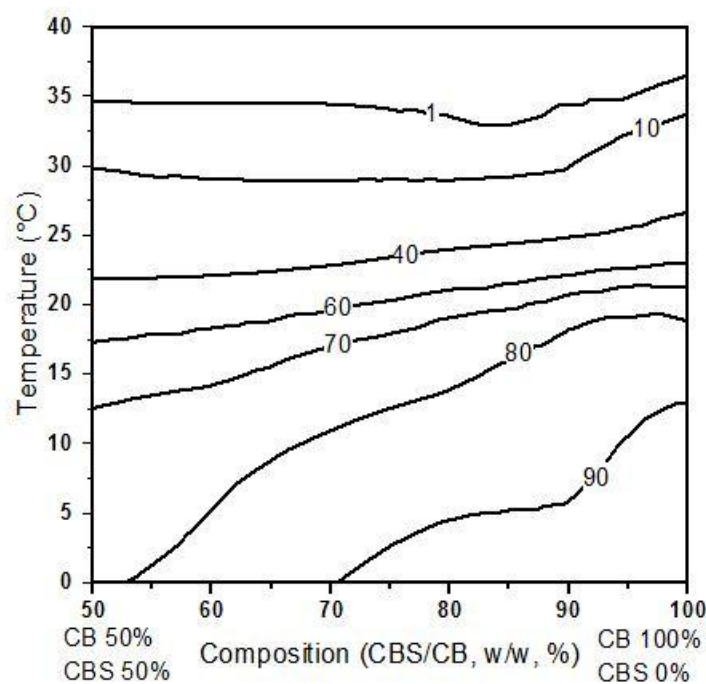


Figure 4.5. Binary iso-solid phase diagrams constructed with OriginPro 9.1 software for blend of enzymatically produced CBS and commercial CB. Numbers in curves represent the percentage of solids.

4.3.2.3 Polymorphism

The polymorphism of individual enzymatically produced CBS (interesterified B2), non-interesterified B2 and commercial CB were identified by XRD at 24°C (Figure 4.6). CB exhibited multiple diffraction peaks at $d = 3.8\text{--}4.3$, 4.5 and 5.2 Å, indicating a combination of β' and β polymorphs. This finding was in agreement with previous studies [37,94]. Multiple diffraction peaks at $d = 3.8\text{--}4.3$ Å representing the β' forms were observed for non-interesterified B2. After interesterification, interesterified B2 (enzymatically produced CBS) displayed a major diffraction peak at 4.5 Å, indicating the β -form. In addition, higher peak intensity at 4.2 Å of the interesterified B2 was observed, showing the β' -form. However, the intensity of the diffraction peak at $d = 4.5$ Å (β -form) of the enzymatically produced CBS was smaller compared to CB (Figure 4.6). This was probably due to the different composition of POST and StOST TAGs between enzymatically produced CBS and CB (Table 4.3).

The polymorphism of the different mixtures (a-f) of enzymatically produced CBS and CB is shown in Figure 4.6. With increasing concentration of enzymatically produced CBS in blends a-f, a decreasing of the major diffraction peaks at $d = 4.5$ Å (β form) was observed. This

could be due to the presence of decreased proportion of SUS TAGs particularly POSt and StOSt (Table 4.3). Blends a to c (5 to 20% of CBS in CB) exhibited diffraction peaks at $d = 3.8\text{--}4.2\text{ \AA}$ with a major peak at $d = 4.5\text{ \AA}$, representing mixtures of β' and β polymorphs. For blends d-f, the peak intensity at $d = 4.5\text{ \AA}$ decreased while the peaks at $d = 3.8\text{--}4.3\text{ \AA}$ increased with a gradual change in peak locations. Similar polymorphic pattern was also observed when more than 10% of enzymatically produced CB-like fat was blended with CB [153]. In the present study, the major peak at $d = 4.5\text{ \AA}$ for blends a-c remained unchanged indicating no change in the polymorphism when 5 to 20% of developed CBS was added with CB (Figure 4.6).

4.3.2.4 Crystal morphology

The crystal morphology of enzymatically produced CBS (interesterified B2), commercial CB and their binary blends (a-f) was observed using PLM at 24°C (Figure 4.7). CB showed spherulitic crystals with needle-like branching outward from the central nuclei, ranging between 10 and 100 μm in diameter (Figure 4.7). The morphology of commercial CB was found to be consistent with that observed by Sonwai *et al.* [131], who reported needle-like crystals. The PLM of enzymatically produced CBS revealed a densely packed granular structure with spherulitic crystals, ranging between 1 and 100 μm in diameter. With the addition of enzymatically developed CBS (interesterified B2) in blends a-f, the spherulitic needle-like crystals shifted to granular small crystals (Figure 4.7). This behavior could be explained by the variations in TAG content between developed CBS and CB (Table 4.3). Another possible reason for the variations in crystalline structures (size and shape) could be the differences in textural properties between CBS and CB [106]. No significant change in crystal microstructure (size and shape) was observed when the developed CBS was added up to 20% with CB (blends a-c) (Figure 4.7). Therefore, blends a to c (5-20% of CBS in CB) could be potentially used as suitable blends for chocolate formulation.

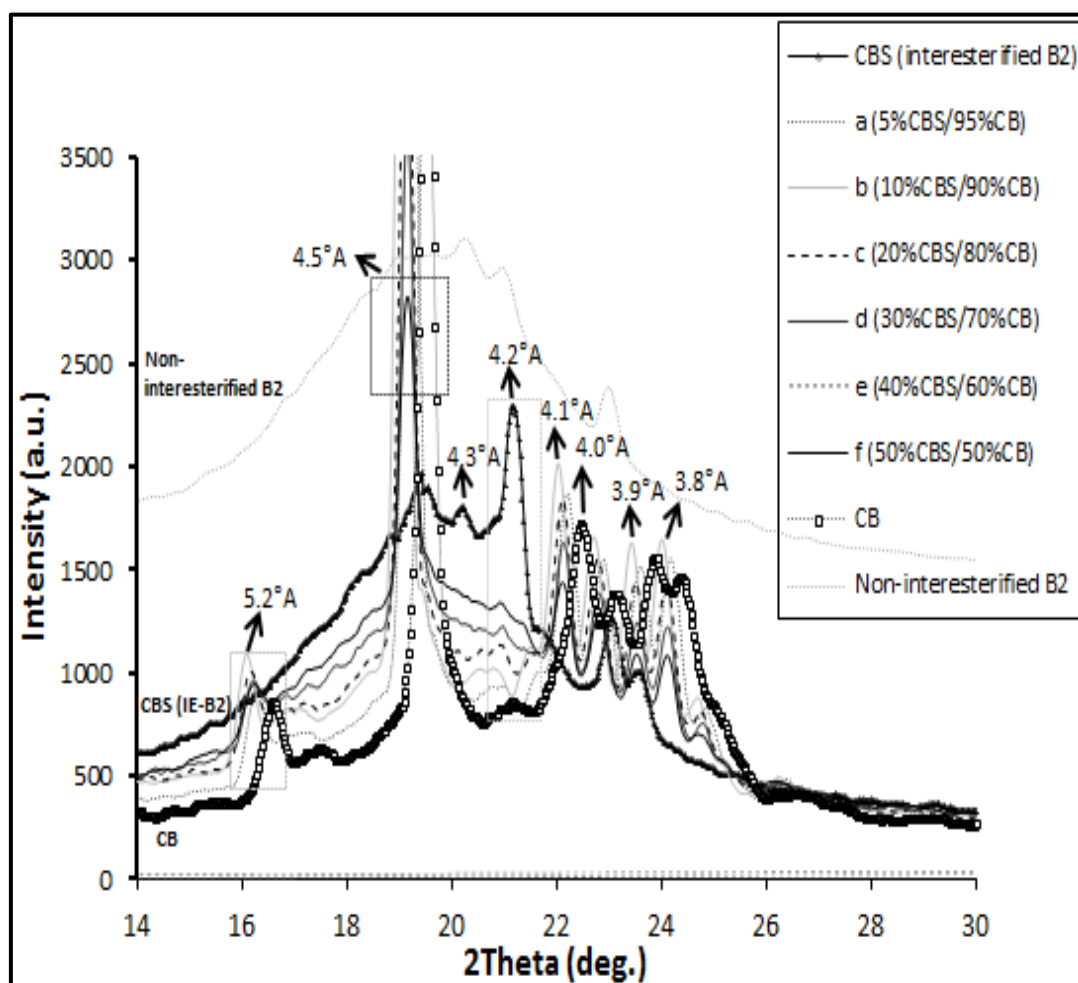


Figure 4.6. X-ray diffractograms of —●— enzymatically produced CBS (interesterified B2),□..... commercial CB and their blends: a (5%CBS/95%CB), — b (10%CBS/90%CB), - - - c (20%CBS/80%CB), — d (30%CBS/70%CB), ===== e (40%CBS/60%CB) and — f (50%CBS/50%CB), and non-interesterified B2.

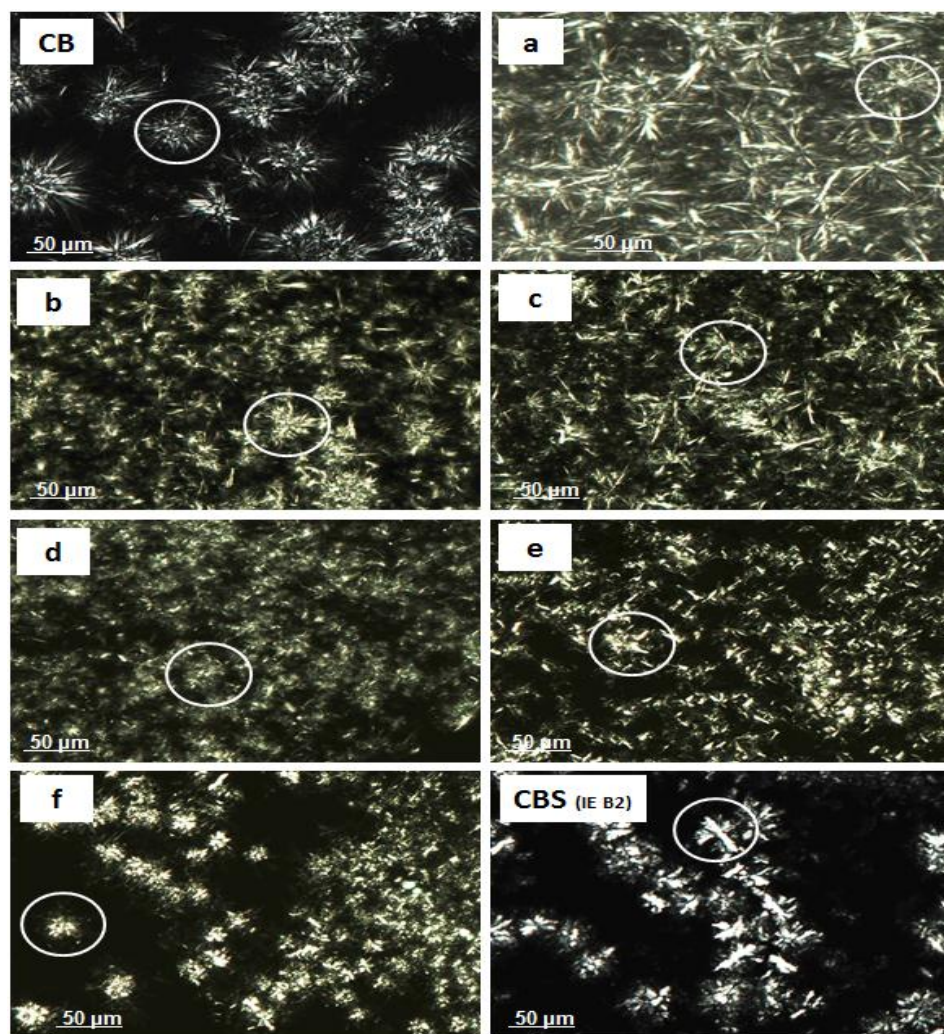


Figure 4.7. Overview of crystal morphology for enzymatically produced CBS (interesterified B2), commercial CB and their blends: a (5%CBS/95%CB), b (10%CBS/90%CB), c (20%CBS/80%CB), d (30%CBS/70%CB), e (40%CBS/60%CB) and f (50%CBS/50%CB).

4.4 Conclusion

Sample B2 (80% ternary blend/15% stearic/5% oleic) showed comparable major fatty acids composition to commercial CB which was selected to produce CBS through enzymatic interesterification. A melting endotherm at 33.5°C, similar to CB was obtained using 4% (w/w) enzyme and after incubating 6 h reaction time at 60°C. POST (28.4%) and StOSt (19.5%) percentage of the interesterified B2 was significantly ($P < 0.05$) increased along with a gradual decrease in POP (17.7%) compared to non-interesterified B2. The interesterified B2 had considerably lower SFC values up to 30°C than CB. Furthermore, the sample displayed a desirable diffraction peak at 4.5 Å indicating the β form, but much smaller than CB due to the differences of POST and StOSt. In the second phase of this research, enzymatically produced CBS was blended with CB to screen their possible application in chocolates. The melting peak became broad upon the addition of CBS, due to the differences of SUS TAG particularly POST/StOSt. However, the peak temperature remained unchanged. In addition, the onset and endset of the melting peak were comparable to CB up to 20% of CBS (blends a-c). The iso-solid diagrams also showed a desirable monotectic effect at 15-25°C, whereas a eutectic effect was observed above 25°C when more than 20% CBS was added. No change in the intensity of diffraction peaks (polymorphism) was observed for blends a-c with similar crystal morphology as per CB. Overall, enzymatic interesterification is able to produce CBS with similar melting profile and comparable TAGs composition to CB. 5 to 20% of enzymatically produced CBS could be potentially added with CB for use in chocolate production without altering the physicochemical properties significantly.

Chapter 5

Work that is presented in this chapter is published in *LWT-Food Science and Technology*, (2017), 82: 420-428 with minor adjustments in Figure/Table number to fit into the current thesis format. A copy of the research paper is included as appendix J in page 158.

5 Physical properties of enzymatically produced CBS and CB mixture, and physical and sensory characteristics of dark chocolate made from the enzymatically produced CBS

5.1 Introduction

Enzymatic interesterification of fats and oils for the formulation of cocoa butter substitute (CBS) has been receiving a lot of attention. Triacylglycerol (TAG) composition of fats and oils is modified to change the physical properties particularly melting profile similar to cocoa butter (CB) for using in confectionery applications [133]. Chemical modification in the production of these types of TAGs is generally not applicable because of deficiency in positional specificity [74,151].

CB, the main ingredient of chocolate, is expensive among all the vegetable fats/oils due to its limited supply and high market demand. Hence, researchers are looking for alternatives to CB. CBS is an alternative to CB and have a similar melting profile to that of cocoa butter, but with different chemical composition [18,27,53,135,140]. In the literature, modification of kokum fat, mango fat, sal fat with methyl palmitate-stearate [133]; and palm oil with soybean oil [1] using enzymatic interesterification has been studied in producing CBS. Reports on the production of CBS from cheap and available palm oils fraction are not available. In our preliminary study [19], palm mid-fraction was mixed with refined, bleached and deodorized palm kernel oil and palm stearin to produce CBS and the results showed several melting temperatures instead of a single melting peak between 30 and 35°C as shown by CB. Melting is the main characteristic that is used for the evaluation of an enzymatically modified CB-like fats [35]. Therefore, enzymatic interesterification was used to modify CBS to show similar melting characteristic and triacylglycerol composition as per CB as mentioned in Chapter 4. Subsequently, 5 to 50% of CBS (w/w) were mixed with CB in order to investigate the compatibility of CBS/CB mixture; in which 5-20% CBS was found to be compatible with CB in terms of solid fat content as a function of temperature and polymorphism.

In the present study, dark chocolate is used as model chocolate, which is made up of CB along with sugar, ground cocoa solids and soy lecithin [153]. However, milk chocolate has not been considered in this study to avoid any overlapping melting or other interaction between CBS and milk fat (i.e., milk fat may interfere on the physical properties of CBS).

The important ingredient of CB and its crystal structure is responsible for the rheological properties, appropriate texture and sensory perception of chocolate [90,140]. The rheological properties of the chocolate depend on many factors such as temperature, composition and processing conditions. During dark chocolate processing, composition and crystallization of CB play an important role in obtaining good quality product. The chocolate composition determines different interactions that occur between ingredients whilst crystallization is the most important step in chocolate processing i.e. refining, conching and tempering [55,126] to ensure the desired sensory characteristics.

The melting characteristic of dark chocolate is very important in order to evaluate the effects of CB polymorphism. CB has complex polymorphs namely γ , α , β' and β (or Roman numbering, I-VI) in ascending stability [94,118]. Polymorphic transitions of CB take place via either a solid-state transition or by melt-mediation. During the manufacturing process, tempering is usually conducted at set temperature and time regime to get the desirable $\beta(V)$ crystal form with melting temperature of 32-34°C, which is preferred in chocolate to impart the desired good snap, glossy appearance and sensory mouth-feel [136]. However, poorly tempered chocolate can develop a sticky greyish-white surface namely fat bloom upon storage. Bloom formation may also arise due to slight (*i.e.*, $\pm 2-3^\circ\text{C}$) or larger temperature variations, which cause the melting and re-crystallisation of TAG in CB, where the liquid fat from the chocolate matrix migrates through pores and microfractures to the surface forming bloom [118].

Since the melting, rheological, textural and polymorphism are the main properties used for the quality assurance of chocolate, it is important to understand how the enzymatically produced palm oil-based CBS influences the physical properties of CB. Therefore, the objective of the present work was to investigate the melting, rheological, textural properties, bloom formation and sensory profile of dark chocolate made with enzymatically produced CBS.

5.2 Materials and methods

5.2.1 Materials

The materials of this chapter are similar to the previous chapter as described in section 4.2.1. Cocoa powder (10-12% fat, pH 6.8-7.2, moisture 5 g/100 g, Guan Chong Cocoa Sdn. Bhd., Johor, Malaysia), icing sugar (MSM Prai Sdn. Bhd., Selangor, Malaysia.) and Soy lecithin

(moisture 0.19 g/100 g, Cargill, Shanghai, China) were employed. CBS was produced from palm mid-fraction/refined bleached deodorized palm kernel oil/palm stearin mixture added with commercial stearic-oleic acid through enzymatic interesterification as discussed in chapter 4.

5.2.2 Chocolate production

Production of standard dark chocolates was performed using the method described by Kadivar *et al.* [74] with minor modification at Cocoa processing lab, Malaysian Cocoa Board, Nilai. Formulation of standard dark chocolate was according to the following composition (w/w): 48% icing sugar, 30.90% CB, 20.5% cocoa powder and 0.6% soy lecithin. For two different chocolate formulations, CBS was added at the levels of 5% and 20% of CB (1.5% and 6.2% of CBS were replaced from 30.90% of CB). Experimental samples (1 kg batch for each formulation) were prepared by mixing sugar, cocoa powder and 2/3 of melted CBS+CB fat in a mortar and pestle mill (Pascal, UK) at low speed for 10 min at 45°C. Then the mixture was refined using a 3-roll refiner (Pascal, UK) at ambient temperature to get a particle size <35 µm. After refining, the mixture was transferred to the conche (Mortar and Pestle mill, Pascal, UK) and then mixed with the rest of the melted CBS+CB fat at 45°C for 4 h. In the following phase, the mixture became a paste as the viscosity reduced. To obtain the desired flow characteristics, soy lecithin was added and mixed for another 2 h.

In the next step, the liquid chocolate was tempered manually according to the method described by Talbot [136]. Tempering was performed to produce the desired β crystals in the chocolate products. Tempering was carried out as follows: i) chocolate was melted at 45°C to remove crystal history, ii) approximately 2/3 of the chocolate mixture was poured onto a marble slab and mixed with a flexible spatula until the product reached 27°C to produce seed crystals and iii) the thickened chocolate was then mixed with the remaining 1/3 warm chocolate (40°C) to get the overall temperature of 31-32°C, in order to melt the unstable crystal polymorphs [24,25,136]. Temperature was measured using an Aasted-Mikroverk Chocometer (Aasted-Mikroverk ApS, Farum, Denmark) to ensure accurate tempering temperature for chocolate. The tempered chocolate was poured into plastic chocolate molds (dimensions bar, 98mm × 30mm × 11mm) and cooled at 13±1°C for 60 min to solidify the chocolate [40]. The chocolate bars were de-moulded and subsequently stored at room temperature.

5.2.3 Triacylglycerol (TAG) analysis

The TAG profiles of individual CB and enzymatically produced CBS were analysed using high performance liquid chromatography equipped with RID, according to AOCS Official Method Ce 5b-89 as discussed in previous section 2.2.4 [18].

5.2.4 Melting profile

Melting profile of the dark chocolates was determined using differential scanning calorimetry (DSC Pyris 4000 DSC, Perkin-Elmer Ltd., Norwalk, USA) equipped with nitrogen gas flow rate of 20 ml/min, following the method of Kadivar *et al.* [74]. Surface of the chocolate was scraped off with a scalpel and 2-4 mg of the chocolate slivers was hermetically sealed in an aluminum pan. An empty, covered aluminum pan was used as the reference. When the system reached the equilibrium conditions at 20°C, the pan was put in the DSC cell and the melting thermograms were recorded by heating from 20 to 65°C at 5°C/min. Onset temperature (T_{onset}), endset temperature (T_{endset}), maximum peak temperature (T_{max}), melting enthalpy (ΔH) and peak area were calculated from the melting thermogram using DSC software. T_{onset} is the temperature at which the corresponding crystal form starts to melt; T_{end} represents the temperature at which liquefaction of the sample is completed; ΔH_{melt} is the amount of energy required for complete melting of the sample; T_{max} is the temperature at which maximum melting occurs; and peak area is equivalent to the heat taken up by the sample during melting [5,38].

5.2.5 Polarised light microscopy (PLM)

To measure the micrographs in terms of fat particle size of the chocolates, a polarized light microscope (PLM, Olympus BX51, Tokyo, Japan) fitted with a digital camera (Nikon, DS-File, Tokyo, Japan) was used at room temperature. Approximately 10 μg of the melted chocolate was then placed on a glass microscope slide. A coverslip was placed on top of the sample and centred on the melted sample to ensure uniform thickness. PLM images were captured using 20 \times objective lens after the slides were kept at room temperature for 4 h to solidify the particles.

5.2.6 Particle size distribution (PSD)

To measure the PSD of the chocolates, a MasterSizer 3000 (Laser Diffraction Particle Size Analyser, Malvern Instruments Ltd., Malvern, Worcestershire, UK) equipped with a Hydro EV was used. Approximately 0.5 g of chocolate slivers was mixed with 10 ml of isopropanol. The sample (~0.2 ml) was dispersed in isopropanol until an obscuration of 10.5% as recommended by the instrument software. The sample was sonicated for 2 min to ensure particles were independently dispersed and thereafter maintained by stirring during the measurement. PSD was determined based on the Mie-Theory using the refractive index 1.59 for dark chocolate [6]. Results were provided as a relative volume (%) of particles in size compared with particle size curves (Malvern MasterSizer Micro Software). PSD parameter was obtained at the largest particle size D_{90} (>90% finer) [16].

5.2.7 Flow behavior

In order to examine flow behavior of the chocolates, a Rheometer RS600 (HAAKE RheoStress 600, Thermo Electron Corp., Karlsruhe, Germany) fitted with a plate-plate geometry was used. Chocolate samples were melted at 50°C for 1 h and approximately 2 g of the samples was placed onto a preheated plate in a gap of 1 mm. The measurement procedure was based on the method of ICA [65] and Afoakwa *et al.* [3] with minor modifications. Temperature of the bottom plate was set at 40°C to prevent solidification of the fat crystals. A stepped flow procedure was applied by increasing the shear rate logarithmically from 2 s^{-1} to 110 s^{-1} . Yield stress (Pa) and viscosity (Pa s) were measured at 65 s^{-1} [74].

5.2.8 Texture analysis

Hardness (N, the maximum force required to penetrate the sample) of the chocolates was measured with a Texture Analyser (TA-XT plus, Stable Microsystems Ltd., Surrey, UK) equipped with 2 kg load cell and probe (P/2N needle stainless) using the following parameters: product height 10 mm, penetration depth 5 mm, pre-speed 1 mm/s, test speed 2 mm/s, post speed 10 mm/s and the duration of the test at ~ 1-2 min [74].

5.2.9 Bloom formation on chocolate surface

Bloom formation on chocolates, stored at $24\pm1^\circ\text{C}$ and $29\pm1^\circ\text{C}$, was captured and examined every two weeks for a total of 3 months using a stereomicroscope (Nikon, SMZ1500, Tokyo,

Japan) fitted with a digital Nikon camera (Nikon, Digital Sight DS-2Mv, Tokyo, Japan), according to previously described method [81].

5.2.10 Polymorphism

To identify the polymorphic transformations of chocolate, a D8 Discover X-ray Diffraction (Bruker, Karlsruhe, Germany) fitted with Cu-K α radiation ($k = 1.5418 \text{ \AA}$, voltage 40 kV and current 40 mA) was used at room temperature. Surface of the chocolates was chopped with a scalpel. To eliminate the interference of sugar crystals, approximately 5 g of the chocolate slivers were mixed in 500 ml of cold water, shaken and allowed to stand at room temperature for 4 h to dissolve the sugar, according to the method of Cebula *et al.* [30]. The suspension was filtered through a Buchner funnel with whatman filter paper (0.45 μm) under a vacuum pump to dry the samples. The sugar free chocolate samples were mounted onto the XRD sample holder. The samples were analysed at 2θ angles of 10° to 30° with a scan rate of $1.5^\circ/\text{min}$. Short (d) spacing (\AA) was determined using the EVA-diffraction software (Bruker, Karlsruhe, Germany). Assignments of polymorphs were based on the following short spacing characteristics of CB: α form ($d = 4.15 \text{ \AA}$); β' forms ($d = 3.8\text{--}4.3 \text{ \AA}$) and β forms ($d = 4.5/4.6 \text{ \AA}$) [37]. Unbloomed chocolate was used as a control.

5.2.11 Sensory evaluation

Sensory evaluation was performed using a 9-point hedonic scale (1 = dislike extremely, 9 = like extremely) where participants evaluated the sensory attributes i.e. glossiness, hardness, waxiness, greasy to touch (sticky), mouth-feel (smooth, melting), overall acceptability and taste acceptance of the dark chocolates. One hundred participants (students and staffs) from Monash University Malaysia were selected. Participants were asked to pick one sample which is different from the other two in a triangle test. Three formulations of dark chocolate (each weighing $\sim 3 \text{ g}$) were served at $23 \pm 1^\circ\text{C}$ in sealed plastic bags. Samples were coded using three digit random numbers. Participants were asked to take a small bite of biscuit and then drink water to rinse their palate after tasting each chocolate (Human Ethics Approval Number: CF16/2097-2016001042).

5.2.12 Statistical analysis

Data were statistically analysed by t-test and one-way analysis of variance using the SPSS software, version-20 (IBM Corp., Chicago, USA). Tukey's test was applied to determine the

significant differences at $P < 0.05$ level. Rheometer and PSD analyses were performed in duplicate. DSC, XRD, TA and PLM analyses were conducted in triplicate.

5.3 Results and discussion

5.3.1 TAG composition

The TAG profiles of individual CB and enzymatically produced CBS are presented in Table 5.1. CB contained three main TAGs: POSt (39.2%), StOSt (29.7%) and POP (18.1%), which is in agreement with previous studies [18,21]. As shown in Table 5.1, enzymatically produced CBS had comparable POP, while significantly ($P < 0.05$) lower composition of POSt and StOSt to CB. In addition, CBS contained additional tri-saturated TAGs (PPP, LaLaLa, PPSt and LaLaM) and di-unsaturated TAG (PLO) which appear only in traceable quantity in CB.

Table 5.1. Overview of TAGs composition of individual CB and enzymatically produced CBS.

TAG (area %)		CB	CBS
SSS	PPP	0.1±0.0a	8.4±0.2b
	PPSt	0.5±0.0a	2.4±0.4b
	StPSt	-	1.2±0.2
	LaLaLa	-	4.7±0.3
	LaLaM	-	2.3±0.1
	MMM	-	1.1±0.2
	Total	0.6	20.1
SUS	POP	18.1±0.8a	17.7±1.6a
	POSt	39.2±1.2a	28.4±1.2b
	StOSt	29.7±0.7a	19.5±0.8b
	LaOLa	-	0.7±0.2
	AOSt	1.9±0.5a	0.6±0.1b
	PLP	1.1±0.0a	1.4±0.3a
	MLP	0.6±0.0a	1.4±0.2b
	Total	90.6	69.7
SUU	PLL	0.5±0.0a	0.8±0.0a
	PLO	0.6±0.2b	6.1±0.7a
	POO	2.8±0.4a	1.3±0.2b
	StOO	2.4±0.1a	1.3±0.0b
	Total	6.3	9.5
UUU	LLO	0.4±0.0a	0.1±0.0a
	OOL	0.7±0.1a	0.2±0.0a
	OOO	1.4±0.2a	0.4±0.0b
	Total	2.5	0.7

Values within the same row with different letters are significantly different ($P<0.05$). Each value in the table represents the mean \pm SD of two measurements. [▲] Abbreviations: Triacylglycerol (TAG), cocoa butter (CB), cocoa butter substitute (CBS), total content of tri-saturated (SSS), total content of mono-unsaturated (SUS), total content of di-unsaturated (SUU), total content of poly-unsaturated (UUU), P palmitic, St stearic, O oleic, La lauric, L linoleic, M myristic, A arachidic.

5.3.2 Melting behavior

Melting properties of different chocolate samples were shown in Figure 5.1. Thermal parameters: T_{onset} , T_{end} , ΔH_{melt} , T_{max} and peak area of the melting endotherms of dark chocolate samples were compared.

In the present study, chocolate formulated with CB showed a sharp melting peak near 33°C with T_{onset} (27.5°C), T_{end} (35.5°C), area (64.2 mJ) and ΔH_{melt} (34.1 J/g). These findings were consistent with the literature [39]. The melting peak and T_{end} of the chocolate with 5% and 20% CBS were similar to CB-chocolate (Figure 5.1). However, 20% CBS-chocolate had significantly ($P < 0.05$) higher ΔH_{melt} and broader peak area with a small shoulder peak compared to the CB-chocolate. This is probably due to the lower melting TAGs specially LaLaLa and PPP (Table 5.1). Similar results were also reported in a previous research [74], where chocolate with 25% CB-like fat showed a broader melting peak and lower T_{onset} . According to Clercq *et al.* [38] the melting profile of dark chocolate should have a narrow melting peak leading to a quick melt down at 37°C (body temperature), producing a cool sensation and smooth mouth-feel. In the current study, there were no significant ($P \geq 0.05$) differences in ΔH_{melt} and peak area between 5% CBS-chocolate and CB-chocolate (Figure 5.1), indicating 5% CBS-added chocolate is comparable to CB-chocolate.

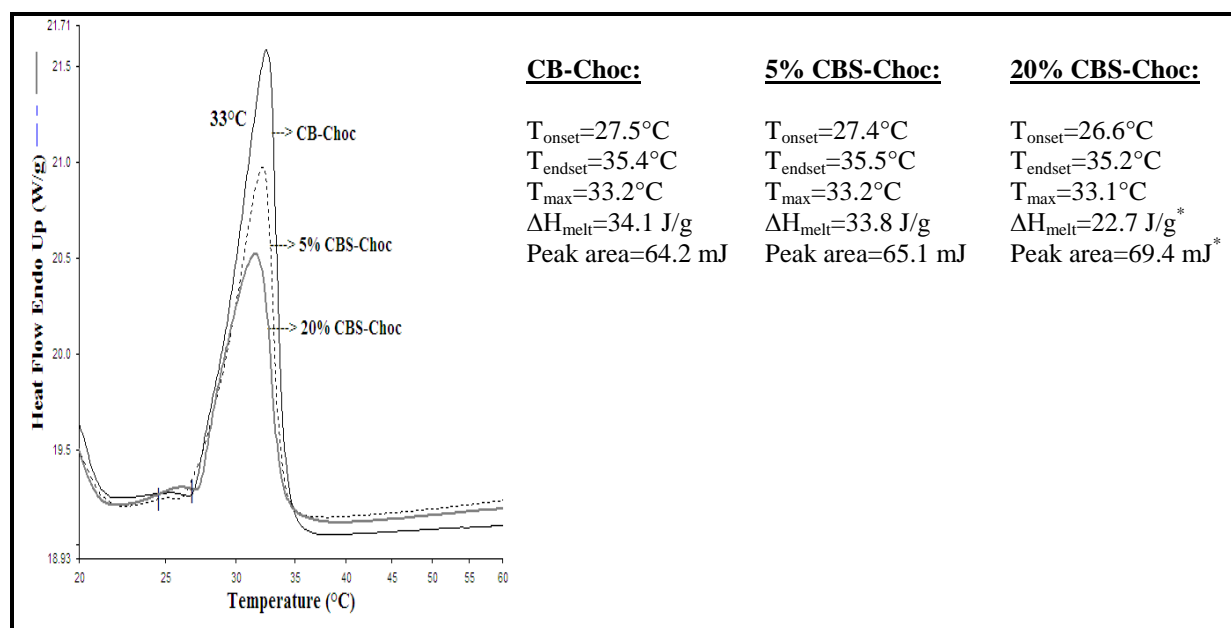


Figure 5.1. DSC Melting thermograms of CB-chocolate, 5% CBS-chocolate and 20% CBS-chocolate. *Significantly different from CB-chocolate, $P<0.05$. All measurements were performed in triplicate and the standard error for each sample was below 1.2%.

5.3.3 Particle size distribution (PSD) of the dark chocolates

Polarised light microscopy (PLM) was used to observe the variations in fat-particle phase, sugar crystalline network and cocoa particle interaction from the dark chocolates as shown in Figure 5.2. All the three samples showed similar micrographs under PLM (Figure 5.2A-C). Sugar and fat crystals exhibited polarization (bright image), whereas cocoa solids (amorphous) did not show polarization, or appeared as dark. This finding was in accordance with the literature [8]. In addition, non-fat particulates were visible in the chocolates, such as irregularly large-shaped sugar crystals ($\sim 25 \mu\text{m}$, bright image) and brownish-red small cocoa particles.

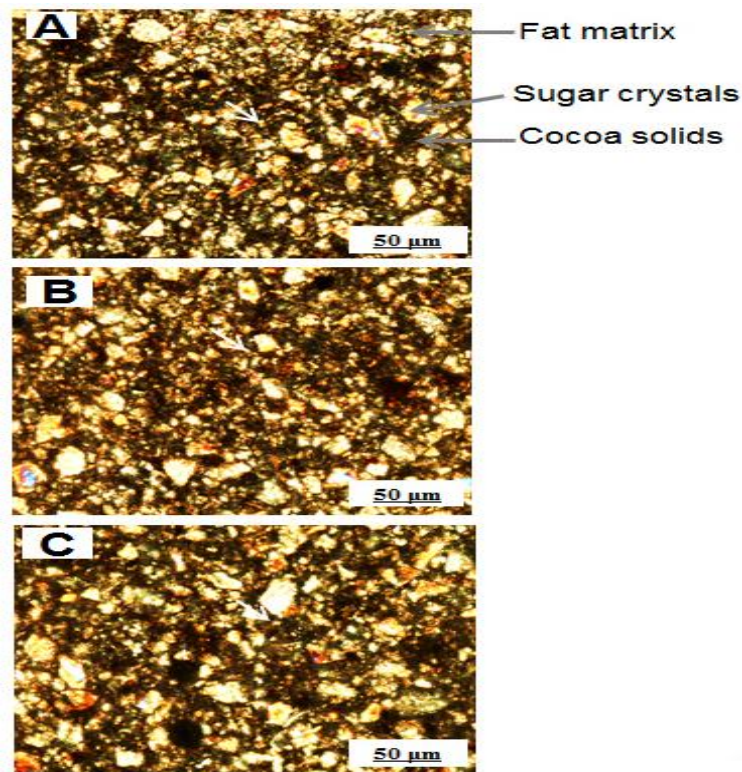


Figure 5.2. PLM micrographs (20 \times lens) of A) CB-chocolate, B) 5% CBS-chocolate and C) 20% CBS-chocolate at 24°C.

In this study, master-sizer was used to confirm the PSD of the chocolate samples. Figure 5.3 shows volume density of the selected samples against size distributions using D_{90} (>90% finer). Chocolate produced with CB showed particle size approximately 18 μm , which is in agreement with the previous research [6]. Similar PSD was observed for chocolate with 5% CBS. However, 20% CBS-added chocolate had a slightly higher PSD ($\sim 24 \mu\text{m}$) than the CB-chocolate (Figure 5.3). As stated by Beckett [15], PSD has a direct influence on rheological, textural and sensory characteristics. The largest particles are responsible for mouth-feel notably grittiness, whereas smaller particles improve flow properties and hardness. For good dark chocolate, PSD should be less than 35 μm [3]. Overall, chocolate with 5% and 20% CBS was within the range of PSD of less than 35 μm .

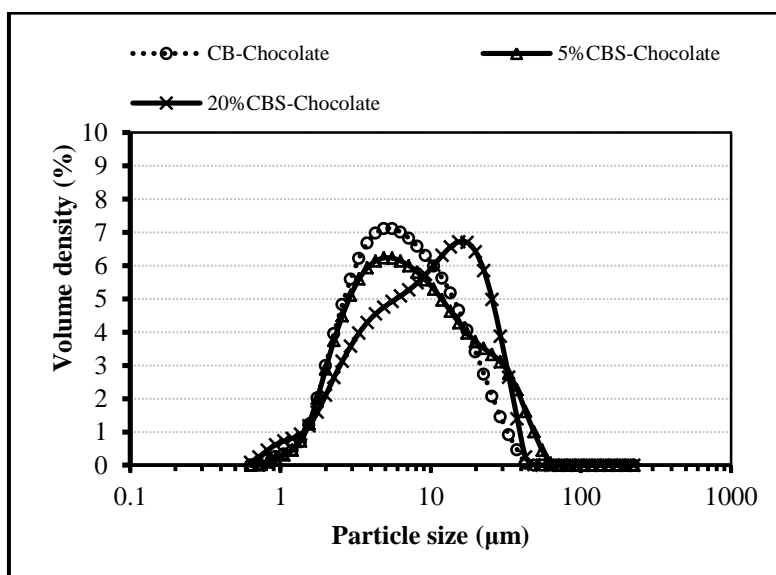


Figure 5.3. Particle size distribution of CB-chocolate, 5% CBS-chocolate and 20% CBS-chocolate at D_{90} (>90% finer).

5.3.4 Flow behavior

Dark chocolate is a solid suspension of sugar and cocoa powder in cocoa butter, which shows non-Newtonian flow behavior [39]. The Casson model was fitted to the flow curves to study the Casson yield stress and viscosity. Yield stress is the amount of energy required to initiate chocolate flow. Plastic viscosity is related to the energy needed to maintain the flow of a fluid. High viscous chocolates are not desirable due to sticky mouth-feel [39].

Figure 5.4 shows the Casson yield stress and viscosity as a function of shear rate between 2 and 65 s^{-1} for the chocolate samples. When the shear rate gradually increased, the Casson plastic viscosity correspondingly decreased while yield stress increased. The viscosity and yield stress of the CB-chocolate were found approximately 2 Pa s and 15 Pa , respectively, at shear rate 65 s^{-1} (Figure 5.4A&B). These results were in accordance with a previous study [74] for dark chocolate. Similar trend in plastic viscosity was also observed for the chocolate with 5% CBS and 20% CBS (Figure 5.4). Likewise, 5% CBS-chocolate showed similar yield stress to the CB-chocolate, whereas 20% CBS-chocolate had slightly lower yield stress (12.2 Pa). This variation was likely due to the function of CB replaced by enzymatically produced CBS and the high PSD (24 μm) (Figure 5.3). PSD and rheological parameters are highly linked as the higher PSD denotes lower surface area available to interact, which leads to higher viscosity and/or yield stress [9].

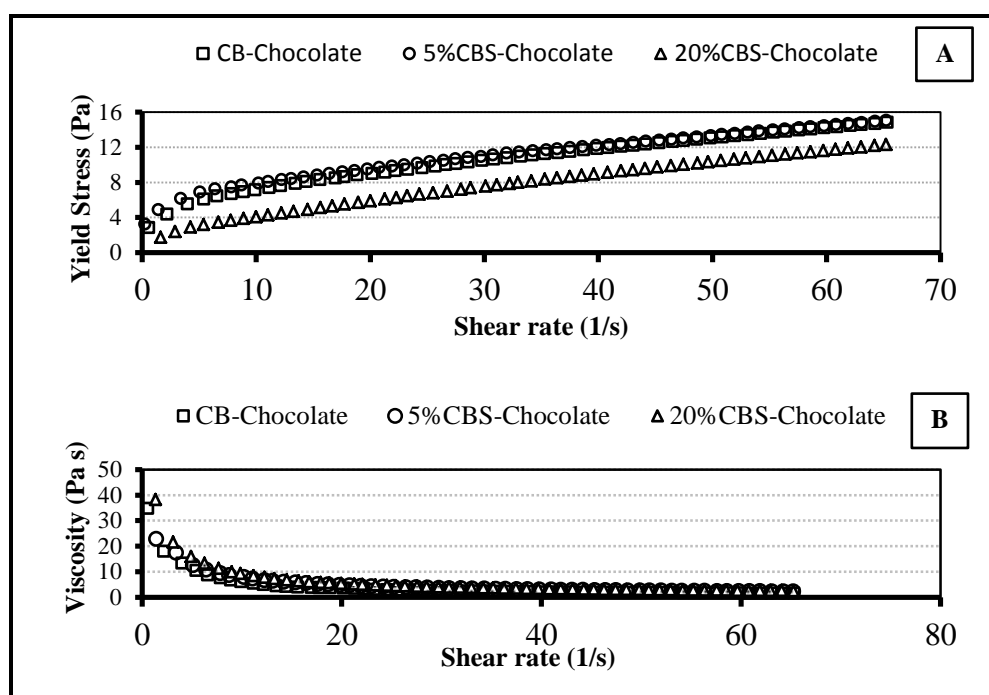


Figure 5.4. A) Casson yield stress (Pa) and B) Casson viscosity (Pa s) of CB-chocolate, 5% CBS-chocolate and 20% CBS-chocolate.

5.3.5 Textural behavior

As stated by Afoakwa *et al.* [2], a good quality chocolate is a solid product with a good snap at 24°C (room temperature) and shiny appearance along with easy melting in the mouth, giving a pleasant mouth-feel sensation. Hardness of dark chocolate samples, expressed in maximum force (N), was measured by penetration test as shown in Figure 5.5. Hardness of the CB-chocolate at 24°C showed approximately 13 N, which is in agreement with previous studies [39,74]. Similar hardness value was observed for 5% CBS-added chocolate (Figure 5.5). However, there was significantly ($P < 0.05$) lower hardness of the chocolate with 20% CBS in comparison to the CB-chocolate and 5% CBS-added chocolate. This may be due to the broader melting temperature (Figure 5.1) and high PSD (Figure 5.3). The large particle size in the chocolate creates weak interaction between particles, resulting in a lower maximum force required to penetrate the product [7]. Zarringhalami *et al.* [153] also found no significant differences between a reference chocolate and the chocolates with 5% and 10% CB-like fat, but the chocolates with 15% and 20% CB-like fat had significantly lower hardness. In the current study, 5% CBS-chocolate had a textural behavior in terms of hardness similar to that of CB-chocolate (Figure 5.5).

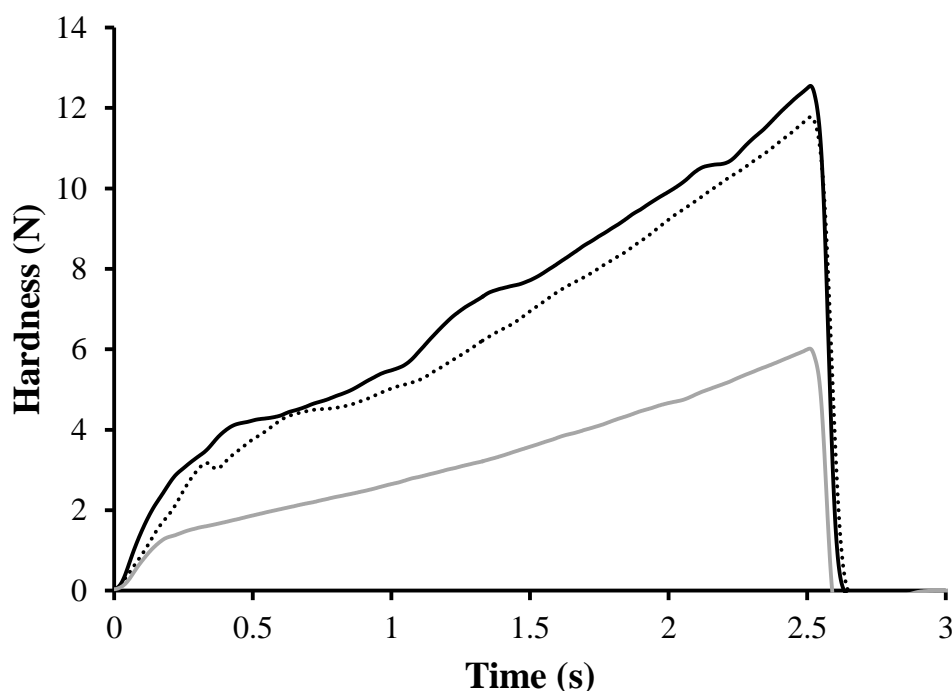


Figure 5.5. Hardness of — CB-chocolate, 5% CBS-chocolate and — 20% CBS-chocolate at 24°C.

5.3.6 Bloom formation and X-ray diffraction during storage

Fat bloom is a physical defect that involves the loss of gloss, smoothness and an undesirable discoloration on the chocolate surface which is the main concern for chocolate manufacturer. Bloom formation is determined by stereomicroscope and confirmed by X-ray diffraction of the chocolate samples during storage at $24\pm1^{\circ}\text{C}$ and $29\pm1^{\circ}\text{C}$ until 12 weeks as shown in Figure 5.6.

Chocolate produced with CB, 5% CBS and 20% CBS at $24\pm1^{\circ}\text{C}$ and stored up to 8 weeks did not show bloom, however after 8 weeks the CB-chocolate and 5% CBS-chocolate began to form white-greyish haze on the surface. At $29\pm1^{\circ}\text{C}$, noticeable bloom formation was observed for CB-chocolate and 5% CBS-chocolate after 2 weeks. This phenomenon can be explained by many factors such as fluctuation of temperature during storage time, recrystallization of fats and sugar crystal, and poor tempering [61,92]. However, no obvious bloom formation was observed for chocolate formulated with 20% CBS at $24\pm1^{\circ}\text{C}$ and $29\pm1^{\circ}\text{C}$ until 12 weeks (Figure 5.6). This may be likely due to the more complex crystalline structures that inhibit bloom [92,108,153]. Another possible reason may be the presence of

medium and high-melting TAG in CBS (Table 5.1). Due to fluctuation of temperature, phase behavior of the TAG becomes disrupted, leading to the formation of large surface crystals [30,36,63]. Beckett [16] stated that the use of high-melting TAG in chocolate allows the melted chocolate to set again with temperature fluctuation. However, the medium-melting TAGs inhibit fat bloom if the storage temperature is higher than the melting temperature of those TAGs. In summary, both chocolates with 5% and 20% CBS can be stored at 24°C to prevent bloom formation.

XRD patterns of bloomed and control chocolates are presented in Figure 5.7. Control chocolates showed a major diffraction peak at $d = 4.5 \text{ \AA}$, indicating β polymorphs and multiple peaks at $d = 3.7\text{-}4.1 \text{ \AA}$, corresponding to the characteristic of β' polymorphs. For bloomed chocolate with CB and 5% CBS, the peak intensity at $d = 3.7$ and 4.0 \AA increased slightly, whereas the 4.5 \AA peak remained unchanged. This result was in agreement with the previous research [132] for bloomed chocolate, who reported that the peak intensity at $d = 3.6$ and 3.8 \AA increased along with a reduced peak at $d = 3.9 \text{ \AA}$. Wang *et al.* [146] also found the diffraction peaks at $d = 3.7, 3.8, 4.2$ and 4.6 \AA for bloomed CBS-chocolate while peaks at $d = 3.8$ and 4.2 \AA for control CBS-chocolate. Likewise in the present study for the bloomed chocolates, the diffraction peak at $d = 4.1 \text{ \AA}$ shifted toward larger d -spacing along with an increased peak height tending to the β polymorphism (Figure 5.7A&B). However, the major diffraction peak at $d = 4.5 \text{ \AA}$ with two peaks at 3.7 and 3.9 \AA were observed for the control chocolate with 20% CBS, indicating no change in the polymorphism transformation during storage at $24\pm1^\circ\text{C}$ and $29\pm1^\circ\text{C}$ (Figure 5.7C). This finding was also confirmed by stereomicroscope (Figure 5.6).

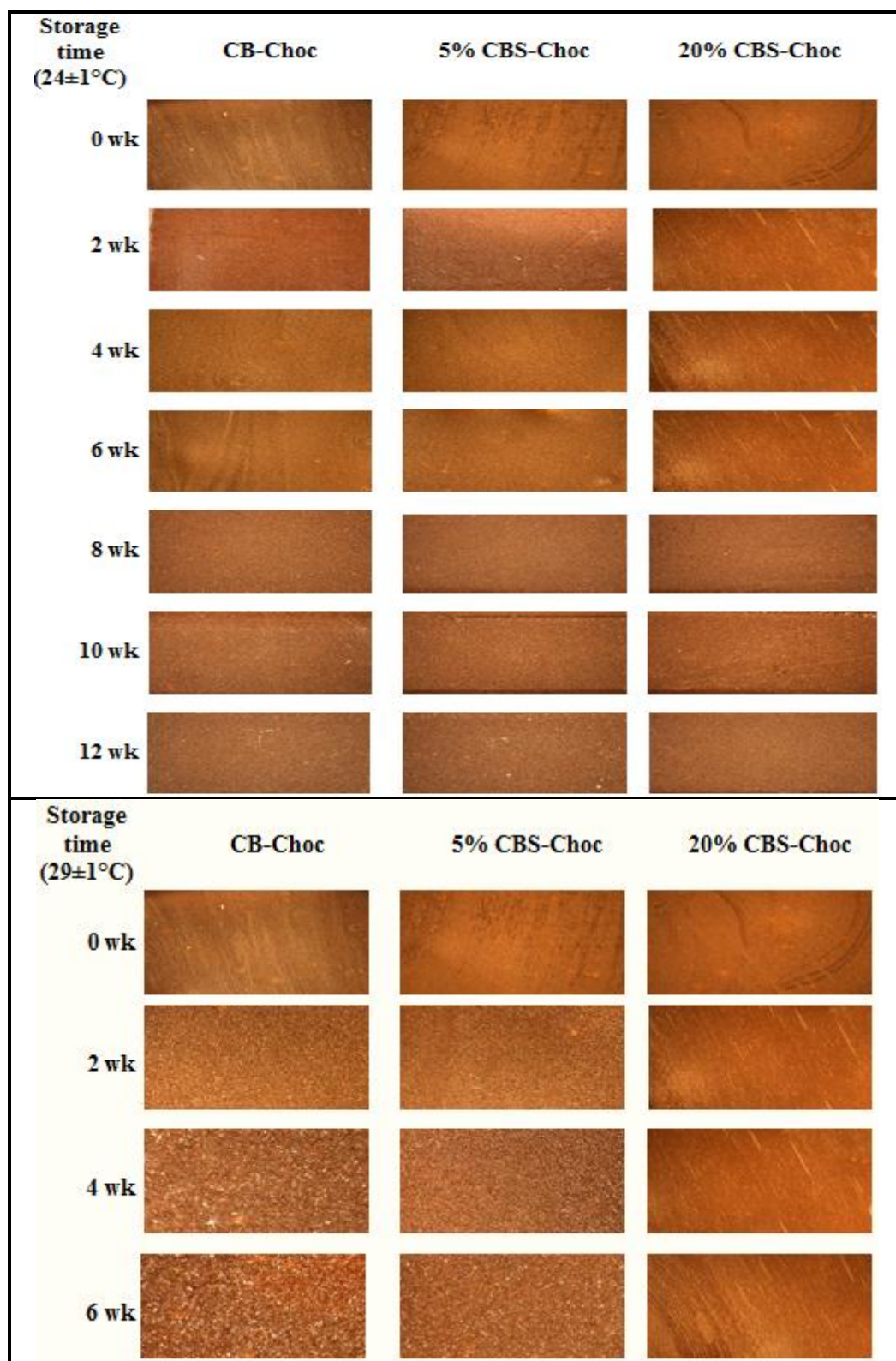


Figure 5.6. Bloom formation of CB-chocolate, 5% CBS-chocolate and 20% CBS-chocolate stored at 24±1°C and 29±1°C.

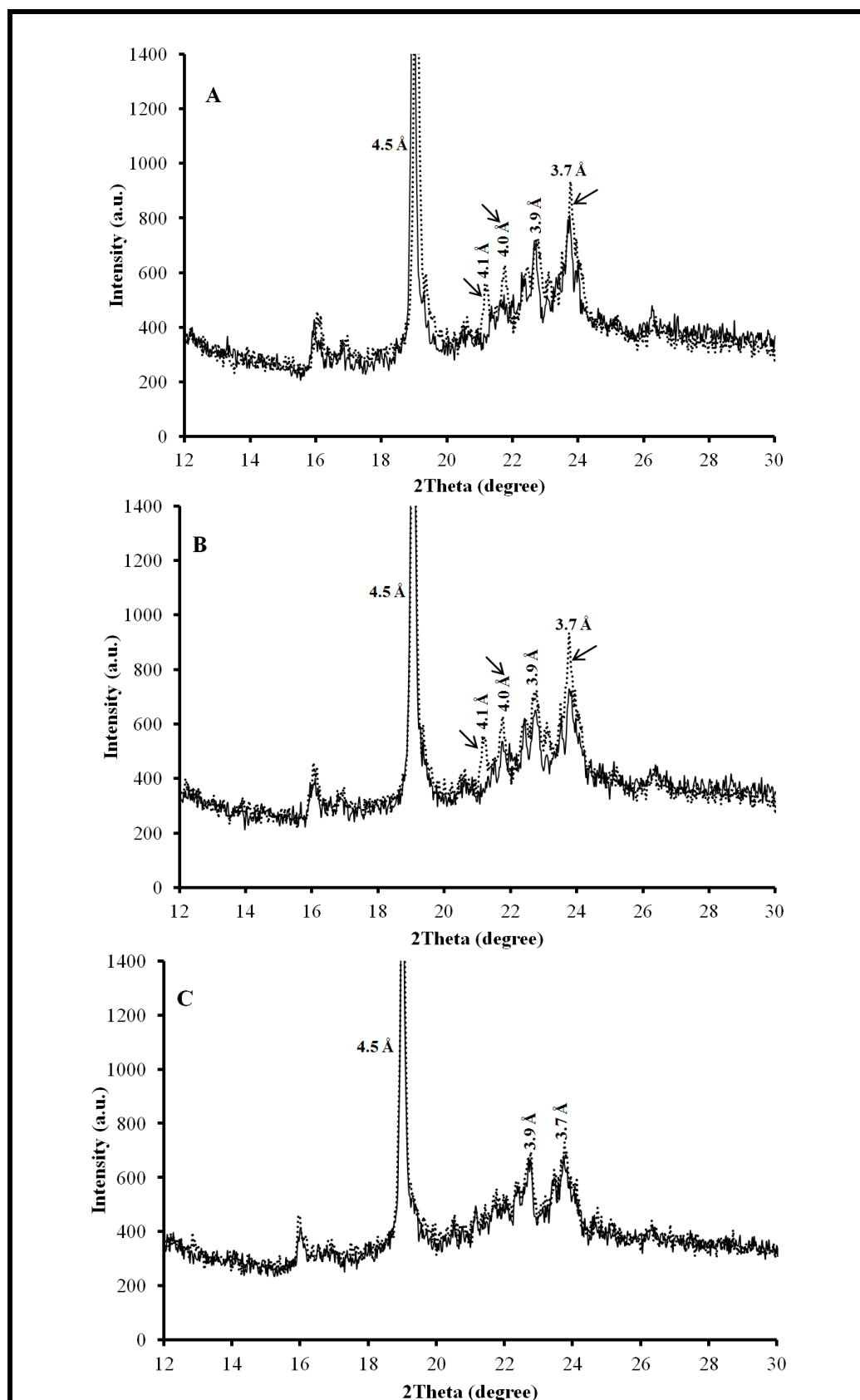


Figure 5.7. X-ray diffraction spectrum of A) — CB-chocolate and bloomed-chocolate, B) — 5% CBS-chocolate and bloomed-chocolate and C) — 20% CBS-chocolate and bloomed-chocolate.

5.3.7 Sensory evaluation

There was no significant ($P \geq 0.05$) difference in sensory characteristics between CB-chocolate and 5% CBS chocolate (Figure 5.8). However, chocolate with 20% CBS had significantly ($P < 0.05$) different sensory characteristics in terms of taste acceptance, overall acceptability and hardness compared to the CB-chocolate. In triangle test, 52 out of 100 panelists were able to identify chocolate with 20% CBS as different from the other two samples of CB-chocolate and 5% CBS-added chocolate (data not shown). Therefore, it could be concluded that panelists did not find any difference between the CB-chocolate and 5% CBS-added chocolate. De-Clercq *et al.* [39] found that full CB-like fat replacement of CB influenced the sensory characteristics of chocolate. In the current study, panelists were not able to distinguish any differences between CB-chocolate and chocolate made with 5% CBS, thus indicating comparable sensory profile between CB-chocolate and 5% CBS-added chocolate.

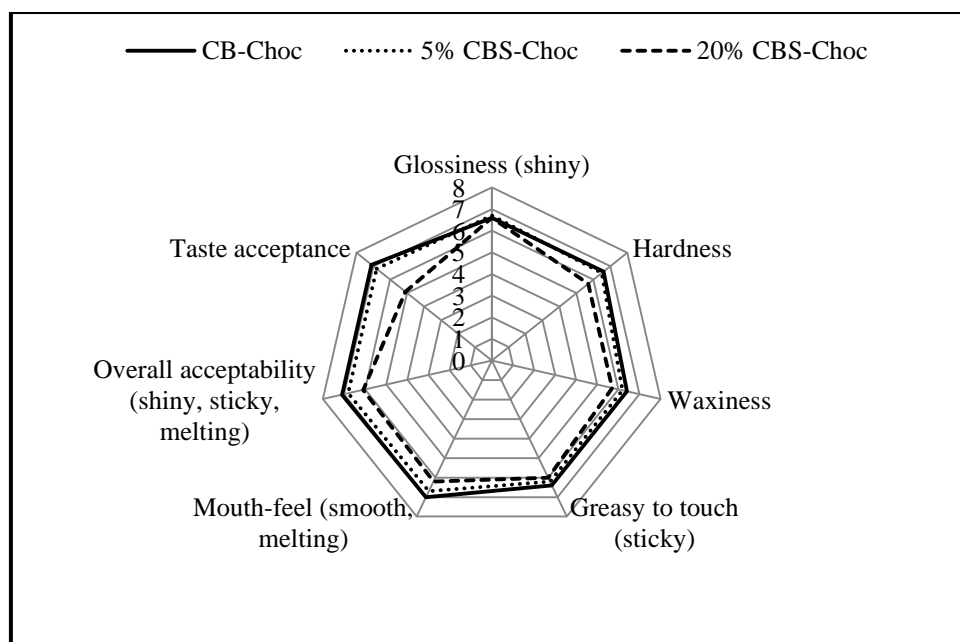


Figure 5.8. Sensory evaluation of CB-chocolate, 5% CBS-chocolate and 20% CBS-chocolate.

5.4 Conclusion

Dark chocolate formulated with CB (without CBS), 5% CBS and 20% CBS was characterized using DSC melting, PSD, rheological, bloom formation and sensory properties. There was no significant ($P \geq 0.05$) difference in melting behavior between the CB-chocolate and 5% CBS chocolate. Although all the chocolates remained similar melting peak temperature, there were significant ($P < 0.05$) differences in peak area and melting enthalpy between 20% CBS-chocolate and CB-chocolate. 20% CBS-chocolate had significantly higher PSD with lower hardness and yield stress compared to CB-chocolate, but its viscosity was comparable to 5% CBS-chocolate and CB-chocolate. Stereomicroscope images of all the chocolate samples did not show bloom at 24°C for up to 8 weeks. However, at 29±1°C, bloom formation was observed for 5% CBS-chocolate and CB-chocolate after two weeks. Noticeable changes in X-ray diffraction peaks (polymorphism) were observed for the bloomed chocolate. There was no significant difference in sensory characteristics between 5% CBS-chocolate and CB-chocolate. Additionally, chocolate with 20% CBS was found to be different in terms of taste from the other two samples in a triangle test. The overall characterization suggested that the chocolate with 5% CBS was comparable to CB-chocolate in terms of physical and sensory characteristics. However, 20% CBS-chocolate showed significantly lower sensory properties particularly taste acceptance and hardness compared to CB-chocolate. All in all, both 5% and 20% CBS-chocolates need to be stored at 24°C to prevent bloom formation.

Chapter 6

6 General conclusions and Future work

6.1 General conclusions

This study was designed to develop CBSs by blending or modifying different palm oil fractions such as PMF, RBDPKO and RBDPS and characterize their physicochemical properties. The developed CBS was added with commercial CB and the mixture was investigated for compatibility. The blend of CBS and CB was then used to make dark chocolate, and the physical and sensory characteristics of dark chocolate were evaluated. The study was carried out in four phases as follows:

Firstly, the physical and chemical properties of binary mixtures of PMF, RBDPKO and RBDPS were examined to produce CBSs. Results showed that all the PMF/RBDPKO and RBDPS/RBDPKO blends had mixtures of short/long-chain fatty acids (lauric, myristic, palmitic and oleic) with corresponding TAGs. In contrast, the PMF/RBDPS blends showed only high percentage of long-chain fatty acids (palmitic and oleic) with corresponding TAGs. Among all the binary blends, 20-40% of PMF in RBDPKO, 30-50% of RBDPS in RBDPKO and 50-80% of PMF in RBDPS showed a desirable monotectic behavior at 10-25°C. Although the polymorphism and TAGs (particularly POS and StOSt) composition were different from that of CB, the broad melting endotherms (20-38°C) of these blends approximated to that of CB, showing potential for use as CBSs.

Secondly, the physical and chemical characteristics of ternary mixture of PMF, RBDPKO and RBDPS were examined. The ternary fat mixtures were combined based on the results of binary fat mixtures. Eight ternary blends of various ratios (%w/w) of PMF/RBDPKO/RBDPS were selected for this study. 14.9% PMF/59.6% RBDPKO/25.5% RBDPS blend showed comparable physicochemical properties to that of CB in terms of palmitic/oleic fatty acids constituent, POP composition and crystal morphology. Although its melting profile (18.5 and 37°C), polymorphism, stearic fatty acid and POST/StOSt composition were different from that of CB, it exhibited a desirable monotectic effect at 20-25°C with less than 50% SFC at 20°C which showed some potential for use as CBS.

In the subsequent phase of this study, commercial stearic and oleic fatty acids at different ratios (%w/w) were added to this suggested ternary blend (14.9% PMF/59.6% RBDPKO/25.5% RBDPS) to resemble the major fatty acids composition to CB. Results showed that the constituent of stearic and oleic fatty acids improved, but the palmitic acid composition decreased considerably for all samples compared to CB. Taking this into account, another ternary blend was selected and examined. This blend (33.3% PMF/33.3% RBDPKO/33.3% RBDPS) had a higher amount of palmitic acid with other fatty acids and multiple melting peaks as per the suggested ternary blend. After the addition of different ratios (%w/w) of commercial stearic-oleic fatty acids to this blend, all the samples showed increased in stearic/oleic acids and decreased in palmitic acid. Among all the four blends, blend 80% ternary mixture/15% stearic/5% oleic showed major fatty acids closely resembling that of CB. However, the blend showed undesirable multiple melting peaks and the TAG composition remained unchanged. Generally, TAGs, responsible for the melting profile, do not react with commercial stearic/oleic fatty acids without the help of enzymatic interesterification. Enzymatic interesterification rearranges the fatty acids of a TAG and this process changes the melting profile. Hence, the effect of enzymatic interesterification on the physicochemical properties of the blend (80% ternary blend/15% stearic/5% oleic) was investigated. The goal was to develop suitable CBS with properties particularly TAG composition and melting profile resembling those of CB.

The blend under optimized interesterification conditions (4% lipase enzyme for 6 h reaction time at 60°C reaction temperature) showed a single melting endotherm at 33.5°C, which is similar to commercial CB. However, after 8 h treatment with 4% enzyme concentration, two endotherms were observed between 16.5 and 35.5°C due to the rearrangement of fatty acids. The composition of POSt (28.4%) and StOSt (19.5%) of the interesterified fat was significantly ($P < 0.05$) increased along with a gradual decrease in POP (17.7%) compared to non-interesterified fat. Additionally, the interesterified fat revealed a desirable X-ray diffraction peak (albeit smaller) at near 4.5 Å indicating the β polymorph. Even though the interesterified fat showed lower SFC values up to 30°C compared to CB, it has potential for use as CBS.

Subsequently, the enzymatically produced CBS was mixed with commercial CB at different ratios (%w/w) to screen their possible application in chocolate production. 5 to 20% of CBS mixed with CB showed similar melting profile with comparable TAG composition,

polymorphism (predominant β -crystals) and crystal morphology to that of CB. Additionally, these blends (5 to 20% of CBS in CB) exhibited a desirable monotectic effect at 15-25°C, making them suitable for use in chocolate production.

Finally, the physical and sensory properties of dark chocolates made with enzymatically produced CBS were evaluated. Dark chocolates with CB (without CBS), 5% CBS and 20% CBS were produced. The chocolates with 5% and 20% CBS showed melting characteristic (melting peak temperature) similar to CB-chocolate. Significant ($P < 0.05$) differences in PSD, flow behavior, hardness and sensory characteristics (especially taste acceptance and hardness) were observed for 20% CBS-chocolate whilst no significant differences ($P \geq 0.05$) were observed for 5% CBS-chocolate compared to CB-chocolate. Stereomicroscope images of all the chocolate samples did not show bloom at 24°C for up to 8 weeks. Conversely, at $29 \pm 1^\circ\text{C}$, bloom formation was only observed for 5% CBS-chocolate and CB-chocolate after two weeks. Noticeable changes in X-ray diffraction peaks (polymorphism) were observed for bloomed chocolate. Overall, 5% CBS-chocolate was similar to CB-chocolate in terms of physical and sensory profile while 20% CBS-chocolate showed reasonably lower sensory profiles particularly taste acceptance and hardness compared to CB-chocolate. Both chocolates with 5% and 20% CBS should be stored at 24°C to prevent bloom formation. Figure 6.1 summarizes the overall production of CBS through blending and enzymatic interesterification of different palm oil fractions, and their melting and chemical composition.

6.1.1 Overall conclusions

In the present study, CBS was produced by blending and enzymatic interesterification of PMF, RBDPKO and RBDPS. The composition of major fatty acids (24.8% palmitic, 32.3% stearic and 29.1% oleic), TAGs (17.7% POP, 28.4% POSt and 19.5% StOSt), and melting endotherm (33.5°C) of the enzymatically developed CBS were comparable to those of CB. 5-20% of CBS in CB showed satisfactory compatibility (desirable monotectic effect) without altering the physicochemical properties of CB. The novelty of the current study lies in PMF/RBDPKO/RBDPS could be enzymatically interesterified to produce CBS that was able to make dark chocolate with similar physical and sensorial characteristics compared to CB-only-chocolate. Therefore, CBS developed in this study could be applied in chocolate formulations and other confectionery applications as to partially replace CB. The current study provides fundamental understanding on the phase behavior and physicochemical

properties of the developed CBS and CB mixture for chocolate application. Table 6.1 summarizes the overall production cost of CBS.

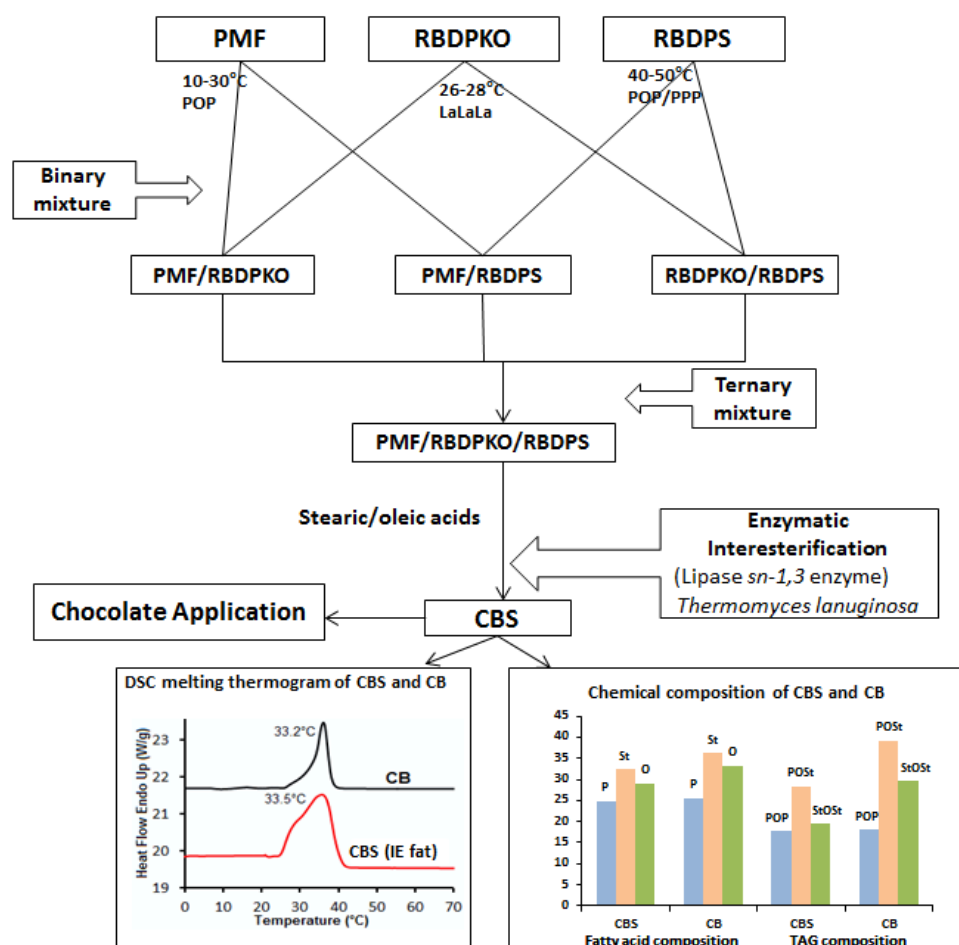


Figure 6.1: Schematic diagram of the production of produced CBS in chocolate application.

Table 6.1: Overall production cost of CBS.

Sample	Price/kg (RM)	Supplier	Production cost (RM)
CB	35	Le Bourne Sdn Bhd	CB = 35
PMF	4	Sime-Darby	5% replace = 33.25
RBDPKO	5	Research	20% replace = 28
RBDPS	4		100% replace = 6.1
Commercial stearic fatty acid	8	KLK Oleo Sdn Bhd	
Commercial oleic fatty acid	10		
Lipase enzyme	400	Novozyme	
CBS	6.1		
(PMF/RBDPKO/ RBDPS = 800g, Stearic = 150g, Oleic =150g, Enzyme =4%)			

6.2 Suggestions for future work

Findings from the current study can be extended as follows:

From the microstructure point of this study, further work can be carried out to study the nano-structure mechanism of produced palm oils-based CBS using cryo-transmission electronmicroscopy (Cryo-TEM). Furthermore, the dark chocolates made with CBS could be further analysed to understand the mechanism of bloom formation using atomic force microscopy (AFM) combined with field emission scanning electron microscopy (FESEM).

X-ray diffraction was used at ambient temperature for the polymorphism mechanism of chocolate made with the CBS. Further research is necessary to correlate the polymorphism in temperature controlled conditions with the DSC melting behavior.

Chocolate's image structure using Fourier transform infrared (FTIR) and Raman spectroscopy can be further studied to correlate with other imaging techniques such as FESEM and AFM.

References

- [1] **Abigor, R. D., Marmer, W.N., Foglia, T. A., Jones, K. C., DiCiccio, R. J., Ashby, R., Uadia, P. O.** Production of cocoa butter-like fats by the lipase-catalyzed interesterification of palm oil and hydrogenated soybean oil, *Journal of the American Oil Chemists' Society*. 2003, **80**, 1193-1196.
- [2] **Afoakwa, E. O.** Chocolate science and technology. (2nd Ed), John Wiley & Sons Ltd, Chichester (UK). 2016.
- [3] **Afoakwa, E. O., Paterson, A., Fowler, M.** Effects of particle size distribution and composition on rheological properties of dark chocolate, *European Food Research and Technology*. 2008, **226**, 1259-1268.
- [4] **Afoakwa, E. O., Paterson, A., Fowler, M.** Factors influencing rheological and textural qualities in chocolate—a review, *Trends in Food Science & Technology*. 2007, **18**, 290-298.
- [5] **Afoakwa, E. O., Paterson, A., Fowler, M., Vieira, J.** Characterization of melting properties in dark chocolates from varying particle size distribution and composition using differential scanning calorimetry, *Food Research International*. 2008, **41**, 751-757.
- [6] **Afoakwa, E. O., Paterson, A., Fowler, M. Vieira, J.** Effects of tempering and fat crystallisation behaviour on microstructure, mechanical properties and appearance in dark chocolate systems, *Journal of Food Engineering*. 2008, **89**, 128-136.
- [7] **Afoakwa, E. O., A. Paterson, M. Fowler, Vieira, J.** Influence of tempering and fat crystallization behaviours on microstructural and melting properties in dark chocolate systems, *Food Research International*. 2009, **42**, 200-209.
- [8] **Afoakwa, E. O., Paterson, A., Fowler, M., Vieira, J.** Microstructure and mechanical properties related to particle size distribution and composition in dark chocolate, *International Journal of Food Science & Technology*. 2009, **44**, 111-119.
- [9] **Aidoo, R. P., Clercq, N. D., Afoakwa, E. O., Dewettinck, K.** Optimisation of processing conditions and rheological properties using stephan mixer as conche in small-scale chocolate processing, *International Journal of Food Science & Technology*. 2014, **49**, 740-746.
- [10] **Albak, F., Tekin, A.** Variation of total aroma and polyphenol content of dark chocolate during three phase of conching, *Journal of Food Science and Technology*. 2016, **53**, 848-855.
- [11] **Ali, A. M., Dimick, P.** Melting and solidification characteristics of confectionery fats: anhydrous milk fat, cocoa butter and palm kernel stearin blends, *Journal of the American Oil Chemists' Society*. 1994, **71**, 803-806.
- [12] **Alkerwi, A. A., Sauvageot, N., Crichton, G. E., Elias, M. F., Stranges, S.** Daily chocolate consumption is inversely associated with insulin resistance and liver enzymes in the Observation of Cardiovascular Risk Factors in Luxembourg study, *British Journal of Nutrition*. 2016, **115**, 1661-1668.
- [13] **Asep, E., Jinap, S., Tan, T. J., Russly, A., Harcharan, S., Nazimah, S.** The effects of particle size, fermentation and roasting of cocoa nibs on supercritical fluid extraction of cocoa butter, *Journal of Food Engineering*. 2008, **85**, 450-458.
- [14] **Beckett, S. T.** Industrial chocolate manufacture and use. John Wiley & Sons, Chichester, 2011, pp. 246-250.
- [15] **Beckett, S. T.** Industrial chocolate manufacture and use, 3rd Ed, Blackwell, Oxford, 1999, pp. 153-465.

- [16] **Beckett, S. T.** The Science of Chocolate, (2nd Ed), RSC Publishing, Cambridge. 2008, pp. 12-124.
- [17] **Belščak, A., Komes, D., Horžić, D., Ganić, K. K., Karlović, D.** Comparative study of commercially available cocoa products in terms of their bioactive composition, *Food Research International*. 2009, **42**, 707-716.
- [18] **Biswas, N., Cheow, Y. L., Tan, C. P., Siow, L. F.** Blending of Palm Mid-Fraction, Refined Bleached Deodorized Palm Kernel Oil or Palm Stearin for Cocoa Butter Alternative, *Journal of the American Oil Chemists' Society*. 2016, **93**, 1415-1427.
- [19] **Biswas, N., Cheow, Y. L., Tan, C. P., Kanagaratnam, S., Siow, L. F.** Cocoa Butter Substitute (CBS) Produced from Palm Mid-fraction/Palm Kernel Oil/Palm Stearin for Confectionery Fillings, *Journal of the American Oil Chemists' Society*. 2017a, **94**, 235-245.
- [20] **Bloomer, S., Adlercreutz, P., Mattiasson, B.** Triglyceride interesterification by lipases. 1. Cocoa butter equivalents from a fraction of palm oil, *Journal of the American Oil Chemists' Society*. 1990, **67**, 519-524.
- [21] **Bootello, M. A., Hartel, R. W., Garcés, R., Martínez-Force, E., Salas, J. J.** Evaluation of high oleic-high stearic sunflower hard stearins for cocoa butter equivalent formulation, *Food Chemistry*. 2012, **134**, 1409-1417.
- [22] **Bootello, M. A., Hartel, R. W., Levin, M., Martínez-Blanes, J. M., Real, C., Garcés, R., Martínez-Force, E., Salas, J. J.** Studies of isothermal crystallisation kinetics of sunflower hard stearin-based confectionery fats, *Food Chemistry*. 2013, **139**, 184-195.
- [23] **Bragg, W. H., Bragg, W. L.** The reflection of X-rays by crystals, Proceedings of the Royal Society of London. Series A, Containing Papers of a Mathematical and Physical Character. 1913, **88**, 428-438.
- [24] **Bricknell, J., Hartel, R. W.** Relation of fat bloom in chocolate to polymorphic transition of cocoa butter, *Journal of the American Oil Chemists' Society*. 1998, **75**, 1609-1615.
- [25] **Briggs, J. L., Wang, T.** Influence of shearing and time on the rheological properties of milk chocolate during tempering, *Journal of the American Oil Chemists' Society*. 2004, **81**, 117-121.
- [26] **Buchgraber, M., Ulberth, F., Anklam, E.** Cluster analysis for the systematic grouping of genuine cocoa butter and cocoa butter equivalent samples based on triglyceride patterns, *Journal of Agricultural and Food Chemistry*. 2004, **52**, 3855-3860.
- [27] **Calliauw, G., Foubert, I., De Greyt, W., Dijckmans, P., Kellens, M., Dewettinck, K.** Production of cocoa butter substitutes via two-stage static fractionation of palm kernel oil, *Journal of the American Oil Chemists' Society*. 2005, **82**, 783-789.
- [28] **Campos, R.** Fat Crystal Networks, ed. A.G Marangoni, Marcel Dekker, New York, (1st Ed), Experimental methodology, CRC Press, Taylor & Francis Group 2005, pp 267-348.
- [29] **Campos, R., Ollivon, M., Marangoni, A. G.** Molecular composition dynamics and structure of cocoa butter, *Crystal Growth & Design*. 2009, **10**, 205-217.
- [30] **Cebula, D., Ziegleder, G.** Studies of Bloom Formation Using X-Ray Diffraction from Chocolates after Long-Term Storage, *Lipid/Fett*. 1993, **95**, 340-343.
- [31] **Cebula, D. J., Smith, K. W.** Differential scanning calorimetry of confectionery fats: Part II—Effects of blends and minor components, *Journal of the American Oil Chemists' Society*. 1992, **69**, 992-998.

- [32] **Chaiseri, S., Dimick, P. S.** Lipid and hardness characteristics of cocoa butters from different geographic regions, *Journal of the American Oil Chemists' Society*. 1989, **66**, 1771-1776.
- [33] **Chapman, G., Akehurst, E., Wright, W.** Cocoa butter and confectionery fats. Studies using programmed temperature X-ray diffraction and differential scanning calorimetry, *Journal of the American Oil Chemists Society*. 1971, **48**, 824-830.
- [34] **Chong, C., Hoh, Y., Wang, C.** Fractionation procedures for obtaining cocoa butter-like fat from enzymatically interesterified palm olein, *Journal of the American Oil Chemists' Society*. 1992, **69**, 137-140.
- [35] **Çiftçi, O. N., Fadiloğlu, S., Göğüş, F.** Conversion of olive pomace oil to cocoa butter-like fat in a packed-bed enzyme reactor, *Bioresource Technology*. 2009, **100**, 324-329.
- [36] **Couzens, P., Wille, H.** Fat migration in composite confectionery products, *Manufacturing Confectioner*. 1997, **77**, 45-47.
- [37] **D'Souza, V.** Short spacings and polymorphic forms of natural and commercial solid fats: a review, *Journal of the American Oil Chemists' Society*. 1990, **67**, 835-843.
- [38] **De Clercq, N., Depypere, F., Delbaere, C., Nopens, I., Bernaert, H., Dewettinck, K.** Influence of cocoa butter diacylglycerols on migration induced fat bloom in filled chocolates, *European Journal of Lipid Science and Technology*. 2014, **116**, 1388-1399.
- [39] **De Clercq, N., Kadivar, S., Van de Walle, D., De Pelsmaeker, S., Ghellynck, X., Dewettinck, K.** Functionality of cocoa butter equivalents in chocolate products, *European Food Research and Technology*. 2016, **243**, 309-321.
- [40] **De Clercq, N., Moens, K., Depypere, F., Ayala, J. V., Calliauw, G., De Greyt, W., Dewettinck, K.** Influence of cocoa butter refining on the quality of milk chocolate, *Journal of Food Engineering*. 2012, **111**, 412-419.
- [41] **De Magalhaes, J. T., Sodré, G. A., Viscogliosi, H., Grenier-Loustalot, M. F.** Occurrence of Ochratoxin A in Brazilian cocoa beans, *Food Control*. 2011, **22**, 744-748.
- [42] **Delbaere, C., Davy, V. W., Depypere, F., Gellynck, X., Dewettinck, K.** Relationship between chocolate microstructure, oil migration and fat bloom in filled chocolates, *European Journal of Lipid Science and Technology*. 2016, **118**, 1800-1826.
- [43] **DeMan, J.** X-ray diffraction spectroscopy in the study of fat polymorphism, *Food Research International*. 1992, **25**, 471-476.
- [44] **Dionisi, F., Golay, P. A., Hug, B., Baumgartner, M., Callier, P., Destailats, F.** Triacylglycerol analysis for the quantification of cocoa butter equivalents (CBE) in chocolate: feasibility study and validation, *Journal of Agricultural and Food Chemistry*. 2004, **52**, 1835-1841.
- [45] **Directive.** Directive 2000/36/EC of the European parliament and of the council relating to cocoa and chocolate products intended for human consumption, 2000, pp. 19-25.
- [46] **Dollah, S., Abdulkarim, S. M., Ahmad, S. H., Khoramnia, A., Mohd Ghazali, H.** Physico-chemical properties of Moringa oleifera seed oil enzymatically interesterified with palm stearin and palm kernel oil and its potential application in food, *Journal of the Science of Food and Agriculture*. 2016, **96**, 3321-3333.
- [47] **FAO.** Food and Agriculture Organization. Committee on Commodity Problems. International Cocoa Organization. The Future of the World Cocoa Economy: Boom or Bust? 69th Session, 28-30 May 2012, Rome, Italy.

- [48] **Fauzi, S. H. M., Rashid, N. A., Omar, Z.** Effects of chemical interesterification on the physicochemical, microstructural and thermal properties of palm stearin, palm kernel oil and soybean oil blends, *Food Chemistry*. 2013, **137**, 8-17.
- [49] **Fernandes, V. A., Müller, A. J., Sandoval, A. J.** Thermal, structural and rheological characteristics of dark chocolate with different compositions, *Journal of Food Engineering*. 2013, **116**, 97-108.
- [50] **Fiebig, H. J., Lüttke, J.** Solid fat content in fats and oils-determination by pulsed nuclear magnetic resonance spectroscopy [C-IV 3g (2003)], *European Journal of Lipid Science and Technology*. 2003, **105**, 377-380.
- [51] **Firestone, D.** Official methods and recommended practices of the AOCS, Oils and Fats Analysis-Standards, 6th Ed, Champaign. AOCS 2009.
- [52] **Foubert, I., Vanrolleghem, P., Thas, O., Dewettinck, K.** Influence of chemical composition on the isothermal cocoa butter crystallization, *Journal of Food Science*. 2004, **69**, 478-487.
- [53] **Garti, N., Widlak, N. R.** Cocoa butter and related compounds, Urbana, IL: AOCS Press. 2012.
- [54] **Gill, P., Sauerbrunn, S., Reading, M.** Modulated differential scanning calorimetry, *Journal of Thermal Analysis and Calorimetry*. 1993, **40**, 931-939.
- [55] **Glicerina, V., Balestra, F., Dalla Rosa, M., Romani, S.** Rheological, textural and calorimetric modifications of dark chocolate during process, *Journal of Food Engineering*. 2013, **119**, 173-179.
- [56] **Gold, I. L., Ukhun, M., Akoh, C.** Characteristics of eutectic compositions of restructured palm oil olein, palm kernel oil and their mixtures, *Journal of the American Oil Chemists' Society*. 2011, **88**, 1659-1667.
- [57] **Goto, M., Kodali, D., Small, D., Honda, K., Kozawa, K., Uchida, T.** Single crystal structure of a mixed-chain triacylglycerol: 1, 2-dipalmitoyl-3-acetyl-sn-glycerol, *Proceedings of the National Academy of Sciences*. 1992, **89**, 8083-8086.
- [58] **Gu, L., House, S. E., Wu, X., Ou, B., Prior, R. L.** Procyanidin and catechin contents and antioxidant capacity of cocoa and chocolate products, *Journal of Agricultural and Food Chemistry*. 2006, **54**, 4057-4061.
- [59] **Gunstone, F.** Vegetable oils in food technology: composition, properties and uses. John Wiley & Sons, CRC Press, 2011, pp. 291-343.
- [60] **Haines, P., Reading, M., Wilburn, F.** Differential thermal analysis and differential scanning calorimetry, *Handbook of Thermal analysis and calorimetry*. 1998, **1**, 279-361.
- [61] **Hartel, R. W.** Chocolate: fat bloom during storage, *Manufacturing Confectioner*. 1999, **79**, 89-99.
- [62] **Himawan, C., Starov, V., Stapley, A.** Thermodynamic and kinetic aspects of fat crystallization, *Advances in Colloid and Interface Science*. 2006, **122**, 3-33.
- [63] **Hodge, S., Rousseau, D.** Fat bloom formation and characterization in milk chocolate observed by atomic force microscopy, *Journal of the American Oil Chemists' Society*. 2002, **79**, 1115-1121.
- [64] **Humphrey, K., Narine, S. S.** Lipid phase behavior. In: Marangoni AG (ed), *Fat Crystal Networks*. Dekker, New York. 2004, pp. 83-114.
- [65] **ICA.** International Confectionery Association. Viscosity of cocoa and chocolate products. Analytical Method 46. CAOBISCO, rue Defacqz 1, B-1000 Brussels, Belgium, 2000.
- [66] **ICCO.** International Cocoa and Commodities Organisation. Celebration of Cocoa 2000. K.P. Partners in Publishing, London 2000.

- [67] **ICCO.** International Cocoa Organization. ICCO monthly averages of daily prices, December 2016., 2016.
- [68] **Jahurul, M., Zaidul, I., Norulaini, N., Sahena, F., Abedin, M., Ghafoor, K., Omar, A. M.** Characterization of crystallization and melting profiles of blends of mango seed fat and palm oil mid-fraction as cocoa butter replacers using differential scanning calorimetry and pulse nuclear magnetic resonance, *Food Research International*. 2014c, **55**, 103-109.
- [69] **Jahurul, M., Zaidul, I., Norulaini, N., Sahena, F., Jinap, S., Azmir, J., Sharif, K., Omar, A. M.** Cocoa butter fats and possibilities of substitution in food products concerning cocoa varieties, alternative sources, extraction methods, composition, and characteristics, *Journal of Food Engineering*. 2013, **117**, 467-476.
- [70] **Jahurul, M., Zaidul, I., Norulaini, N. N., Sahena, F., Abedin, M., Mohamed, A., Omar, A. M.** Hard cocoa butter replacers from mango seed fat and palm stearin, *Food Chemistry*. 2014a, **154**, 323-329.
- [71] **Jahurul, M., Zaidul, I., Norulaini, N. N., Sahena, F., Kamaruzzaman, B., Ghafoor, K., Omar, A.** Cocoa butter replacers from blends of mango seed fat extracted by supercritical carbon dioxide and palm stearin, *Food Research International*. 2014b, **65**, 401-406.
- [72] **Jensen, L.** Crystal Structure of beta-Tricaprin, *Nature*. 1963, **197**, 681-682.
- [73] **Jonfia-Essien, W., West, G., Alderson, P., Tucker, G.** Phenolic content and antioxidant capacity of hybrid variety cocoa beans, *Food Chemistry*. 2008, **108**, 1155-1159.
- [74] **Kadivar, S., De Clercq, N., Mokbul, M., Dewettinck, K.** Influence of enzymatically produced sunflower oil based cocoa butter equivalents on the phase behavior of cocoa butter and quality of dark chocolate, *LWT-Food Science and Technology*. 2016, **66**, 48-55.
- [75] **Kadivar, S., De Clercq, N., Van de Walle, D., Dewettinck, K.** Optimisation of enzymatic synthesis of cocoa butter equivalent from high oleic sunflower oil, *Journal of the Science of Food and Agriculture*. 2014, **94**, 1325-1331.
- [76] **Kaphueakngam, P., Flood, A., Sonwai, S.** Production of cocoa butter equivalent from mango seed almond fat and palm oil mid-fraction, *Asian Journal of Food and Agro-Industry*. 2009, **2**, 441-447.
- [77] **Keen, C. L., Holt, R. R., Oteiza, P. I., Fraga, C. G., Schmitz, H. H.** Cocoa antioxidants and cardiovascular health, *The American Journal of Clinical Nutrition*. 2005, **81**, 298S-303S.
- [78] **Kellens, M., Gibon, V., Hendrix, M., De Greyt, W.** Palm oil fractionation, *European Journal of Lipid Science and Technology*. 2007, **109**, 336-349.
- [79] **Khatoon, S., Khan, M. I., Jeyarani, T.** Enzymatic interesterification of palm and coconut stearin blends, *International Journal of Food Science & Technology*. 2012, **47**, 2259-2265.
- [80] **Kim, S., Kim, I. H., Akoh, C. C., Kim, B. H.** Enzymatic production of cocoa butter equivalents high in 1-palmitoyl-2-oleoyl-3-stearin in continuous packed bed reactors, *Journal of the American Oil Chemists' Society*. 2014, **91**, 747-757.
- [81] **Kinta, Y., Hartel, R. W.** Bloom formation on poorly-tempered chocolate and effects of seed addition, *Journal of the American Oil Chemists' Society*. 2010, **87**, 19-27.
- [82] **Koh, S. P., Arifin, N., Tan, C. P., Yusoff, M., Long, K., Lai, O.** Deep frying performance of enzymatically synthesized palm-based medium-and long-chain triacylglycerols (MLCT) oil blends, *Food and Bioprocess Technology*. 2011, **4**, 124-135.

- [83] **Kuleasan, S., Tekin, A.** Alkaline neutralization of crude soybean oil by various adsorbents, *European Journal of Lipid Science and Technology*. 2008, **110**, 261-265.
- [84] **Kummerow, F. A.** The negative effects of hydrogenated trans fats and what to do about them, *Atherosclerosis*. 2009, **205**, 458-465.
- [85] **Larsson, K., Larsson, K.** *Lipids: molecular organization, physical functions and technical applications*. Oily Press Dundee, UK; pp 7-47 1994.
- [86] **Lin, S. Y., Wang, S. L.** Advances in simultaneous DSC–FTIR microspectroscopy for rapid solid-state chemical stability studies: some dipeptide drugs as examples, *Advanced Drug Delivery Reviews*. 2012, **64**, 461-478.
- [87] **Lipp, M., Anklam, E.** Review of cocoa butter and alternative fats for use in chocolate—part A. Compositional data, *Food Chemistry*. 1998, **62**, 73-97.
- [88] **Liu, K. J., Chang, H. M., Liu, K. M.** Enzymatic synthesis of cocoa butter analog through interesterification of lard and tristearin in supercritical carbon dioxide by lipase, *Food Chemistry*. 2007, **100**, 1303-1311.
- [89] **Liu, K. J., Cheng, H. M., Chang, R. C., Shaw, J. F.** Synthesis of cocoa butter equivalent by lipase-catalyzed interesterification in supercritical carbon dioxide, *Journal of the American Oil Chemists' Society*. 1997, **74**, 1477-1482.
- [90] **Loisel, C., Lecq, G., Keller, G., Ollivon, M.** Dynamic crystallization of dark chocolate as affected by temperature and lipid additives, *Journal of Food Science*. 1998, **63**, 73-79.
- [91] **Lonchamp, P., Hartel, R. W.** Fat bloom in chocolate and compound coatings, *European Journal of Lipid Science and Technology*. 2004, **106**, 241-274.
- [92] **Lonchamp, P., Hartel, R. W.** Surface bloom on improperly tempered chocolate, *European Journal of Lipid Science and Technology*. 2006, **108**, 159-168.
- [93] **Marangoni, A. G.** Fat Crystal Networks, *Lipids -- Microstructure; Crystals -- Mathematical models; Crystallography*, Chapter 9. Experimental Methodology, CRC Press, pp. 267-348. 2004.
- [94] **Marangoni, A. G., McGauley, S. E.** Relationship between crystallization behavior and structure in cocoa butter, *Crystal Growth & Design*. 2003, **3**, 95-108.
- [95] **Marangoni, A. G., Rousseau, D.** Engineering triacylglycerols: the role of interesterification, *Trends in Food Science & Technology*. 1995, **6**, 329-335.
- [96] **Marangoni, A. G., Wesdorp, L. H.** Structure and Properties of Fat Crystal Networks. *Crystallography and Polymorphism (Chapter 1)*, 2nd Ed, Taylor & Francis Group, NY, CRC Press, pp. 1-24. 2012.
- [97] **Marty, S., Marangoni, A. G.** Effects of cocoa butter origin, tempering procedure, and structure on oil migration kinetics, *Crystal Growth & Design*. 2009, **9**, 4415-4423.
- [98] **MCB.** Malaysian Cocoa Board, Department of Statistic Malaysia. Production of Cocoa Beans, 2016.
- [99] **McGauley, S. E., Marangoni, A. G.** Static crystallization behavior of cocoa butter and its relationship to network microstructure, *Physical properties of lipids*. New York: Marcel Dekker. 2002, 85-123.
- [100] **Metin, S., Hartel, R. W.** Crystallization of Fats and Oils. In: Shahidi F, editor., *Bailey's industrial oil and fat products*. New York: Wiley Interscience. 2005.
- [101] **Miller, K. B., Hurst, W. J., Flannigan, N., Ou, B., Lee, C., Smith, N., Stuart, D. A.** Survey of commercially available chocolate-and cocoa-containing products in the United States. 2. Comparison of flavan-3-ol content with nonfat cocoa solids, total polyphenols, and percent cacao, *Journal of Agricultural and Food Chemistry*. 2009, **57**, 9169-9180.

- [102] **Mohamed, I. O.** Enzymatic Synthesis of Cocoa Butter Equivalent from Olive Oil and Palmitic-Stearic Fatty Acid Mixture, *Applied Biochemistry and Biotechnology*. 2015, **175**, 757-769.
- [103] **Mohamed, I. O.** Lipase-Catalyzed Acidolysis of Palm Mid Fraction Oil with Palmitic and Stearic Fatty Acid Mixture for Production of Cocoa Butter Equivalent, *Applied Biochemistry and Biotechnology*. 2013, **171**, 655-666.
- [104] **Mursu, J., Voutilainen, S., Nurmi, T., Rissanen, T. H., Virtanen, J. K., Kaikkonen, J., Nyyssönen, K., Salonen, J. T.** Dark chocolate consumption increases HDL cholesterol concentration and chocolate fatty acids may inhibit lipid peroxidation in healthy humans, *Free Radical Biology and Medicine*. 2004, **37**, 1351-1359.
- [105] **Nair, K. P.** The agronomy and economy of important tree crops of the developing world, Elsevier, London, 2010, pp. 131-180.
- [106] **Narine, S. S., Marangoni, A. G.** The difference between cocoa butter and Salatrim® lies in the microstructure of the fat crystal network, *Journal of the American Oil Chemists' Society*. 1999, **76**, 7-13.
- [107] **Norizzah, A., Chong, C., Cheow, C., Zaliha, O.** Effects of chemical interesterification on physicochemical properties of palm stearin and palm kernel olein blends, *Food Chemistry*. 2004, **86**, 229-235.
- [108] **Osborn, H., Akoh, C.** Enzymatically modified beef tallow as a substitute for cocoa butter, *Journal of Food Science*. 2002, **67**, 2480-2485.
- [109] **Quast, L. B., Luccas, V., Ribeiro, A. P. B., Cardoso, L. P., Kieckbusch, T. G.** Physical properties of tempered mixtures of cocoa butter, CBR and CBS fats, *International Journal of Food Science & Technology*. 2013, **48**, 1579-1588.
- [110] **Rabasco Álvarez, A. M., González Rodríguez, M. L.** Lipids in pharmaceutical and cosmetic preparations, *Grasas y aceites*. 2000 **51**, 74-96.
- [111] **Ramel, P. R., Co, E. D., Acevedo, N. C., Marangoni, A. G.** Structure and functionality of nanostructured triacylglycerol crystal networks, *Progress in Lipid Research*. 2016, **64**, 231-242.
- [112] **Ray, J.** Production and characterisation of cocoa butter equivalents from high oleic sunflower oil by enzymatic rearrangement. PhD thesis, Loughborough University, Loughborough, England 2013.
- [113] **Ray, J., Nagy, Z. K., Smith, K. W., Bhaggan, K., Stapley, A. G.** Kinetic study of the acidolysis of high oleic sunflower oil with stearic-palmitic acid mixtures catalysed by immobilised *Rhizopus oryzae* lipase, *Biochemical Engineering Journal*. 2013, **73**, 17-28.
- [114] **Regulation, M. F.** Malaysian law on food and drugs, Malaysian Law Publishers 1985.
- [115] **Reshma, M., Saritha, S., Balachandran, C., Arumughan, C.** Lipase catalyzed interesterification of palm stearin and rice bran oil blends for preparation of zero trans shortening with bioactive phytochemicals, *Bioresource Technology*. 2008, **99**, 5011-5019.
- [116] **Reyes-Hernández, J., Dibildox-Alvarado, E., Charó-Alonso, M., Toro-Vazquez, J.** Physicochemical and rheological properties of crystallized blends containing trans-free and partially hydrogenated soybean oil, *Journal of the American Oil Chemists' Society*. 2007, **84**, 1081-1093.
- [117] **Rodríguez, A., Castro, E., Salinas, M. C., López, R., Miranda, M.** Interesterification of tallow and sunflower oil, *Journal of the American Oil Chemists' Society*. 2001, **78**, 431-436.

- [118] **Rousseau, D., Smith, P.** Microstructure of fat bloom development in plain and filled chocolate confections, *Soft Matter*. 2008, **4**, 1706-1712.
- [119] **Sabariah, S., Ali, A. M., Chong, C.** Chemical and physical characteristics of cocoa butter substitutes, milk fat and Malaysian cocoa butter blends, *Journal of the American Oil Chemists' Society*. 1998, **75**, 905-910.
- [120] **Saberi, A. H., Lai, O. M., Toro-Vázquez, J. F.** Crystallization kinetics of palm oil in blends with palm-based diacylglycerol, *Food Research International*. 2011, **44**, 425-435.
- [121] **Sato, K.** Crystallization behaviour of fats and lipids—a review, *Chemical Engineering Science*. 2001, **56**, 2255-2265.
- [122] **Sato, K.** Molecular aspects in fat polymorphism, AOCS Press: Champaign IL, USA. 2001, pp. 1-15.
- [123] **Sato, K., Goto, M., Yano, J., Honda, K., Kodali, D. R., Small, D. M.** Atomic resolution structure analysis of β' polymorph crystal of a triacylglycerol: 1, 2-dipalmitoyl-3-myristoyl-sn-glycerol, *Journal of Lipid Research*. 2001, **42**, 338-345.
- [124] **Sato, K., Ueno, S.** Physical properties of fats in food, *Fats in Food Technology*. Chichester: Wiley. 2014, pp. 1-38.
- [125] **Schmelzer, J. M., Hartel, R. H.** Interactions of milk fat and milk fat fractions with confectionery fats, *Journal of Dairy Science*. 2001, **84**, 332-344.
- [126] **Servais, C., Ranc, H., Roberts, I.** Determination of chocolate viscosity, *Journal of Texture Studies*. 2003, **34**, 467-497.
- [127] **Shukla, V. K. S.** Edible oil and fat products: Products and applications. in: Shahidi, Fereidoon (Ed.), *Bailey's Industrial Oil and Fat Products*, Vol. 4, 6th Edn., John Wiley & Sons Ltd., Hoboken, NJ, 2005, pp. 159-173.
- [128] **Shukla, V. K. S.** Cocoa butter properties and quality, *Lipid Technology*, 1995, **7**, 54-57.
- [129] **Smith, K. W., Cain, F. W., Talbot, G.** Nature and composition of fat bloom from palm kernel stearin and hydrogenated palm kernel stearin compound chocolates, *Journal of Agricultural and Food Chemistry*. 2004, **52**, 5539-5544.
- [130] **Soares, F. A. S. D. M., da Silva, R. C., da Silva, K. C. G., Lourenço, M. B., Soares, D. F., Gioielli, L. A.** Effects of chemical interesterification on physicochemical properties of blends of palm stearin and palm olein, *Food Research International*. 2009, **42**, 1287-1294.
- [131] **Sonwai, S., Kaphueakngam, P., Flood, A.** Blending of mango kernel fat and palm oil mid-fraction to obtain cocoa butter equivalent, *Journal of Food Science and Technology*. 2014, **51**, 2357-2369.
- [132] **Sonwai, S., Rousseau, D.** Structure evolution and bloom formation in tempered cocoa butter during long-term storage, *European Journal of Lipid Science and Technology*. 2006, **108**, 735-745.
- [133] **Sridhar, R., Lakshminarayana, G., Kaimal, T.** Modification of selected Indian vegetable fats into cocoa butter substitutes by lipase-catalyzed ester interchange, *Journal of the American Oil Chemists Society*. 1991, **68**, 726-730.
- [134] **Steinberg, F. M., Bearden, M. M., Keen, C. L.** Cocoa and chocolate flavonoids: implications for cardiovascular health, *Journal of the American Dietetic Association*. 2003, **103**, 215-223.
- [135] **Talbot, G.** *Application of Fats in Confectionery*. Kennedy's Publications, Loughton, UK, 2006, pp. 125-137.
- [136] **Talbot, G.** *Science and Technology of Enrobed and Filled Chocolate, Confectionery and Bakery Products*, CRC Press, Woodhead Publishing Limited, New York. 2009, pp. 53-79, 344-361, 255-283.

- [137] **Talbot, G.** Vegetable fats, Industrial Chocolate Manufacture and Use, Springer, 1994, pp. 242-257.
- [138] **Tan, C. P., Man, Y. C.** Differential scanning calorimetric analysis of palm oil, palm oil based products and coconut oil: effects of scanning rate variation, *Food Chemistry*. 2002, **76**, 89-102.
- [139] **Timms, R. E.** Phase behaviour of fats and their mixtures, Progress in Lipid Research. 1984, **23**, 1-38.
- [140] **Timms, R. E.** Production and characteristic properties. In Timms RE.,(Ed), Confectionery fats handbook: properties, production and application. The Oily Press, Bridwater, England, 2003, pp. 191-254.
- [141] **Torbica, A. M., Pajin, B. S., Omorjan, R. P., Lončarević, I. S., Tomić, J. M.** Physical properties of chocolate with addition of cocoa butter equivalent of moderate hardness, *Journal of the American Oil Chemists' Society*. 2014, **91**, 39-48.
- [142] **Toro-Vazquez, J. F., Pérez-Martínez, D., Dibildox-Alvarado, E., Charó-Alonso, M., Reyes-Hernández, J.** Rheometry and polymorphism of cocoa butter during crystallization under static and stirring conditions, *Journal of the American Oil Chemists' Society*. 2004, **81**, 195-202.
- [143] **Undurraga, D., Markovits, A., Erazo, S.** Cocoa butter equivalent through enzymic interesterification of palm oil midfraction, *Process Biochemistry*. 2001, **36**, 933-939.
- [144] **Vereecken, J., Foubert, I., Smith, K. W., Dewettinck, K.** Relationship between crystallization behavior, microstructure, and macroscopic properties in trans-containing and trans-free filling fats and fillings, *Journal of Agricultural and Food Chemistry*. 2007, **55**, 7793-7801.
- [145] **Wang, F., Liu, Y., Jin, Q., Meng, Z., Wang, X.** Characterization of cocoa butter substitutes, milk fat and cocoa butter mixtures, *European Journal of Lipid Science and Technology*. 2011, **113**, 1145-1151.
- [146] **Wang, F., Liu, Y., Shan, L., Jin, Q., Wang, X., Li, L.** Blooming in cocoa butter substitutes based compound chocolate: Investigations on composition, morphology and melting behavior, *Journal of the American Oil Chemists' Society*. 2010, **87**, 1137-1143.
- [147] **Wang, H. X., Wu, H., Ho, C. T., Weng, X. C.** Cocoa butter equivalent from enzymatic interesterification of tea seed oil and fatty acid methyl esters, *Food Chemistry*. 2006, **97**, 661-665.
- [148] **Werneck, M. M., Allil, R., Ribeiro, B., de Nazaré, F.** A guide to fiber bragg grating sensors, Current Trends in Short-and Long-Period Fibre Gratings; InTech: Rijeka, Croatia. 2013, pp. 1-24.
- [149] **Wille, R., Lutton, E.** Polymorphism of cocoa butter, *Journal of the American Oil Chemists Society*. 1966, **43**, 491-496.
- [150] **Williams, S. D., Ransom-Painter, K. L., Hartel, R. W.** Mixtures of palm kernel oil with cocoa butter and milk fat in compound coatings, *Journal of the American Oil Chemists' Society*. 1997, **74**, 357-366.
- [151] **Xu, X.** Production of specific-structured triacylglycerols by lipase-catalyzed reactions: a review, *European Journal of Lipid Science and Technology*. 2000, **102**, 287-303.
- [152] **Zaidul, I., Norulaini, N. N., Omar, A. M., Smith, R.** Blending of supercritical carbon dioxide (SC-CO₂) extracted palm kernel oil fractions and palm oil to obtain cocoa butter replacers, *Journal of Food Engineering*. 2007, **78**, 1397-1409.
- [153] **Zarringhalami, S., Sahari, M. A., Barzegar, M., Hamidi-Esfehani, Z.** Enzymatically modified tea seed oil as cocoa butter replacer in dark chocolate, *International Journal of Food Science & Technology*. 2010, **45**, 540-545.

- [154] **Zhang, H., Smith, P., Adler-Nissen, J.** Effects of degree of enzymatic interesterification on the physical properties of margarine fats: solid fat content, crystallization behavior, crystal morphology, and crystal network, *Journal of Agricultural and Food Chemistry*. 2004, **52**, 4423-4431.
- [155] **Zhou, S. L., Zhang, F. Q., Jin, Q. Z., Liu, Y. F., Shan, L., Zhang, T., Zou, X. Q., Wang, X. G.** Characterization of palm kernel oil, palm stearin, and palm olein blends in isosolid diagrams, *European Journal of Lipid Science and Technology*. 2010, **112**, 1041-1047.

Appendix A List of chemicals used in this study

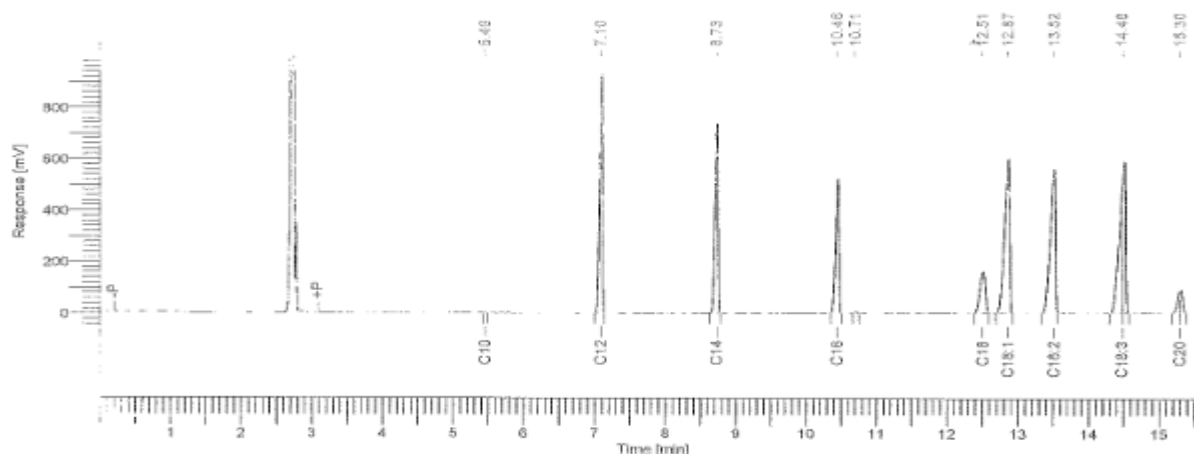
Table A.1. List of chemicals.

Chemicals	Grade	Company
Acetone	HPLC grade (99%)	Fisher Scientific, Loughborough, UK
Acetonitrile	Assay (GC, 99.99%)	Fisher Scientific, Loughborough, UK
Ethyl alcohol	Analar grade (~95%)	R & M Chemicals, Essex, UK
Isopropanol	Assay (GC, 99.98%)	Fisher Scientific, Loughborough, UK
Sodium hydroxide	ACS reagent	R & M Chemicals, Essex, UK
Heptane	HPLC grade (99%)	Fisher Scientific, Loughborough, UK
Hexane	HPLC grade (95%)	Fisher Scientific, Loughborough, UK
Toluene	Assay (GC, 99.97%)	Fisher Scientific, Loughborough, UK
Methanol	Assay (GC, 99.99%)	Fisher Scientific, Loughborough, UK
Toluene	HPLC grade ($\geq 99.5\%$)	Fisher Scientific, Loughborough, UK
Sulfuric acid	HPLC grade ($\geq 99.5\%$)	Fisher Scientific, Loughborough, UK
Lipase enzyme	Lipozyme TL IM (<i>Thermomyces lanuginosa</i> lipase)	Novozymes, Bagsvaerd, Denmark
FAME	Analytical standard	Lab Science Solution Sdn. Bhd., Selangor, Malaysia
TAG standards	Analytical standard	Sigma Aldrich, St. Louis, MO

Appendix B (Chapter 2) GC chromatogram

Software Version : 6.3.0.0445 Date : 11/27/2014 2:14:12 AM
 Operator : TCWS Sample Name : STD
 Sample Number : Study :
 AutoSampler : NONE Rack/Vial : 0/0
 Instrument Name : Clarus 500 Channel : A
 Instrument Serial # : 650N5080905 A/D mV Range : 1000
 Delay Time : 0.00 min End Time : 15.67 min
 Sampling Rate : 12.5000 pts/s
 Sample Volume : 1.000000 ul
 Sample Amount : 1.0000 Area Reject : 0.000000
 Data Acquisition Time : 11/27/2014 1:24:54 AM Dilution Factor : 1.00
 Cycle : 1

Raw Data File : C:\GC\Data\DR LEE FONG SIO\STD_C12-C18_attn-4_27_11_14.raw
 Inst Method : C:\GC\Method\FAME_STANDARD_ATTEN-4_27_11_14 from C:\GC\Data\DR LEE FONG SIO\STD_C12-C18_attn-4_27_11_14.raw
 Proc Method : C:\GC\Method\FAME_STANDARD_ATTEN-4_27_11_14.mth from
 Calib Method : C:\GC\Method\FAME_STANDARD_ATTEN-4_27_11_14.mth from
 Report Format File : C:\GC\Report Format\FAME.rpt
 Sequence File : C:\GC\Method\STD_C12-C18_attn-4_27_11_14.seq



FAME REPORT

Peak #	Component Name	Time [min]	Area [uV*sec]	Height [uV]	Area [%]	Norm. Area [%]	BL
1	C10	5.460	2490.70	1538.07	0.02	0.02	BB
2	C12	7.100	2478858.13	926368.91	15.00	15.00	BB
3	C14	8.733	2060282.83	735583.06	12.46	12.46	BB
4	C16	10.456	1662261.50	520527.22	10.06	10.06	BB
5		10.707	14804.03	6639.20	0.09	0.09	BB
6	C18	12.513	832528.12	158424.77	5.04	5.04	BB
7	C18:1	12.868	2840936.27	595126.98	17.19	17.19	BB
8	C18:2	13.516	2755285.99	554541.12	16.67	16.67	BB

Figure B.1. Example of GC chromatogram of FAME standards.

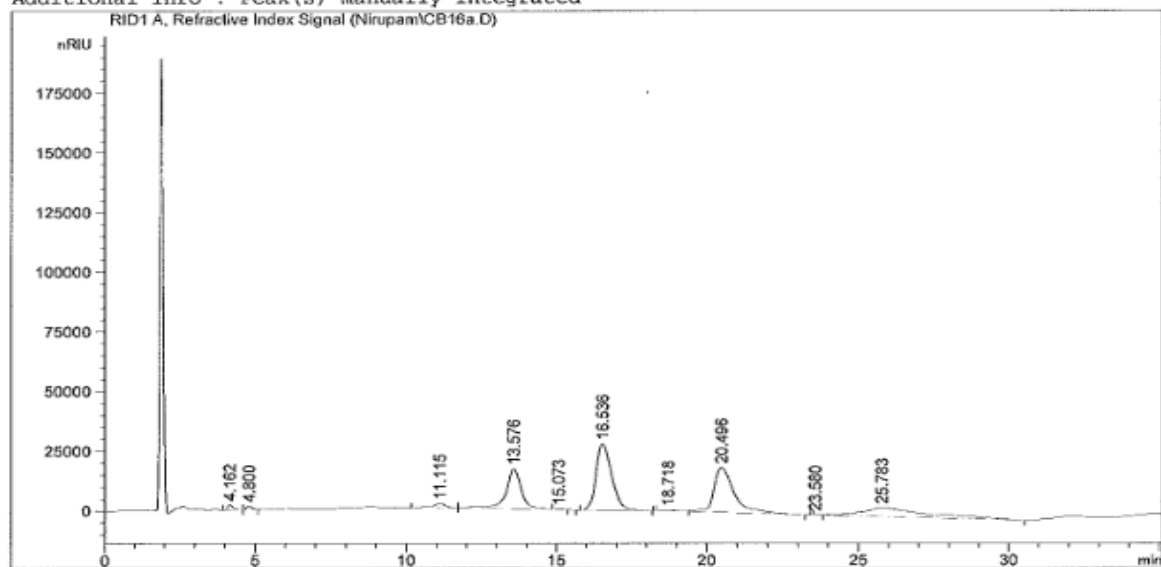
Appendix C (Chapter 2) HPLC chromatogram

Data File C:\Chem32\1\Data\Nirupam\CB16a.D
Sample Name: CB16_12

```
=====
Acq. Operator   : SYSTEM
Sample Operator : SYSTEM
Acq. Instrument : HPLC
Injection Date  : 12/16/2015 11:14:25 AM
Location       : 1
Inj Volume     : 10.000 µl

Acq. Method    : C:\Chem32\1\Methods\Nirupam.M
Last changed   : 12/16/2015 10:55:07 AM by SYSTEM
                (modified after loading)
Analysis Method: C:\Chem32\1\Methods\Nirupam.M
Last changed   : 12/16/2015 11:59:02 AM by SYSTEM
                (modified after loading)
Sample Info    : Acetone/ACN (70/30 v/v)
                Column temp 35 degree C
                10 uL,
```

Additional Info : Peak(s) manually integrated



Area Percent Report

```
Sorted By      : Signal
Multiplier     : 1.0000
Dilution       : 1.0000
Sample Amount:  : 1.00000 [ng/ul] (not used in calc.)
Do not use Multiplier & Dilution Factor with ISTDs
```

Signal 1: RID1 A, Refractive Index Signal

Peak #	RetTime [min]	Type	Width [min]	Area [nRIU*s]	Height [nRIU]	Area %
1	4.162	BB	0.1909	2.66462e4	2136.47998	0.8413
2	4.800	BB	0.1953	1.82808e4	1486.25330	0.5772
3	11.115	BB	0.4201	5.37110e4	1842.31470	1.6958

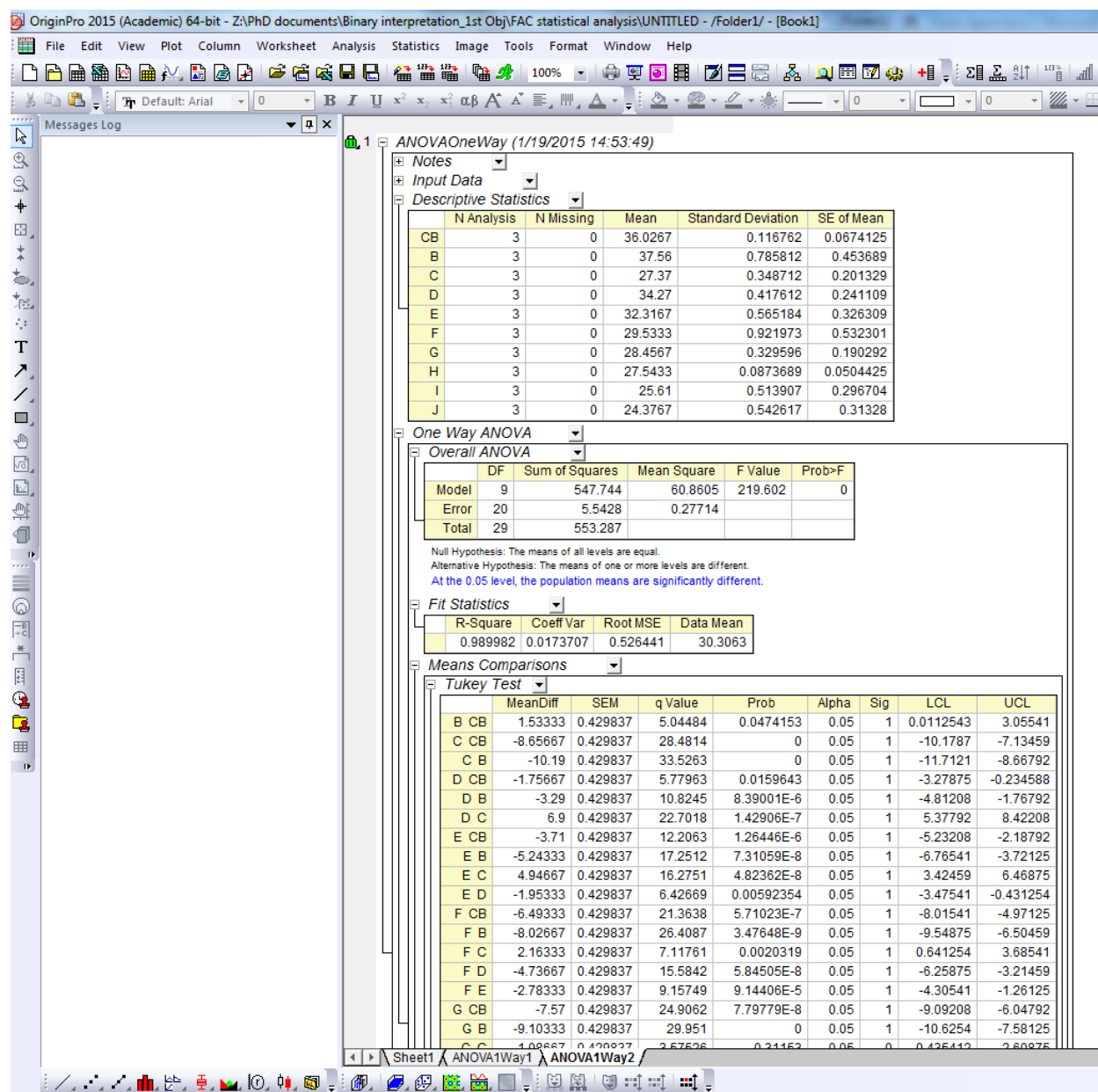
HPLC 12/16/2015 12:00:48 PM SYSTEM

Page 1 of 2

Figure C.1. Example of HPLC chromatogram of cocoa butter.

Appendix D (Chapter 2) Statistical analysis using OriginPro software

Table D.1. Statistical analysis of the data in Chapter 2.



Appendix E (Chapter 5) Statistical analysis using SPSS software

Table E.1: Statistical analysis of the data in Chapter 5.

DSC melting.spv [Document4] - IBM SPSS Statistics Viewer

File Edit View Data Transform Insert Format Analyze Direct Marketing Graphs Utilities Add-ons Window Help

Output Log Oneway Title Notes Active Dataset ANOVA Post Hoc Tests Multiple Comparisons Homogeneous Subset Title Onset Endset MeltingEnthalpy

Oneway

[DataSet0]

ANOVA

		Sum of Squares	df	Mean Square	F	Sig.
Onset	Between Groups	8.027	2	4.013	29.607	.001
	Within Groups	.813	6	.136		
	Total	8.840	8			
Endset	Between Groups	.162	2	.081	.474	.644
	Within Groups	1.027	6	.171		
	Total	1.189	8			
MeltingEnthalpy	Between Groups	43.262	2	21.631	94.048	.000
	Within Groups	1.380	6	.230		
	Total	44.642	8			

Post Hoc Tests

Multiple Comparisons

Tukey HSD

Dependent Variable	(I) Samples	(J) Samples	Mean Difference (I-J)	Std. Error	Sig.	95% Confidence Interval	
						Lower Bound	Upper Bound
Onset	CB-Chocolate	5%CBS-Chocolate	.1333	.3006	.899	-.789	1.056
		20%CBS-Chocolate	2.0667*	.3006	.001	1.144	2.989
	5%CBS-Chocolate	CB-Chocolate	-.1333	.3006	.899	-1.056	.789
		20%CBS-Chocolate	1.9333*	.3006	.002	1.011	2.856
	20%CBS-Chocolate	CB-Chocolate	-2.0667*	.3006	.001	-2.989	-1.144
		5%CBS-Chocolate	-1.9333*	.3006	.002	-2.856	-1.011
Endset	CB-Chocolate	5%CBS-Chocolate	-.0333	.3377	.995	-1.070	1.003
		20%CBS-Chocolate	.2667	.3377	.723	-.770	1.303
	5%CBS-Chocolate	CB-Chocolate	.0333	.3377	.995	-1.003	1.070
		20%CBS-Chocolate	.3000	.3377	.667	-.736	1.336
	20%CBS-Chocolate	CB-Chocolate	-.2667	.3377	.723	-1.303	.770
		5%CBS-Chocolate	-.3000	.3377	.667	-1.336	.736
MeltingEnthalpy	CB-Chocolate	5%CBS-Chocolate	-.4667	.3916	.500	-1.668	.735
		20%CBS-Chocolate	4.4000*	.3916	.000	3.199	5.601
	5%CBS-Chocolate	CB-Chocolate	.4667	.3916	.500	-.735	1.668
		20%CBS-Chocolate	4.8667*	.3916	.000	3.665	6.068
	20%CBS-Chocolate	CB-Chocolate	-4.4000*	.3916	.000	-5.601	-3.199
		5%CBS-Chocolate	-4.8667*	.3916	.000	-6.068	-3.665

*. The mean difference is significant at the 0.05 level.

Appendix F (Chapter 5) Sensory questionnaire form

Sensory evaluation form

You are given three samples (245, 274 and 237) of chocolate. Please evaluate the chocolate formulations using the 9-point hedonic scale given in Table 1. Please remove chocolates from the plastic bag to examine the glossiness (Q1) before further tasting. Participants are asked to eat a small bite of biscuit and then drink water to rinse their palate after tasting each type of chocolate.

Table 1: Hedonic scale responses

Scale point	Description
1	Dislike extremely
2	Dislike very much
3	Dislike moderately
4	Dislike slightly
5	Neither like or dislike
6	Like slightly
7	Like moderately
8	Like very much
9	Like extremely

Question 1

Please taste and rank the samples carefully using the above scale point.

Characteristics	245	274	237
Glossiness (shiny)			
Hardness			
Waxiness			
Greasy to touch (sticky)			
Mouth-feel (smooth, melting behavior)			
Overall acceptability (shiny, sticky, melting)			
Taste acceptance			

Question 2

Triangle test

Please evaluate all three samples (245, 274 and 237), in order from left to right, then circle **ONE** sample which is different from the other two.

245

274

237

Thank you for your participation!

Appendix G (Chapter 5) Control chocolate and bloomed chocolate

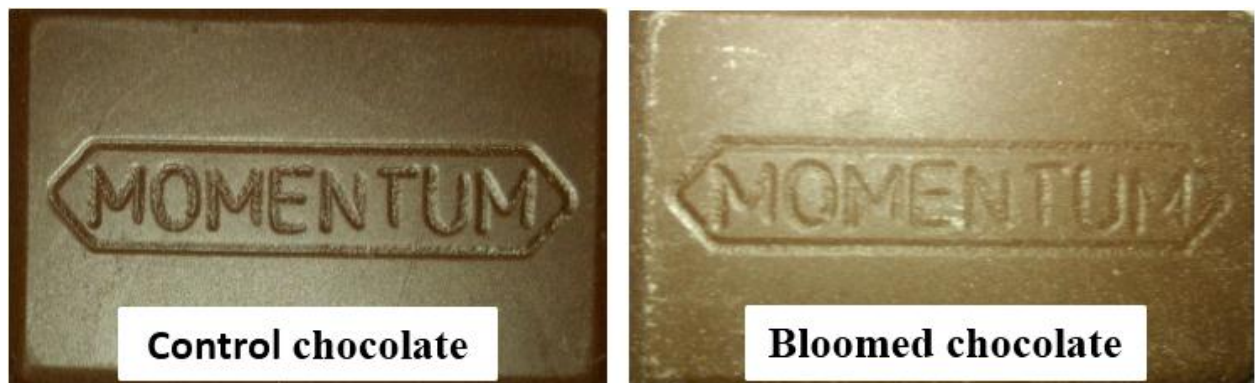


Figure G.1. Example of control chocolate (un-bloomed) and bloomed chocolate.

Appendix H (Chapter 2) Publications during enrolment

J Am Oil Chem Soc (2016) 93:1415–1427
DOI 10.1007/s11746-016-2880-z



ORIGINAL PAPER

Blending of Palm Mid-Fraction, Refined Bleached Deodorized Palm Kernel Oil or Palm Stearin for Cocoa Butter Alternative

N. Biswas¹ · Y. L. Cheow¹ · C. P. Tan² · L. F. Siow¹

Received: 5 October 2015 / Revised: 31 May 2016 / Accepted: 2 August 2016 / Published online: 13 August 2016
© AOCS 2016

Abstract This study evaluated the physicochemical properties of palm mid-fraction (PMF), refined bleached deodorized palm kernel oil (RBDPKO) and refined bleached deodorized palm stearin (RBDPS) as binary mixtures in terms of their fatty acid compositions (GC), triacylglycerols (HPLC), solid fat contents (p-NMR), melting behaviors (DSC) and polymorphisms (XRD) for cocoa butter (CB) alternative formulations. All the PMF/RBDPKO and RBDPS/RBDPKO blends showed mixtures of short/long-chain fatty acids with corresponding triacylglycerols. 10–70 % PMF in RBDPKO showed a eutectic effect between 20 and 30 °C. However, a monotectic effect was observed at 10–15 °C for 20–40 % PMF in RBDPKO and 40–80 % of RBDPS in RBDPKO. For PMF/RBDPS blends, a monotectic effect was observed at less than 30 °C. Broad endotherms at 20–38 °C were observed for 30–50 % RBDPS in RBDPKO which are closer to CB, with polymorphs of $\beta'_1 > \beta'_2 \gg \beta_2$ based on XRD analysis. 50–80 % PMF in RBDPS exhibited significantly higher contents of long-chain fatty acids with the exception of stearic and lower constituents of monounsaturated triacylglycerols compared to CB. Broad endotherms were observed at 20–38 °C for 50–80 % PMF in RBDPS which are closer to CB, with $\beta'_1 \gg \beta'_2 > \beta_2$. Therefore, 20–40 % PMF in RBDPKO, 30–50 % RBDPS in RBDPKO and 50–80 % PMF in

RBDPS could be used as CB substitutes because of their comparable physicochemical behaviors.

Keywords Iso-solid diagram · Differential scanning calorimetry · *Elaeis guineensis* · Solid fat content · Cocoa butter alternative

Introduction

Cocoa butter (CB) is a natural fat obtained from cocoa seeds (*Theobroma cacao*), commonly used as an important ingredient for the production of chocolate. CB consists of three main triacylglycerols (TAGs): glycerol-1,3-dipalmitate-2-oleate (POP; P palmitic, O oleic), glycerol-1-palmitate-2-oleate-3-stearate (POST; St stearic) and glycerol-1,3-distearate-2-oleate (StOST) [1, 2]. These TAGs are responsible for the melting profiles, crystallization and polymorphisms of CB, which becomes highly solid at 20 °C and melts between 30 and 35 °C [3]. This melting profile is desired in confectionery applications such as chocolates. CB has a complex polymorphic behavior, with an α polymorph (melting temperature, T_m 17–24 °C, short spacing at 4.15 Å); a β'_1 polymorph (T_m 26–30 °C, 3.8 and 4.2 Å); a β'_2 polymorph (T_m 24–26 °C, 4.1 and 4.3 Å); a β_1 polymorph (T_m 34–36 °C, 3.7 and 4.6 Å) and a β_2 polymorph (T_m 32–34 °C, 4.5 Å) [4]. Generally, the stable polymorph (β_2) is preferred in chocolates as it melts at a high melting temperature with small to moderate crystal sizes allowing for smooth products [5].

Cocoa butter is very expensive among all commercial fats and oils due to its low availability and strong market demand. Therefore, many studies have been performed to produce alternatives to CB by blending different proportions of palm kernel oil and palm oil [6–8], palm

✉ L. F. Siow
siow.lee.fong@monash.edu

¹ School of Science, Monash University Malaysia,
47500 Bandar Sunway, Selangor D.E., Malaysia

² Department of Food Technology, Faculty of Food Science
and Technology, Universiti Putra Malaysia (UPM),
43400 Serdang, Selangor D.E., Malaysia

mid-fraction and mango kernel fat [9], palm kernel oil and milk fat [7], and palm stearin and mango seed fat [10]. Among cocoa butter alternatives (CBAs), cocoa butter substitutes (CBSs) are derived from lauric fats such as palm kernel oil and coconut oil, cocoa butter replacers (CBRs) are obtained from hydrogenation of non-lauric vegetable oils such as hydrogenated mango seed fat, and cocoa butter equivalents (CBEs) are derived from stearate-rich fats such as mango seed, sal, shea, kokum and illipe [9]. The melting profile of CBSs is similar to that of CB but chemical composition and crystallization behavior in terms of stable polymorphic forms are completely different to CB. CBEs show similar melting profile, polymorphism and chemical composition with CB [28].

Palm mid-fraction (PMF) is a fraction of palm oil (*Elaeis guineensis*) that is obtained through re-fractionation, either from palm olein or palm stearin; it has a melting point between 9.8 and 32.8 °C [1]. Of the three main TAGs, PMF contains 51.8 % of symmetrical monounsaturated POP. Most importantly, PMF shows a steep solid fat content versus temperature curve, which is similar to that of CB. These physicochemical properties make PMF suitable for the production of CBA [1, 9].

The fraction from palm kernel oil, extracted by fractionation, refined, bleached and deodorized (RBDPKO) is a semi-solid fat at room temperature with a melting point of approximately 26–28 °C [11]. It contains a high percentage of short-chain fatty acids: lauric acid (12:0, 47.7 %) and myristic acid (14:0, 22.6 %) [8]. Although this oil contains high levels of undesirable lauric and myristic acids, it is widely used as a suitable raw material for the production of confectionery [7]. In this application, RBDPKO shows melting and crystallization behaviors similar to CB but differ considerably chemically. In CB, the constituents of long-chain fatty acids such as palmitic (16:0, 24.4 %), stearic (18:0, 33.6 %), and oleic acids (18:1, 37.0 %) are high, while the short-chain fatty acids such as lauric acid and myristic acid constituents occur in very low amounts [1]. In RBDPKO, the concentration of short-chain fatty acid constituents is high, while the concentration of long-chain fatty acid constituents is relatively low compared with CB. Hence, the high short-chain fatty acids content and the low long-chain fatty acids (palmitic/oleic) content of RBDPKO makes it unsuitable as a direct CB substitute. However, by blending RBDPKO with palmitic acid and oleic acid-rich fats such as PMF or palm stearin, it is possible to decrease the short-chain fatty acid concentration and increase the long-chain fatty acid concentration. This may produce high-quality CBSs with a fatty acid composition closer to CB. RBDPKO is now gaining more interest as a suitable CBS in confectionery [12].

Refined bleached deodorized palm stearin (RBDPS) is obtained by fractionating refined palm oil to separate olein from palm stearin. RBDPS is a solid fat with a high melting point (44–56 °C) which needs to be mixed with lower melting oils such as PMF and RBDPKO in order to obtain a melting profile similar to CB. Moreover, this oil has a low level of linoleic acid (18:2), making it less prone to oxidation [13]. RBDPS has been well reviewed and reported to be a suitable CBA [14, 17].

Binary systems of fats/oils have been recently gaining interest for producing CBAs for compound chocolates and other confectionery applications because fats/oils such as PMF, RBDPKO and RBDPS are comparatively cheap and are readily available in the market. Recent studies have produced CBRs by blending palm kernel oil and palm oil [8] and mango seed fat and palm stearin [10], and have also been reported as having fatty acid composition, solid fat content and slip melting point closer to commercial CB. Some studies have also investigated the compatibility and melting behavior via chemical interesterification of palm oil olein and palm kernel oil [6], and palm stearin and palm kernel olein [25] for producing confectionery products such as spreads. From the literature, it has also been noted that there are a few reports on the melting behavior, compatibility and microstructure of palm kernel oil, palm stearin or palm olein for producing margarines, shortenings and fat spreads [26, 27]. Hence, the production of CBAs especially CBSs with PMF, RBDPKO or RBDPS remains an unexplored area of research. Oil blending in the current study is helpful in understanding their potential application in confectionery. CBSs produced from blending of fat mixtures could be used as a suitable partial replacement of CB.

In the present study, PMF, RBDPKO and RBDPS were mixed two at a time at different proportions to determine their suitability as a CBA. PMF has a high percentage of POP, RBDPKO has a short melting range, and RBDPS has a wider range of melting points. These oils/fats were mixed to see how close their physicochemical characteristics resemble those of CB. Hence, the objective of this study was to evaluate the fatty acid composition, triacylglycerol, solid fat content, melting behavior and polymorphism of PMF/RBDPKO, RBDPS/RBDPKO and PMF/RBDPS mixtures for CBS formulations.

Materials and Methods

Materials

Palm mid-fraction (PMF), refined bleached deodorized palm kernel oil (RBDPKO) and refined bleached deodorized palm stearin (RBDPS) were obtained from Sime

Darby Research. Cocoa butter (CB) was purchased from Le Bourne. All chemicals and solvents used were of Analytical Reagent or HPLC grades (Fisher Scientific, USA). Fatty acid methyl ester (FAME) standards and TAG standards were obtained from Lab Science Solution and Sigma Aldrich.

Preparation of Oil Blends

Mixtures (w/w) of two fats (PMF/RBDPKO, RBDPS/RBDPKO and PMF/RBDPS) were prepared from 0 to 100 % in 10 % increments. The samples were melted at 80 °C, mixed thoroughly and then stored at room temperature for further analysis.

Fatty Acid Analysis

Fatty acid composition was determined in terms of fatty acid methyl esters (FAME). The samples (50 mg) were weighed and dissolved in 1 ml of heptane inside a 1.5-ml centrifuge tube. The mixtures were then added to 50 µl of 1 M sodium methoxide in anhydrous methanol and then mixed vigorously for 1 min by using a vortex mixer. After the sedimentation of sodium glycerolate, 1 µl of the clear supernatant was injected into a gas chromatograph (Perkin Elmer Clarus 500 GC, USA) fitted with an elite FFAP column (30 m length × 0.32 mm i.d. × 0.25 µm film thickness). A flame ionization detector (FID) was used to detect the FAME [15]. The injection and detection temperatures were both 250 °C. The oven temperature was programmed as follows: heat from 110 to 140 °C (30 °C/min), hold at 140 °C for 1 min, heat from 140 to 240 °C (15 °C/min) and hold for 7 min at 240 °C. The carrier gas (helium) flow rate was 0.9 ml/min. The peaks were identified by comparing the retention times with the FAME standards and quantified by using a peak area normalization method.

Triacylglycerol (TAG) Analysis

The TAG profiles of the mixtures were analyzed by using high-performance liquid chromatography (HPLC series 1260; Agilent, CA, USA) according to AOCS Official Method, Ce 5b-89. The column used was ZORBAX C-18 (4.6 × 250 mm, 5 µm; Agilent) and maintained at 35 °C by a column oven. Isocratic elution was carried out at a flow rate of 1.5 ml/min with a mixture of acetone/acetonitrile (70:30, v/v) as the mobile phase. A refractive index detector (RID 1260 Infinity; CA, USA) was used. The injection volume with an auto-injector was 10 µL of 5 % (w/v) oil in acetone. TAG peaks were identified based on the retention time of TAG standards. The percentage of TAGs was determined by using a peak area of the chromatogram.

Solid Fat Content (SFC) Analysis

The SFC of the mixtures was determined by pulsed nuclear magnetic resonance with a Bruker Minispec PC 120 NMR analyzer (Karlsruhe, Germany), following the method developed by Fiebig and Lüttke [16]. The fat samples (2–3 g) were placed into the NMR tubes and melted at 80 °C for 30 min followed by tempering at 60 °C for 5 min, 0 °C for 90 min, 26 °C for 40 h, 0 °C for 90 min, and finally kept it for 30 min at the desired measuring temperatures of 5, 10, 15, 20, 25, 30, 35, 40 and 45 °C before SFC is measured. Iso-solid phase diagrams of the fat mixtures were constructed with OriginPro 9.1 software (OriginLab, Northampton, USA) based on the SFC value obtained from NMR for each temperature ranging from 5 to 40 °C.

Melting Behavior

Melting behavior of fat mixtures was determined using differential scanning calorimetry (DSC; Pyris 4000 DSC; Perkin-Elmer, USA), following the method developed by Williams et al. [7]. Nitrogen gas was used at a flow rate of 20 ml/min. The instrument was calibrated with indium and *n*-dodecane. The samples (5–10 mg) were hermetically sealed in an aluminum pan. An empty, covered aluminum pan was used as the reference. The samples were cooled at –50 °C for 5 min and then heated to 80 °C. The melting thermograms were recorded at a heating rate of 5 °C/min from –50 to 80 °C.

Crystal Analysis

The polymorphic forms of the fat crystals were determined with a D8 Discover X-ray Diffractometer (Bruker, Germany) by using Cu-K α radiation ($k = 1.5418$ Å, voltage 40 kV and current 40 mA). The samples were kept at 5 °C for 24 h and mounted on flat stainless steel plates with a rectangular hole immediately before XRD analysis. The samples were analyzed at 2θ angles of 5° to 30° at ambient temperature with a scan rate of 1.5°/min. X-ray data was processed using the diffraction software to calculate the absorption intensity background, intensity and peak width in degrees for each crystalline form and the relative contents of the β'_1 , β'_2 and β_2 crystals. The β'_1 , β'_2 and β_2 polymorphs were calculated from the intensity of the short spacings at 3.8 and 4.2 Å, 4.1 and 4.3 Å, and 4.5 Å, respectively [4]. Each polymorph present was calculated using the formula:

$$\begin{aligned} \% \beta'_1 &= \frac{I_{\beta'_1} \times 100}{I_{\beta'_1} + I_{\beta'_2} + I_{\beta_2}}; \quad \% \beta'_2 = \frac{I_{\beta'_2} \times 100}{I_{\beta'_1} + I_{\beta'_2} + I_{\beta_2}}; \\ \% \beta_2 &= \frac{I_{\beta_2} \times 100}{I_{\beta'_1} + I_{\beta'_2} + I_{\beta_2}} \end{aligned}$$

Table 1 Fatty acid composition (peak area %) for PMF/RBDPKO mixtures

Blend	Fatty acid composition							
	<C _{12:0}	C _{12:0}	C _{14:0}	C _{16:0}	C _{18:0}	C _{18:1}	C _{18:2}	C _{20:0}
A (100:0)	–	0.16 ± 0.11 j	1.0 ± 0.09 k	49.40 ± 0.10 a	4.59 ± 0.09 b	37.68 ± 0.10 a	7.17 ± 0.10 a	–
B (90:10)	0.77 ± 0.13	4.86 ± 0.25 i	2.56 ± 0.10 j	45.71 ± 0.18 b	4.18 ± 0.11 b	35.28 ± 0.10 b	6.64 ± 0.13 b	–
C (80:20)	1.32 ± 0.21	8.40 ± 0.08 h	3.77 ± 0.10 i	41.85 ± 0.21 c	4.26 ± 0.04 b	34.16 ± 0.12 c	6.24 ± 0.10 b	–
D (70:30)	2.03 ± 0.10	14.82 ± 0.14 g	5.96 ± 0.08 h	35.79 ± 0.12 d	4.04 ± 0.05 bc	31.69 ± 0.10 e	5.67 ± 0.04 c	–
E (60:40)	2.36 ± 0.16	17.47 ± 0.11 f	6.93 ± 0.05 g	33.93 ± 0.04 e	3.87 ± 0.20 cd	30.11 ± 0.11 f	5.33 ± 0.12 cd	–
F (50:50)	2.78 ± 0.14	20.34 ± 0.21 e	8.07 ± 0.13 f	31.16 ± 0.10 f	3.72 ± 0.15 cd	28.84 ± 0.11 g	5.09 ± 0.10 d	–
G (40:60)	3.29 ± 0.10	25.72 ± 0.07 d	10.04 ± 0.10 e	26.36 ± 0.12 g	3.48 ± 0.08 cd	26.45 ± 0.12 h	4.66 ± 0.10 e	–
H (30:70)	4.17 ± 0.17	30.72 ± 0.14 c	11.89 ± 0.12 d	21.58 ± 0.25 i	3.27 ± 0.07 cd	24.24 ± 0.10 i	4.20 ± 0.06 e	–
I (20:80)	6.13 ± 0.08	37.34 ± 0.12 b	13.06 ± 0.18 c	17.31 ± 0.45 j	2.57 ± 0.13 e	20.15 ± 0.14 j	3.44 ± 0.10 f	–
J (10:90)	3.92 ± 0.17	37.73 ± 0.11 b	14.77 ± 0.28 b	15.90 ± 0.10 k	2.95 ± 0.07 cde	21.20 ± 0.14 k	3.53 ± 0.12 f	–
K (0:100)	7.74 ± 0.07	46.79 ± 0.10 a	16.21 ± 0.21 a	8.77 ± 0.17 l	2.20 ± 0.14 e	15.78 ± 0.16 l	2.51 ± 0.11 g	–
CB	–	Trace	0.73 ± 0.02 k	25.69 ± 0.28 h	36.15 ± 0.26 a	33.24 ± 0.19 d	3.13 ± 0.22 f	1.04 ± 0.07

Values within the same column with different letters are significantly different ($p < 0.05$). Each value in the table represents the mean ± SD of three measurements

PMF palm mid-fractions, RBDPKO refined bleached deodorized palm kernel oil, CB cocoa butter

Table 2 Fatty acid composition (peak area %) for RBDPS/RBDPKO mixtures

Blend	Fatty acid composition							
	<C _{12:0}	C _{12:0}	C _{14:0}	C _{16:0}	C _{18:0}	C _{18:1}	C _{18:2}	C _{20:0}
A (100:0)	–	0.23 ± 0.08 k	1.17 ± 0.05 j	54.28 ± 0.28 a	4.47 ± 0.14 b	33.39 ± 0.20 a	6.46 ± 0.10 a	–
B (90:10)	0.96 ± 0.03	10.15 ± 0.12 j	4.49 ± 0.21 i	42.15 ± 0.34 b	4.54 ± 0.12 b	31.88 ± 0.08 b	5.83 ± 0.14 b	–
C (80:20)	1.08 ± 0.10	11.21 ± 0.40 i	4.75 ± 0.10 i	42.96 ± 0.54 c	4.39 ± 0.21 bc	30.03 ± 0.13 c	5.58 ± 0.24 bc	–
D (70:30)	1.7 ± 0.10	13.73 ± 0.21 h	6.04 ± 0.14 h	39.56 ± 0.31 d	4.22 ± 0.21 bc	29.46 ± 0.17 d	5.29 ± 0.30 cd	–
E (60:40)	1.97 ± 0.08	16.73 ± 0.40 g	7.32 ± 0.21 g	37.02 ± 0.12 e	4.0 ± 0.10 cd	27.96 ± 0.24 e	5.0 ± 0.12 d	–
F (50:50)	2.73 ± 0.11	22.27 ± 0.12 f	9.05 ± 0.14 f	31.43 ± 0.32 f	3.74 ± 0.12 d	26.21 ± 0.21 f	4.57 ± 0.14 e	–
G (40:60)	3.4 ± 0.20	27.68 ± 0.10 e	11.12 ± 0.21 e	25.49 ± 0.14 g	3.52 ± 0.10 de	24.59 ± 0.24 g	4.20 ± 0.14 e	–
H (30:70)	3.42 ± 0.21	29.59 ± 0.10 d	12.01 ± 0.40 d	23.99 ± 0.20 h	3.40 ± 0.14 de	23.45 ± 0.13 h	4.14 ± 0.21 e	–
I (20:80)	4.38 ± 0.07	32.07 ± 0.21 c	13.70 ± 0.12 c	20.40 ± 0.13 i	3.25 ± 0.21 e	22.41 ± 0.10 i	3.79 ± 0.18 f	–
J (10:90)	4.8 ± 0.13	34.30 ± 0.57 b	16.97 ± 0.70 b	15.81 ± 0.21 j	3.12 ± 0.15 e	21.46 ± 0.40 j	3.54 ± 0.10 fg	–
K (0:100)	7.74 ± 0.07	46.79 ± 0.10 a	16.21 ± 0.21 a	8.77 ± 0.17 k	2.20 ± 0.14 f	15.78 ± 0.16 k	2.51 ± 0.11 f	–
CB	–	Trace	0.73 ± 0.02 k	25.69 ± 0.28 g	36.15 ± 0.26 a	33.24 ± 0.19 a	3.13 ± 0.22 g	1.04 ± 0.07

Values within the same column with different letters are significantly different ($p < 0.05$). Each value in the table represents the mean ± SD of three measurements

RBDPS refined bleached deodorized palm stearin, RBDPKO refined bleached deodorized palm kernel oil, CB cocoa butter

where $I\beta'_1$, $I\beta'_2$ and $I\beta_2$ were the peak intensities of the β'_1 , β'_2 and β_2 polymorphs, respectively.

Statistical Analysis

The data were statistically analyzed by one-way analysis of variance (ANOVA) using the OriginPro 9.1 software (OriginLab). Tukey's test was applied to determine the significant differences at 95 % confidence level. NMR data represented single determination. DSC diagrams and XRD analyses were conducted in triplicate.

Results and Discussion

Fatty acid Composition

The fatty acid profiles of the different mixtures of PMF/RBDPKO, RBDPS/RBDPKO and PMF/RBDPS are shown in Tables 1, 2 and 3. The compositions of all selected fat samples (Tables 1, 2, 3) are consistent with earlier findings [1, 7, 9, 11], who reported that the fatty acid profiles of CB are as described in the "Introduction". PMF and RBDPS are rich in palmitic (51.9 and 68 %) and

Table 3 Fatty acid composition (peak area %) for PMF/RBDPS mixtures

Blend	Fatty acid composition							
	<C _{12:0}	C _{12:0}	C _{14:0}	C _{16:0}	C _{18:0}	C _{18:1}	C _{18:2}	C _{20:0}
A (100:0)	–	0.16 ± 0.11 a	1.0 ± 0.09 a	49.40 ± 0.10 a	4.59 ± 0.09 c	37.68 ± 0.10 a	7.17 ± 0.10 a	–
B (90:10)	0.02 ± 0.03	0.15 ± 0.06 a	0.96 ± 0.03 a	49.66 ± 0.46 b	4.76 ± 0.17 bc	37.55 ± 0.11 a	6.90 ± 0.10 ab	–
C (80:20)	0.03 ± 0.01	0.16 ± 0.06 a	0.98 ± 0.05 a	49.86 ± 0.31 b	4.79 ± 0.12 bc	37.28 ± 0.17 a	6.90 ± 0.14 ab	–
D (70:30)	0.03 ± 0.01	0.16 ± 0.07 a	0.96 ± 0.03 a	50.04 ± 1.36 c	4.81 ± 0.52 bc	37.18 ± 0.75 a	6.82 ± 0.32 ab	–
E (60:40)	0.03 ± 0.01	0.16 ± 0.12 a	0.97 ± 0.09 a	50.87 ± 1.08 d	4.78 ± 0.41 bc	36.43 ± 0.47 b	6.76 ± 0.21 ab	–
F (50:50)	0.04 ± 0.03	0.16 ± 0.08 a	1.0 ± 0.14 a	51.34 ± 0.57 e	4.80 ± 0.41 bc	36.06 ± 0.64 b	6.65 ± 0.10 b	–
G (40:60)	0.07 ± 0.02	0.17 ± 0.05 a	1.01 ± 0.10 a	51.89 ± 0.40 e	4.76 ± 0.18 bc	35.48 ± 0.54 c	6.62 ± 0.21 b	–
H (30:70)	0.10 ± 0.01	0.19 ± 0.05 a	1.07 ± 0.12 a	52.44 ± 0.21 f	4.75 ± 0.12 bc	34.72 ± 0.32 d	6.73 ± 0.17 b	–
I (20:80)	0.09 ± 0.02	0.19 ± 0.12 a	1.07 ± 0.14 a	52.58 ± 0.80 f	4.90 ± 0.08 b	34.44 ± 0.23 d	6.73 ± 0.12 b	–
J (10:90)	0.11 ± 0.03	0.19 ± 0.02 a	1.04 ± 0.08 a	52.96 ± 0.65 g	5.0 ± 0.21 b	34.19 ± 0.13 de	6.51 ± 0.24 b	–
K (0:100)	–	0.23 ± 0.08 a	1.17 ± 0.05 a	54.28 ± 0.28 h	4.47 ± 0.14 bc	33.39 ± 0.20 e	6.46 ± 0.10 b	–
CB	–	Trace	0.73 ± 0.02 a	25.69 ± 0.28 i	36.15 ± 0.26 a	33.24 ± 0.19 e	3.13 ± 0.22 c	1.04 ± 0.07

Values within the same column with different letters are significantly different ($p < 0.05$). Each value in the table represents the mean ± SD of three measurements

PMF palm mid-fractions, RBDPS refined bleached deodorized palm stearin, CB cocoa butter

oleic (36.1 and 21 %) acids, respectively. RBDPKO contains a high percentage of lauric acid (48.3 %), followed by myristic (15.6 %), oleic (15.1 %), palmitic (8 %), and linoleic (3 %) acids. Since none of these fats mimicked the fatty acid profile of cocoa butter, it was decided that they should be blended in different proportions and combinations. In Tables 1, 2 and 3, the fatty acid constituents among the blends were significantly ($p < 0.05$) affected by the ratios of the mixtures. In PMF/RBDPKO mixtures (Table 1), the constituents of the short-chain fatty acids (lauric and myristic) increased gradually ($p < 0.05$) with increasing RBDPKO. Although the compositions of long-chain fatty acids, such as palmitic, oleic and linoleic acids, are closer to commercial CB (Table 1), the compositions of the short-chain fatty acids are significantly higher ($p < 0.05$) in blends G to I (20–40 % PMF in RBDPKO). A similar trend was also observed in mixtures F to H (30–50 % RBDPS in RBDPKO) of the RBDPS/RBDPKO blends as described in Table 2. In the PMF/RBDPS mixtures (Table 3), the palmitic and oleic acids with the exception of stearic were significantly ($p < 0.05$) higher in mixtures B to F (50–90 % PMF in RBDPS) compared with commercial CB. Calliau and co-workers [12] also produced CBSs via a two-stage static fraction of palm kernel oil, and reported the fatty acid profiles: lauric (56.3 %), myristic (19.6 %), palmitic (8.9 %) and stearic (2.0 %). Jahurul and co-workers [17] also studied the fatty acids in different blends of mango seed fat extracted by supercritical carbon dioxide and palm stearin in various ratios to obtain CB replacers, and reported that the fatty acid profiles of certain blends were closer to commercial CB. Therefore, the fatty acid compositions of mixtures G to I

of PMF/RBDPKO, mixtures F to H of RBDPS/RBDPKO and mixtures B to F of PMF/RBDPS were the closest to commercial CB compared to other fat mixtures. Though these fatty acids are chemically different from those present in CB, they may be similar in their solid fat content and melting behaviors to CB, thus making them suitable substitutes for CB.

Triacylglycerol Composition

The TAG profiles of the different mixtures are shown in Table 4. CB contains predominantly mono-unsaturated TAGs (88.2 % SUS: POP, POST and StOST; P palmitic, O oleic, St stearic), which is consistent with previous studies [1] described in the “Introduction”. PMF and RBDPS are high in SUS (60.1 and 40.7 %), followed by di-unsaturated (SUU: PLL, POO, StOO; L linoleic) TAGs (26.9 and 21.6 %). RBDPKO is rich in trisaturated TAGs (70.4 % SSS: LaLaLa, LaLaM, MMM; La lauric, M myristic). In Table 4, variations of TAG constituents were observed among the blends. All the blends of PMF/RBDPKO, RBDPS/RBDPKO and PMF/RBDPS had a mixture of SSS, SUS, SUU and UUU (polyunsaturated; OOL, OOO, LLO) TAGs. In respect of PMF/RBDPKO mixtures, SUS and SUU contents decreased significantly, while SSS content increased with the addition of RBDPKO. A similar trend was also observed for the RBDPS/RBDPKO and PMF/RBDPS mixtures. There were significant differences ($p < 0.05$) among all the binary mixtures except some blends of UUU TAGs (Table 4). The StOST TAG is responsible for β crystal formation, whereas POP/POST TAGs are responsible for β' crystals [18]. Therefore, these TAGs,

Table 4 Overview of TAGs (peak area %) in PMF/RBDPKO mixtures, RBDPS/RBDPKO mixtures, and PMF/RBDPS mixtures

Blend	PMF/RBDPKO				RBDPS/RBDPKO				PMF/RBDPS				Others			
	SSS	SUS	SUU	Others	SSS	SUS	SUU	Others	SSS	SUS	SUU	Others	SUS	SUU	Others	
A (100:0)	4.8 ± 0.1 k	60.1 ± 1.7 b	26.9 ± 0.7 a	7.4 ± 0.2 a	0.8	29.1 ± 1.8 k	40.7 ± 1.7 b	21.6 ± 1.2 a	6.1 ± 0.7 a	2.5	4.8 ± 0.4 k	60.1 ± 0.4 b	26.9 ± 1.1 a	7.4 ± 0.4 a	0.8	
B (90:10)	10.6 ± 0.5 j	58.2 ± 0.8 c	25.2 ± 0.4 b	5.2 ± 0.2 bc	0.8	33.7 ± 1.1 j	39.2 ± 1.1 c	17.8 ± 1.4 b	5.7 ± 0.5 ab	3.6	7.3 ± 0.1 j	58.3 ± 0.5 c	26.5 ± 1.0 ab	7.1 ± 0.1 ab	0.8	
C (80:20)	18.5 ± 0.4 i	52.3 ± 1.1 d	23.1 ± 0.6 c	4.9 ± 0.2 c	1.2	36.5 ± 1.2 i	38.7 ± 0.7 d	15.7 ± 1.2 c	5.5 ± 0.1 bc	3.6	8.1 ± 0.1 i	57.6 ± 0.4 d	26.2 ± 0.8 b	6.8 ± 0.1 bc	1.3	
D (70:30)	20.7 ± 0.1 b	50.7 ± 0.8 e	22.4 ± 0.5 d	4.7 ± 0.1 cd	1.5	37.3 ± 1.1 b	38.3 ± 0.3 e	15.2 ± 0.4 c	5.4 ± 0.2 bc	3.8	10.1 ± 0.2 b	56.1 ± 1.8 e	25.7 ± 0.8 cd	6.8 ± 0.1 bc	1.3	
E (60:40)	27.9 ± 0.5 g	44.7 ± 0.5 f	21.0 ± 0.7 e	4.7 ± 0.1 cd	1.7	42.0 ± 0.7 g	36.8 ± 0.8 f	12.3 ± 0.5 d	5.1 ± 0.5 cd	3.8	11.7 ± 0.1 g	55.4 ± 1.4 f	25.2 ± 1.0 d	6.4 ± 0.1 cd	1.3	
F (50:50)	31.5 ± 0.7 f	42.3 ± 0.7 g	19.7 ± 0.2 f	4.6 ± 0.1 cd	1.9	43.0 ± 0.5 f	36.4 ± 0.4 fg	11.7 ± 0.4 e	5.1 ± 0.2 cd	3.8	12.4 ± 0.2 f	54.7 ± 1.2 g	24.8 ± 0.7 e	6.4 ± 0.1 cd	1.7	
G (40:60)	38.7 ± 1.0 e	41.0 ± 0.9 h	13.4 ± 0.1 g	4.5 ± 0.1 cde	2.4	45.5 ± 1.2 e	36.1 ± 0.8 g	9.5 ± 0.1 f	4.7 ± 0.2 d	4.2	14.8 ± 0.2 e	52.7 ± 0.8 h	24.4 ± 0.4 ef	6.4 ± 0.1 cd	1.7	
H (30:70)	42.3 ± 0.8 d	39.4 ± 0.5 i	11.2 ± 0.1 h	4.5 ± 0.2 cde	2.6	50.5 ± 1.3 d	32.4 ± 0.4 h	8.2 ± 0.1 g	4.7 ± 0.4 d	4.2	15.0 ± 0.1 d	52.1 ± 0.3 h	24.1 ± 0.2 f	6.4 ± 0.1 cd	2.4	
I (20:80)	45.7 ± 0.7 c	37.8 ± 0.4 j	9.5 ± 0.5 i	4.3 ± 0.1 cde	2.7	61.5 ± 1.4 c	21.7 ± 0.8 i	7.9 ± 0.4 gh	4.5 ± 0.1 de	4.4	19.8 ± 0.2 c	48.3 ± 0.4 i	23.3 ± 0.6 g	6.2 ± 0.1 cd	2.4	
J (10:90)	60.8 ± 1.1 b	24.2 ± 0.4 k	7.3 ± 0.2 j	4.3 ± 0.2 cde	3.4	69.0 ± 1.2 b	14.7 ± 0.4 j	7.4 ± 0.1 h	4.5 ± 0.2 de	4.4	21.0 ± 0.4 b	47.1 ± 0.5 j	22.7 ± 0.5 h	6.2 ± 0.1 cd	3.0	
K (0:100)	70.4 ± 1.4 a	14.2 ± 0.4 l	6.8 ± 0.2 k	4.1 ± 0.2 e	4.5	70.4 ± 1.7 a	14.2 ± 0.5 j	6.8 ± 0.2 i	4.1 ± 0.4 e	4.5	29.1 ± 1.2 a	40.7 ± 0.5 k	21.6 ± 0.4 i	6.1 ± 0.1 d	3.5	
CB	0.7 ± 0.1 i	88.2 ± 0.7 a	5.3 ± 0.2 i	0.4 ± 0.0 f	5.4	0.7 ± 1.8 i	88.2 ± 1.5 a	5.3 ± 0.2 j	0.4 ± 0.0 f	5.4	0.7 ± 0.0 i	88.2 ± 1.3 a	5.3 ± 0.5 j	0.4 ± 0.0 e	5.4	

Values within the same column with different letters are significantly different ($p < 0.05$). Each value in the table represents the mean \pm SD of two measurements

TAG Triacylglycerols, trisaturated (SSS: LaLaLa, LaLaM, MM, PPP; La lauric, M myristic, P palmitic), monounsaturated (SUS: LaLaO, POP, POS, SIOS; O oleic, S stearic), diunsaturated (SUU: PLL, POO, SOO; L linoleic), polyunsaturated (UUU: OOL, OOO, LLO), PMF palm mid-fractions, RBDPKO refined bleached deodorized palm kernel oil, RBDPS refined bleached deodorized palm stearin, CB coconut butter

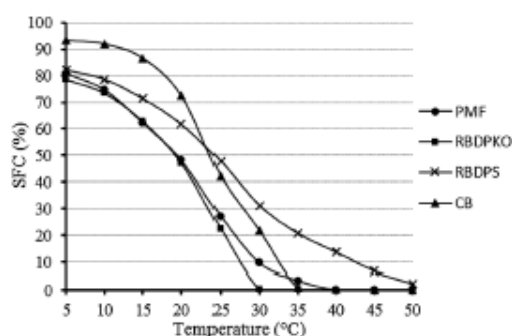


Fig. 1 SFC versus temperature profiles for CB (filled triangle), PMF (filled circle), RBDPKO (filled square) and RBDPS (multiplication symbol)

though being chemically different from those of CB, they may have a significant influence on the solid fat content, melting properties and polymorphism of the mixtures, making them suitable substitutes for CB.

Solid Fat Content and Iso-solid Diagrams of the Blends

The SFC profiles of individual CB, PMF, RBDPKO and RBDPS are shown in Fig. 1. CB showed a high SFC ($\geq 70\%$) up to 20 °C, followed by a rapid SFC drop between 20 and 35 °C, and 0 % SFC was observed at and above 40 °C. This is presumably due to its high content of SUS TAGs (Table 4). This finding is consistent with earlier studies by Kadivar et al. [19], who reported a high SFC ($\geq 75\%$) at 20 °C, and a rapid decrease from 25 to 35 °C and 0 % at and above body temperature. PMF and RBDPKO exhibited a high SFC ($\geq 50\%$) up to 20 °C, followed by a rapid decrease from 20 to 30 °C. PMF was completely liquefied at 35 °C, while RBDPKO showed 0 % SFC at and above 40 °C. These variations in the SFC are mainly caused by the differences in the fatty acids (Table 1) and TAGs of PMF and RBDPKO (Table 4). RBDPS exhibited the highest SFC ($\geq 60\%$) at less than 25 °C and melted completely at and above 50 °C (Fig. 1), possibly due to its high content of SSS TAGs (Table 4).

The phase behavior of fat mixtures can be explained by iso-solid phase diagrams [20], which have been used to illustrate the eutectic and monotectic effects as it is useful to understand the compatibility of mixed fat systems at a given temperature [21]. For example, the eutectic effect occurs when theoretically the contour lines of constant SFC are not straight, with some blend compositions having lower melting temperatures than expected. This indicates that the fat mixtures are not compatible (eutectic). The monotectic effect (compatibility) is seen by a straight

line connecting the SFC of each pure component, indicating that fats in a blend are well mixed [19, 22]. In Fig. 2a, the PMF/RBDPKO mixtures especially 10–70 % PMF in RBDPKO displayed a eutectic effect at temperatures above 15 °C ($\text{SFC} \leq 40\%$). A eutectic effect was observed at 5 °C for 30–90 % PMF in RBDPKO. However, the contour lines were almost straight for 20–50 % PMF in RBDPKO between 10 and 15 °C (Fig. 2a). This may be due to the considerable contents of SUS and UUU TAGs (which have similar melting profiles and polymorphs) in PMF and RBDPKO (Table 4). A similar iso-solid diagram (monotectic effect) was observed between 10 and 20 °C for 40–80 % RBDPS in RBDPKO (Fig. 2b). This behavior was also observed by Bootello and co-workers [1] for sunflower hard stearins (SHSs) and PMF mixtures. They also reported a eutectic effect for 20–60 % SHS-65 in PMF between 10 and 20 °C, and a monotectic effect for 70–85 % SHS-95 in PMF above 20 °C. Therefore, according to the iso-solid diagrams, 20–50 % PMF at 10–15 °C and 40–80 % RBDPS at 10–20 °C could be blended with RBDPKO to avoid the undesirable eutectic effect which is responsible for an unpleasant mouth feeling and softer texture [1].

In Fig. 2c, the iso-solid lines of PMF/RBDPS mixtures were almost linear and exhibited a monotectic effect at less than 30 °C. The absence of a eutectic effect in Fig. 2c indicated that PMF and RBDPS do not show incompatibilities, as these oils contained a similar pattern of long-chain fatty acids (Table 3) with corresponding TAGs (Table 4). Approximately 40 % of SFC was observed at 25 °C for 50–80 % PMF in RBDPS and this is also within the monotectic area of the iso-solid diagram (Fig. 2c). This observation is in accordance with Timms [22], who suggests a fat adequate for confectionery usage should display at least 40 % SFC value at 25 °C. Therefore, 50–80 % PMF in RBDPS could be used as CBSs because of the monotectic effect and SFC profiles.

Melting Behavior

The DSC melting curves of the selected individual fats CB, PMF, RBDPKO and RBDPS are shown in Fig. 3a–c. CB exhibited one sharp endotherm (T_1) at approximately 33 °C with one/two small endotherms (Fig. 3a). The small endotherms may be due to the considerable contents of SSS and SUU TAGs (Table 4). The onset temperature (T_{Onset}) at 22.1 °C, endset temperature (T_{Endset}) at 37.2 °C and melting enthalpy (ΔH) at 114.2 J/g were also observed for CB (Table 5). PMF exhibited two broad endotherms (T_1 10 °C and T_2 22 °C) with an exotherm (endothermic trough) between them. Melting is one of the endothermic behaviors and crystallization is one of the exothermic behaviors. This exotherm is likely caused by the polymorphic transformation during the DSC melting [11]. PMF also showed T_{Onset}

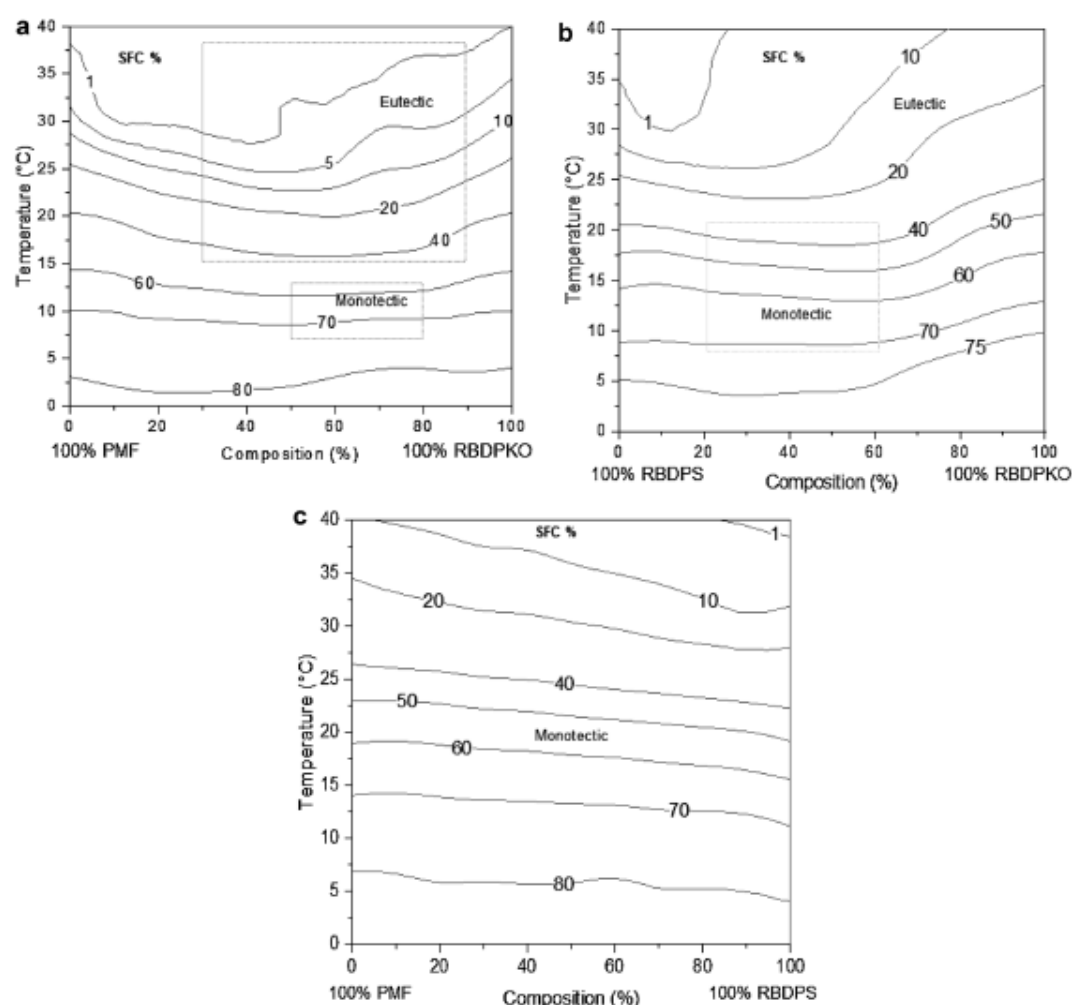


Fig. 2 Binary iso-solid phase diagrams for mixtures of **a** PMF/RBDPKO, **b** RBDPS/RBDPKO, and **c** PMF/RBDPS

(4.5 °C), T_{Endset} (27.3 °C) and ΔH (34.8 J/g) as described in Table 5. RBDPKO had a broad endotherm (T_1) at approximately 27 °C, with multiple small peaks. The T_{Onset} , T_{Endset} and ΔH of RBDPKO were observed at 17.2, 29.8 °C and 84.9 J/g, respectively (Table 5). RBDPS exhibited two distinct broad endotherms at 10 and 40 °C (T_1 and T_2) with an exotherm between them (Fig. 3b). The lower temperature endotherm (T_1) is probably related to the small content of the oleic fraction, while the higher temperature endotherm (T_2) corresponded to the stearin fraction (Fig. 3b). The melting of RBDPS started at −4.1 °C and ended at 55.2 °C, with melting enthalpy at 73.9 J/g (Table 5). Similar DSC

melting profiles have been reported by other researchers [1, 11], namely endothermic peaks at 32.5 °C for commercial CB, 9.8–32.8 °C for PMF, −9.12 to 26.03 °C for RBDPKO, and −18.4 to 55.0 °C for RBDPS.

The DSC melting profiles of the different binary mixtures of PMF/RBDPKO, RBDPS/RBDPKO and PMF/RBDPS are shown in Fig. 3a–c. All mixtures of PMF/RBDPKO showed one primary broad endothermic peak between 15.7 and 25.8 °C with one/two small shoulder peaks (Fig. 3a). The shoulder peaks are probably caused by the presence of UUU TAGs from both PMF and RBDPKO (Table 4). Mixtures B to F of PMF/RBDPKO showed one

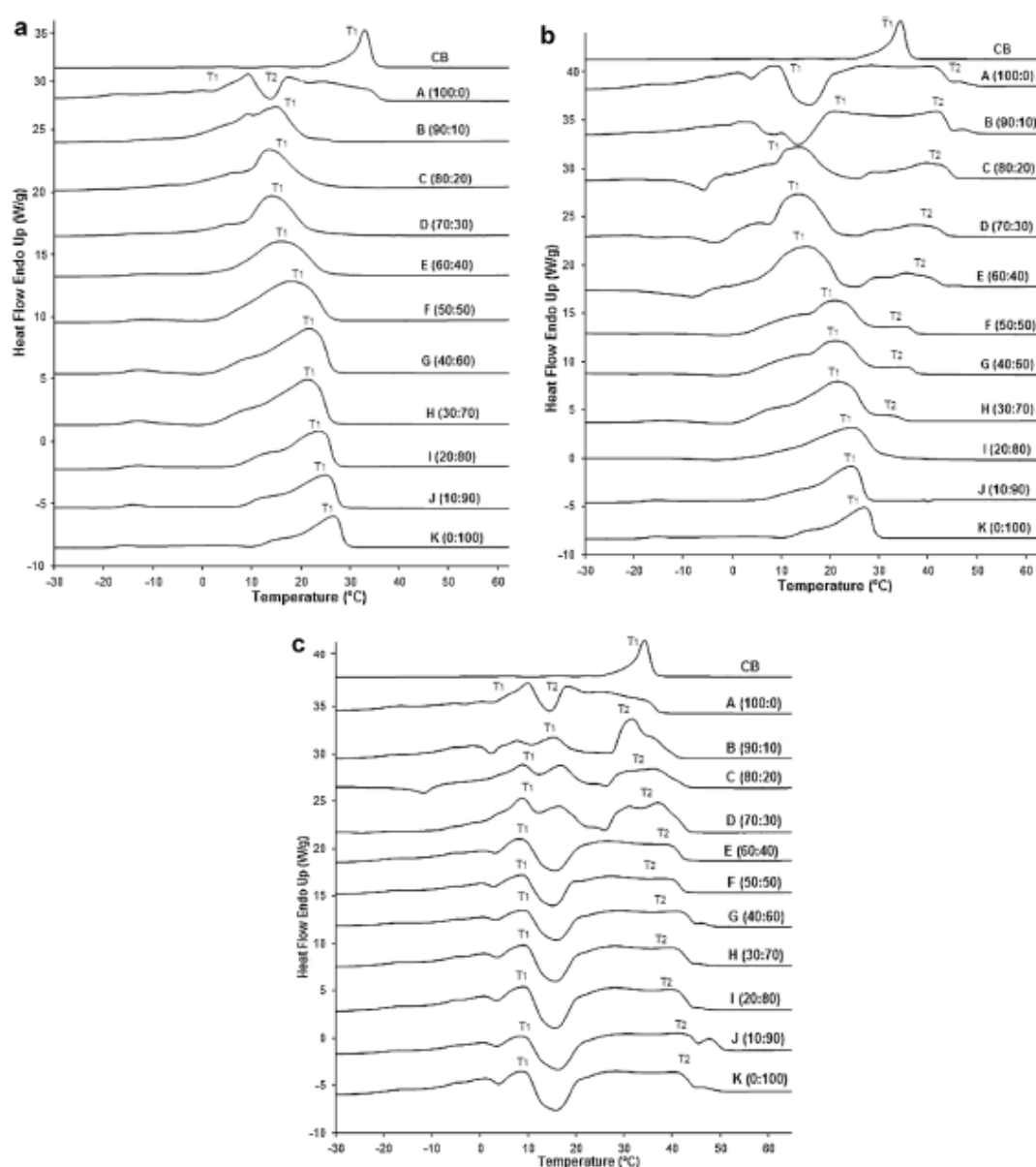


Fig. 3 Differential scanning calorimetry melting curves of **a** PMF/RBDPKO mixtures, **b** RBDPS/RBDPKO mixtures, and **c** PMF/RBDPS mixtures

broad endotherm between 16 and 20 °C with a small exothermic peak, different onset temperature (T_{Onset}), endset temperature (T_{Endset}) and melting enthalpy (ΔH). The exothermic peak can probably be explained by the polymorphic transformation in PMF. The T_{Onset} , T_{Endset} and melting

enthalpy of these blends ranged from 4.8 to 9.2 °C, 27.5 to 28.4 °C and 42.2 to 61.2 J/g, respectively (Table 5). However, the T_{Onset} from 10.4 to 16.4 °C, T_{Endset} from 28.3 to 29.3 °C and melting enthalpy from 64.7 to 80.9 J/g were observed for blends G to J of PMF/RBDPKO. There were

also significant differences ($p < 0.05$) among all the blends except blends C and D of the T_{Endset} temperature (Table 5). The blends G to J also exhibited one broad endotherm at 25 and 26 °C with two small shoulder peaks. The small difference of the melting peak could be due to the variation of fatty acids, SSS and SUS TAGs in PMF and RBDPKO (Tables 1, 4). Moreover, this behavior agreed with the monotectic formation in the iso-solid diagram (Fig. 2a). These findings are in agreement with those reported by Jahurul and co-workers [23], who obtained CB replacers by blending supercritical carbon-dioxide extracted mango seed fat and palm oil mid-fraction. They also reported two maxima at 16.4 and 19.1 °C, with T_{Onset} (−14.1 to −15.2 °C), T_{Endset} (36.3–36.8 °C) and ΔH (68–69.3 J/g) closer to commercial CB. In the present study, mixtures G to J with 10–40 % PMF in RBDPKO showed one maxima at 25–26 °C with T_{Onset} , T_{Endset} and ΔH , which are close to commercial CB (Fig. 3a). Therefore, mixtures G to J of PMF in RBDPKO may be used as CBS-based filling fats requiring to have less than 50 % SFC at 20 °C with melting temperature ranging between 21 and 23 °C [5].

In Fig. 3b, the RBDPS/RBDPKO mixtures showed one or two broad endotherms with multiple small peaks. The shoulder peaks may be due to the presence of unsaturated fatty acids, SUU and UUU TAGs in RBDPS and RBDPKO (Tables 2, 4). Mixtures B to H with 30–90 % RBDPS in RBDPKO demonstrated two broad endotherms (T_1 and T_2) at temperatures ranging from 5 to 36 °C. The lower temperature endotherm (T_1) is possibly related to the presence of low melting SUU and UUU TAGs from both RBDPS

and RBDPKO (Table 4). However, the high-temperature endotherm (T_2) indicates the presence of high melting SSS (PPP) and SUS TAGs from RBDPS (Table 4). In addition, these results suggest eutectic formation although the iso-solid phase diagram for the 40–80 % RBDPS in RBDPKO showed monotectic behavior at 10–20 °C (Fig. 2b). With respect to the mixtures I and J, the DSC melting curves exhibited one broad endotherm at approximately 26 °C (T_1). This may be due to the presence of medium melting SSS TAGs from RBDPKO (Table 4). With decreasing RBDPS in the mixtures, the T_{Onset} increased while the T_{Endset} both decreased significantly ($p < 0.05$), and ranging from −3.7 to 16.4 °C and 53.7–34.7 °C, respectively. The increase in T_{Onset} can be explained by the presence of increased proportions of short-chain saturated fatty acids and SSS TAGs (Tables 2, 4). The decrease in T_{Endset} could be due to the presence of decreased long-chain palmitic and oleic fatty acids, SUS (especially POP) and SUU (especially POO) TAGs (Tables 2, 4). Melting enthalpies (75.8–82.7 J/g) also decreased gradually ($p < 0.05$) with the addition of RBDPKO in the mixtures (Table 5). This observation is consistent with a previous report by Jahurul and co-workers [10], who successfully produced hard CB replacers by blending supercritical carbon dioxide extracted mango seed fat and palm stearin. And they also reported melting profiles (17.6–36.9 °C) with T_{Onset} (−13.4 °C) and T_{Endset} (40.0 °C) closer to CB. A recent study by Bootello and co-workers [1] also reported two maxima, at 22.8 and 36.51 °C, for commercial CB. In the present study, mixtures F to H with 30–50 % RBDPS in RBDPKO showed melting profiles of

Table 5 Overview of T_{Onset} , T_{Endset} and melting enthalpy (ΔH) in PMF/RBDPKO mixtures, RBDPS/RBDPKO mixtures, and PMF/RBDPS mixtures

Blend	PMF/RBDPKO			RBDPS/RBDPKO			PMF/RBDPS		
	T_{Onset} (°C)	T_{Endset} (°C)	ΔH (J/g)	T_{Onset} (°C)	T_{Endset} (°C)	ΔH (J/g)	T_{Onset} (°C)	T_{Endset} (°C)	ΔH (J/g)
A (100:0)	4.5 ± 0.1 j	27.3 ± 1.2 f	34.8 ± 0.3 i	−4.1 ± 0.1 k	55.2 ± 0.3 a	73.9 ± 1.0 i	4.5 ± 0.3 b	27.3 ± 1.1 k	34.8 ± 1.0 k
B (90:10)	4.8 ± 0.1 j	27.5 ± 0.9 f	42.2 ± 0.3 k	−3.7 ± 0.3 j	53.7 ± 0.8 b	75.8 ± 1.2 k	4.2 ± 0.3 bc	32.1 ± 1.0 j	41.7 ± 0.7 j
C (80:20)	5.7 ± 0.1 i	27.6 ± 0.8 f	44.6 ± 0.5 j	−3.4 ± 0.3 j	52.4 ± 0.6 c	77.4 ± 0.8 j	4.0 ± 0.3 bc	33.6 ± 1.2 i	50.3 ± 1.0 i
D (70:30)	6.8 ± 0.3 h	27.8 ± 0.6 f	50.3 ± 0.3 i	−2.2 ± 0.3 i	49.3 ± 0.1 d	78.1 ± 0.7 i	3.7 ± 0.1 cd	35.4 ± 0.3 h	57.6 ± 0.8 h
E (60:40)	8.3 ± 0.3 g	28.1 ± 0.7 e	55.4 ± 0.3 h	−0.5 ± 0.0 h	46.4 ± 1.1 e	79.6 ± 0.6 h	3.6 ± 0.5 cd	37.2 ± 1.2 g	66.4 ± 0.5 g
F (50:50)	9.2 ± 0.3 f	28.3 ± 0.9 de	61.2 ± 0.3 g	5.4 ± 0.3 g	42.3 ± 1.2 f	80.4 ± 0.8 g	3.2 ± 0.3 d	42.1 ± 0.3 f	68.5 ± 0.7 f
G (40:60)	10.4 ± 0.3 e	28.5 ± 1.1 de	64.7 ± 0.5 f	9.7 ± 0.7 f	39.4 ± 1.0 g	81.2 ± 0.5 f	2.6 ± 0.2 e	44.3 ± 1.0 e	69.4 ± 1.0 e
H (30:70)	12.5 ± 0.2 d	28.7 ± 1.0 d	71.2 ± 1.1 e	13.2 ± 0.8 e	37.6 ± 0.8 h	81.8 ± 0.5 e	2.3 ± 0.2 e	45.6 ± 1.1 d	70.4 ± 0.7 d
I (20:80)	14.7 ± 0.1 c	29.1 ± 1.1 c	74.6 ± 1.2 d	14.8 ± 0.7 d	36.4 ± 0.8 i	82.3 ± 0.7 d	1.7 ± 0.3 f	49.4 ± 1.0 c	70.6 ± 0.8 d
J (10:90)	16.4 ± 0.4 b	29.3 ± 0.3 bc	80.9 ± 0.3 c	16.4 ± 1.0 c	34.7 ± 0.6 j	82.7 ± 0.8 c	−0.8 ± 0.0 g	50.7 ± 0.8 b	72.1 ± 0.5 c
K (0:100)	17.2 ± 0.6 b	29.8 ± 0.3 b	84.9 ± 0.8 b	17.2 ± 0.8 b	29.8 ± 0.7 k	84.9 ± 1.1 b	−4.1 ± 0.0 h	55.2 ± 0.7 a	73.9 ± 1.2 b
CB	22.1 ± 0.3 a	37.2 ± 0.6 a	114.2 ± 0.7 a	22.1 ± 0.4 a	37.2 ± 0.4 i	114.2 ± 1.0 a	22.1 ± 0.5 a	37.2 ± 0.3 g	114.2 ± 0.8 a

Values within the same column with different letters are significantly different ($p < 0.05$). Each value in the table represents the mean ± SD of three measurements

PMF palm mid-fractions, RBDPKO refined bleached deodorized palm kernel oil, RBDPS refined bleached deodorized palm stearin, CB cocoa butter

20–38 °C with T_{Onset} , T_{Endset} and ΔH , which are the closest to commercial CB. Therefore, mixtures F to H of RBDPS/RBDPKO can be used as CBSs in compound chocolates because of their compatibility (Fig. 2b) and melting profiles (Fig. 3b; Table 5).

In Fig. 3c, the PMF/RBDPS mixtures showed two broad endotherms (T_1 and T_2) with an exotherm between them. As the RBDPS increased in the mixtures, the higher temperature endotherm (T_2) increased from 30 to 40 °C. This may be due to the increased proportion of SSS TAGs (PPP) from RBDPS (Table 4). All the mixtures showed different T_{Onset} , T_{Endset} , and ΔH . For example, the T_{Onset} at 4.2 °C and T_{Endset} at 32.1° were observed for mixture B, whereas T_{Onset} was at −0.8 °C and T_{Endset} at 50.7 °C for mixture J (Table 5). There were gradual increases in the ΔH of all mixtures (41.7–70.6 J/g) with the addition of RBDPS (Table 5). This behavior was probably caused by the presence of increased proportions of saturated fatty acids and SSS (especially PPP) TAGs (Tables 3, 4). These findings also agreed with the monotectic effect in the iso-solid diagram (Fig. 2c). Most of the PMF/RBDPS mixtures were significantly different ($p < 0.05$) for the T_{Onset} , T_{Endset} and melting enthalpy (Table 5). These findings are consistent with a previous report by Sonwai and co-workers [9], who reported the melting profiles of a mango kernel fat/palm oil mid-fraction blend that resemble CB with two maxima at 17 and 36.2 °C. In another study, Chaiseri and Dimik [24] also noted two maxima, at 11.6 and 22.8 °C, for commercial CB. Similarly, in the present study, mixtures C to F

with 50–80 % PMF in RBDPS showed melting characteristics of 20–38 °C with T_{Onset} , T_{Endset} and ΔH , which are the closest to commercial CB. Therefore, mixtures C to F of PMF in RBDPS can be used as CBSs in compound chocolates due to their monotectic effect with approximately 40 % SFC value at 25 °C (Fig. 2c) and melting profiles (Fig. 3c; Table 5).

Polymorphisms

The purpose of the microstructure study using XRD was to observe if the crystalline microstructure of binary mixtures resembles that of CB. The polymorphic forms obtained by XRD were confirmed using DSC melting thermograms (Fig. 3a–c). The polymorphic structures of the different fat mixtures are presented in Table 6. CB showed a mixture of β'_1 , β'_2 and β_2 crystals due to the presence of 88.2 % SUS (Table 4), and this agrees with the earlier studies [4]. PMF and RBDPKO showed only β'_1 and β'_2 polymorphs, while RBDPS exhibited a mixture of β'_1 , β'_2 and β_2 polymorphs. For PMF/RBDPKO mixtures, the proportion of β'_1 crystal decreased gradually while the proportion of β'_2 crystal increased accordingly ($p < 0.05$) with the addition of RBDPKO. This behavior could be due to the decreased proportion of SUS (especially POP) and increased proportion of SSS TAGs (Table 4). In DSC melting thermograms, blends G to J with 10–40 % PMF in RBDPKO showed a melting temperature of 25–26 °C which is close to CB with a mixture of β'_1 and β'_2 polymorphs ($\beta'_1 \gg \beta'_2$) (Fig. 3a; Table 6).

Table 6 Overview of polymorphic forms (%)^a in PMF/RBDPKO mixtures, RBDPS/RBDPKO mixtures, and PMF/RBDPS mixtures

Blend	PMF/RBDPKO			RBDPS/RBDPKO			PMF/RBDPS		
	β'_1	β'_2	β_2	β'_1	β'_2	β_2	β'_1	β'_2	β_2
A (100:0)	82.4 ± 0.9 a	17.6 ± 1.2 a	–	34.7 ± 0.7 i	37.1 ± 1.2 a	28.2 ± 1.2 b	82.4 ± 0.2 a	17.6 ± 0.7 a	–
B (90:10)	80.7 ± 0.7 b	19.3 ± 1.1 b	–	35.4 ± 1.1 h	37.0 ± 0.7 a	27.6 ± 0.4 c	72.7 ± 1.5 b	18.3 ± 0.8 b	9.0 ± 0.4 k
C (80:20)	80.2 ± 1.2 b	19.8 ± 1.0 b	–	36.9 ± 0.7 g	36.8 ± 0.7 a	26.3 ± 0.4 d	67.3 ± 0.4 c	18.7 ± 0.7 b	14.0 ± 0.8 j
D (70:30)	74.5 ± 0.7 c	25.5 ± 1.1 c	–	37.5 ± 0.7 f	36.8 ± 0.7 a	25.7 ± 0.7 e	64.0 ± 0.3 d	19.0 ± 0.1 c	17.0 ± 0.7 i
E (60:40)	72.3 ± 0.8 d	27.7 ± 0.7 d	–	40.0 ± 0.7 ef	36.8 ± 1.2 a	23.2 ± 0.7 f	59.1 ± 0.7 e	19.5 ± 0.2 c	21.4 ± 0.7 h
F (50:50)	71.4 ± 1.1 e	28.6 ± 0.7 e	–	40.4 ± 0.2 e	36.8 ± 1.1 a	22.8 ± 0.7 g	57.5 ± 0.7 f	19.7 ± 0.7 c	22.8 ± 0.8 g
G (40:60)	70.4 ± 1.4 f	29.6 ± 0.3 f	–	42.0 ± 0.2 e	36.8 ± 1.4 a	21.2 ± 0.8 h	55.4 ± 0.8 g	21.4 ± 0.7 d	23.2 ± 0.4 f
H (30:70)	66.2 ± 0.4 g	33.8 ± 0.3 g	–	43.6 ± 1.1 d	36.7 ± 0.2 a	19.7 ± 0.7 i	51.4 ± 0.7 h	24.3 ± 0.7 e	24.3 ± 0.4 e
I (20:80)	64.7 ± 0.4 h	35.3 ± 0.2 h	–	47.7 ± 0.3 c	36.7 ± 0.7 a	15.6 ± 0.7 j	47.1 ± 0.7 i	27.2 ± 1.2 f	25.7 ± 1.2 d
J (10:90)	64.2 ± 0.4 h	35.8 ± 0.3 h	–	51.0 ± 1.4 b	36.7 ± 0.7 a	12.3 ± 0.3 k	41.7 ± 0.8 j	31.2 ± 0.2 g	27.1 ± 0.4 c
K (0:100)	63.3 ± 0.4 i	36.7 ± 0.2 i	–	63.3 ± 1.4 a	36.7 ± 0.3 a	–	34.7 ± 0.9 k	37.1 ± 0.7 h	28.2 ± 0.4 b
CB	25.4 ± 0.7 j	4.1 ± 0.2 j	70.5 ± 0.4	25.4 ± 0.7 j	4.1 ± 0.2 b	70.5 ± 0.4 a	25.4 ± 0.7 i	4.1 ± 0.2 i	70.5 ± 0.4 a

Values within the same column with different letters are significantly different ($p < 0.05$). Each value in the table represents the mean ± SD of three measurements

PMF palm mid-fractions, RBDPKO refined bleached deodorized palm kernel oil, RBDPS refined bleached deodorized palm stearin, CB cocoa butter

^a Determined by X-ray diffraction

A similar trend was observed for PMF/RBDPS mixtures. In the PMF/RBDPS mixtures, the percentage of β_2 crystal increased ($p < 0.05$) with increasing RBDPS (Table 6). This may be related to the presence of increased proportions of SSS TAGs especially PPP (Table 4). Blends C to F with 50–80 % PMF in RBDPS showed a mixture of β'_1 , β'_2 and β_2 polymorphs ($\beta'_1 \gg \beta'_2 > \beta_2$) with melting temperatures of 20–38 °C which are close to CB (Table 6; Fig. 3c).

For RBDPS in RBDPKO mixtures, the proportion of the β'_1 crystal increased, while the proportion of β'_2 and β_2 crystals gradually decreased with increasing RBDPKO. There were significant differences ($p < 0.05$) in the amount of β'_1 and β_2 polymorphs among all the blends; however, blends C to J showed similar percentages of the β'_2 polymorph (Table 6). These variations in the crystals are likely due to the differences in the TAGs contents (Table 4). Blends F to H (30–50 % RBDPS in RBDPKO) showed melting temperatures of 20–38 °C which are close to CB with a mixture of β'_1 , β'_2 and β_2 polymorphs ($\beta'_1 > \beta'_2 \gg \beta_2$) (Fig. 3b; Table 6). A similar observation was reported in the blends of mango kernel fat and PMF, which revealed a mixture of β' and β polymorphs closer to CB [9]. In the present study, the amounts of β'_1 and β'_2 crystals were found to be higher than CB for all the mixtures, while the amount of β_2 crystal was reasonably lower compared to commercial CB. In a previous study, more than 70 % β' crystals compared to the β crystal have been reported to be desirable for compound chocolates and coatings [21]. Therefore, 20–40 % PMF in RBDPKO, 30–50 % RBDPS in RBDPKO and 50–80 % of PMF in RBDPS mixtures may be used as CBSs in compound chocolates.

Conclusions

The melting profiles of 20–40 % PMF in RBDPKO, 30–50 % RBDPS in RBDPKO and 50–80 % of PMF in RBDPS mixtures can approximate that of CB, even though the polymorphism, fatty acid profile and TAG composition are different. Furthermore, 20–40 % PMF in RBDPKO and 30–50 % RBDPS in RBDPKO mixtures showed a monotectic behavior at 10–20 °C, suitable to be used as CBSs in compound chocolates and fillings. Up to 50–80 % of PMF in RBDPS mixtures also displayed a monotectic behavior at less than 30 °C, making the mixture potentially of use as CBSs in compound chocolates and other confectionery applications.

Acknowledgments The authors would like to thank School of Science and Grant No. (FRGS/1/2013/SG01/MUSM/03/2) for supporting the current study. The authors are grateful to the Malaysia Cocoa Board for SFC determinations and Mr Nasrun for XRD technical support.

References

1. Bootello MA, Hartel RW, Garcés R, Martínez-Force E, Salas JJ (2012) Evaluation of high oleic-high stearic sunflower hard stearins for cocoa butter equivalent formulation. *Food Chem* 134:1409–1417
2. Gunstone F (2011) Vegetable oils in food technology: composition, properties and uses. Wiley, London, pp 291–343
3. Jahurul M, Zaidul I, Norulaini N, Sahena F, Jinap S, Azmir J, Sharif K, Omar AM (2013) Cocoa butter fats and possibilities of substitution in food products concerning cocoa varieties, alternative sources, extraction methods, composition, and characteristics. *J Food Eng* 117:467–476
4. d'Souza V (1990) Short spacings and polymorphic forms of natural and commercial solid fats: a review. *J Am Oil Chem Soc* 67:835–843
5. Talbot G (2009) Fats for confectionery coatings and fillings. In: Talbot G (ed) Science and technology of enrobed and filled chocolate, confectionery and bakery products. Woodhead Publishing Ltd, pp 53–79
6. Gold IL, Ukhun M, Akoh C (2011) Characteristics of eutectic compositions of restructured palm oil olein, palm kernel oil and their mixtures. *J Am Oil Chem Soc* 88:1659–1667
7. Williams SD, Ransom-Painter KL, Hartel RW (1997) Mixtures of palm kernel oil with cocoa butter and milk fat in compound coatings. *J Am Oil Chem Soc* 74:357–366
8. Zaidul I, Norulaini NN, Omar AM, Smith R (2007) Blending of supercritical carbon dioxide (SC-CO₂) extracted palm kernel oil fractions and palm oil to obtain cocoa butter replacers. *J Food Eng* 78:1397–1409
9. Sonwai S, Kaphueakngam P, Flood A (2014) Blending of mango kernel fat and palm oil mid-fraction to obtain cocoa butter equivalent. *J Food Sci Technol* 51:2357–2369
10. Jahurul M, Zaidul I, Norulaini NN, Sahena F, Abedin M, Mohamed A, Omar AM (2014) Hard cocoa butter replacers from mango seed fat and palm stearin. *Food Chem* 154:323–329
11. Tan C, Che Man Y (2002) Differential scanning calorimetric analysis of palm oil, palm oil based products and coconut oil: effects of scanning rate variation. *Food Chem* 76:89–102
12. Calliauw G, Foubert I, De Greyt W, Dijckmans P, Kellens M, Dewettinck K (2005) Production of cocoa butter substitutes via two-stage static fractionation of palm kernel oil. *J Am Oil Chem Soc* 82:783–789
13. Soares FASDM, da Silva RC, da Silva KCG, Lourenço MB, Soares DF, Gioielli LA (2009) Effects of chemical interesterification on physicochemical properties of blends of palm stearin and palm olein. *Food Res Int* 42:1287–1294
14. Kellens M, Gibon V, Hendrix M, De Greyt W (2007) Palm oil fractionation. *Eur J Lipid Sci Technol* 109(336):349
15. Saberi AH, Lai O-M, Toro-Vázquez JF (2011) Crystallization kinetics of palm oil in blends with palm-based diacylglycerol. *Food Res Int* 44:425–435
16. Fiebig HJ, Lüttke J (2003) Solid fat content in fats and oils-determination by pulsed nuclear magnetic resonance spectroscopy [C-IV 3 g (2003)]. *Eur J Lipid Sci Technol* 105:377–380
17. Jahurul M, Zaidul I, Norulaini NN, Sahena F, Kamaruzzaman B, Ghafoor K, Omar A (2014) Cocoa butter replacers from blends of mango seed fat extracted by supercritical carbon dioxide and palm stearin. *Food Res Int* 65:401–406
18. Toro-Vázquez JF, Pérez-Martínez D, Dibildox-Alvarado E, Charó-Alonso M, Reyes-Hernández J (2004) Rheometry and polymorphism of cocoa butter during crystallization under static and stirring conditions. *J Am Oil Chem Soc* 81:195–202
19. Kadivar S, De Clercq N, Mokbul M, Dewettinck K (2016) Influence of enzymatically produced sunflower oil based cocoa butter

- equivalents on the phase behavior of cocoa butter and quality of dark chocolate. *LWT-Food Sci Technol* 66:48–55
20. Humphrey KL, Narine SS (2004) Lipid phase behavior. In: Marangoni AG (ed) *Fatcrystal networks*. Dekker, New York, pp 83–114
 21. Wang F, Liu Y, Jin Q, Meng Z, Wang X (2011) Characterization of cocoa butter substitutes, milk fat and cocoa butter mixtures. *Eur J Lipid Sci Technol* 113:1145–1151
 22. Timms R (1984) Phase behaviour of fats and their mixtures. *Prog Lipid Res* 23:1–38
 23. Jahurul M, Zaidul I, Norulaini N, Sahena F, Abedin M, Ghafoor K, Omar AM (2014) Characterization of crystallization and melting profiles of blends of mango seed fat and palm oil mid-fraction as cocoa butter replacers using differential scanning calorimetry and pulse nuclear magnetic resonance. *Food Res Int* 55:103–109
 24. Chaiseri S, Dimick PS (1989) Lipid and hardness characteristics of cocoa butters from different geographic regions. *J Am Oil Chem Soc* 66:1771–1776
 25. Norizzah A, Chong C, Cheow C, Zaliha O (2004) Effects of chemical interesterification on physicochemical properties of palm stearin and palm kernel olein blends. *Food Chem* 86:229–235
 26. Fauzi SHM, Rashid NA, Omar Z (2013) Effects of chemical interesterification on the physicochemical, microstructural and thermal properties of palm stearin, palm kernel oil and soybean oil blends. *Food Chem* 137:8–17
 27. Zhou SL, Zhang FQ, Jin QZ, Liu YF, Shan L, Zhang T, Zou XQ, Wang XG (2010) Characterization of palm kernel oil, palm stearin, and palm olein blends in isosolid diagrams. *Eur J Lipid Sci Technol* 112:1041–1047
 28. Talbot G (2006) *Application of fats in Confectionery*. Kennedy's Publications, pp 125–137

Appendix I (Chapter 3) Publications during enrolment

Author's personal copy

J Am Oil Chem Soc (2017) 94:235–245
DOI 10.1007/s11746-016-2940-4



ORIGINAL PAPER

Cocoa Butter Substitute (CBS) Produced from Palm Mid-fraction/Palm Kernel Oil/Palm Stearin for Confectionery Fillings

Nirupam Biswas¹ · Yuen Lin Cheow¹ · Chin Ping Tan² · Silvaruby Kanagaratnam³ · Lee Fong Siow¹

Received: 13 June 2016 / Accepted: 10 December 2016 / Published online: 3 January 2017
© AOCs 2017

Abstract This study investigated the physicochemical properties of ternary mixtures of palm mid-fraction (PMF):refined bleached deodorized palm kernel oil (RBDPKO):refined bleached deodorized palm stearin (RBDPS) for cocoa butter substitute (CBS). Fatty acid constituents, triacylglycerol constituents, solid fat contents (SFCs), melting behavior, polymorphism and crystal morphology were determined using gas chromatography (GC), high-performance liquid chromatography (HPLC), differential scanning calorimetry (DSC), pulsed nuclear magnetic resonance (p-NMR), X-ray diffraction (XRD) and polarized light microscopy (PLM), respectively. Eight blends of various ratios of ternary mixtures were investigated based on the previously studied binary fat mixtures. The composition of palmitic (P) and oleic (O), POP, and crystal morphology (size and shape) of the PMF/RBDPKO/RBDPS [14.9/59.6/25.5 (%w/w)] mixture were comparable to cocoa butter (CB), while its melting profile (18.5 and 37 °C), SFC at 20 °C and polymorphism were different from CB. The iso-solid diagrams of the mixture displayed a monotectic effect at 20–25 °C. Therefore, the 14.9/59.6/25.5 PMF/RBDPKO/RBDPS mixture could be used as a CBS in confectionery fillings because of the

crystal morphology and monotectic behaviors comparable to those of CB.

Keywords Ternary · Crystal · Cocoa butter · Iso-solid diagram · Polarizer

Introduction

Cocoa butter (CB) is traditionally used for the formulation of chocolates, coatings, confectionery fillings and other confectionery products. CB is solid at room temperature and melts quickly above 30–32 °C [1]. This behavior produces a stable confectionery product that releases flavors in the mouth at body temperature without any undesirable waxy texture. CB consists of three main triacylglycerols (TAGs): glycerol-1,3-dipalmitate-2-oleate (POP; P = palmitic, O = oleic; 13.6–15.5%), glycerol-1-palmitate-2-oleate-3-stearate (POST; St = stearic; 33.7–40.5%) and glycerol-1,3-distearate-2-oleate (StOSt, 23.8–31.2%) [1, 2]. These TAGs dominate the melting characteristic and solid fat content as a function of temperature and polymorphic transformations of chocolate, providing chocolate's textural and sensory properties [3]. CB exhibits complex polymorphic forms, namely γ , α , β' and β in ascending stability [4]. The stable polymorph (β) is typically preferred in chocolates and coatings because it melts at high melting temperature with small to moderate crystal sizes, allowing for smooth mouth-feel products [5]. The metastable β' polymorph is desirable for confectionery fillings and compound chocolates because it melts at low temperature with a fine arrangement and a large surface area of solid crystals [5, 6].

CB is expensive compared to other commercial vegetable fats and oils because of its limited supply and high

✉ Lee Fong Siow
siow.lee.fong@monash.edu

¹ School of Science, Monash University Malaysia, 47500 Bandar Sunway, Selangor D.E., Malaysia

² Department of Food Technology, Faculty of Food Science and Technology, Universiti Putra Malaysia, 43400 UPM Serdang, Selangor D.E., Malaysia

³ Malaysian Palm Oil Board, Persiaran Institusi Bandar Baru Bangi, 43000 Kajang, Selangor, Malaysia

market demand. Therefore, manufacturers are looking for alternatives to CB. CB alternatives (CBAs) can be classified into three groups: CB substitutes (CBSs) derived from lauric fats, CB replacers (CBRs) obtained from hydrogenation of vegetable oils, and CB equivalents (CBEs) derived from polymorphic and non-lauric fats. Among them, CBSs are generally used in confectionery fillings such as truffles, compound chocolates and other confectionery products [5]. CBSs contain high amounts of lauric acid (12:0, 54.6%), followed by myristic acid (14:0, 20.7%), palmitic acid (16:0, 9.2%) and stearic acid (18:0, 8.7%), resulting in short-chain TAGs [7]. CBSs show solid fat content (monotectic behavior) as a function of temperature and crystal morphology (size and shape) similar to those of CB, while the polymorphism, melting profile, TAG composition and fatty acid profile are different from CB [8–10]. In addition, CBSs with a low melting temperature of 21–23 °C are used in confectionery fillings [5].

Palm mid-fraction (PMF) is a fraction of palm oil (*Elaeis guineensis*) with melting points between 9.8 and 32.8 °C [2]. PMF contains 51.8% of POP among three main TAGs. Most importantly, PMF shows a steep solid fat content versus temperature curve, which is similar to that of CB. Moreover, PMF tends to crystallize in the β' form and is, therefore, an attractive option for producing confectionery fillings and fat spreads [11].

Refined, bleached and deodorized palm kernel oil (RBDPKO) refers to extract palm kernel oil that has been refined, bleached and deodorized. It is a semi-solid fat at room temperature, with a melting point of approximately 26–28 °C. The oil contains a high percentage of short-chain fatty acids such as lauric (12:0, 47.7%) and myristic acids (14:0, 22.6%) [10]. Although this oil contains high levels of undesirable short-chain fatty acids, it is broadly used as a suitable raw material for the production of confectioneries [12]. In this application, RBDPKO shows melting characteristic and crystallization behavior similar to those of CB, but the two chemical formulations differ considerably. In CB, the constituents of long-chain fatty acids such as palmitic (16:0, 24.4%), stearic (18:0, 33.6%), and oleic acids (18:1, 37.0%) are high, whereas short-chain fatty acids such as lauric acid and myristic acid constituents occur in very low amounts [2]. In RBDPKO, the concentration of short-chain fatty acids is high, whereas the concentration of long-chain fatty acids is relatively low compared to that of CB. Hence, the high short-chain fatty acid content and low long-chain fatty acids (palmitic/oleic) content of RBDPKO makes it unsuitable as a direct CBS. Blending RBDPKO with palmitic and oleic acid-rich fats such as PMF and/or palm stearin, however, makes it possible to decrease the short-chain fatty acid concentration whilst increase the long-chain fatty acid concentration. This process may produce high-quality CBSs with fatty acid compositions more

similar to that of CB. RBDPKO is now gaining more interest as a suitable CBS in confectionery products [13].

Refined, bleached and deodorized palm stearin (RBDPS) is obtained by fractionating refined palm oil to separate olein from palm stearin. The physical properties of RBDPS differ from other palm oil products because it is a solid fat with a high melting point (44–56 °C), that needs to be mixed with lower melting point oils such as PMF and RBDPKO to yield a melting profile similar to that of CB. In addition, this oil contains a low amount of linoleic acid (18:2), making it less prone to oxidation [12]. The applications of RBDPS have been well-reviewed, and the stearin has also been reported to be a suitable coating material [14, 15].

In compound chocolates, coatings and fillings, different vegetable fats such as palm kernel oil, palm kernel stearin, palm oil or cocoa butter are commonly modified or blended. The modification of palm kernel oil to CBS is traditionally performed through hydrogenation. This process, however, has always been regarded to produce trans-fatty acids that increase undesirable low-density lipoprotein cholesterol [16]. Therefore, many studies have been performed to produce for CBS-based compound chocolates and coatings by blending different proportions of palm kernel oil, palm kernel stearin, palm oil or cocoa butter [6, 11, 17, 18]. Vereecken *et al.* studied the crystallization behavior, microstructure and macroscopic properties of the lauric-based and palm-based fats for confectionery fillings [19]. However, no information has been obtained with respect to the melting behavior, polymorphisms and crystal morphology of ternary mixtures of PMF/RBDPKO/RBDPS, which are important in producing CBSs in confectionery fillings.

Iso-solid phase diagrams have been used to illustrate the eutectic and monotectic behavior of binary/ternary fat mixtures because they are useful in understanding the compatibility of mixed fat systems [6]. For instance, the eutectic effect occurs, when the contour lines of constant solid fat content are not straight, with some blend compositions having lower melting temperatures than expected. This indicates that the fat blends are not compatible (eutectic). The monotectic effect (dilution effect) is manifested by a straight line connecting the SFC of each pure component, indicating fats in a blend are mixed well (monotectic) [20].

PMF, RBDPKO and RBDPS oils are less expensive than other vegetable oil products, making them cost-effective ingredients in confectionery fillings and compound chocolates. The present study aims to evaluate the physical and chemical characteristics of ternary fat mixtures of PMF/RBDPKO/RBDPS in terms of their fatty acid profiles, triacylglycerol constituents, melting behavior, solid fat content, polymorphism and crystal morphology to produce better CBSs in confectionery fillings. The ternary fat mixtures were combined based on our preliminary study of binary fat mixtures [21].

Table 1 Experimental design of PMF/RBDPKO/RBDPS mixtures

Proportion by weight (%)			
Code	PMF	RBDPKO	RBDPS
A(e)	11.1	44.4	44.4
B(g)	25.0	37.5	37.5
C(h)	33.3	33.3	33.3
D(f)	28.6	42.8	28.6
E(c)	14.9	59.6	25.5
F(d)	31.0	48.3	20.7
G(a)	16.6	66.6	16.6
H(b)	26.6	62.0	11.4

Small letters, (a)–(h), are used to label samples with decreasing order of RBDPKO; capital letters, A–H, are used to label samples with decreasing order of RBDPS

PMF Palm mid-fraction, RBDPKO refined, bleached and deodorized palm kernel oil, RBDPS refined, bleached and deodorized palm stearin

Materials and Methods

Materials

PMF, RBDPKO and RBDPS were obtained from Sime Darby Research Sdn. Bhd. CB was purchased from Le Bourne Sdn. Bhd (Selangor, Malaysia). All chemicals and solvents used were of analytical reagent or HPLC grades (Fisher Scientific Comp., USA). Fatty acid methyl ester (FAME) standards and TAG standards were obtained from Lab Science Solution Sdn. Bhd. and Sigma-Aldrich.

Preparation of Fat Blend

Blends (%w/w) of PMF, RBDPKO and RBDPS were mixed in various ratios (Table 1) according to binary fat mixtures in our preliminary study [21]. The blends were melted at 80 °C for 30 min to erase crystal memory. The samples were kept at 25 °C for further analysis.

Example of ternary relation from binary mixtures: PMF:RBDPKO:RBDPS = (PMF:RBDPKO) × (PMF:RBDPS). Where, PMF:RBDPKO = 2:3 (40/60); RBDPKO:RBDPS = 1:1 (50/50); therefore, PMF:RBDPKO:RBDPS = 2:3:3 (25/37.5/37.5).

Fatty Acid Analysis

Fatty acid composition of the investigated fat mixtures was determined in terms of FAME, following the method developed by Saberi *et al.* [22]. The samples (50 mg) were weighed and dissolved in 1 ml of heptane inside a 1.5-ml centrifuge tube. The mixtures were then added to 50 µl of

1 M sodium methoxide in anhydrous methanol and then mixed vigorously for 1 min by using a vortex mixer. After the sedimentation of sodium glycerolate, 1 µl of the clear supernatant was injected into a gas chromatograph (Perkin Elmer Clarus 500 GC, Waltham, USA) fitted with an elite-FFAP column (30-m length × 0.32-mm i.d. × 0.25-µm film thickness). A flame ionization detector (FID) was used to detect the FAME. The injection and detection temperatures were both at 250 °C. The oven temperature was programmed as follows: heat from 110 to 140 °C (30 °C/min), hold at 140 °C for 1 min, heat from 140 to 240 °C (15 °C/min) and hold for 7 min at 240 °C. The carrier gas (helium) flow rate was 0.9 ml/min. The peaks were identified by comparing retention times with FAME standards and quantified by using a peak area normalization method.

Triacylglycerol (TAG) Analysis

The TAG profiles of the selected samples were analyzed using high-performance liquid chromatography (Agilent HPLC series 1260, CA, USA) according to AOCS Official Method Ce 5b-89. The column used was a ZORBAX C-18 (4.6 × 250 mm, 5 µm, Agilent Technologies, CA, USA) and maintained at 35 °C by a column oven. Isocratic elution was carried out at a flow rate of 1.5 ml/min with a mixture of acetone/acetonitrile (70:30, v/v) as the mobile phase. A refractive index detector (RID 1260 Infinity, CA, USA) was used. The injection volume with an auto-injector was 10 µL of 5% (w/v) oil in acetone. TAG peaks were identified based on the retention time of TAG standards. The percentage of TAGs was determined by using a peak area of the chromatogram.

Solid Fat Content (SFC)

SFC of the selected fats was determined by using pulsed nuclear magnetic resonance (p-NMR) with a Bruker Minispec PC 120 NMR analyzer (Karlsruhe, Germany), according to the AOCS Official Method Cd 16b-93 for stabilizing confectionery fats. The method was also used in previous researches [19, 23, 24]. Samples were melted at 100 °C for 15 min and filled into NMR tubes (10-mm o.d. × 75-mm length, up to 3 cm in height). Samples were tempered at 60 °C for 5 min, followed by 0 °C for 90 min, 26 °C for 40 h, 0 °C for 90 min, and finally kept for 60 min at the desired measuring temperatures of 5, 10, 15, 20, 25, 30, 35, 37, 40, and 45 °C before SFC was measured. The melting profiles were drawn by plotting SFC against temperature. Iso-solid phase diagrams of the fat mixtures were constructed with OriginPro 9.1 software (OriginLab Corp., Northampton, MA, USA) based on SFC values obtained from NMR at 10, 20 and 25 °C.

Melting Behaviour

Melting behavior of the fat mixtures was determined using differential scanning calorimetry (DSC, Pyris 4000 DSC, Perkin-Elmer Ltd., USA). Nitrogen gas was used at a flow rate of 20 ml/min. The instrument was calibrated with indium and *n*-dodecane. The samples (5–8 mg) were hermetically sealed in an aluminum pan. An empty, covered aluminum pan was used as the reference. The samples were cooled to $-50\text{ }^{\circ}\text{C}$ at $10\text{ }^{\circ}\text{C}/\text{min}$, held at $-50\text{ }^{\circ}\text{C}$ for 5 min and then heated to $80\text{ }^{\circ}\text{C}$ at $5\text{ }^{\circ}\text{C}/\text{min}$ [25].

Polymorphism

The polymorphic forms of the fat crystals were determined at room temperature ($24\text{ }^{\circ}\text{C}$) with a D8 Discover X-ray diffractometer (Bruker, Germany) fitted with Cu-K α radiation ($k = 1.5418\text{ \AA}$, voltage 40 kV and current 40 mA). The samples were analysed at 2θ angles of 10° – 30° with a scan rate of $1.5^{\circ}/\text{min}$. Short (d) spacing (\AA) was determined using the EVA-diffraction software (Bruker, Germany). Assignments of polymorphs were based on the following short spacing characteristics of CB: α form ($d = 4.15\text{ \AA}$); β' forms ($d = 3.8$ – 4.3 \AA) and β forms ($d = 4.5$ – 4.6 \AA) [4].

Crystal Morphology

Polarized light microscopy (PLM, Olympus BX51, Tokyo, Japan) equipped with a digital camera (Nikon, DS-Filc, Tokyo, Japan) at $24\text{ }^{\circ}\text{C}$ was used to observe the crystal network microstructure of individual CB, PMF, RBDPKO, RBDPS and ternary mixtures of PMF/RBDPKO/RBDPS. The method described by Narine and Marangoni [26] was used for the crystallization of fat blends. The sample was melted at $80\text{ }^{\circ}\text{C}$ for 20 min to destroy crystal memory. About $15\text{ }\mu\text{l}$ of melted sample was placed on a glass slide, heated to $80\text{ }^{\circ}\text{C}$, and covered carefully by a coverslip. The slides were then stored in a temperature-controlled cabinet at $24 \pm 1\text{ }^{\circ}\text{C}$ for 48 h to ensure proper crystallization. The liquid phase appears black, while the solid phase appears grey. NIS-Element Imaging Software (Version 4.20, Nikon Instruments Inc. Melville, USA) was used to obtain images.

Statistical Analysis

Data were statistically analysed by one-way analysis of variance (ANOVA) using the OriginPro 9.1 software (OriginLab Corp., Northampton, MA, USA). Tukey's test was applied to determine the significant differences at a $P < 0.05$ level. NMR analysis was performed in duplicate. DSC diagrams, XRD and PLM analyses were conducted in triplicate.

Table 2 Fatty acid composition (% peak area)^a of PMF/RBDPKO/RBDPS mixtures

FA (%)	Blend										CB
	(a)	(b)	(c)	(d)	(e)	(f)	(g)	(h)			
C _{8:0}	2.75 \pm 0.1a	2.58 \pm 0.1a	2.47 \pm 0.4a	2.07 \pm 0.1b	2.04 \pm 0.0b	1.78 \pm 0.1c	1.70 \pm 0.2c	1.69 \pm 0.4c	–	–	–
C _{10:0}	2.24 \pm 0.1a	2.05 \pm 0.4a	2.01 \pm 0.1a	1.76 \pm 0.1b	1.71 \pm 0.0b	1.47 \pm 0.1bc	1.43 \pm 0.4bc	1.38 \pm 0.4bc	–	–	–
C _{12:0}	30.32 \pm 0.7a	29.69 \pm 0.5b	29.06 \pm 0.6c	26.47 \pm 0.3d	26.36 \pm 0.5d	23.31 \pm 0.4e	23.27 \pm 0.7e	23.24 \pm 0.3e	Trace	Trace	Trace
C _{14:0}	10.26 \pm 0.8a	9.63 \pm 0.1b	9.14 \pm 0.1c	8.86 \pm 0.4d	8.74 \pm 0.4d	8.17 \pm 0.3e	8.11 \pm 0.9e	8.09 \pm 0.4e	0.73 \pm 0.0f	0.73 \pm 0.0f	0.73 \pm 0.0f
C _{16:0}	24.85 \pm 0.2f	24.88 \pm 0.2f	25.74 \pm 0.4e	26.89 \pm 0.9d	29.46 \pm 1.1c	30.76 \pm 0.1b	30.82 \pm 0.8b	33.00 \pm 0.7a	25.69 \pm 0.2e	25.69 \pm 0.2e	25.69 \pm 0.2e
C _{18:0}	3.00 \pm 0.1d	3.09 \pm 0.4d	3.12 \pm 0.0d	3.96 \pm 0.4b	3.37 \pm 0.4c	3.36 \pm 0.4c	3.34 \pm 0.5c	3.29 \pm 0.4c	36.15 \pm 0.5a	36.15 \pm 0.5a	36.15 \pm 0.5a
C _{18:1}	22.56 \pm 0.4 g	23.34 \pm 0.8f	24.51 \pm 0.8e	25.14 \pm 0.8d	25.26 \pm 0.9d	26.62 \pm 0.1c	26.78 \pm 0.8b	26.84 \pm 0.7b	33.24 \pm 0.3a	33.24 \pm 0.3a	33.24 \pm 0.3a
C _{18:2}	4.02 \pm 0.1c	4.74 \pm 0.1b	3.95 \pm 0.4c	4.85 \pm 0.4b	3.06 \pm 0.4d	4.53 \pm 0.1b	4.55 \pm 0.4b	2.47 \pm 0.3e	3.13 \pm 0.4d	3.13 \pm 0.4d	3.13 \pm 0.4d
C _{20:0}	–	–	–	–	–	–	–	–	1.04 \pm 0.1	1.04 \pm 0.1	1.04 \pm 0.1
SFA	73.42 \pm 1.1a	71.92 \pm 1.0b	71.54 \pm 1.1c	70.01 \pm 1.1d	71.68 \pm 1.1c	68.85 \pm 0.6e	68.67 \pm 1.4e	70.69 \pm 1.1f	63.63 \pm 1.0g	63.63 \pm 1.0g	63.63 \pm 1.0g
USFA	26.58 \pm 0.7f	28.08 \pm 0.8e	28.46 \pm 0.9d	29.99 \pm 0.4b	28.32 \pm 0.3de	31.15 \pm 0.8b	31.33 \pm 0.4b	29.31 \pm 0.5c	36.37 \pm 0.7a	36.37 \pm 0.7a	36.37 \pm 0.7a

FA Fatty acid, SFA saturated fatty acid, USFA unsaturated fatty acid, PMF palm mid-fraction, RBDPKO refined, bleached and deodorized palm kernel oil, RBDPS refined, bleached and deodorized palm stearin, CB cocoa butter

^a Values within the same row with different letters are significantly different ($P < 0.05$); Each value in the table represents the mean \pm standard deviation (SD) of three measurements

Table 3 Overview of TAGs (peak area %)† in PMF/RBDPKO/RBDPS mixtures

TAG	Blend	PMF										RBDPKO	RBDPS	CB
		(a)	(b)	(c)	(d)	(e)	(f)	(g)	(h)					
CLa	1.7 ± 0.01	1.5 ± 0.01	1.0 ± 0.0	0.8 ± 0.0	–	–	–	–	–	–	–	8.7 ± 0.01	–	–
CLaLa	6.4 ± 0.01	5.7 ± 0.04	5.3 ± 0.01	5.3 ± 0.01	2.4 ± 0.07	2.4 ± 0.01	2.4 ± 0.07	2.1 ± 0.07	2.1 ± 0.01	–	–	11.4 ± 0.50	–	–
LaLaLa	18.1 ± 0.01	17 ± 0.01	15.4 ± 0.40	15.1 ± 0.40	14.3 ± 1.10	13.7 ± 0.07	13.7 ± 1.10	13.2 ± 0.05	10.3 ± 0.70	–	–	27.2 ± 1.10	–	–
LaLaM	10.2 ± 0.03	9.7 ± 0.01	9.2 ± 0.01	8.8 ± 0.01	7.5 ± 0.01	6.8 ± 0.02	6.8 ± 0.01	6.4 ± 0.02	6.4 ± 0.01	0.9 ± 0.01	–	17.0 ± 0.01	–	–
LaMM	7.2 ± 0.01	6.7 ± 0.07	6.7 ± 0.01	6.4 ± 0.01	4.8 ± 0.01	4.3 ± 0.02	4.3 ± 0.01	3.8 ± 0.01	3.4 ± 0.01	–	–	15.1 ± 0.50	–	–
MMM	4.7 ± 0.01	4.4 ± 0.31	3.8 ± 0.01	3.4 ± 0.01	2.6 ± 0.00	2.2 ± 0.01	2.2 ± 0.01	1.7 ± 0.01	1.2 ± 0.01	0.7 ± 0.01	–	8.4 ± 0.01	0.7 ± 0.00	–
PLP	4.1 ± 0.01	3.8 ± 0.01	3.7 ± 0.01	3.4 ± 0.01	3.4 ± 0.01	3.1 ± 0.01	3.1 ± 0.01	2.6 ± 0.03	2.3 ± 0.01	6.2 ± 0.01	–	–	6.1 ± 0.01	0.6 ± 0.01
PLP	1.4 ± 0.01	1.7 ± 0.01	3.7 ± 0.01	2.3 ± 0.01	1.2 ± 0.01	2.8 ± 0.01	2.8 ± 0.01	2.4 ± 0.02	6.7 ± 0.40	10.2 ± 1.20	–	–	5.5 ± 0.01	2.1 ± 0.01
POO	6.2 ± 0.05	5.4 ± 0.01	5.0 ± 0.01	3.8 ± 0.01	4.6 ± 0.01	3.5 ± 0.03	3.5 ± 0.01	5.4 ± 0.01	2.1 ± 0.01	12.9 ± 1.10	–	–	13.5 ± 0.50	–
POP	34.7 ± 0.10	34.3 ± 1.20	25.4 ± 1.50	34.6 ± 1.10	37.5 ± 1.10	38.6 ± 1.10	38.6 ± 1.10	39.4 ± 1.20	44.2 ± 1.70	50.7 ± 1.4	0.9 ± 0.01	0.9 ± 0.01	32.1 ± 1.10	18.1 ± 0.70
PPP	4.4 ± 0.01	3.8 ± 0.01	5.4 ± 0.01	4.8 ± 0.01	10.3 ± 0.01	8.9 ± 0.02	8.9 ± 0.01	9.7 ± 0.01	10.1 ± 0.01	3.2 ± 0.01	1.1 ± 0.01	1.1 ± 0.01	28.4 ± 1.10	0.7 ± 0.01
POST	0.4 ± 0.01	5.4 ± 0.01	7.1 ± 0.01	5.9 ± 0.01	4.2 ± 0.01	5.7 ± 0.01	5.7 ± 0.01	5.0 ± 0.01	7.6 ± 0.01	9.1 ± 0.01	–	–	3.8 ± 0.01	39.2 ± 1.10
StOSt	–	–	0.7 ± 0.01	0.5 ± 0.01	–	0.2 ± 0.01	0.2 ± 0.01	–	1.2 ± 0.01	1.9 ± 0.01	–	–	–	29.7 ± 1.10
SSS	51.0 ± 1.20	47.3 ± 0.70	45.8 ± 1.70	43.8 ± 0.70	41.9 ± 1.10	38.3 ± 1.10	38.3 ± 1.10	36.9 ± 0.40	33.5 ± 1.20	4.8 ± 0.01	80.2 ± 1.50	29.1 ± 0.01	29.1 ± 0.01	0.7 ± 0.00
SUS	35.1 ± 0.11	39.7 ± 0.40	33.2 ± 0.50	41 ± 0.01	41.7 ± 1.00	44.5 ± 1.10	44.5 ± 1.10	44.4 ± 1.10	53.0 ± 1.10	61.7 ± 1.10	0.9 ± 0.00	35.9 ± 0.60	35.9 ± 0.60	87.0 ± 1.20
SUU	7.6 ± 0.02	7.1 ± 0.01	8.7 ± 0.01	6.1 ± 0.01	5.8 ± 0.01	6.3 ± 0.01	6.3 ± 0.01	7.8 ± 0.01	8.8 ± 0.01	23.1 ± 0.70	2.4 ± 0.01	19.0 ± 0.01	19.0 ± 0.01	2.1 ± 0.01
UUU	4.1 ± 0.01	3.8 ± 0.01	3.7 ± 0.01	3.4 ± 0.01	3.4 ± 0.01	3.1 ± 0.02	3.1 ± 0.02	2.6 ± 0.00	2.3 ± 0.01	6.2 ± 0.01	–	6.1 ± 0.01	6.1 ± 0.01	0.6 ± 0.01
Others	0.5	0.6	7.6	4.9	7.2	7.8	7.8	8.3	2.4	4.2	7.8	9.9	9.9	9.6

TAG Triacylglycerol, C capric, La lauric, M myristic, P palmitic, O oleic, St stearic, L linoleic, SSS saturated, SUS monounsaturated, SUU polyunsaturated, PMF palm mid-fraction, RBDPKO refined, bleached and deodorized palm kernel oil, RBDPS refined, bleached and deodorized palm stearin, CB cocoa butter

† Each value in the table represents the mean ± standard deviation of two measurements

Results and Discussion

Fatty Acid Composition

Table 2 shows the fatty acid profiles of ternary mixtures of PMF/RBDPKO/RBDPS. When the RBDPKO decreased in the mixtures, the concentration of short-chain fatty acids (lauric and myristic) significantly ($P < 0.05$) decreased along with a gradual increase in the concentration of long-chain fatty acids such as palmitic and oleic (Table 2). The fatty acid concentrations in all ternary blends were significantly ($P < 0.05$) affected by the ratios of the mixtures. Calliauw and co-workers [10] also produced CBSs via two-stage static fraction of palm kernel oil, and reported the fatty acid profiles: lauric (56.3%), myristic (19.6%), palmitic (8.9%) and stearic (2.0%). Zaidul *et al.* also studied the fatty acids in different blends of supercritical carbon dioxide extracted palm kernel oil fractions and palm oil in various ratios to obtain CB replacers, and they reported that the fatty acid profiles of certain blends were comparable to those of commercial CB [27]. In the present study, the concentrations of long-chain fatty acids such as palmitic, oleic and linoleic with the exception of stearic and short-chain fatty acids in blend (c) were observed to be comparable to those of commercial CB (Table 2).

Triacylglycerol (TAG) Composition

The TAG profiles of the different PMF/RBDPKO/RBDPS mixtures are shown in Table 3. CB contains predominantly monounsaturated TAGs: POP (18.1%), POST (39.2%) and StOSt (29.7%). PMF contains high concentrations of unsaturated TAGs: POP (50.7%), POO (12.9%), PLP (10.2%; L = linoleic) and POST (9.1%). RBDPS has high concentrations of both saturated and unsaturated TAGs: PPP (28.4%) and POP (32.1%). RBDPKO is rich in saturated TAGs: LaLaLa (La = lauric), LaLaM (M = myristic) and LaMM at 27.2, 17.0 and 15.1%, respectively. These findings are consistent with the results reported in previous studies [2, 28]. Blending of PMF/RBDPKO/RBDPS shows variations in TAG constituents (Table 3). All eight mixtures of the PMF/RBDPKO/RBDPS blend contained a mixture of SSS (trisaturated), SUS (monounsaturated), SUU (diunsaturated) and UUU (polyunsaturated) TAGs. In the mixtures, the trisaturated SSS TAGs, CLaLa (C = capric), LaLaLa, LaLaM, LaMM and MMM, decreased, whereas the unsaturated SUS TAGs, especially POP and PLP, increased gradually ($P < 0.05$) with the reduction of RBDPKO. This can be explained by the presence of a decreasing amount of short-chain saturated fatty acids and increasing amounts of both long-chain saturated and unsaturated fatty acids (Table 2). The most remarkable difference between the ternary mixtures and CB was the content of SUS TAGs, especially POST and StOSt. Sabariah *et al.* reported that CBS contains

a mixture of short-chain fatty acids: lauric, myristic, and long-chain fatty acids: palmitic, stearic with corresponding TAGs [7]. In the present study, the constituent of POP with the exception of POST and StOSt TAGs in blend (c) was found to be comparable to that of CB.

Melting Behavior

DSC melting curves of ternary mixtures of PMF/RBDPKO/RBDPS are shown in Fig. 1. All ternary mixtures

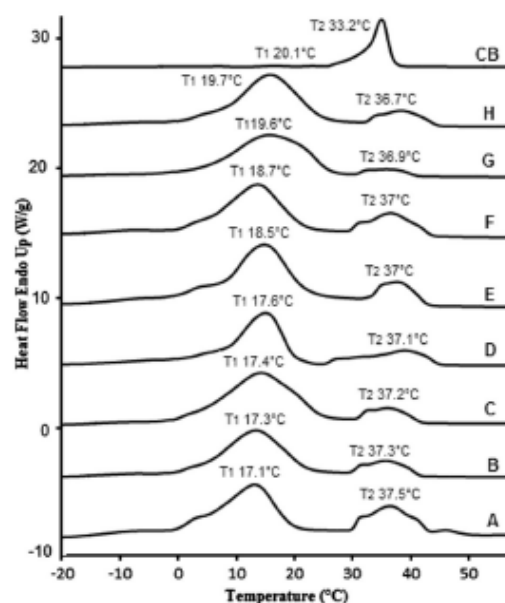


Fig. 1 DSC melting curves for ternary mixtures (A–H) of PMF/RBDPKO/RBDPS

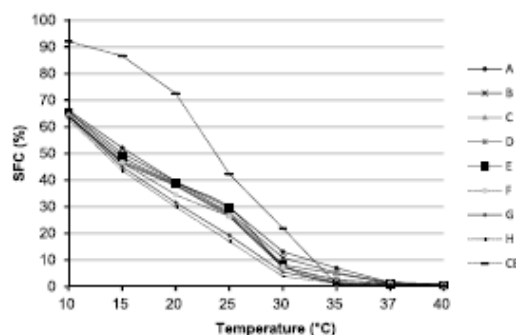


Fig. 2 Solid fat content of ternary mixtures (A–H) of PMF/RBDPKO/RBDPS

demonstrated two broad endothermic peaks, with T_1 ranging from 17.1–19.7 °C and T_2 ranging from 36.7–37.5 °C. Only small differences in melting temperatures were observed among all the eight blends. These differences are most likely caused by the variation in fatty acid constituents (Table 2) and TAG contents in PMF, RBDPKO and RBDPS (Table 3). When the RBDPS was reduced in mixtures A–H, the first broad endothermic peak (T_1) slowly increased towards a temperature of 19.7 °C and the second peak (T_2) decreased to 36.7 °C. For instance, blend A with 44.4% RBDPS showed its first broad endotherm (T_1) at 17.1 °C and second endotherm (T_2) at 37.5 °C, whereas

the first endotherm (T_1) was observed at 19.7 °C and the second endotherm (T_2) was observed at 36.7 °C for mixture H with 11.4% RBDPS. This observation is consistent with a previous report by Jahurul *et al.* [25], who successfully produced high melting profiles of CB replacers by blending supercritical carbon dioxide-extracted mango seed fat with palm stearin. The authors reported the melting profiles of mango seed fat/palm stearin blends that resemble CB with two endotherms at 17.6 and 36.9 °C. Sonwai *et al.* also produced CBE by blending mango kernel fat and PMF, and reported two maxima at 22.8 and 36.5 °C [9]. In the current study, blend E of 14.9/59.6/25.5 PMF/RBDPKO/RBDPS

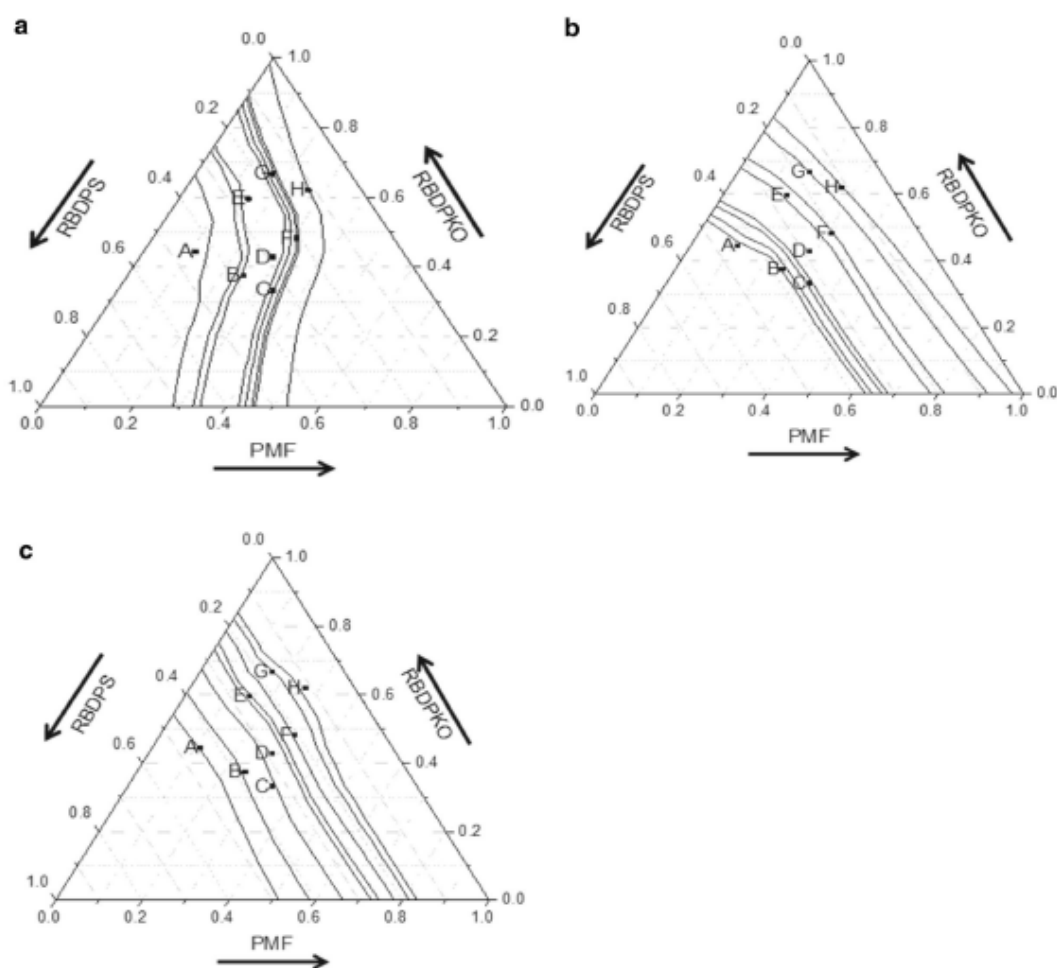


Fig. 3 Ternary iso-solid phase diagrams for PMF/RBDPKO/RBDPS mixtures at **a** 10 °C, **b** 20 °C, and **c** 25 °C. The *straight lines* represent a monotectic effect and *curves* represent a eutectic effect

contains 25.74% palmitic, 24.51% oleic and 3.95% linoleic acids (Table 2). The melting profile of blend E spanning from 18.5 to 37 °C (Fig. 1) is reasonably different from commercial CB, leading to its potential use as a CBS in confectionery fillings [5, 29].

Solid Fat Content (SFC)

The SFC profiles of the investigated fat samples are shown in Fig. 2. CB showed a high SFC ($\geq 70\%$) up to 20 °C, followed by a steep decline between 25 and 35 °C and 0% SFC was detected at or above 37 °C (Fig. 2). This finding is in agreement with previous studies by Kadivar *et al.* [30], who reported there was more than 75% SFC up to 20 °C, followed by a steep decrease between 25 and 35 °C and no solids above the body temperature. It was observed from Fig. 2 that the SFC of all the eight ternary mixtures decreased gradually with increasing temperature. The SFC of the ternary mixtures showed a maximum decline at temperatures ranging from 15 to 25 °C. This behavior was likely caused by the decreased proportion of unsaturated fatty acids (Table 2) and SUS TAGs (Table 3), which melted over this temperature range. The SFCs for mixtures A–E were found to be different from those of mixtures F to H (Fig. 2). In the present study, blend E showed approximately 40% SFC at 20 °C and 30% SFC at 25 °C which are comparatively lower than that of CB (Fig. 2). This was close to a report by Timms [31] who suggested that confectionery fat (e.g., chocolate) should exhibit approximately 63% SFC at 20 °C, 40% SFC at 25 °C and 0% SFC at 37 °C. In another study of Talbot [5], fat with less than 50% SFC at 20 °C is suitable as confectionery fillings. In this regard, blend E could potentially be used as a CBS in confectionery fillings.

Iso-Solid Diagrams of Ternary Blends

Ternary iso-solid phase diagrams of PMF/RBDPKO/RBDPS mixtures at 10, 20 and 25 °C are shown in Fig. 3. The ternary blends showed slightly curvatures at 10 °C, which indicated the eutectic effect (Fig. 3a). This behavior could be caused by the differences in SSS TAGs and SFC at low temperature among PMF, RBDPKO and RBDPS (Fig. 2). As the temperature increased from 10 to 25 °C, the eutectic effect gradually shifted to a monotectic effect. The contour lines of all the 8 mixtures were nearly straight at 25 °C (Fig. 3c), indicating the fats are compatible. In the case of blend E (14.9/59.6/25.5 PMF/RBDPKO/RBDPS), approximately 30% of SFC was observed at 25 °C (Fig. 2), which is within the monotectic area of the iso-solid diagram (Fig. 3c).

Polymorphism

The polymorphic structures of individual PMF, RBDPKO, RBDPS, their ternary mixtures (A–H) and commercial CB were identified by XRD at 24 °C (Fig. 4). CB showed multiple diffraction peaks at $d = 3.8$ – 4.3 and 4.5 Å, indicating a mixture of β' and β polymorphs. Two diffraction peaks at $d = 3.8$ and 4.3 Å indicate the β' forms were observed for individual PMF. Similar XRD patterns were found for RBDPS with a major diffraction peak near 4.5 Å, representing the β form. RBDPKO exhibited mainly three diffraction peaks at $d = 3.8$, 4.1 and 4.3 Å which are characterized by the β' forms. These findings are in agreement with previous studies [4, 11, 31, 32].

Sato [33] reported that fat with high levels of PPP and SSS TAGs was responsible for β forms and POP/POST were responsible for β' forms. RBDPS had a high percentage of PPP while PMF was rich in POP (Table 3), so RBDPS tends to have β crystals whereas PMF tends to have β' crystals. Timms [31] stated that palm kernel oil tends to crystalize in the stable β' form due to the presence of a high percentage of LaLaLa TAG. In the present study, it was observed that with decreasing the concentration of RBDPS in the blends A–H resulted in disappearance of the major diffraction peak at $d = 4.5$ Å (β formation; Fig. 4). This could be explained by the decreased proportion of PPP in RBDPS (Table 3). Blends A to E exhibited diffraction peaks at $d = 3.8$, 4.2 and 4.3 Å with a major peak at $d = 4.5$ Å, representing combinations of β' and β polymorphs. For blends F–H, peaks at $d = 3.8$ – 4.3 Å (only β' formation) were observed. Vereecken *et al.* [19] reported that the β' form is desired for confectionery fillings because it melts at low temperature with a fine arrangement, whilst the β form gives hardness as well as rough and

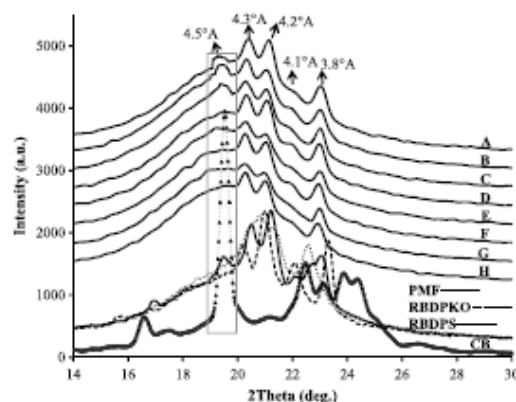


Fig. 4 X-ray diffractograms of PMF, RBDPKO, RBDPS, their blends and commercial CB at 24 °C

sandy textures. Blend E with 14.9/59.6/25.5 PMF/RBDPKO/RBDPS showed comparable fatty acid composition to CB, but its melting profile (18.5–37 °C) and 30% SFC at 25 °C with polymorphism are different from CB, making it potentially useful as a CBS in confectionery fillings.

Crystal Morphology

The crystal morphologies of individual PMF, RBDPKO, RBDPS, their ternary blend and CB were observed using PLM at 24 °C (Fig. 5). Commercial CB displayed

spherulitic crystals (10–100 μm in diameter) consisting of needle-like crystals branching outward from the central nuclei (Fig. 5a). The microstructure of individual PMF showed continuous granular crystals in the shape of very small spherulites (10–50 μm in diameter) with an orderly packed structure (Fig. 5b). Similar granular crystals (densely packed) were observed for RBDPS with a size of less than 20 μm in diameter (Fig. 5d). Large spherulitic crystals (100–300 μm in diameter) with a tight nucleus were observed in RBDPKO (Fig. 5c). The morphology of RBDPKO was found to be consistent with

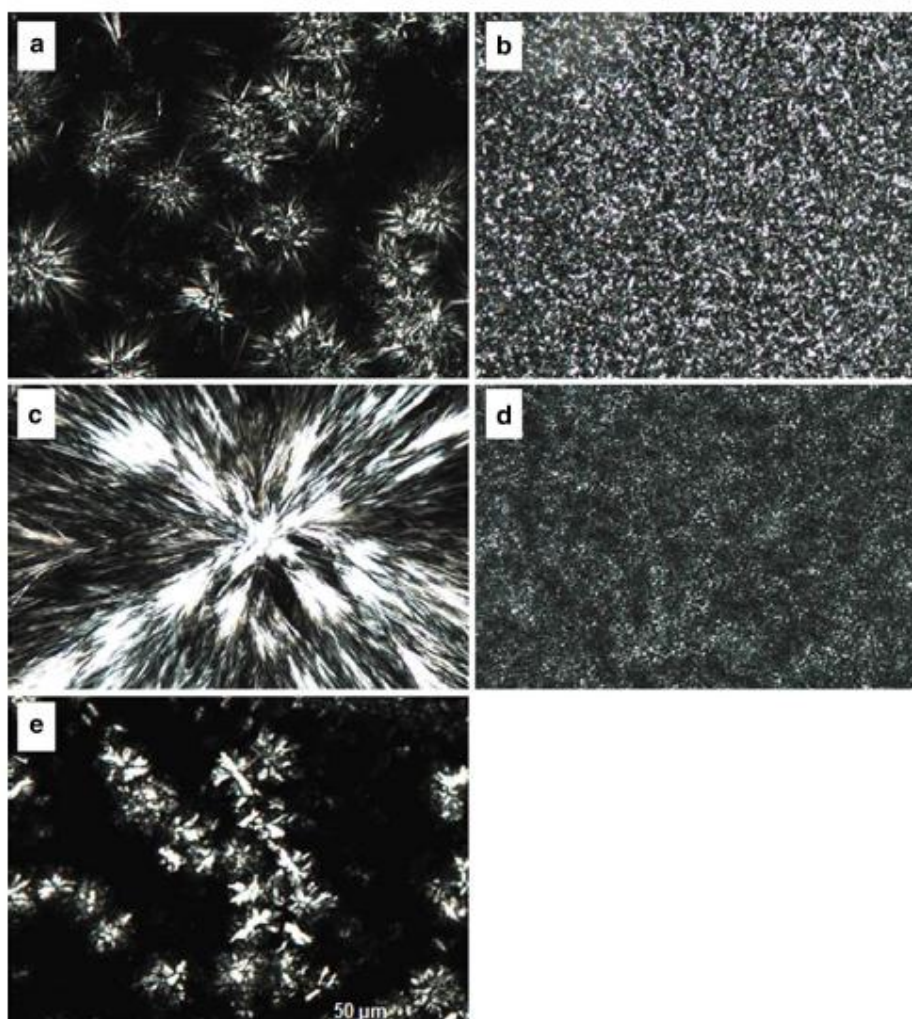


Fig. 5 Polarised light microphotographs ($\times 40$ lens) of **a** individual CB, **b** PMF, **c** RBDPKO, **d** RBDPS and **e** ternary blend of PMF/RBDPKO/RBDPS (14.9/59.6/25.5, %w/w) obtained at 24 °C

that observed by Schmelzer *et al.* [34], who reported large spherulitic crystals.

The crystal network morphologies of all ternary blends were found to be a mixture of tightly packed spherulites and granular structures. With the addition of RBD-PKO in the formulations, the spherulitic granular crystals shifted to large needle-like crystals. This variation could be related to the differences in the fatty acid composition (Table 2) and TAG species (Table 3). Another possible reason for the differences in crystalline structure (size and shape) could be the differences in textural properties among PMF, RBDPKO and RBDPS [35]. A blend of 14.9/59.6/25.5 PMF/RBDPKO/RBDPS showed small spherulites ($\geq 50 \mu\text{m}$ in diameter) consisting of needle-like crystals radiating and branching outward from the central nuclei (Fig. 5e). This behavior was explained by Jahurul *et al.* who reported spherulites exhibiting needle-like structures when blending mango seed fat and PMF [36]. No drastic change in microstructure in terms of size and shape was observed between CB and the 14.9/59.6/25.5 PMF/RBDPKO/RBDPS blend. However, CB still had densely and orderly packed crystals compared to the ternary blend (Fig. 5).

Conclusion

The crystal morphology, palmitic acid and oleic acid with POP content of blend E (14.9/59.6/25.5 PMF/RBDPKO/RBDPS) closely approximated those of CB, although its melting profile and polymorphism are different from CB. In addition, blend E showed a monotectic behavior at 20–25 °C with less than 50% SFC at 20 °C, making it suitable to be used as a CBS in confectionery fillings.

Acknowledgements The authors would like to thank the School of Science for supporting the current study and are grateful for grant number FRGS/1/2013/SG01/MUSM/03/2. The authors are also grateful for the SFC determinations conducted by the Malaysia Palm Oil Board, and Mr. Nasrun from the School of Engineering for XRD technical support.

References

- Gunstone F (2011) Vegetable oils in food technology: composition, properties and uses. Wiley, CRC Press, pp 291–343
- Bootello MA, Hartel RW, Garcés R, Martínez-Force E, Salas JJ (2012) Evaluation of high oleic-high stearic sunflower hard stearins for cocoa butter equivalent formulation. *Food Chem* 134(3):1409–1417
- Afoakwa EO (2010) Chocolate production and consumption patterns. In: Afoakwa EO (ed) *Chocolate science and technology*. Wiley & Blackwell, West Sussex, pp 1–10
- D'Souza V (1990) Short spacings and polymorphic forms of natural and commercial solid fats: a review. *J Am Oil Chem Soc* 67(11):835–843
- Talbot G (2009) Fats for confectionery coatings and fillings. In: *Science and technology of enrobed and filled chocolate, confectionery and bakery products*. Woodhead Publishing, Cambridge, UK, pp 53–79
- Wang F, Liu Y, Jin Q, Meng Z, Wang X (2011) Characterization of cocoa butter substitutes, milk fat and cocoa butter mixtures. *Eur J Lipid Sci Technol* 113(9):1145–1151
- Sabariah S, Ali AM, Chong C (1998) Chemical and physical characteristics of cocoa butter substitutes, milk fat and Malaysian cocoa butter blends. *J Am Oil Chem Soc* 75(8):905–910
- Lippe M, Anklam E (1998) Review of cocoa butter and alternative fats for use in chocolate—part A. *Compos Data Food Chem* 62(1):73–97
- Talbot G (2006) *Application of Fats in Confectionery*. Kennedy's Publications, Loughton, UK, pp 125–137
- Calliauw G, Foubert I, De Greyt W, Dijkmans P, Kellens M, Dewettinck K (2005) Production of cocoa butter substitutes via two-stage static fractionation of palm kernel oil. *J Am Oil Chem Soc* 82:783–789
- Sonwai S, Kaphueakngam P, Flood A (2014) Blending of mango kernel fat and palm oil mid-fraction to obtain cocoa butter equivalent. *J Food Sci Technol* 51(10):2357–2369
- Soares FASDM, da Silva RC, da Silva KCG, Lourenço MB, Soares DF, Gioielli LA (2009) Effects of chemical interesterification on physicochemical properties of blends of palm stearin and palm olein. *Food Res Int* 42(9):1287–1294
- Williams SD, Ransom-Painter KL, Hartel RW (1997) Mixtures of palm kernel oil with cocoa butter and milk fat in compound coatings. *J Am Oil Chem Soc* 74(4):357–366
- Kellens M, Gibon V, Hendrix M, De Greyt W (2007) Palm oil fractionation. *Eur J of Lipid Sci Technol* 109(4):336–349
- Lonchamp P, Hartel RW (2004) Fat bloom in chocolate and compound coatings. *Eur J Lipid Sci Technol* 106(4):241–274
- Kummerow FA (2009) The negative effects of hydrogenated trans fats and what to do about them. *Atherosclerosis* 205:458–465
- Wang F, Liu Y, Shan L, Jin Q, Wang X, Li L (2010) Blooming in cocoa butter substitutes based compound chocolate: investigations on composition, morphology and melting behavior. *J Am Oil Chem Soc* 87(10):1137–1143
- Pease JJ (1985) Confectionery fats from palm oil and lauric oil. *J Am Oil Chem Soc* 62(2):426–430
- Vereecken J, Foubert I, Smith KW, Dewettinck K (2007) Relationship between crystallization behavior, microstructure, and macroscopic properties in trans-containing and trans-free filling fats and fillings. *J Agric Food Chemistry* 55(19):7793–7801
- Timms R (1984) Phase behaviour of fats and their mixtures. *Prog Lipid Res* 23(1):1–38
- Biswas N, Cheow Y, Tan C, Siow L (2016) Blending of palm mid-fraction. *J Am Oil Chem Soc* 93:1415–1427
- Saberi AH, Lai O-M, Toro-Vázquez JF (2011) Crystallization kinetics of palm oil in blends with palm-based diacylglycerol. *Food Res Int* 44(1):425–435
- Osborn H, Akoh C (2002) Enzymatically modified beef tallow as a substitute for cocoa butter. *J Food Sci* 67:2480–2485
- NorAini I, Embong M, Aminah A, Maimon C (1995) Physical characteristics of shortenings based on modified palm oil, milk-fat and low melting milkfat fraction. *Lipid/Fett* 97:253–260
- Jahurul M, Zaidul I, Norulaini NN, Sabena F, Abedin M, Mohamed A, Omar AM (2014) Hard cocoa butter replacers from mango seed fat and palm stearin. *Food Chem* 154:323–329
- Narine SS, Marangoni AG (1999) The difference between cocoa butter and Salatrim® lies in the microstructure of the fat crystal network. *J Am Oil Chem Soc* 76(1):7–13
- Zaidul I, Norulaini NN, Omar AM, Smith R (2007) Blending of supercritical carbon dioxide (SC-CO₂) extracted palm kernel oil

- fractions and palm oil to obtain cocoa butter replacers. *J Food Eng* 78(4):1397–1409
28. Tan C, Man YC (2002) Differential scanning calorimetric analysis of palm oil, palm oil based products and coconut oil: effects of scanning rate variation. *Food Chem* 76(1):89–102
 29. Rodríguez A, Castro E, Salinas MC, López R, Miranda M (2001) Interesterification of tallow and sunflower oil. *J Am Oil Chem Soc* 78(4):431–436
 30. Kadivar S, De Clercq N, Mokbul M, Dewettinck K (2016) Influence of enzymatically produced sunflower oil based cocoa butter equivalents on the phase behavior of cocoa butter and quality of dark chocolate. *LWT-Food Sci Technol* 66:48–55
 31. Timms RE (2003) Production and characteristic properties. In: Timms RE (ed) *Confectionery fats handbook: properties, production and application*. The Oily Press, Bridwater, pp 191–254
 32. Zhou SL, Zhang FQ, Jin QZ, Liu YF, Shan L, Zhang T, Zou XQ, Wang XG (2010) Characterization of palm kernel oil, palm stearin, and palm olein blends in isosolid diagrams. *Eur J Lipid Sci Technol* 112(9):1041–1047
 33. Sato K (2001) Molecular aspects in fat polymorphism. AOCS Press, Champaign, pp 1–15
 34. Schmelzer JM, Hartel R (2001) Interactions of milk fat and milk fat fractions with confectionery fats. *J Dairy Sci* 84(2):332–344
 35. Çiftçi ON, Fadiloğlu S, Goğuş F (2009) Conversion of olive pomace oil to cocoa butter-like fat in a packed-bed enzyme reactor. *Biores Technol* 100(1):324–329
 36. Jahurul M, Zaidul I, Norulaini N, Sahena F, Abedin M, Ghaffoor K, Omar AM (2014) Characterization of crystallization and melting profiles of blends of mango seed fat and palm oil mid-fraction as cocoa butter replacers using differential scanning calorimetry and pulse nuclear magnetic resonance. *Food Res Int* 55:103–109

Appendix J (Chapter 5) Publications during enrolment

LWT - Food Science and Technology 82 (2017) 420–428



Contents lists available at ScienceDirect

LWT - Food Science and Technology

journal homepage: www.elsevier.com/locate/lwt

Physical, rheological and sensorial properties, and bloom formation of dark chocolate made with cocoa butter substitute (CBS)

Nirupam Biswas^a, Yuen Lin Cheow^a, Chin Ping Tan^b, Lee Fong Siow^{a,*}^a School of Science, Monash University Malaysia, 47500 Bandar Sunway, Selangor D.E., Malaysia^b Department of Food Technology, Faculty of Food Science and Technology, Universiti Putra Malaysia, 43400 UPM Serdang, Selangor D.E., Malaysia

ARTICLE INFO

Article history:

Received 2 March 2017

Received in revised form

13 April 2017

Accepted 15 April 2017

Available online 18 April 2017

Keywords:

Dark chocolate

Fat bloom

Polarized light microscopy

Melting

Polymorphism

ABSTRACT

This study examined the physical properties of enzymatically produced palm oil-based cocoa butter substitute (CBS) in dark chocolate. Melting profile, particle size distribution (PSD), rheological, textural behaviors, bloom formation and polymorphism were analysed using differential scanning calorimetry (DSC), master-size/polarized light microscopy (PLM), rheometer, stereomicroscope and x-ray diffraction (XRD), respectively. Dark chocolates were produced with cocoa butter (CB, without CBS), 5 g CBS (formulation-1) and 20 g CBS/100 g blend (formulation-2). Both chocolates with addition of CBS showed maximum melting temperature similar to CB-chocolate. However, the peak area and melting enthalpy for formulation-2 were significantly ($P < 0.05$) different from CB-chocolate. Significant differences ($P < 0.05$) in PSD, flow behavior, hardness and sensory characteristics were observed for formulation-2 whilst no significant difference ($P \geq 0.05$) was observed for formulation-1. Stereomicroscope images of all the chocolate samples did not show bloom at 24 °C for up to 8 weeks. Conversely, at 29 ± 1 °C, bloom formation was only observed for CB-chocolate and formulation-1 after two weeks of storage. Noticeable changes in XRD peaks were observed for bloomed chocolate. Overall, chocolate with formulation-1 was similar to CB-chocolate in terms of physical and sensory properties. However, chocolate with formulation-2 exhibited significantly lower sensory profiles particularly taste acceptance and hardness compared to CB-chocolate.

© 2017 Elsevier Ltd. All rights reserved.

1. Introduction

Enzymatic interesterification of fats and oils for the formulation of cocoa butter substitute (CBS) has been receiving a lot of attention. Triacylglycerol (TAG) composition of fats and oils is modified to change the physical properties particularly melting profile similar to cocoa butter (CB) for using in confectionery applications (Asghar, Pasha, Murtaza, & Ali, 2017; Sridhar, Lakshminarayana, & Kaimal, 1991). Chemical modification in the production of these types of TAGs is generally not applicable because of deficiency in positional specificity (Kadivar, De Clercq, Mokbul, & Dewettinck, 2016; Xu, 2000).

CB, the main ingredient of chocolate, is expensive among all the vegetable fats/oils due to its limited supply and high market demand. Hence, researchers are looking for alternatives to CB. CBS is an alternative to CB and have a similar melting profile to that of

cocoa butter, but with different chemical composition (Biswas, Cheow, Tan, & Siow, 2016; Calliauw et al., 2005; Garti & Widlak, 2015; Talbot, 2006). In the literature, modification of kokum fat, mango fat, sal fat with methyl palmitate-stearate (Sridhar et al., 1991); and palm oil with soybean oil (Abigor et al., 2003) using enzymatic interesterification has been studied in producing CBS. Reports on production of CBS from cheap and available palm oils fraction are not available. In our preliminary study (Biswas, Cheow, Tan, Kanagaratnam, & Siow, 2017), palm mid-fraction was mixed with refined, bleached and deodorized palm kernel oil and palm stearin to produce CBS and the results showed several melting temperatures instead of a single melting peak between 30 and 35 °C as shown by CB. Melting is the main characteristic that is used for the evaluation of an enzymatically modified CB-like fats (Çiftçi, Fadiloğlu, & Göğüş, 2009). Therefore, enzymatic interesterification was used to modify CBS to show similar melting characteristic and triacylglycerol composition as per CB in our earlier phase of this study (unpublished data). Subsequently, 5–50 g of CBS/100 g blend were mixed with CB in order to investigate the compatibility of CBS/CB mixture; in which 5–20 g CBS/100 g blend was found to be

* Corresponding author.

E-mail address: siow.lee.fong@monash.edu (L.F. Siow).

compatible with CB in terms of solid fat content as a function of temperature and polymorphism.

European Union Directive 2000/36/EC and Food Standards Agency 2003 limit the use of vegetable fats in chocolates to 5 g/100 g blend. The non-EU countries have their own regulations. For example, the United States does not allow the use of CB alternatives in chocolates, but permits its use as coatings on chocolate products. Generally, most countries permit more than 5 g CB alternatives/100 g blend in chocolates, but this is labelled as “compound chocolate” (Beckett, 2011; De Clercq et al., 2016; Kadivar, De Clercq, Van de Walle, & Dewettinck, 2014).

In the present study, dark chocolate is used as model chocolate, which is made up of CB along with sugar, ground cocoa solids and soy lecithin (Asghar et al., 2017; Zarringhalami, Sahari, Barzegar, & Hamidi-Esfahani, 2010). However, milk chocolate has not been considered in this study to avoid any overlapping melting or other interaction between CBS and milk fat (i.e., milk fat may interfere on the physical properties of CBS). The important ingredient of CB and its crystal structure is responsible for the rheological properties, appropriate texture and sensory perception of chocolate (Aidoo, Afoakwa, & Dewettinck, 2015; Loisel, Lecq, Keller, & Ollivon, 1998; Timms, 2003). The rheological properties of the chocolate depend on many factors such as temperature, composition and processing conditions. During dark chocolate processing, composition and crystallization of CB play an important role in obtaining good quality product. The chocolate composition determines different interactions that occur between ingredients whilst crystallization is the most important step in chocolate processing i.e. refining, conching and tempering (Glicerina, Balestra, Dalla Rosa, & Romani, 2013; Servais, Ranc, & Roberts, 2003) to ensure the desired sensory characteristics.

The melting characteristic of dark chocolate is very important in order to evaluate the effects of CB polymorphism. CB has complex polymorphs namely γ , α , β' and β (or Roman numbering, I–VI) in ascending stability (Marangoni & McGauley, 2003; Rousseau & Smith, 2008). Polymorphic transitions of CB take place via either a solid-state transition or by melt-mediation. During the manufacturing process, tempering is usually conducted at set temperature and time regime to get the desirable $\beta(V)$ crystal form with melting temperature of 32–34 °C which is preferred in chocolate to impart the desired good snap, glossy appearance and sensory mouth-feel (Talbot, 2009). However, poorly tempered chocolate can develop a sticky greyish-white surface namely fat bloom upon storage. Bloom formation may also arise due to slight (i.e., ± 2 –3 °C) or larger temperature variations which cause the melting and re-crystallisation of TAG in CB, where the liquid fat from the chocolate matrix migrates through pores and microfractures to the surface forming bloom (Rousseau & Smith, 2008).

Since the melting, rheological, textural and polymorphism are the main properties used for the quality assurance of chocolate, it is important to understand how the enzymatically produced palm oil-based CBS influences the physical properties of CB. Therefore, the objective of the present work was to investigate the melting, rheological, textural properties, bloom formation and sensory profile of dark chocolate made with enzymatically produced CBS.

2. Materials and methods

2.1. Materials

Cocoa powder (10–12 g fat/100 g, pH 6.8–7.2, moisture 5 g/100 g, Guan Chong Cocoa Sdn. Bhd), icing sugar (MSM Prai Sdn. Bhd.), Cocoa butter (Le Bourne Sdn. Bhd.), Soy lecithin (moisture 0.19 g/100 g, Cargill, Shanghai, China) were employed. Palm mid-fraction, refined bleached deodorized palm kernel oil and palm

stearin were obtained from Sime-Darby Research Sdn. Bhd. In our preliminary study (Biswas et al., 2017), the major palmitic, oleic acids and POP composition of the mixture of palm mid-fraction/refined bleached deodorized palm kernel oil/palm stearin closely approximated those of CB, although its melting profile was different from CB. Subsequently, CBS with desirable melting profile and comparable fatty acids/TAGs composition as per CB was produced from palm mid-fraction/refined bleached deodorized palm kernel oil/palm stearin mixture added with commercial stearic-oleic acid through enzymatic interesterification (unpublished data) and was used in the current study. TAG standards were obtained from Sigma Aldrich (St. Louis, MO). All other reagents and solvents were of analytical or HPLC grade.

2.2. Chocolate production

Production of standard dark chocolates was performed using the method described by Kadivar et al (Kadivar et al., 2016), with minor modification at Cocoa processing lab, Malaysian Cocoa Board, Nilai. Formulation of standard dark chocolate was according to the following composition (w/w): 48 g icing sugar/100 g blend, 30.90 g CB/100 g blend, 20.5 g cocoa powder/100 g blend and 0.6 g soy lecithin/100 g blend. For two different chocolate formulations, CBS was added at the levels of 5 g and 20 g in 100 g CB (1.5 g and 6.2 g of CBS were replaced from 30.90 g of CB). Experimental samples (1 kg batch for each formulation) were prepared by mixing sugar, cocoa powder and 2/3 of melted CBS + CB fat in a mortar and pestle mill (Pascal, UK) at low speed for 10 min at 45 °C. Then the mixture was refined using a 3-roll refiner (Pascal, UK) at ambient temperature to get a particle size <35 μ m. After refining, the mixture was transferred to the conche (Mortar and Pestle mill, Pascal, UK) and then mixed with the rest of the melted CBS + CB fat at 45 °C for 4 h. In the following phase, the mixture became a paste as the viscosity reduced. To obtain the desired flow characteristics, soy lecithin was added and mixed for another 2 h.

In the next step, the liquid chocolate was tempered manually according to the method described by Talbot (Talbot, 1994). Tempering was performed to produce the desired β crystals in the chocolate products. Tempering was carried out as follows: i) chocolate was melted at 45 °C to remove crystal history, ii) approximately 2/3 of the chocolate mixture was poured onto a marble slab and mixed with a flexible spatula until the product reached 27 °C to produce seed crystals and iii) the thickened chocolate was then mixed with the remaining 1/3 warm chocolate (40 °C) to get the overall temperature of 31–32 °C, in order to melt the unstable crystal polymorphs (Bricknell & Hartel, 1998; Briggs & Wang, 2004; Talbot, 1994). Temperature was measured using an Aasted-Mikroverk Chocometer (Aasted-Mikroverk ApS, Farum, Denmark) to ensure accurate tempering temperature for chocolate. The tempered chocolate was poured into plastic chocolate molds (dimensions bar, 98 mm \times 30 mm \times 11 mm) and cooled at 13 ± 1 °C for 60 min to solidify the chocolate (De Clercq et al., 2012). The chocolate bars were de-moulded and subsequently stored at room temperature.

2.3. Triacylglycerol (TAG) analysis

The TAG profiles of individual CB and enzymatically produced CBS were analysed using high performance liquid chromatography (Agilent HPLC series 1260, Santa Clara, USA) equipped with Column ZORBAX C-18 (4.6 \times 250 mm, 5 μ m, Agilent Technologies, Santa Clara, USA) according to AOCs Official Method Ce 5b-89 as discussed in our previous study (Biswas et al., 2016).

2.4. Melting profile

Melting profile of the dark chocolates was determined using differential scanning calorimetry (DSC Pyris 4000 DSC, Perkin-Elmer Ltd., Norwalk, USA) equipped with nitrogen gas flow rate of 20 ml/min, following the method of Kadivar et al. (2016). Surface of the chocolate was scraped off with a scalpel and 2–4 mg of the chocolate slivers was hermetically sealed in an aluminum pan. An empty, covered aluminum pan was used as the reference. When the system reached the equilibrium conditions at 20 °C, the pan was put in the DSC cell and the melting thermograms were recorded by heating from 20 to 65 °C at 5 °C/min. Onset temperature (T_{onset}), endset temperature (T_{end}), maximum peak temperature (T_{max}), melting enthalpy (ΔH) and peak area were calculated from the melting thermogram using DSC software. T_{onset} is the temperature at which the corresponding crystal form starts to melt; T_{end} represents the temperature at which liquefaction of the sample is completed; ΔH_{melt} is the amount of energy required for complete melting of the sample; T_{max} is the temperature at which maximum melting occurs; and peak area is equivalent to the heat taken up by the sample during melting (Afoakwa, Paterson, Fowler, & Vieira, 2008a; De Clercq et al., 2014).

2.5. Polarised light microscopy (PLM)

To measure the micrographs in terms of fat particle size of the chocolates, a polarized light microscope (PLM, Olympus BX51, Tokyo, Japan) fitted with a digital camera (Nikon, DS-Filc, Tokyo, Japan) was used at room temperature. Approximately 10 µg of the melted chocolate was then placed on a glass microscope slide. A coverslip was placed on top of the sample and centred on the melted sample to ensure uniform thickness. PLM images were captured using 20 × objective lens after the slides were kept at room temperature for 4 h to solidify the particles.

2.6. Particle size distribution (PSD)

To measure the PSD of the chocolates, a MasterSizer 3000 (Laser Diffraction Particle Size Analyser, Malvern Instruments Ltd., Malvern, Worcestershire, UK) equipped with a Hydro EV was used. Approximately 0.5 g of chocolate slivers was mixed with 10 ml of isopropanol. The sample (~0.2 ml) was dispersed in isopropanol until an obscuration of 10.5% as recommended by the instrument software. The sample was sonicated for 2 min to ensure particles were independently dispersed and thereafter maintained by stirring during the measurement. PSD was determined based on the Mie-Theory using the refractive index 1.59 for dark chocolate (Afoakwa, Paterson, Fowler, & Vieira, 2008b). Results were provided as a relative volume (%) of particles in size compared with particle size curves (Malvern MasterSizer Micro Software). PSD parameter was obtained at the largest particle size D_{90} (>90% finer) (Beckett, 2008).

2.7. Flow behavior

In order to examine flow behavior of the chocolates, a Rheometer RS600 (HAAKE RheoStress 600, Thermo Electron Corp., Karlsruhe, Germany) fitted with a plate-plate geometry was used. Chocolate samples were melted at 50 °C for 1 h and approximately 2 g of the samples was placed onto a preheated plate in a gap of 1 mm. The measurement procedure was based on the method of ICA. (2000) and Afoakwa, Paterson, and Fowler (2008) with minor modifications. Temperature of the bottom plate was set at 40 °C to prevent solidification of the fat crystals. A stepped flow procedure was applied by increasing the shear rate logarithmically from 2 s⁻¹

to 110 s⁻¹. Yield stress (Pa) and viscosity (Pa s) were measured at 65 s⁻¹ (Kadivar et al., 2016).

2.8. Texture analysis

Hardness (N, the maximum force required to penetrate the sample) of the chocolates was measured with a Texture Analyser (TA-XT plus, Stable Microsystems Ltd., Surrey, UK) equipped with 2 kg load cell and probe (P/2N needle stainless) using the following parameters: product height 10 mm, penetration depth 5 mm, pre-speed 1 mm/s, test speed 2 mm/s, post speed 10 mm/s and the duration of the test at ~ 1–2 min (Kadivar et al., 2016).

2.9. Bloom formation on chocolate surface

Bloom formation on chocolates, stored at 24 ± 1 °C and 29 ± 1 °C, was captured and examined every two weeks for a total of 3 months using a stereomicroscope (Nikon, SMZ1500, Tokyo, Japan) fitted with a digital Nikon camera (Nikon, Digital Sight DS-2Mv, Tokyo, Japan), according to previously described method (Kinta & Hartel, 2010).

2.10. Polymorphism

To identify the polymorphic transformations of chocolate, a D8 Discover X-ray Diffraction (Bruker, Karlsruhe, Germany) fitted with Cu-K α radiation (λ = 1.5418 Å, voltage 40 kV and current 40 mA) was used at room temperature. Surface of the chocolates was chopped with a scalpel. To eliminate the interference of sugar crystals, approximately 5 g of the chocolate slivers were mixed in 500 ml of cold water, shaken and allowed to stand at room temperature for 4 h to dissolve the sugar, according to the method of Cebula and Ziegler (1993). The suspension was filtered through a Buchner funnel with whatman filter paper (0.45 µm) under a vacuum pump to dry the samples. The sugar free chocolate samples were mounted onto the XRD sample holder. The samples were analysed at 2 θ angles of 10°–30° with a scan rate of 1.5°/min. Short (d) spacing (Å) was determined using the EVA-diffraction software (Bruker, Karlsruhe, Germany). Assignments of polymorphs were based on the following short spacing characteristics of CB: α form (d = 4.15 Å); β' forms (d = 3.8–4.3 Å) and β forms (d = 4.5/4.6 Å) (D'Souza, 1990). Unbloomed chocolate was used as a control.

2.11. Sensory evaluation

Sensory evaluation was performed using a 9-point hedonic scale (1 = dislike extremely, 9 = like extremely) where participants evaluated the sensory attributes i.e. glossiness, hardness, waxiness, greasy to touch (sticky), mouth-feel (smooth, melting), overall acceptability and taste acceptance of the dark chocolates. One hundred participants (students and staffs) from Monash University Malaysia were selected. Participants were asked to pick one sample which is different from the other two in a triangle test. Three formulations of dark chocolate (each weighing ~3 g) were served at 23 ± 1 °C in sealed plastic bags. Samples were coded using three digit random numbers. Participants were asked to take a small bite of biscuit and then drink water to rinse their palate after tasting each chocolate.

2.12. Statistical analysis

Data were statistically analysed by *t*-test and one-way analysis of variance using the SPSS software, version-20 (IBM Corp., Chicago, USA). Tukey's test was applied to determine the significant differences at P < 0.05 level. DSC, PSD, Rheometer, XRD, TA and PLM

analyses were conducted in triplicate.

3. Results and discussion

3.1. TAG composition

The TAG profiles of individual CB and enzymatically produced CBS are presented in Table 1. CB contained three main TAGs: POST (39.2 g/100 g), StOSt (29.7 g/100 g) and POP (18.1 g/100 g), which is in agreement with previous studies (Biswas et al., 2016; Bootello, Hartel, Garcés, Martínez-Force, & Salas, 2012). As shown in Table 1, enzymatically produced CBS had comparable POP, while significantly ($P < 0.05$) lower composition of POST and StOSt to CB. In addition, CBS contained additional tri-saturated TAGs (PPP, LaLaLa, PPSt and LaLaM) and di-unsaturated TAG (PLO) which appear only in traceable quantity in CB.

3.2. Melting behavior

Melting properties of different chocolate samples were shown in Fig. 1 and Table 2. Thermal parameters: T_{onset} , T_{end} , ΔH_{melt} , T_{max} and peak area of the melting endotherms of dark chocolate samples were compared.

In the present study, chocolate formulated with CB showed a sharp melting peak near 33 °C with T_{onset} (27.5 °C), T_{end} (35.5 °C), area (64.2 mJ) and ΔH_{melt} (34.1 J/g). These findings were consistent with the literature (De Clercq et al., 2016). The melting peak and T_{end} of the chocolate with 5 g CBS/100 g blend and 20 g CBS/100 g blend were similar to CB-chocolate (Fig. 1, Table 2). However, chocolate with 20 g CBS/100 g blend had significantly ($P < 0.05$) higher ΔH_{melt} and broader peak area with a small shoulder peak compared to the CB-chocolate. This is probably due to the lower melting TAGs specially LaLaLa and PPP (Table 1). Similar results were also reported in a previous research (Kadivar et al., 2016), where chocolate with 25 g CB-like fat/100 g blend showed a broader melting peak and lower T_{onset} . According to De Clercq et al. (2014), the melting profile of dark chocolate should have a narrow

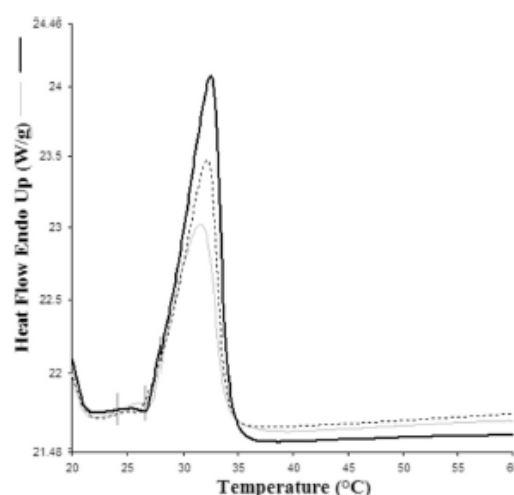


Fig. 1. DSC Melting thermograms of — CB-chocolate, - - - 5 g CBS/100 g chocolate blend and . . . 20 g CBS/100 g chocolate blend.

melting peak leading to a quick melt down at 37 °C (body temperature), producing a cool sensation and smooth mouth-feel. In the current study, there were no significant ($P \geq 0.05$) differences in ΔH_{melt} and peak area between 5 g CBS/100 g chocolate blend and CB-chocolate (Table 2), indicating 5 g CBS/100 g chocolate blend is comparable to CB-chocolate.

3.3. Particle size distribution (PSD) of the dark chocolates

Polarised light microscopy (PLM) was used to observe the

Table 1
Overview of TAGs composition of individual CB and enzymatically produced CBS.

TAG (area %) ^a		CB	CBS
SSS	PPP	0.1 ± 0.0a	8.4 ± 0.2b
	PPSt	0.5 ± 0.0a	2.4 ± 0.4b
	StPSt	—	1.2 ± 0.2
	LaLaLa	—	4.7 ± 0.3
	LaLaM	—	2.3 ± 0.1
	MMM	—	1.1 ± 0.2
	Total	0.6	20.1
SUS	POP	18.1 ± 0.8a	17.7 ± 1.6a
	POSt	39.2 ± 1.2a	28.4 ± 1.2b
	StOSt	29.7 ± 0.7a	19.5 ± 0.8b
	LaOLa	—	0.7 ± 0.2
	AOSt	1.9 ± 0.5a	0.6 ± 0.1b
	PLP	1.1 ± 0.0a	1.4 ± 0.3a
	MLP	0.6 ± 0.0a	1.4 ± 0.2b
SUU	Total	90.6	69.7
	PLL	0.5 ± 0.0a	0.8 ± 0.0a
	PLO	0.6 ± 0.2b	6.1 ± 0.7a
	POO	2.8 ± 0.4a	1.3 ± 0.2b
	StOO	2.4 ± 0.1a	1.3 ± 0.0b
	Total	6.3	9.5
UUU	LLO	0.4 ± 0.0a	0.1 ± 0.0a
	OOL	0.7 ± 0.1a	0.2 ± 0.0a
	OOO	1.4 ± 0.2a	0.4 ± 0.0b
	Total	2.5	0.7

Values within the same row with different letters are significantly different ($P < 0.05$). Each value in the table represents the mean ± SD of two measurements.

^a Abbreviations: Triacylglycerol (TAG), cocoa butter (CB), cocoa butter substitute (CBS), total content of tri-saturated (SSS), total content of mono-unsaturated (SUS), total content of di-unsaturated (SUU), total content of poly-unsaturated (UUU); P palmitic, St stearic, O oleic, La lauric, L linoleic, M myristic, A arachidic.

Table 2Overview of Melting profile of CB-chocolate, 5 g CBS/100 g chocolate blend and 20 g CBS/100 g chocolate blend.^a

Melting profile	CB-chocolate	5 g CBS/100 g chocolate blend	20 g CBS/100 g chocolate blend
T _{onset} (°C)	27.5 ± 0.2a	27.4 ± 0.6a	26.6 ± 0.3a
T _{midpoint} (°C)	35.4 ± 0.2a	35.5 ± 0.2a	35.2 ± 0.2a
T _{max} (°C)	33.2 ± 0.6a	33.2 ± 0.4a	33.1 ± 0.5a
ΔH _{melt} (J/g)	34.1 ± 0.4a	33.8 ± 0.6a	22.7 ± 0.6b
Peak area (mJ)	64.2 ± 0.6b	65.1 ± 0.6b	69.4 ± 0.6a

^a Values within the same row with different letters are significantly different ($P < 0.05$). Each value in the table represents the mean ± SD of three measurements.

variations in fat-particle phase, sugar crystalline network and cocoa particle interaction from the dark chocolates as shown in Fig. 2. All three samples showed similar micrographs under PLM (Fig. 2A–C). Sugar and fat crystals exhibited polarization (bright image), whereas cocoa solids (amorphous) did not show polarization, or appeared as dark. This finding was in accordance with the literature (Afoakwa, Paterson, Fowler, & Vieira, 2009b). In addition, non-fat particulates were visible in the chocolates, such as irregularly large-shaped sugar crystals (~25 μm, bright image) and brownish-red small cocoa particles.

In this study, master-sizer was used to confirm the PSD of the chocolate samples. Fig. 3 shows volume density of the selected samples against size distributions using D₉₀ (>90% finer). Chocolate produced with CB showed particle size approximately 18 μm, which is in agreement with the previous research (Afoakwa et al., 2008). Similar PSD was observed for chocolate made with 5 g CBS/100 g blend. However, chocolate made with 20 g CBS/100 g blend had a slightly higher PSD (~24 μm) than the CB-chocolate (Fig. 3). As stated by Beckett, PSD has a direct influence on rheological, textural and sensory characteristics. The largest particles are responsible for mouth-feel notably grittiness, whereas smaller particles improve flow properties and hardness (Beckett, 2011). For good dark chocolate, PSD should be less than 35 μm (Afoakwa et al., 2008). Overall, chocolate made with 5 g CBS/100 g blend and 20 g CBS/100 g blend was within the range of PSD of less than 35 μm.

3.4. Flow behavior

Dark chocolate is a solid suspension of sugar and cocoa powder in cocoa butter, which shows non-Newtonian flow behavior (De Clercq et al., 2016). The Casson model was fitted to the flow curves to study the Casson yield stress and viscosity. Yield stress is the amount of energy required to initiate chocolate flow. Plastic viscosity is related to the energy needed to maintain the flow of a fluid. High viscous chocolates are not desirable due to sticky mouth-feel (De Clercq et al., 2016).

Fig. 4 shows the Casson yield stress and viscosity as a function of shear rate between 2 and 65 s⁻¹ for the chocolate samples. When the shear rate gradually increased, the Casson plastic viscosity correspondingly decreased while yield stress increased. The viscosity and yield stress of the CB-chocolate were found

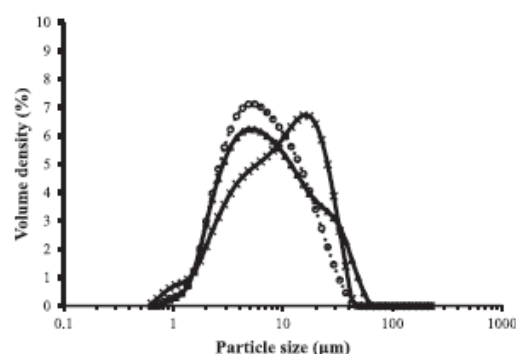


Fig. 3. Particle size distribution of CB-chocolate, — 5 g CBS/100 g chocolate blend and --- 20 g CBS/100 g chocolate blend at D₉₀ (>90% finer).

approximately 2 Pa s and 15 Pa, respectively, at shear rate 65 s⁻¹ (Fig. 4A&B). These results were in accordance with a previous study (Kadivar et al., 2016) for dark chocolate. Similar trend in plastic viscosity was also observed for the chocolate with 5 g CBS/100 g blend and 20 g CBS/100 g blend (Fig. 4). Likewise, chocolate with 5 g CBS/100 g blend showed similar yield stress to the CB-chocolate, whereas chocolate with 20 g CBS/100 g blend had slightly lower yield stress (12.2 Pa). This variation was likely due to the function of CB replaced by enzymatically produced CBS and the high PSD (24 μm) (Fig. 3). PSD and rheological parameters are highly linked as the higher PSD denotes lower surface area available to interact, which leads to higher viscosity and/or yield stress (Aidoo, Clercq, Afoakwa, & Dewettinck, 2014).

3.5. Textural behavior

As stated by Afoakwa (2016), a good quality chocolate is a solid product with a good snap at 24 °C (room temperature) and shiny appearance along with easy melting in the mouth, giving a pleasant mouth-feel sensation. Hardness of dark chocolate samples, expressed in maximum force (N), was measured by penetration test

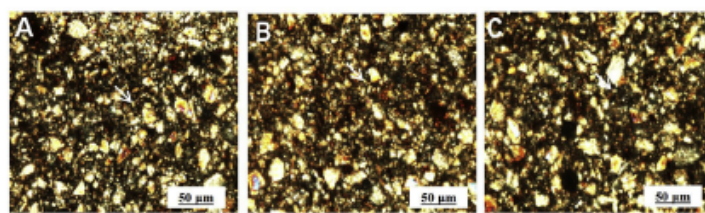


Fig. 2. PLM micrographs (20 × lens) of A) CB-chocolate, B) 5 g CBS/100 g chocolate blend and C) 20 g CBS/100 g chocolate blend at 24 °C.

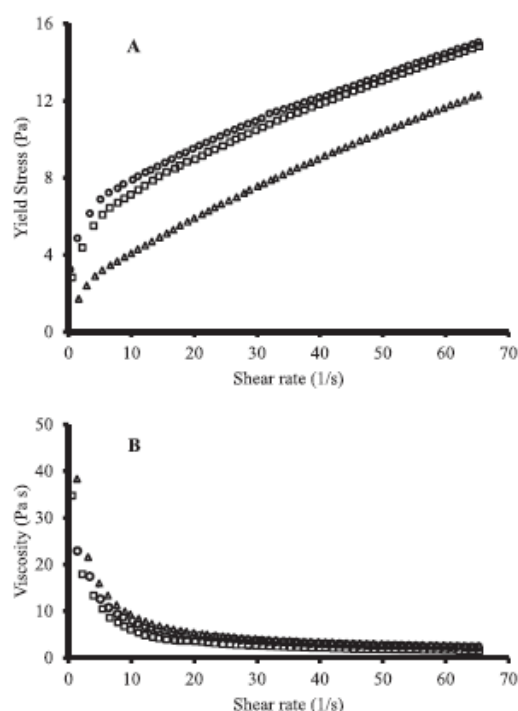


Fig. 4. A) Casson yield stress (Pa) and B) Casson viscosity (Pa s) of □ CB-chocolate, ○ 5 g CBS/100 g chocolate blend and △ 20 g CBS/100 g chocolate blend.

as shown in Fig. 5. Hardness of the CB-chocolate at 24 °C showed approximately 13 N, which is in agreement with previous studies (De Clercq et al., 2016; Kadivar et al., 2016). Similar hardness value was observed for 5 g CBS/100 g chocolate-blend (Fig. 5). However, there was significantly ($P < 0.05$) lower hardness of the chocolate with 20% CBS in comparison to the CB-chocolate and 5 g CBS/100 g chocolate-blend. This may be due to the broader melting

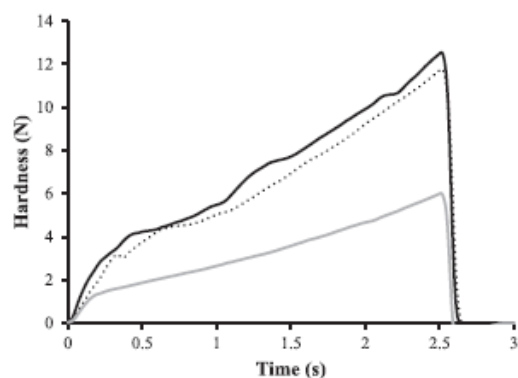


Fig. 5. Hardness of — CB-chocolate, ---- 5 g CBS/100 g chocolate blend and 20 g CBS/100 g chocolate blend at 24 °C.

temperature (Table 2) and high PSD (Fig. 3). The large particle size in the chocolate creates weak interaction between particles, resulting in a lower maximum force required to penetrate the product (Afoakwa, Paterson, Fowler, & Vieira, 2009a). Zarringhalami et al. (2010) also found no significant differences between a reference chocolate and the chocolates with 5 g and 10 g CB-like fat/100 g blend, but the chocolates with 15 g and 20 g CB-like fat/100 g blend had significantly lower hardness. In the current study, 5 g CBS/100 g chocolate-blend had a textural behavior in terms of hardness similar to that of CB-chocolate (Fig. 5).

3.6. Bloom formation and X-ray diffraction during storage

Fat bloom is a physical defect that involves the loss of gloss, smoothness and an undesirable discoloration on the chocolate surface which is the main concern for chocolate manufacturer. Bloom formation is determined by stereomicroscope and confirmed by X-ray diffraction of the chocolate samples during storage at 24 ± 1 °C and 29 ± 1 °C until 12 weeks as shown in Fig. 6.

Chocolate produced with CB, 5 g CBS/100 g blend and 20 g CBS/100 g blend at 24 ± 1 °C and stored up to 8 weeks did not show bloom, however after 8 weeks the CB-chocolate and 5 g CBS/100 g chocolate blend began to form white-greyish haze on the surface. At 29 ± 1 °C, noticeable bloom formation was observed for CB-chocolate and 5 g CBS/100 g chocolate blend after 2 weeks. This phenomenon can be explained by many factors such as fluctuation of temperature during storage time, recrystallization of fats and sugar crystal, and poor tempering (Hartel, 1999; Lonchampt & Hartel, 2006). However, no obvious bloom formation was observed for chocolate formulated with 20 g CBS/100 g blend at 24 ± 1 °C and 29 ± 1 °C until 12 weeks (Fig. 6). This may be likely due to the more complex crystalline structures that inhibit bloom (Lonchampt & Hartel, 2006; Osborn & Akoh, 2002; Zarringhalami et al., 2010). Another possible reason may be the presence of medium and high-melting TAG in CBS (Table 1). Due to fluctuation of temperature, phase behavior of the TAG becomes disrupted, leading to the formation of large surface crystals (Cebula & Ziegler, 1993; Couzens & Wille, 1997; Hodge & Rousseau, 2002). Beckett stated that the use of high-melting TAG in chocolate allows the melted chocolate to set again with temperature fluctuation. However, the medium-melting TAGs inhibit fat bloom if the storage temperature is higher than the melting temperature of those TAGs (Beckett, 2008). In summary, both chocolates with 5 g and 20 g CBS/100 g blend can be stored at 24 °C to prevent bloom formation.

XRD patterns of bloomed and control chocolates are presented in Fig. 7. Control chocolates showed a major diffraction peak at $d = 4.5$ Å, indicating β polymorphs and multiple peaks at $d = 3.7$ – 4.1 Å, corresponding to the characteristic of β' polymorphs. For bloomed chocolate with CB and 5 g CBS/100 g blend, the peak intensity at $d = 3.7$ and 4.0 Å increased slightly, whereas the 4.5 Å peak remained unchanged. This result was in agreement with the previous research (Sonwai & Rousseau, 2006) for bloomed chocolate, who reported that the peak intensity at $d = 3.6$ and 3.8 Å increased along with a reduced peak at $d = 3.9$ Å. Wang et al. (2010) also found the diffraction peaks at $d = 3.7$, 3.8 , 4.2 and 4.6 Å for bloomed CBS-chocolate while peaks at $d = 3.8$ and 4.2 Å for control CBS-chocolate. Likewise in the present study for the bloomed chocolates, the diffraction peak at $d = 4.1$ Å shifted toward larger d -spacing along with an increased peak height tending to the β polymorphism (Fig. 7A&B). However, the major diffraction peak at $d = 4.5$ Å with two peaks at 3.7 and 3.9 Å were observed for the control chocolate with 20 g CBS/100 g blend, indicating no change in the polymorphism transformation during storage at 24 ± 1 °C and 29 ± 1 °C (Fig. 7C). This finding was also confirmed by stereomicroscope (Fig. 6).

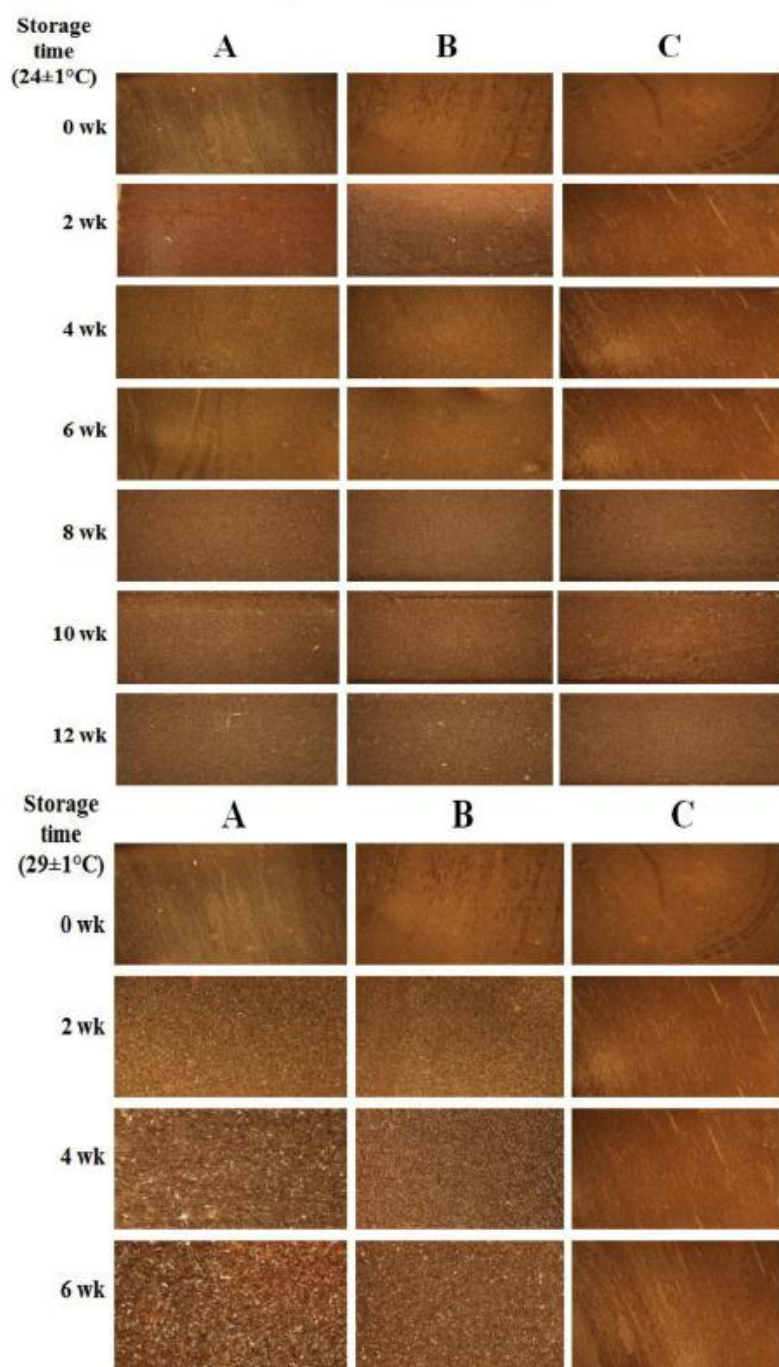


Fig. 6. Bloom formation of A) CB-chocolate, B) 5 g CBS/100 g chocolate blend and C) 20 g CBS/100 g chocolate blend stored at $24 \pm 1^\circ\text{C}$ and $29 \pm 1^\circ\text{C}$.

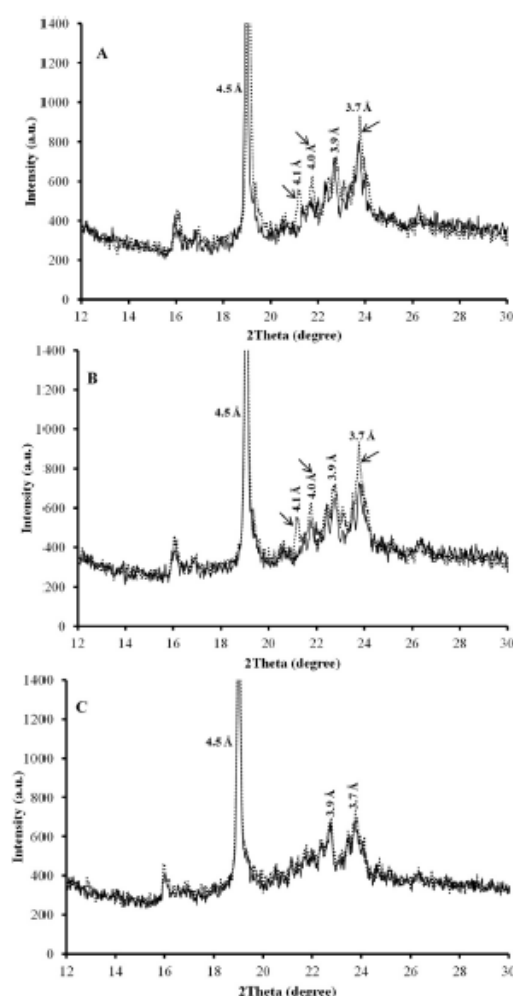


Fig. 7. X-ray diffraction spectrum of A — CB-chocolate and bloomed-chocolate, B — 5 g CBS/100 g chocolate blend and bloomed-chocolate and C — 20 g CBS/100 g chocolate blend and bloomed-chocolate.

3.7. Sensory evaluation

There was no significant ($P \geq 0.05$) difference in sensory characteristics between CB-chocolate and 5 g CBS/100 g chocolate blend (Fig. 8). However, chocolate with 20 g CBS/100 g blend had significantly ($P < 0.05$) different sensory characteristics in terms of taste acceptance, overall acceptability and hardness compared to the CB-chocolate. In triangle test, 52 out of 100 panelists were able to identify chocolate with 20 g CBS/100 g blend as different from the other two samples of CB-chocolate and 5 g CBS/100 g chocolate blend (data not shown). Therefore, it could be concluded that panelists did not find any difference between the CB-chocolate and 5 g CBS/100 g chocolate blend. De Clercq et al. found that full CB-like fat replacement of CB influenced the sensory characteristics

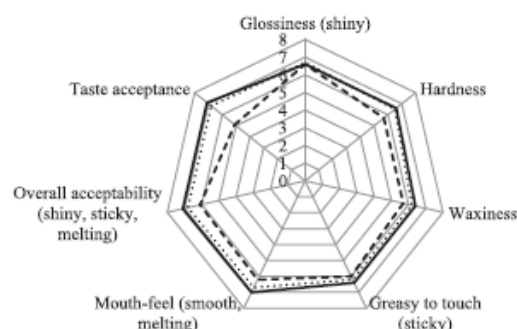


Fig. 8. Sensory evaluation of — CB-chocolate, 5 g CBS/100 g chocolate blend and ----- 20 g CBS/100 g chocolate blend.

of chocolate (De Clercq et al., 2016). In the current study, panelists were not able to distinguish any differences between CB-chocolate and chocolate made with 5 g CBS/100 g blend, thus indicating comparable sensory profile between CB-chocolate and 5 g CBS/100 g chocolate blend.

4. Conclusion

Dark chocolate formulated with CB (without CBS), 5 g CBS and 20 g CBS/100 g blend was characterized using DSC melting, PSD, rheological, bloom formation and sensory properties. There was no significant ($P \geq 0.05$) difference in melting behavior between the CB-chocolate and chocolate with 5 g CBS/100 g blend. Although all the chocolates remained similar melting peak temperature, there were significant ($P < 0.05$) differences in peak area and melting enthalpy between 20 g CBS/100 g chocolate blend and CB-chocolate. Chocolate made with 20 g CBS/100 g blend had significantly higher PSD with lower hardness and yield stress compared to CB-chocolate, but its viscosity was comparable to 5 g CBS/100 g chocolate blend and CB-chocolate. Stereomicroscope images of all the chocolate samples did not show bloom at 24 °C for up to 8 weeks. However, at 29 ± 1 °C, bloom formation was observed for chocolate with 5 g CBS/100 g blend and CB-chocolate after two weeks. Noticeable changes in X-ray diffraction peaks (polymorphism) were observed for the bloomed chocolate. There was no significant difference in sensory characteristics between 5 g CBS/100 g chocolate blend and CB-chocolate. Additionally, chocolate with 20 g CBS/100 g blend was found to be different in terms of taste from the other two samples in a triangle test. The overall characterization suggested that the chocolate with 5 g CBS/100 g blend was comparable to CB-chocolate in terms of physical and sensory characteristics. However, chocolate with 20 g CBS/100 g blend showed significantly lower sensory properties particularly taste acceptance and hardness compared to CB-chocolate. All in all, both chocolates made with 5 g and 20 g CBS/100 g blend need to be stored at 24 °C to prevent bloom formation.

Declaration

The authors have declared no conflicts of interest.

Acknowledgements

The authors would like to thank School of Science, Monash University Malaysia (FRGS/1/2013/SG01/MUSM/03/2) for funding the current study. The Authors are grateful to Malaysia Cocoa Board

for chocolate making facility. Furthermore, we would like to thank Dr Satoshi and Rachel at the School of Medicine, Monash University Malaysia for their technical assistance on stereomicroscope experiment.

References

- Abigor, R. D., Marmer, W. N., Foglia, T. A., Jones, K. C., DiGedo, R. J., Ashby, R., et al. (2003). Production of cocoa butter-like fats by the lipase-catalyzed interesterification of palm oil and hydrogenated soybean oil. *Journal of the American Oil Chemists' Society*, 80(12), 1193–1196.
- Afoakwa, E. O. (2016). *Chocolate science and technology* (2nd ed.). Chichester, UK: John Wiley & Sons Ltd.
- Afoakwa, E. O., Paterson, A., & Fowler, M. (2008). Effects of particle size distribution and composition on rheological properties of dark chocolate. *European Food Research and Technology*, 226(6), 1259–1268.
- Afoakwa, E. O., Paterson, A., Fowler, M., & Vieira, J. (2008a). Characterization of melting properties in dark chocolates from varying particle size distribution and composition using differential scanning calorimetry. *Food Research International*, 41(7), 751–757.
- Afoakwa, E. O., Paterson, A., Fowler, M., & Vieira, J. (2008b). Effects of tempering and fat crystallization behaviour on microstructure, mechanical properties and appearance in dark chocolate systems. *Journal of Food Engineering*, 89(2), 128–136.
- Afoakwa, E. O., Paterson, A., Fowler, M., & Vieira, J. (2009a). Influence of tempering and fat crystallization behaviours on microstructural and melting properties in dark chocolate systems. *Food Research International*, 42(1), 200–209.
- Afoakwa, E. O., Paterson, A., Fowler, M., & Vieira, J. (2009b). Microstructure and mechanical properties related to particle size distribution and composition in dark chocolate. *International Journal of Food Science & Technology*, 44(1), 111–119.
- Aidoo, R. P., Afoakwa, E. O., & Dewettinck, K. (2015). Rheological properties, melting behaviours and physical quality characteristics of sugar-free chocolates processed using inulin/polydextrose bulking mixtures sweetened with stevia and thaumatin extracts. *LWT-Food Science and Technology*, 62(1), 592–597.
- Aidoo, R. P., Clercq, N. D., Afoakwa, E. O., & Dewettinck, K. (2014). Optimisation of processing conditions and rheological properties using stephan mixer as conche in small-scale chocolate processing. *International Journal of Food Science & Technology*, 49(3), 740–746.
- Asghar, A., Pasha, I., Murtaza, G., & Ali, M. (2017). Improving heat stability along with quality of compound dark chocolate by adding optimized cocoa butter substitute (hydrogenated palm kernel stearin) emulsion. *LWT-Food Science and Technology*, 80, 531–536.
- Beckett, S. (2008). *The science of chocolate* (2nd ed.). Cambridge, UK: Royal Society of Chemistry Publishing.
- Beckett, S. T. (2011). *Industrial chocolate manufacture and use*. Chichester: John Wiley & Sons.
- Biswas, N., Cheow, Y. L., Tan, C. P., Kanagaratnam, S., & Siow, L. F. (2017). Cocoa butter substitute (CBS) produced from palm mid-fraction/palm kernel oil/palm stearin for confectionery fillings. *Journal of the American Oil Chemists' Society*, 94(2), 235–245.
- Biswas, N., Cheow, Y., Tan, C., & Siow, L. (2016). Blending of palm mid-fraction, refined bleached deodorized palm kernel oil or palm stearin for cocoa butter alternative. *Journal of the American Oil Chemists' Society*, 93(10), 1415–1427.
- Bootto, M. A., Hartel, R. W., Garcés, R., Martínez-Force, E., & Salas, J. J. (2012). Evaluation of high oleic-high stearic sunflower hard stearins for cocoa butter equivalent formulation. *Food Chemistry*, 134(3), 1409–1417.
- Bricknell, J., & Hartel, R. (1998). Relation of fat bloom in chocolate to polymorphic transition of cocoa butter. *Journal of the American Oil Chemists' Society*, 75(11), 1609–1615.
- Briggs, J. L., & Wang, T. (2004). Influence of shearing and time on the rheological properties of milk chocolate during tempering. *Journal of the American Oil Chemists' Society*, 81(2), 117–121.
- Calliauw, G., Foubert, L., De Greyt, W., Dijkmans, P., Kellens, M., & Dewettinck, K. (2005). Production of cocoa butter substitutes via two-stage static fractionation of palm kernel oil. *Journal of the American Oil Chemists' Society*, 82(11), 783–789.
- Cebula, D., & Ziegler, G. (1993). Studies of bloom formation using X-ray diffraction from chocolates after long-term storage. *Lipid/Fett*, 95(9), 340–343.
- Çiftçi, O. N., Fadiloğlu, S., & Göğüş, F. (2009). Conversion of olive pomace oil to cocoa butter-like fat in a packed-bed enzyme reactor. *Bioresource Technology*, 100(1), 324–329.
- Couzens, P., & Wille, H. (1997). Fat migration in composite confectionery products. *Manufacturing Confectioner*, 77, 45–47.
- DSouza, V. (1990). Short spacings and polymorphic forms of natural and commercial solid fats: A review. *Journal of the American Oil Chemists' Society*, 67(11), 835–843.
- De Clercq, N., Depypere, F., Delbaere, C., Nopens, I., Bernaert, H., & Dewettinck, K. (2014). Influence of cocoa butter diacylglycerols on migration induced fat bloom in filled chocolates. *European Journal of Lipid Science and Technology*, 116(10), 1388–1399.
- De Clercq, N., Kadivar, S., Van de Walle, D., De Pelsmaeker, S., Ghelleyck, X., & Dewettinck, K. (2016). Functionality of cocoa butter equivalents in chocolate products. *European Food Research and Technology*, 243(2), 309–321.
- De Clercq, N., Moens, K., Depypere, F., Ayala, J. V., Calliauw, G., De Greyt, W., et al. (2012). Influence of cocoa butter refining on the quality of milk chocolate. *Journal of Food Engineering*, 111(2), 412–419.
- Garti, N., & Widlak, N. R. (2015). *Cocoa butter and related compounds, confectionery fats* (19). Urbana, USA: AOCS Press.
- Glicerina, V., Balestra, F., Dalla Rosa, M., & Romani, S. (2013). Rheological, textural and calorimetric modifications of dark chocolate during process. *Journal of Food Engineering*, 119(1), 173–179.
- Hartel, R. W. (1999). Chocolate: Fat bloom during storage. *Manufacturing Confectioner*, 79, 89–99.
- Hodge, S., & Rousseau, D. (2002). Fat bloom formation and characterization in milk chocolate observed by atomic force microscopy. *Journal of the American Oil Chemists' Society*, 79(11), 1115–1121.
- ICA. (2000). *International Confectionery Association. Viscosity of cocoa and chocolate products*. Analytical Method 46. CAOISCO, rue Defacqz 1, B-1000 Brussels, Belgium.
- Kadivar, S., De Clercq, N., Mokbul, M., & Dewettinck, K. (2016). Influence of enzymatically produced sunflower oil based cocoa butter equivalents on the phase behavior of cocoa butter and quality of dark chocolate. *LWT-Food Science and Technology*, 66, 48–55.
- Kadivar, S., De Clercq, N., Van de Walle, D., & Dewettinck, K. (2014). Optimisation of enzymatic synthesis of cocoa butter equivalent from high oleic sunflower oil. *Journal of the Science of Food and Agriculture*, 94(7), 1325–1331.
- Kinta, Y., & Hartel, R. W. (2010). Bloom formation on poorly-tempered chocolate and effects of seed addition. *Journal of the American Oil Chemists' Society*, 87(1), 19–27.
- Loisel, C., Lecq, G., Keller, G., & Ollivon, M. (1998). Dynamic crystallization of dark chocolate as affected by temperature and lipid additives. *Journal of Food Science*, 63(1), 73–79.
- Lonchamp, P., & Hartel, R. W. (2006). Surface bloom on improperly tempered chocolate. *European Journal of Lipid Science and Technology*, 108(2), 159–168.
- Marangoni, A. G., & McGauley, S. E. (2003). Relationship between crystallization behavior and structure in cocoa butter. *Crystal Growth & Design*, 3(1), 95–108.
- Osborn, H., & Akoh, C. (2002). Enzymatically modified beef tallow as a substitute for cocoa butter. *Journal of Food Science*, 67(7), 2480–2485.
- Rousseau, D., & Smith, P. (2008). Microstructure of fat bloom development in plain and filled chocolate confections. *Soft Matter*, 4(8), 1706–1712.
- Servais, C., Ranc, H., & Roberts, I. (2003). Determination of chocolate viscosity. *Journal of Texture Studies*, 34(5–6), 467–497.
- Sonwai, S., & Rousseau, D. (2006). Structure evolution and bloom formation in tempered cocoa butter during long-term storage. *European Journal of Lipid Science and Technology*, 108(9), 735–745.
- Sridhar, R., Lakshminarayana, G., & Kaimal, T. (1991). Modification of selected Indian vegetable fats into cocoa butter substitutes by lipase-catalyzed ester interchange. *Journal of the American Oil Chemists Society*, 68(10), 726–730.
- Talbot, G. (1994). *Chocolate temper*. *Industrial chocolate manufacture and use*, Springer, pp. 156–166.
- Talbot, G. (2006). *Application of fats in confectionery*. Loughton, UK: Kennedy's Publications.
- Talbot, G. (2009). *Science and technology of enrobed and filled chocolate, confectionery and bakery products*. New York: CRC Press, Woodhead Publishing Limited, 53–361.
- Timms, R. E. (2003). Production and characteristic properties. In R. E. Timms (Ed.), *Confectionery fats handbook: Properties, production and application*. Bridwater, England: The Oily Press.
- Wang, F., Liu, Y., Shan, L., Jin, Q., Wang, X., & Li, L. (2010). Blooming in cocoa butter substitutes based compound chocolate: Investigations on composition, morphology and melting behavior. *Journal of the American Oil Chemists' Society*, 87(10), 1137–1143.
- Xu, X. (2000). Production of specific-structured triacylglycerols by lipase-catalyzed reactions: A review. *European Journal of Lipid Science and Technology*, 102(4), 287–303.
- Zarringhalami, S., Sahari, M. A., Barzegar, M., & Hamidi-Esfahani, Z. (2010). Enzymatically modified tea seed oil as cocoa butter replacer in dark chocolate. *International Journal of Food Science & Technology*, 45(3), 540–545.